Pyrimidine Functionalized Phosphine Ligands and Their Application in Catalysis

Dissertation zur Erlangung

des Doktorgrades der Naturwissenschaften (Dr. rer. nat.)

genehmigt vom Fachbereich Chemie

der Technischen Universität Kaiserslautern

(D 386)

Vorgelegt von

MSc Saeid Farsadpour

Betreuer der Arbeit: Prof. Dr. W. R. Thiel

Tag der wissenschaftlichen Aussprache: 10.09.2012

Vom Fachbereich Chemie der Technischen Universität Kaiserslautern am 10.09.2012 als Dissertation angenommen.

Dekan: Prof. Dr.-Ing. Jens Hartung

Vorsitzender der Prüfungskommission: Prof. Dr. H. Sitzmann

1. Berichterstatter: Prof. Dr. W. R. Thiel

2. Berichterstatter: Prof. Dr. S. Ernst

Die vorligende Arbeit wurde im Fachbereich Chemie der Technischen Universität Kaiserslautern im Arbeitskreis von Prof. Dr. W. R. Thiel in der Zeit von August 2008 bis August 2012 angefertigt.

In the Name of God

Lovingly Dedicated to

My Wife Leila

Abbreviations

AAS	atomic absorption spectrometry
Å	angstrom
Anal.	analytical
a.u	Arbitrary Unis
BET	Brunauer-Emmet-Teller
BJH	Barrett-Joyner-Halenda
br.	broad
°C	degrees centigrade
calc.	calculated
CID	collision-induced dissociation
CP MAS	Cross Polarization Magic Angle Spinning
d	doublet
DFT	density functional theory
DMF	N,N-dimethylformamide
DMF-DMA	N,N-dimethylformamide dimethyl acetal
DMSO	dimethyl sulfoxide
eq	equivalent
eq.	equation
ESI-MS	electrospray mass spectrometry
Et	ethyl
Et_2O	diethyl ether
EtOH	ethanol
FT-IR	fourier transform infrared spectroscopy
g	gram
GC	gas chromatography
h	hour
Hz	hertz
iPr	isopropanol
IR	infrared
J	coupling constant
kcal	kilocalorie
M	molar

m	multiplet
MCM	Mobil Crystalline Material
Me	Methyl
ml	millilitre
NMR	nuclear magnetic resonance
Ph	Phenyl
ppm	parts per million
ref.	reference
refl.	Reflux
RT	room temperatur
s	Singlet
SEM	Scanning Electron Microscopy
T	temperature in Kelvin
TEM	Transmission Electron Microscopy
T	Triplet
*t*Bu	*tert*-Butyl
temp.	temperature in °C
TG-DTG	Thermogravimetric and Differential Thermogravimetric analysis
THF	tetrahydrofuran
TOF	turn over frequency
TON	turn over number
TPP	triphenylphosphine
XRD	X-ray diffraction
$\tilde{\upsilon}$	wave number in cm^{-1}
δ	chemical shift in ppm

Contents

Introduction

1. Introduction

1.1. Catalysis

Catalysis is the enhancement of the rate of a chemical reaction caused by the participation of a substance called a catalyst. Catalytic reactions have been known for many centuries but in former times people were unable to explain the occurrences they were seeing all around them like fermentation of wine to vinegar, leavening of bread, etc.. The term catalysis was coined by Swedish chemist Jöns Jacob Berzelius more than 150 years ago when he had noticed changes in substances when they were brought in contact with small amounts of certain species called "ferments".[1] Many years later German chemist Wilhelm Ostwald, who was awarded the Nobel Prize for chemistry in 1909 came up with the definition that:

"A catalyst is a compound that increases the rate of a chemical reaction without being consumed by itself and without changing the thermodynamic equilibrium of the reaction".

Since a catalyst brings two chemicals together physically in a way that their chance to react is maximized, it plays the role of a "matchmaker" in a chemical reaction. Catalysts also provide selectivity to more desirable products. All these attributes about catalysis and catalysts translate to energy savings, less pollution, less side products and lower cost reactor materials. Alwin Mittasch (1869-1955) mentioned that "chemistry without catalysis would be a sword without a handle, a light without brilliance or a bell without sound."

During the last century, catalysts have found outstanding applications in human life. Fluid catalytic cracking (FCC) is the most important conversion process used in petroleum refineries, which produces gasoline as well as heating oil, fuel oil, propane, butane, and chemical raw materials that are useful in manufacturing other products such as plastics, textiles, synthetic rubbers, dyes, and cosmetics. Since 1960s, toxic chemicals such as CO, NO_x and hydrocarbon emissions from mobile vehicles are converted into less toxic substances by

Introduction

exhaust emission catalysts. As other important applications, catalysts for polymer production, for pharmaceutical production and for food industry shall be named here.

1.1.1. Types of Catalysts

A catalytic reaction can be either a heterogeneous or a homogeneous one. In a heterogeneous reaction, the catalyst is in a different phase from the reactants (typical examples involve a solid catalyst with the reactants either in a liquid or a gaseous phase). In a homogeneous reaction, the catalyst is in the same phase as the reactants, typically everything will be present as a gas or contained in a single liquid phase. Biocatalysts (enzymes) are often seen as a separate group. In **Table 1** advantages and disadvantages of the both homogeneous and heterogeneous catalysts are listed.

Table 1. Properties of homogeneous and heterogeneous catalysts.

Aspect	Homogenous	Heterogeneous
Catalyst recovery	Difficult and expensive	Easy and straightforward
Thermal stability	Poor	Good
Selectivity	High due to single active sites	Difficult to control selectivity
Reaction Mechanism	Easier to find out	Difficult to find out
Reproducibility	Reproducible results	Difficulties in reproducibility
Reaction conditions	Lower temp. (<250ºC)	Higher temp. & pressure
Active sites	Very well defined	Not well-defined
Catalyst life	Relatively short, regeneration may/may not be possible	Relatively long, regeneration possible
Industrial Application	Pharma, fine & specialty chemical manufacturing, ~15%	Bulk/Commodity products manufacturing ~ 85%

1.1.2. Heterogenization of Homogeneous Catalysts

To reduce the limitations mentioned in **Table 1**, bridging the gap between homogeneous and heterogeneous catalysts has been found to be a good way.[2,3,4,5] This is obtainable by "heterogenization" or "fixing" homogeneous catalysts on support materials to

Introduction

combine benefits of both heterogeneous and homogeneous catalysis.[6,7,8,9] To develop high-performance heterogenized homogeneous catalysts, the concept of interphases chemistry has been introduced by E. Lindner and his coworkers in 1999.[10] An interphase is defined as a region within a material in which a stationary and a mobile component penetrate each other on a molecular level (**Figure 1**). The stationary phase is made of an inert matrix, a flexible spacer, and an active center, while the mobile phase consists of a solvent or a gaseous, liquid, or a solution of reactant. In an ideal interphase, the reactive center is uniform, well-defined, and highly mobile. In this way, an interphase is able to simulate homogeneous reaction conditions, and at the same time it has the advantages of a heterogeneous catalyst.
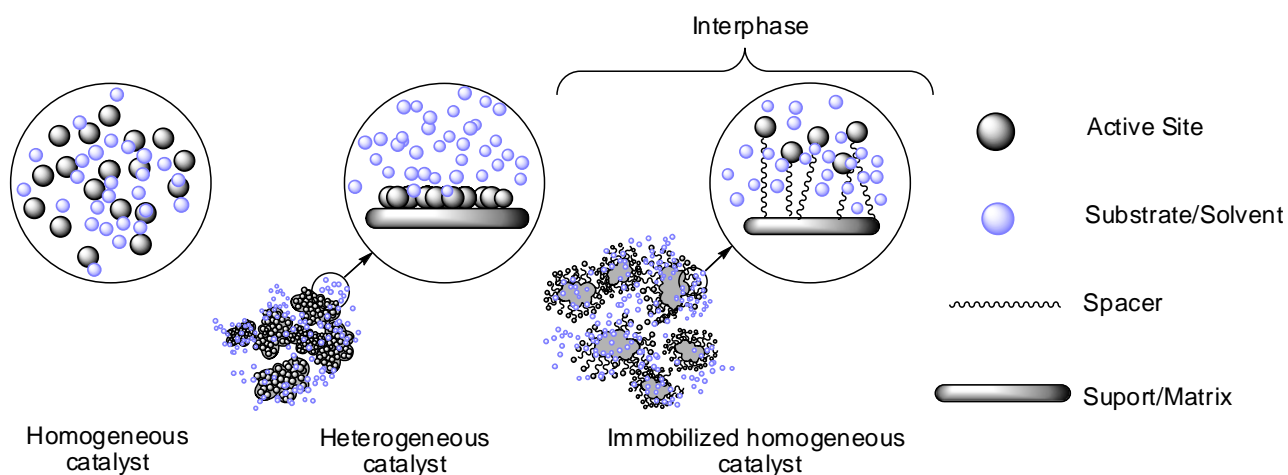
Figure 1. Schematic representation of homogeneous, heterogeneous and immobilized homogeneous catalysts.

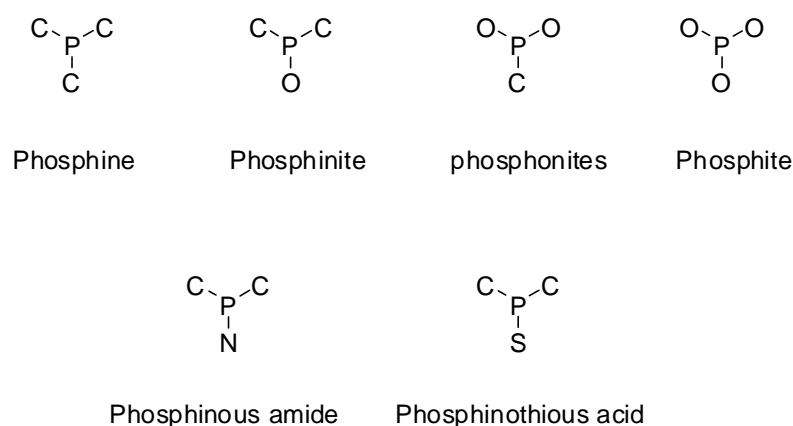## 1.2. Ligands in Transition Metal Catalysis

Finding the best homogeneous catalyst for a particular transformation is a difficult task, since we need to optimize a range of variable inputs such as metal, ligands, co-catalysts, substrates, solvents and reaction conditions including temperature and pressure. Among the

Introduction

variable inputs mentioned above, ligands play the main role in catalyst optimization. Changing the ligands can be an applicable way of modifying the properties of metal complexes. This type of treatments have been examined widely. In addition, using a range of experimental and calculated parameters, steric and electronic properties of ligands can be better understandable. For such ligands, previous analyses of experimental results have established a context of knowledge in which predictions based on certain descriptors can be tested. The explanation of ligand effects on experimental observations can also help us to recognize key properties and thus to have a better design strategy.

1.2.1. Phosphorus-containing Ligands

Among all ligands, phosphines are the most notable for their remarkable electronic and steric abilities. Such trivalent phosphorus compounds, with the general formula PR_3, offer chemists a unique chance to modify their electronic and steric properties. Phosphine ligands are usually strong σ-donor ligands and weak π-acceptors, however, replacing the electron-donating groups by electron with-drawing groups the σ-donating and the π-accepting properties of the phosphorus center can be modified. As an example modifying via replacement of the P–C bonds with P–O, P–N and P–S are shown in **Scheme 1**.

| Phosphine | Phosphinite | phosphonites | Phosphite |

| Phosphinous amide | Phosphinothious acid |

Scheme 1. Several trivalent phosphorus ligand families.

Introduction

The catalytic reactivity and selectivity of a transition-metal complex is affected by the steric factors too. The steric behavior of phosphine ligands is interpreted with the help of so-called cone angle. The cone angle θ for PR_3 (**Figure 2**) was introduced by Tolman[11] in 1977 and is defined as the apex of a cylindrical cone, situated 2.28 Å from the centre of the phosphorus atom, which diverges outwards toward the R groups and borders the van der Waals radii of the peripheral atoms. This angle is applied to point out the approximate amount of space that the ligand consumes around the metal. A bulkier ligand (with a larger cone-angle) tends to have a higher dissociation rate than smaller ligands.
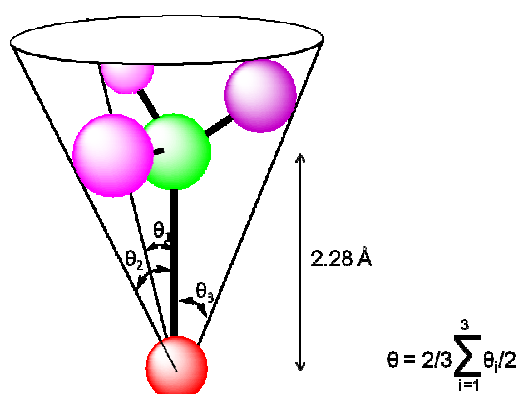
Figure 2. Representation of Tolman's model for calculating the cone angle.

1.2.1.1.   Coordination Chemistry of Phosphine Ligands

For years, it was assumed that π-backdonation occurs from the metal into empty d-orbitals on phosphorus. In 1990, Orpen and his coworkers[12] introduced an acceptable description of π-bonding in transition metal-phosphine (and -phosphite) complexes considering the geometry variations in 24 sets of transition metal-phosphine and -phosphite complexes, from which crystal structures were known for multiple oxidation states of the complexes. One of their examples is shown in **Scheme 2**. Their conclusions were based on the effect of metal oxidation on the M–P π-back-bonding.

Introduction

Co-P	2.218	2.230
P-C	1.846	1.829
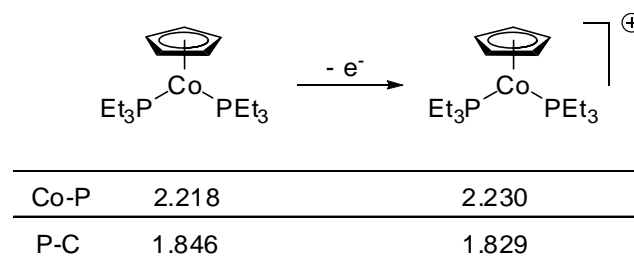
Scheme 2. Length bonds are in Å and resulted from crystal structures determination.[12]

Removing one electron from the metal, the M–P bond length will increase, along with a decrease in P–C bond length which clarifies that π-backdonation occurs into MOs formed by the combination of two d-orbitals on phosphorus and the P–R σ* orbitals.[13,14,15] Generally, ligands, especially phosphorus-containing ones, can also be differentiated according to their coordinating mode (i.e., monodentate, bidentate, polydentate and mixed bidentate; see **Scheme 3**).

monodentate   bidentate   polydentate   mixed bidentate
X= C, N, O, S, etc.
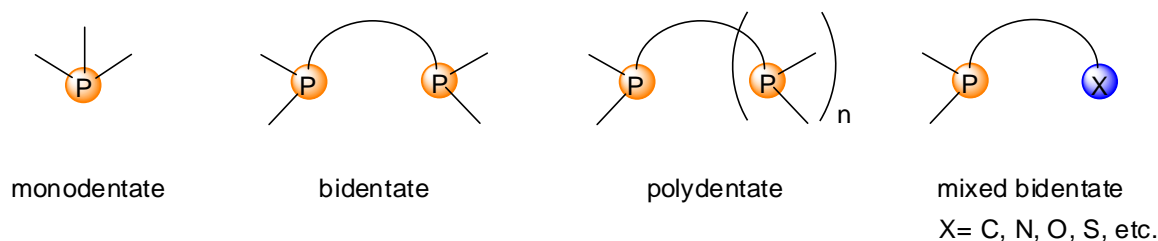
Scheme 3. Coordination modes of trivalent phosphorus ligands.

1.2.1.2.   *Classification of Phosphines as Hemilabile Ligands*

The term "hemilabile" was introduced by J. C. Jeffrey and T. B. Rauchfuss.[16] A hemilabile ligand, a special form of hybrid ligands, consists of one strongly bound donor group and one which binds weakly to the metal center (**Scheme 4**). The bonding and reactivity of the other ligands bound to the metal will be affected by this behavior, in particular those in the *trans* position.

Introduction
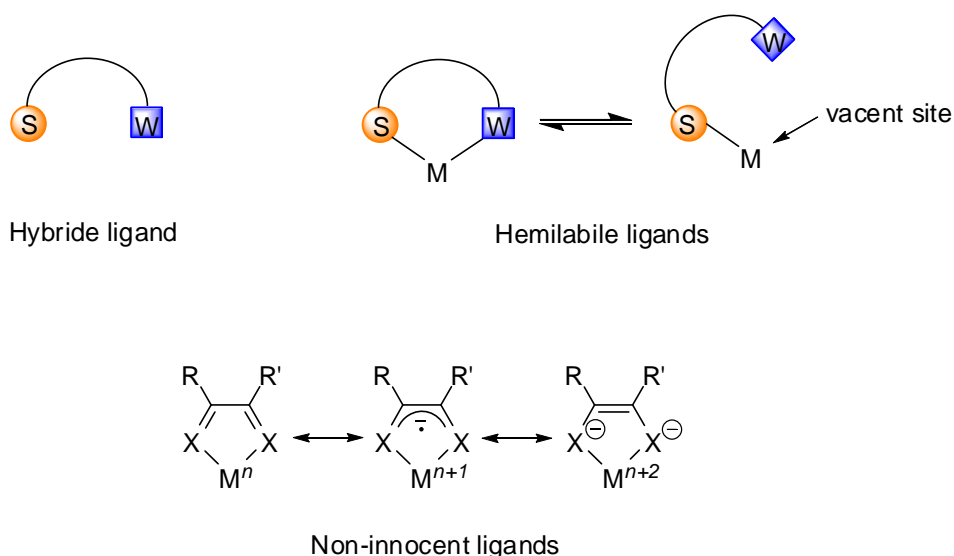
Scheme 4. Representation of hemilability of hybrid ligands. S: strong donor or inert group, W: weak donor or labile group (top). Non-innocent ligands (bottom).

Among all phosphorus-based ligands, phosphorus-oxygen and phosphorus-nitrogen based ligands are the most studied class of functionalized hemilabile phosphines.[17] The oxygen functional groups associated with the phosphorus donor come from alcohol,[18] ether,[19,20] ketone,[21] amide,[22,23] acetal,[24,25] and phosphine oxide[26,27,28,29] groups. Although these various functions open up significant changes in the coordination properties and the hemilability, phosphorus-oxygen based ligands are generally the most weakly chelating type of ligand. Therefore, heterogenization of their complexes as supported catalysts (by anchoring onto solid supports or sol gel processing) is not surprising.[30]

Amine and pyridine moieties are the most common donors associated with phosphorus-nitrogen ligands but amines,[31] imines,[32] or anilides[33] have also been used as the weakly coordinating end of *P,N* chelates.[34] These hybrid ligands are often named as hemilabile ligands but in comparison to the *P,O* ligands, their hemilability is generally low. However, the beneficial effect of *P,N* ligands, for instance, on the rhodium-catalyzed hydroformylation of olefins is documented.[35]

Introduction

1.2.1.3.   General Synthesis of Phosphine Ligands

The central phosphorous–carbon bonds of phosphines are usually formed by reacting either a carbon centered electrophile with a phosphorous nucleophile or a carbon nucleophile with a phosphorous based electrophile (**Scheme 5**). Following the second method, metalated carbon compounds react with phosphorous halides generally without any problems. The solely limitation is the incompatibility of functional groups within R and R' towards the organometallic reagent, narrowing the scope of accessible products. From an other point of view, the gradual formation of multiple phosphorous–carbon bonds in one reaction batch is difficult if metalated phosphines are employed due to their high sensitivity against water and oxygen.
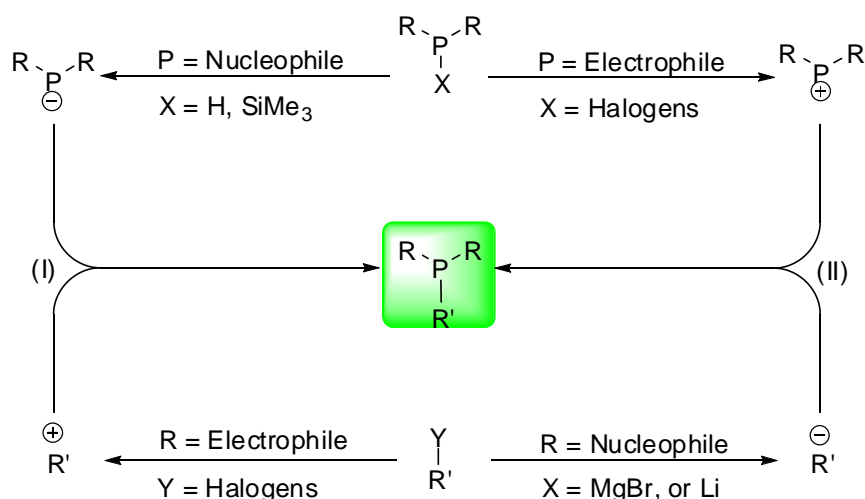
Scheme 5. General synthetic routs leading to phosphine ligands.

In comparison to route (I), deprotonation of phosphines of the type H_yPR_{3-y} (y = 1–3) using organometallic reagents, mostly n-butyllithium, is probably the best way to build up phosphorous–carbon bonds with phosphorous nucleophiles. Alternatively, phosphides can be generated in situ from phosphines in a superbasic medium such as DMSO/KOH.[36,37,38,39,40,41,42,43,44] Using an aryl halide compound as the carbon electrophile, the

Introduction

well-known reactivity of S_NAr-reactions can be observed: aryl fluorides turn out to be the most reactive aryl-X components and electron-withdrawing substituents considerably increase the reactivity of the aryl halide. This type of reaction was intensively investigated in the last 20 years, mainly by Stelzer et al..[36,37,38,39,40,41,42,43,44] This method opens up access to a variety of different phosphine ligands. As an important example, I here mention water-soluble phosphines such as *p*-TPPTS (sodium triphenylphosphine trisulfonate) which can be synthesized without protection of the sulfonic acid sites. However, the scope of reactants is limited by the aggressive superbasic medium. Alternative precursors containing phosphorous nucleophile are silylated phosphines of the type $Ph_{3-x}P(SiMe_3)_x$ (x = 1–3). However there are just a few reports on the application of silylated phosphines for the formation of phosphorous–carbon bonds in which harsh reaction conditions (e. g. high reaction temperature, long reaction time as well as using extremely electron poor RY') were applied. More recently, W. R. Thiel and his coworkers reported the first fluoride catalyzed phosphorous–carbon bond formation which opens up an access to a broad variety of interesting functionalized aryl phosphine structures under very mild reaction conditions in a minimum amount of organic solvent. [45,46,47]

1.2.1.4. *Application of Phosphine Ligands in Homogeneous Transition Metal Catalysis*

Application of phosphine ligands is necessary for nearly all homogeneous catalysis with precious-metals.[48] In catalytic reactions there are some significant parameters which are easily tunable by applying a suitable phosphine ligand. In fact, these parameters which are listed below, can lead to an excellent performance of catalyst.

➢ The solubility of the active species.

➢ The steric effect of the ligand.

➢ The electron density on the metal center.

➢ The reactivity and stability of the catalyst in the catalytic cycle.

Introduction

- ➢ The lifetime and turnover-numbers of the catalyst.

- ➢ The stereoselectivity of the reaction in case of chiral ligands.

According to these features, phosphine ligands are employed in a wide variety of different catalytic reactions, as far as they have found immense importance in all branches of homogeneous catalysis during the last decade, a series of them being of industrial relevance such as hydrogenations,[49,50,51,52] hydrocyanations,[53] hydroformylations,[54,55] hydrosilations,[56] cross-coupling reactions,[57] organometallic polymerizations,[58] or Diels–Alder reactions.[59] Therefore it is not unexpected that the development of phosphine chemistry has obtained a persuasive claim over the last decades, particularly for applications in enantioselective catalysis.[60,61]

1.3. Palladium-Catalyzed Reactions in Presence of Phosphine Ligands.

The widespread utility of the palladium-based catalysts is completely obvious for all chemists. Among these different palladium-catalyzed reactions the so-called cross-coupling reactions have become a very powerful methodology for the formation of C-C and C-heteroatom bonds.

Generally, bond formation will occur when stoichiometric amounts of organometallic reagents such as organoboron, -tin, -zinc, -copper, -silicon, compounds couple with organohalides or pseudohalides with the help of palladium center. As it shown in **Scheme 6**, several coupling reactions have been developed with different substrates. Among all types of ligands, which are the partner in these reactions, phosphorous based ligands have been broadly used.

Introduction
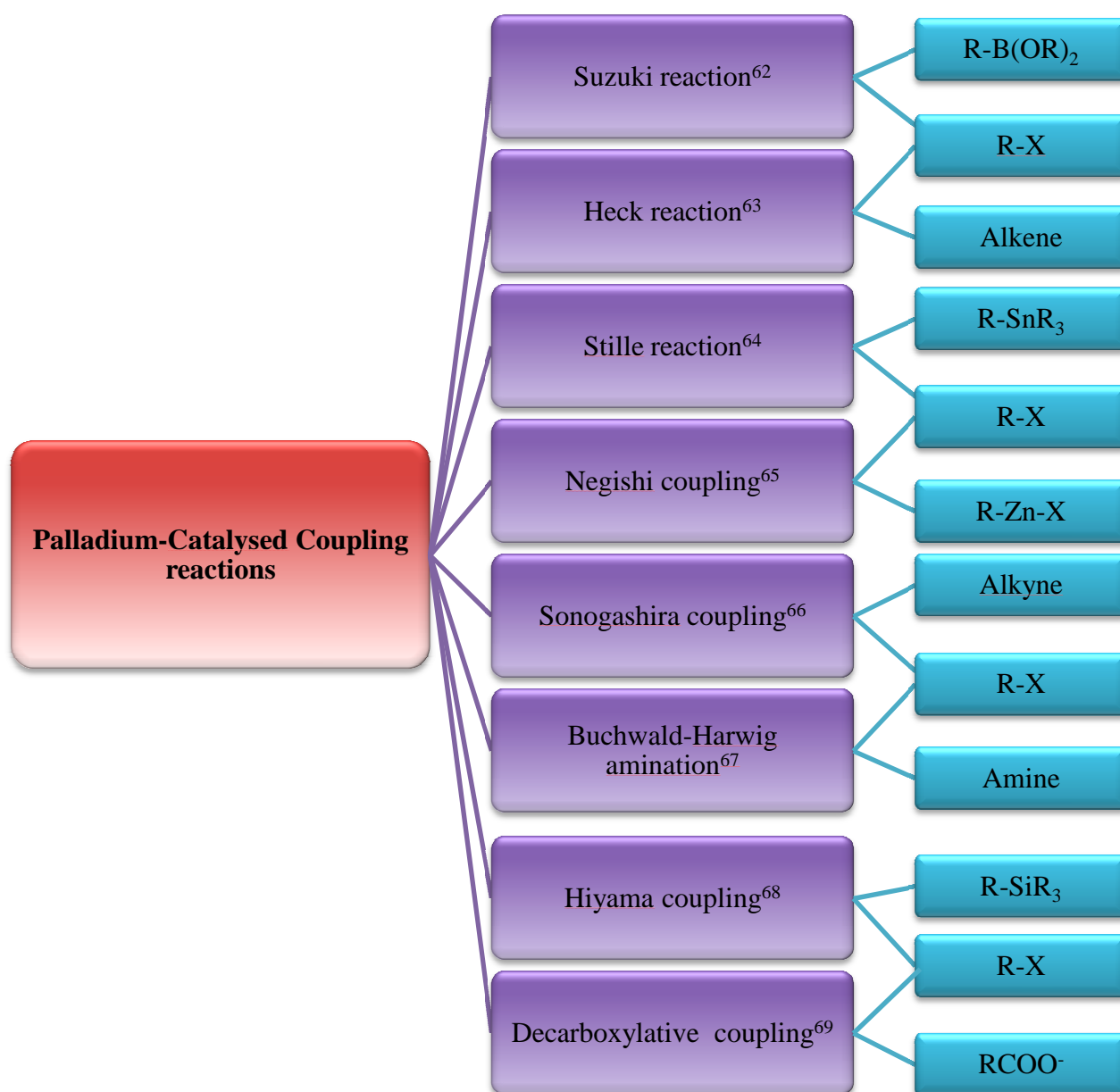
Scheme 6. Overview over palladium-catalyzed coupling reaction. All the references are representing phosphorous based ligands in the corresponding reactions. [62,63,64,65,66,67,68,69]

Most palladium catalyzed coupling reactions are believed to follow a similar catalytic cycle. It generally includes at least three separate steps, oxidative addition, transmetalation, and reductive elimination (**Scheme 7**). The catalytic species can be formed in situ using a palladium source, such as $Pd(PPh_3)_4$ or $Pd(P(t\text{-}Bu)_3)_2$ and the reaction mechanism usually starts with an oxidative addition of an organic halide (R-X) to the catalyst. Subsequently, the second partner undergoes transmetalation, which inserts both coupling partners on the same metal

Introduction

centre. The final step is reductive elimination of the two coupling fragments to give the organic product and to regenerate the catalyst. The properties of the ligand can facilitate two steps of the catalytic cycle. The use of strong σ-donating ligands, such as trialkylphosphines, increases the electron density at the metal site, accelerating the oxidative addition of the substrate to the catalyst. In addition, the bulky ligands – in particular phosphine ligands which exhibit a large cone angle – are able to accelerate the elimination step.
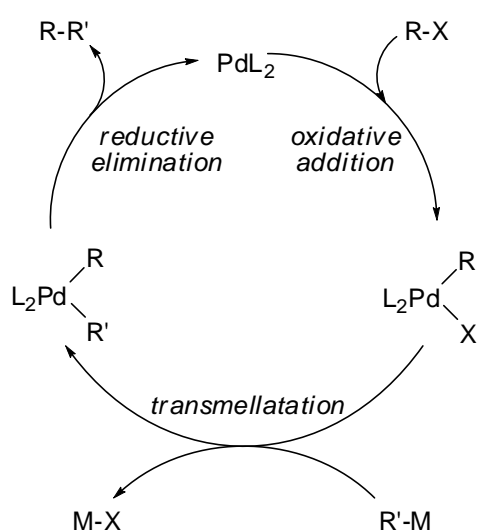
**Scheme 7**. General catalytic cycle for palladium catalyzed coupling reaction.

In addition to coupling reactions which were mentioned above, some type of other reactions catalyzed by palladium phosphine catalyst have been documented e. g. ethene oligomerization,[70,71] [72] [73] formation of linear copolymers of ethylene and acrylonitrile,[74] hydroamination reactions,[75] or Reppe carbonylation.[76]

2. Motivation

Functionalized phosphines are important ligands in coordination chemistry and are frequently applied in transition metal catalysis. Since a couple of years, Thiel's group is engaged in developing novel phosphines such as imino functionalized phosphines,[77] enantiomerically pure *P*,*N*-donors[78] and pyrazole functionalized phosphines[79]. The good results of the previous studies on the role of pyrazole derived ligands in homogeneous catalysis as well as their coordination chemistry towards metal ions were my motivation to change the pyrazolyl group against a pyrimidinyl group and to investigate the coordination chemistry of these new ligands as well as catalytic application of their palladium complexes.


(pyrazolyl)phosphine   (2-aminopyrimidinyl)phophines
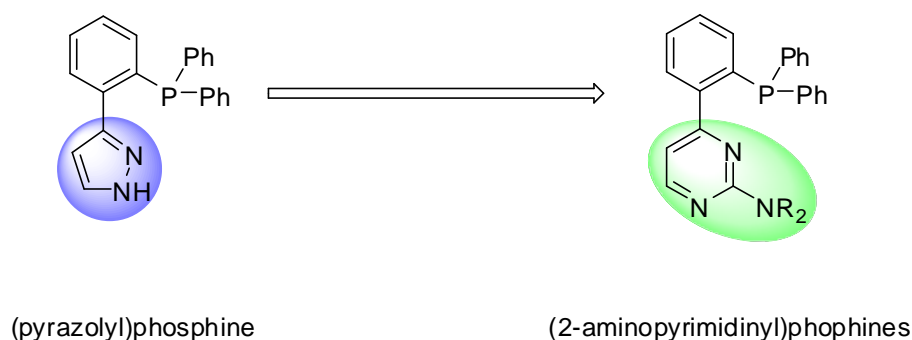
Scheme 8. Replacing the pyrazole against a 2-aminopyrimidine.

Besides from bioinorganic related chemistry,[80] where pyrimidines are known as one of the structure and function directing moieties in nucleobases, these heterocycles have only rarely been used as motifs in coordination compounds. Compared to pyridines they e.g. play a minor role in catalysis, which is quite astonishing, since pyridine chemistry is much more difficult and restricted in terms of chemical diversity than pyrimidine chemistry. The well-established and stepwise synthesis of the pyrimidine ring[81] allows the simple introduction of a multitude of functional groups into the pyrimidine skeleton.

Parallel to this work, ruthenium complexes of (2-aminopyrimidinyl)pyridines were

Motivation

applied as catalyst for the transfer hydrogenation of acetophenone in Prof. Thiel's group. Later on, a new mechanism for the catalyst activation under base-free conditions was proposed on the basis of ESI-MS investigations and ab-initio calculations combined with isotope labelling, proving that the key step in the catalyst self-activation process is a C-H bond cleavage occurring at the pyrimidine part of the bidentate nitrogen donor, which thus switches from an *N,N*- to a *C,N*-coordination mode [82] (**Figure 3**). However all attempts to trap *C,N*-coordinated ruthenium complexes have failed up to now. Therefore from the chose of (2-aminopyrimidinyl)phosphine ligands might help us to see whether *P,C* coordination mode is observable in corresponding metal complexes.
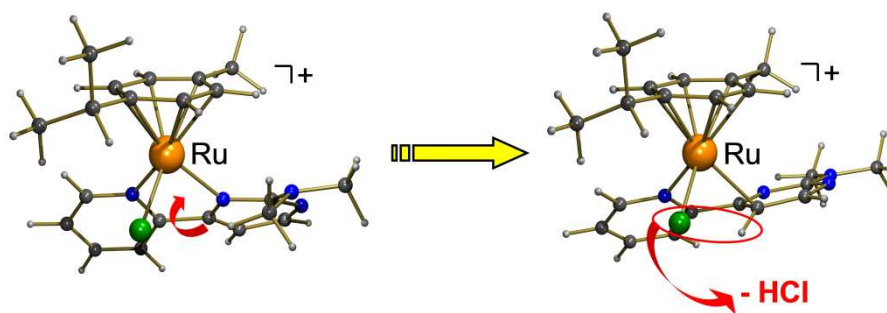

Figure 3. Representation of *N,N*- and *C,N*-coordination mode of (2-aminopyrimidinyl)pyridines towards Ru(II).

The next aim of my work was the synthesis and characterization of phosphanes ligands containing an aminopyrimidine group and their corresponding metal complexes. The NH_2 group of the aminopyrimidine is also a potential site for the introduction of a phosphine substituent leading to bidentate and tridentate ligands (**Scheme 9**). This type of ligands, are also matter of interest in the SFB/TRR-88 (3MET) at the TU Kaiserslautern.

14

Motivation

D = o-C$_5$H$_4$N, Ph
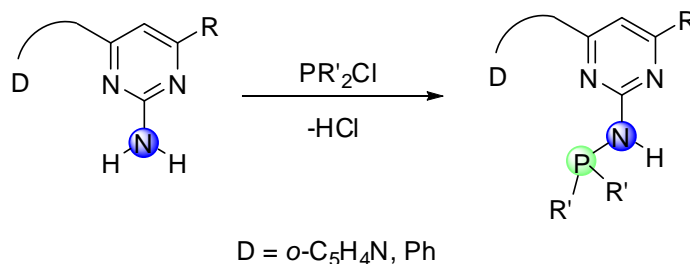
Scheme 9. Introducing a phosphine substituent at the amino group to obtain *PN* and *PNN* ligands.

Along Thiel's group efforts to develop greener synthetic pathways for organic transformations,[83,84,85,86,87,88,89] the next goal of this thesis was to synthesize mesoporous silica materials with immobilized palladium complexes of (2-aminopyrimidinyl)phosphines and study their application as catalysts. To achieve this goal, following tasks will be required (**Scheme 10**):

➢ Synthesis of functionalized (2-aminopyrimidinyl)phosphine ligands by using a suitable spacer.

➢ Synthesis of the corresponding palladium complexes.

➢ Covalent immobilization of the resulting complexes on supports.

➢ Investigation of the immobilized catalysts in liquid phase reactions and studying their catalytic activity, selectivity and reusability.

Motivation
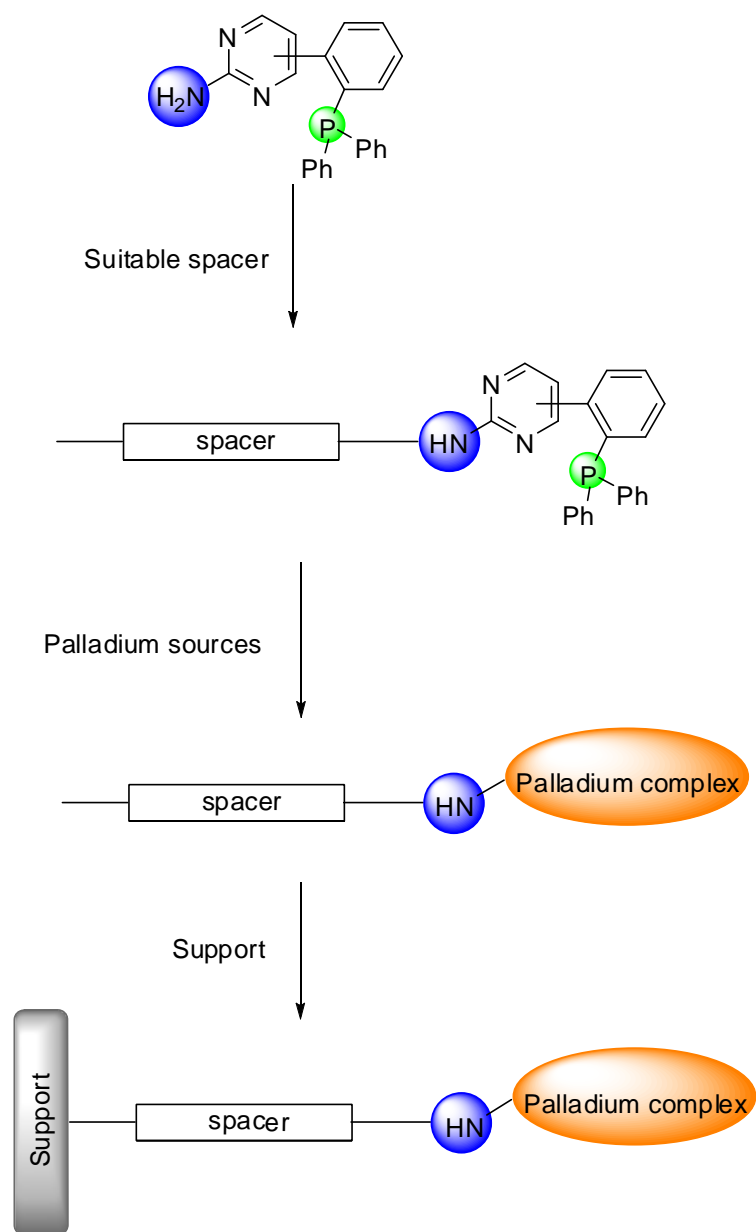
Scheme 10. Immobilization of the palladium complexes via spacer on the support.

Results and Discussion

3. Results and Discussion

3.1. Ligand Synthesis

#### 3.1.1. Synthesis of the Pyrimidinyl Functionalized Phosphine Ligands

3.1.1.1. Large-scale Synthesis of the Precursors

Thiel's group was interested in the field of functionalized phosphine ligands during the last decade. The first triphenylphosphine ligands bearing pyrazoles were obtained by ring closure of [2- or 3-(3-dimethylamino-1-oxoprop-2-en-yl)phenyl]diphenylphosphine **1a,b** with hydrazine.[90]

The synthetic route that led to the target precursors **1a,b** was developed in Thiel's group following a stepwise synthetic route: Starting from 3-bromoacetophenone an overall yield about 50% was obtained (route 1, **Scheme 11**). For this strategy an acetyl group attached to at least one of the phenyl rings of the PPh$_3$ backbone is required. This allows condensing the aromatic acyl derivatives with *N*,*N*-dimethylformamide dimethyl acetale results in the formation of **1**. As shown in **Scheme 11** this classical synthetic route includes five steps containing a protection/deprotection sequence since bromoacetophenone must be protected before reacting it with magnesium.

Following efforts in Thiel's group resulted in developing a short and simple synthetic pathway to obtain precursors **1a** and **1c** (route 2, **Scheme 11**).[45,46] By reacting 2- or 4-fluoroacetophenone with DMFDMA, the acyl group is converted to a 3-dimethylamino-2-propen-1-onyl unit. These products can be coupled with diphenyl(trimethylsilyl)phosphine in the presence of CsF as catalyst to give **1a**, **1c**.

Results and Discussion
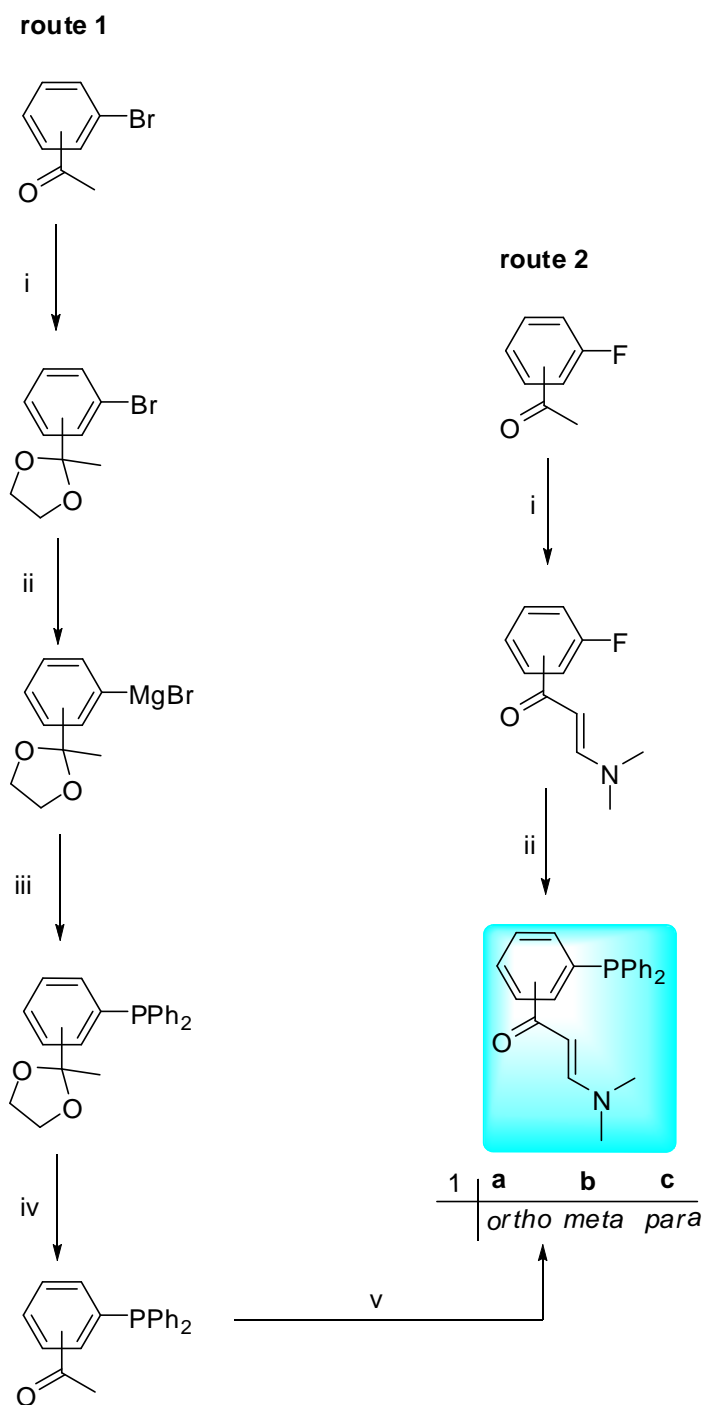
Scheme 11. Route 1, i) TsOH, HOCH$_2$CH$_2$OH, toluene, reflux; ii) Mg, thf, reflux; iii) PPh$_2$Cl, thf, reflux; iv) TsOH, H$_2$O, thf, reflux; v) HC(OMe)$_2$ -NMe$_2$, reflux. Route 2, i) HC(OMe)$_2$-NMe$_2$, reflux; ii) CsF, PPhSi(Me)$_3$, DMF.

Route 2 offers several advantages over route 1:

- The number of synthetic steps is reduced while the chemical yield is increased.

18

Results and Discussion

- A broad variety of interesting functionalized aryl phosphines are accessible in this way.

- The reaction can be performed under very mild reaction conditions.

- Separation processes and purification of intermediates are avoided.

- A minimum amount of organic solvent is used and no salt is formed.

- The work-up process is simple.

Setting this synthetic route up from a mg scale to a kg scale was a part of my project which was done in cooperation with Daniel Dehe from Thiel's group (**Figure 4**). Approximately 1 kg of the coupling product **1c** could be obtained based on around only 600 ml of DMF as a solvent, 95 g of CsF, 600 g of (*E*)-3-(*N,N*-dimethylamino)-1-(4'-fluorophenyl)prop-2-en-1-one and 790 ml of diphenyl(trimethylsilyl)phosphine which was added dropwise via the dropping funnel by using a 4 liter glass reactor sealed with a rubber stopper, equipped with a heating jacket and nitrogen inlet and a mechanical stirrer.[47] The toxic by-product FSiMe$_3$ with boiling point of 16 °C was collected by using a cold trap. Changes in the color intensity were used to monitor the reaction: The reaction is completed when the intense red-orange color of the phosphide anions disappear leading to a bright red solution. The mixture was diluted with H$_2$O and CH$_2$Cl$_2$, the layers were separated and the product was obtained from the organic layer.

Results and Discussion
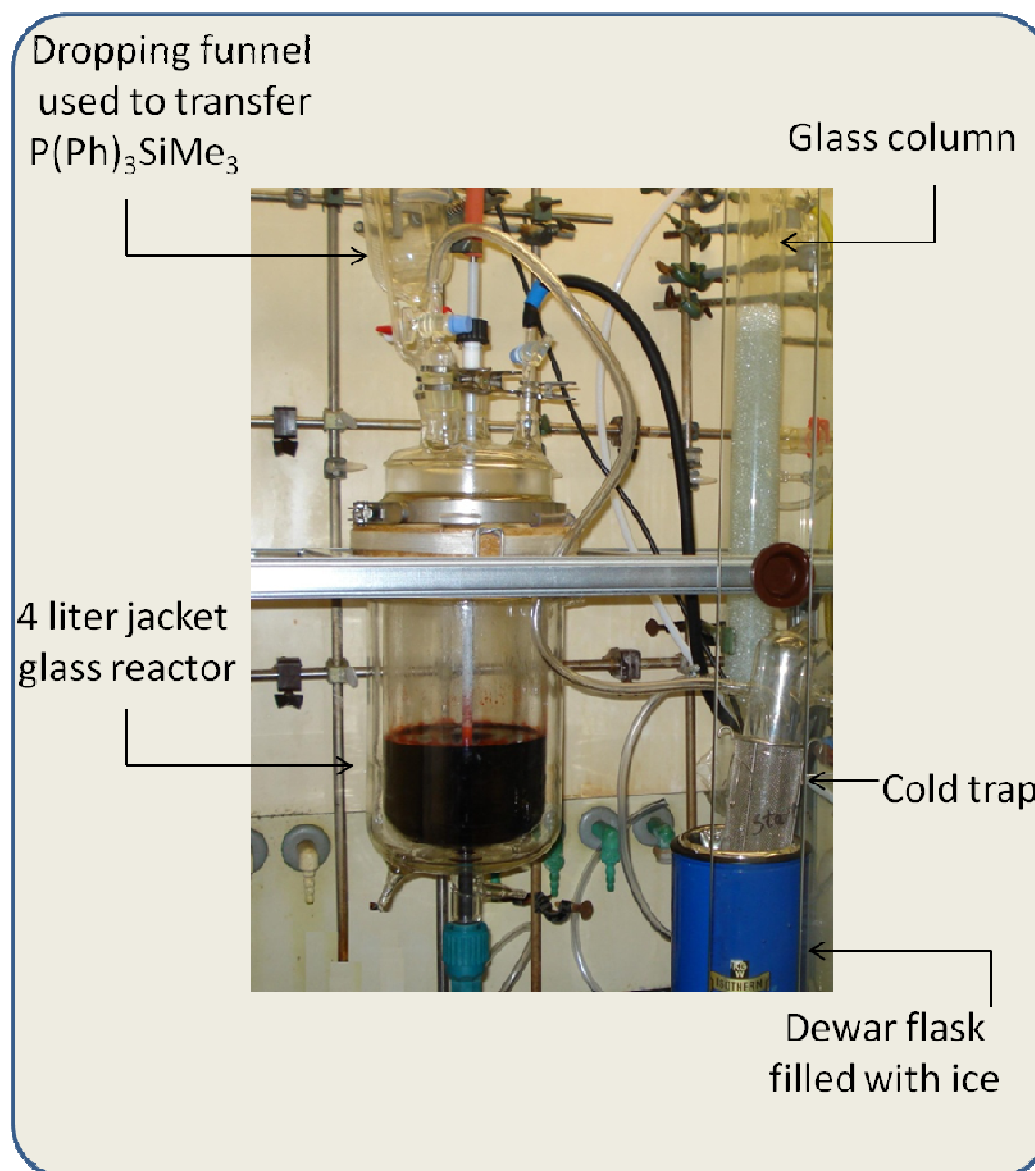
Figure 4. The scale-up platform for the precursors.

3.1.1.2. *Synthesis of Para Substituted 2-aminopyrimidinyl-functionalized Phosphines*

The ring closure of **1c** with an excess of guanidinium salts under a nitrogen atmosphere in presence of KOH in EtOH under reflux conditions resulted in the formation of a 4-(2-amino)pyrimidinyl ring in the para position to the phosphine site (**2a,b**). After removing the solvent, the products **2a,b** were obtained as colorless to pale yellow solids in good yields by recrystallization from ethanol (**Scheme 12**). Synthesis of **2a** by this method was reported previously in Thiel's group.[91] However, there is no report on solvent free reaction of such

20

Results and Discussion

precursors with guanidinium salts. Hence fusing just the guanidinium salts and **1c** was examined. The mixture of **1c** and the corresponding guanidinium carbonate was heated to about 220 °C until all dimethylamine was released. After cooling to RT, the residue was dissolved in CH_2Cl_2, solids were separated by filtration, and the solvent was removed to afford **2a**. However, fusing 1-ethylguanidiumsulfat with **1c** in the aforementioned condition failed. The ring closure of **1c** also is possible with hydrazine monohydrate and resulted in **3**, which was reported in Thiel's group earlier.[46] This series of ligands were synthesized in a scale of about 100 g.
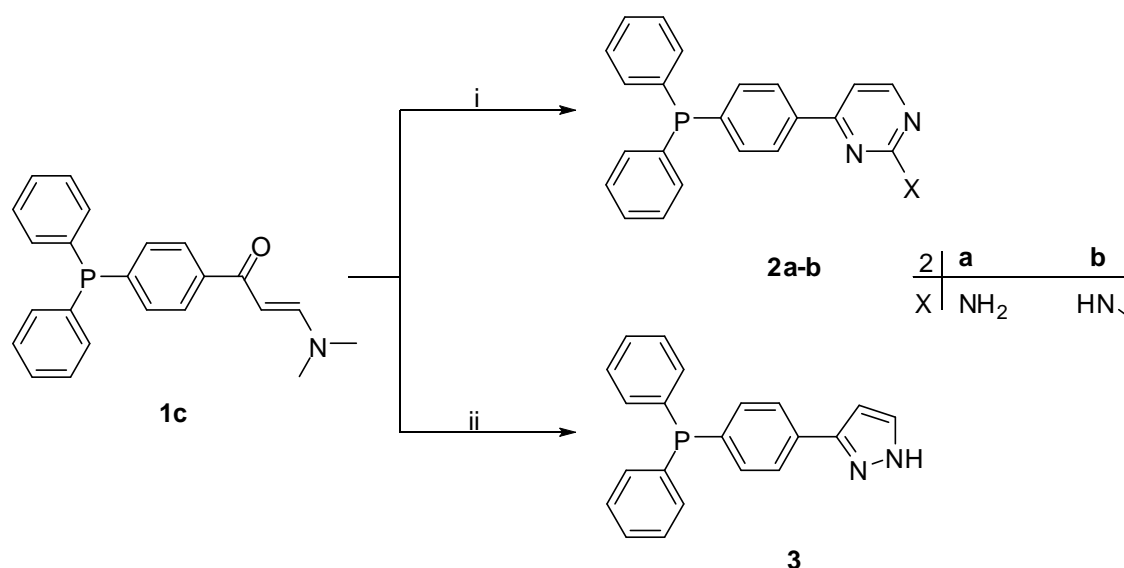
Scheme 12. Synthesis of **2a,b** and 3; i). $[XC(NH_2)_2]_2(CO_3)$, KOH, EtOH, reflux 12 h; ii) $N_2H_4.H_2O$, EtOH, reflux.

The ^1H NMR spectra of **2a,b** show slight differences in chemical shifts of phenylpyrimidinyl hydrogen e.g. in **2a,** protons in the 5- and 6-position of the pyrimidine ring appeared as two doublets at about 7.01 and 8.35, respectively, with a coupling constant of $^3J_{HH}$ = 5.2 Hz. Introducing an electron donating ethyl group on **2b,** these signals of protons shifted slightly to higher field and appear at about 6.94 and 8.32 ppm, respectively. For ligand **3,**

Results and Discussion

containing a pyrazolyl ring, the resonances of the hydrogen atoms at the 3- and 4-positions of the pyrazole ring appear as two doublets at about 6.61 and 7.59 ppm, respectively, which are clearly separated from the other aromatic resonances. Shifts of phosphorus atoms of **2a,b** and **3** in the ^{31}P NMR spectra show that the different functions have only a slight influence on the electron density on the phosphorus atom in comparison to the PPh$_3$ (**Figure 5**).
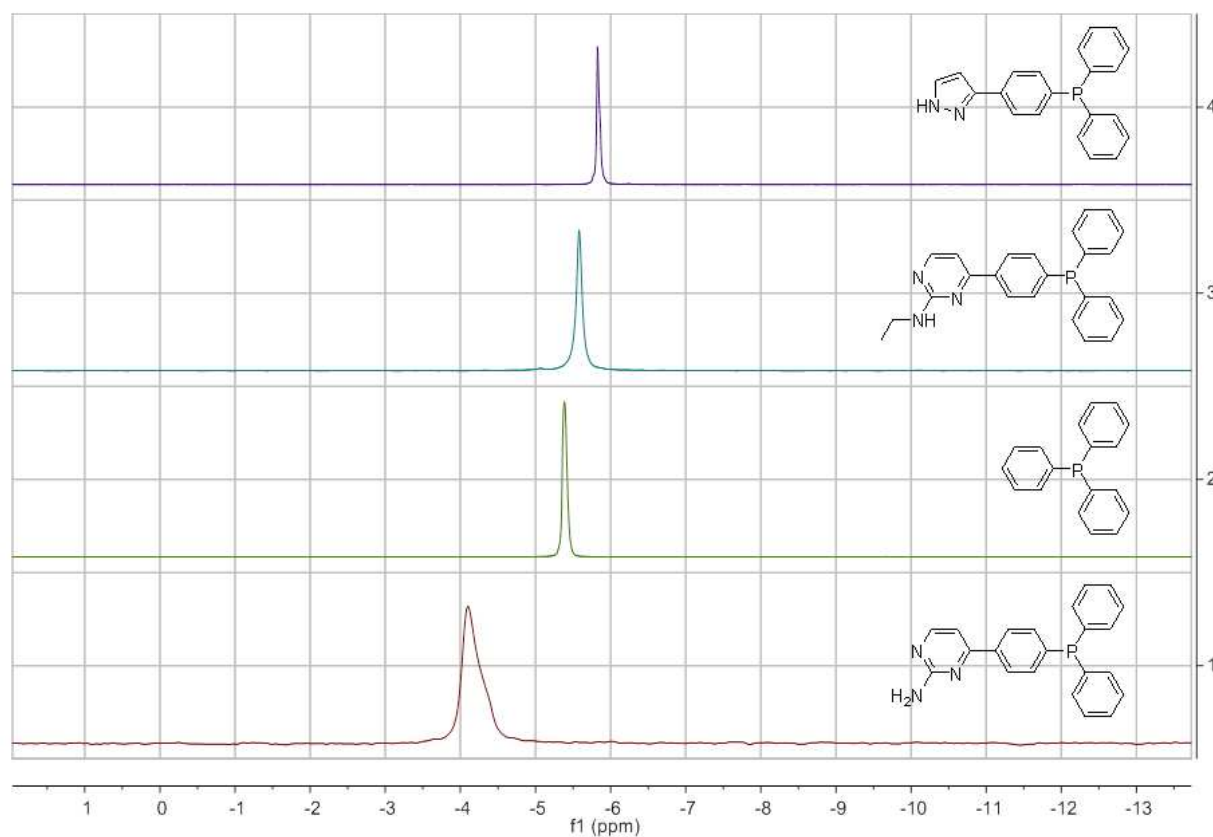

Figure 5. ^{31}P NMR spectra of **2a-b**, **3** and PPh$_3$.

3.1.1.3. *Synthesis of Ortho Substituted 2-aminopyrimidinyl-functionalized phosphines*

Phosphine ligands bearing groups on the *ortho* position that are able to coordinate can be used as chelating ligands. Functional groups in the *ortho* position containing nitrogen, oxygen, sulfur, and also in some case carbenes have been introduced as *PN*, *PO*, *PC* ligands in

Results and Discussion

coordination chemistry as well as in catalysis. It was obvious that with precursor **1a** it will be possible to open up a route to obtain PX (X = N, O, S or C) chelating ligands.

Treatment of precursor **1a** under an atmosphere of nitrogen with an excess of the appropriate guanidinium salt in ethanol under basic conditions gives the 2-aminopyrimidinyl-functionalized phosphines **4a–j** in good yields (**Scheme 13**).


4	a	b	c	d	e	f	g
X	NH$_2$	HN	HN(CH$_2$)$_7$	N	N	N	N

4	h	i	j
X	NH	NH	NH
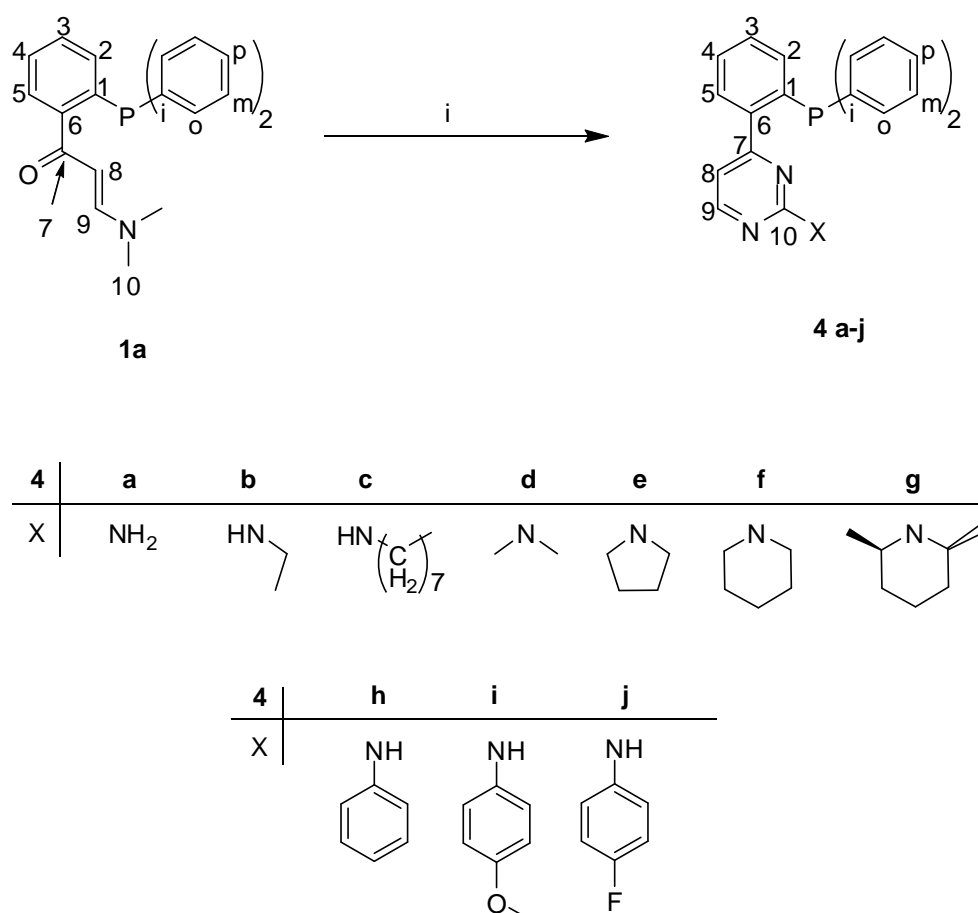
Scheme 13. [XC(NH$_2$)$_2$]$_2$(SO$_4$), KOH, EtOH, reflux 24-48 h.

With bulkier guanidinium salts (e. g. for **4g** and **4c**) the reaction time has to be prolonged to 30-48h in comparison to **4a,b** and **4d-f** for which the reaction was completed in 20 h. With aromatic guanidinium salts possessing an electron withdrawing amino group the reaction time had to be increased too (48 h for **4h-j**). The differences in the reaction times

Results and Discussion

occur probably for two reasons: first, according to the ring closure mechanism (**Scheme 14**), guanidinium salts with sterically hindered substrates will require a longer time for ring closure. Second, activation of inactive aromatic guanidinium salts under basic condition is harder than alkyl based guanidinium salts.
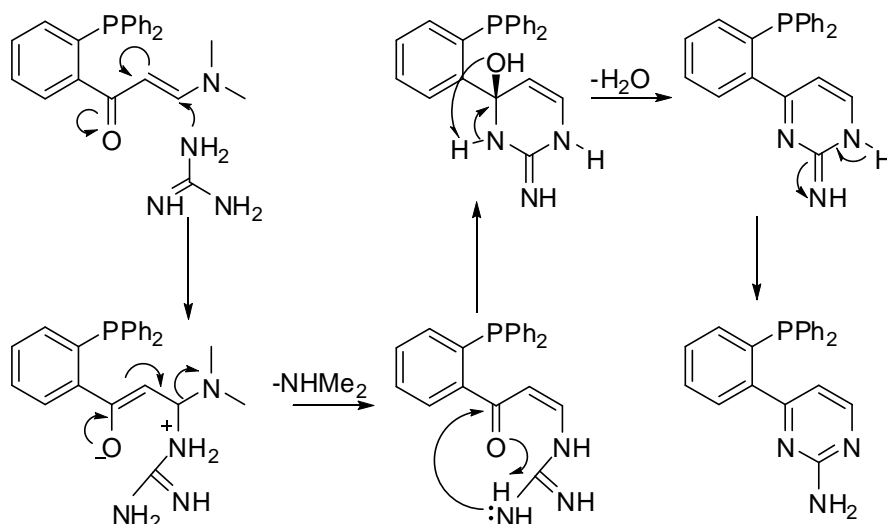
Scheme 14. Mechanism for the ring closure with precursor **1a**.

Single crystals of **4a** and **4f** suitable for X-ray structural analysis were obtained from ethanol. The molecular structures, selected bond lengths and angels are presented in **Figure 6**. Whereas ligand **4f** shows the typical behavior of organic compounds with weak intermolecular interactions, compound **4a** exhibits strong intermolecular hydrogen bonds between the amino group and the nitrogen atoms of the pyrimidine ring leading to a 1D "zig-zag" arrangement.

Results and Discussion
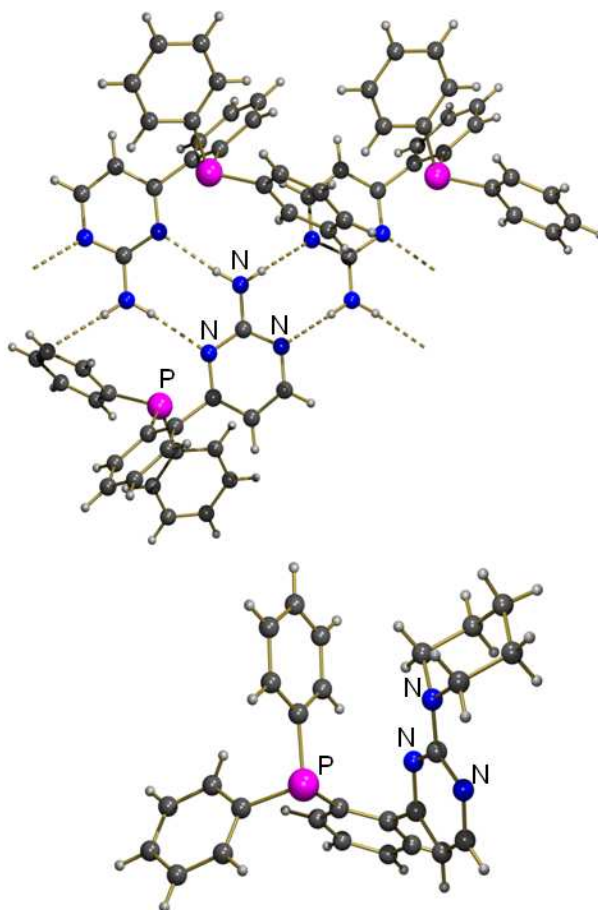
Figure 6. Molecular structure of **4a** (top) and **4f** (bottom) in the solid state.

Characteristic bond lengths [Å] and angles [°] for **4a** : C1–P1 1.8400(15), C6–C7 1.492(2), C7–C8 1.388(2), C8–C9 1.379(2), C9–N2 1.327(2), N2–C10 1.356519, C10–N1 1.3515(18), N1–C7 1.3442(19), C10–N3 1.3425(19), C6–C1–P1 122.66(11), C1–C6–C7 122.02(13), N1–C7–C6 118.68(12), N1–C10–N3 118.37(13), C5–C6–C7–C8 –67.07, P1–C1–C6–C7 1.19.

Characteristic bond lengths [Å] and angles [°] for **4f**: C1–P1 1.8546(17), C6–C7 1.488(2), C7–C8 1.390(2), C8–C9 1.379(3), C9–N2 1.329(2), N2–C10 1.353(2), C10–N1 1.353(2), N1–C7 1.335(2), C10–N3 1.362(2), C6–C1–P1 118.75(12), C1–C6–C7 120.61(15), N1–C7–C6 116.95(14), N1–C10–N3 117.42(15), C5–C6–C7–C8 –52.48, P1–C1–C6–C7 –7.21.

^{1}H NMR and ^{31}P NMR data of **4a-j** are summarized in **Table 2**. The resonances of the *ortho* isomers **4a,b** are shifted to higher field in comparison to corresponding *para* isomers

Results and Discussion

2a,b. The ^{31}P NMR resonances of the ligands are found in the range of –12.05 to –14.35 ppm. The nature of the substituents has just a little influence on the phosphorous center. As shown in **Figure 7**, the resonances of the protons of **4g** are the mostly influenced and are shifted to higher field compared to **4a**, indicating an increase in electron density on the pyrimidinyl ring, which is also reflected in the [13]P NMR resonance.

Table 2. ^{1}H NMR and ^{31}P NMR data of ligands **4a-4j**.

Ligand	H-2	H-3	H-4	H-5	H-8	H-9	[31]P
4a	6.98	7.38	7.47	7.63	6.67	8.16	–12.05
4b	6.98	7.39	7.49	7.61	6.68	8.21	–12.05
4c	6.98	7.37	7.48	7.60	6.66	8.20	–12.03
4d	6.98	7.38	7.48	7.61	6.71	8.31	–12.04
4e	6.97	7.39	7.49	7.63	6.73	8.31	–12.08
4f	6.99	7.39	7.49	7.62	6.75	8.33	–12.23
4g	7.01	7.32-7.39	7.45-7.53	7.45-7.53	6.25	7.99	–14.35

Results and Discussion
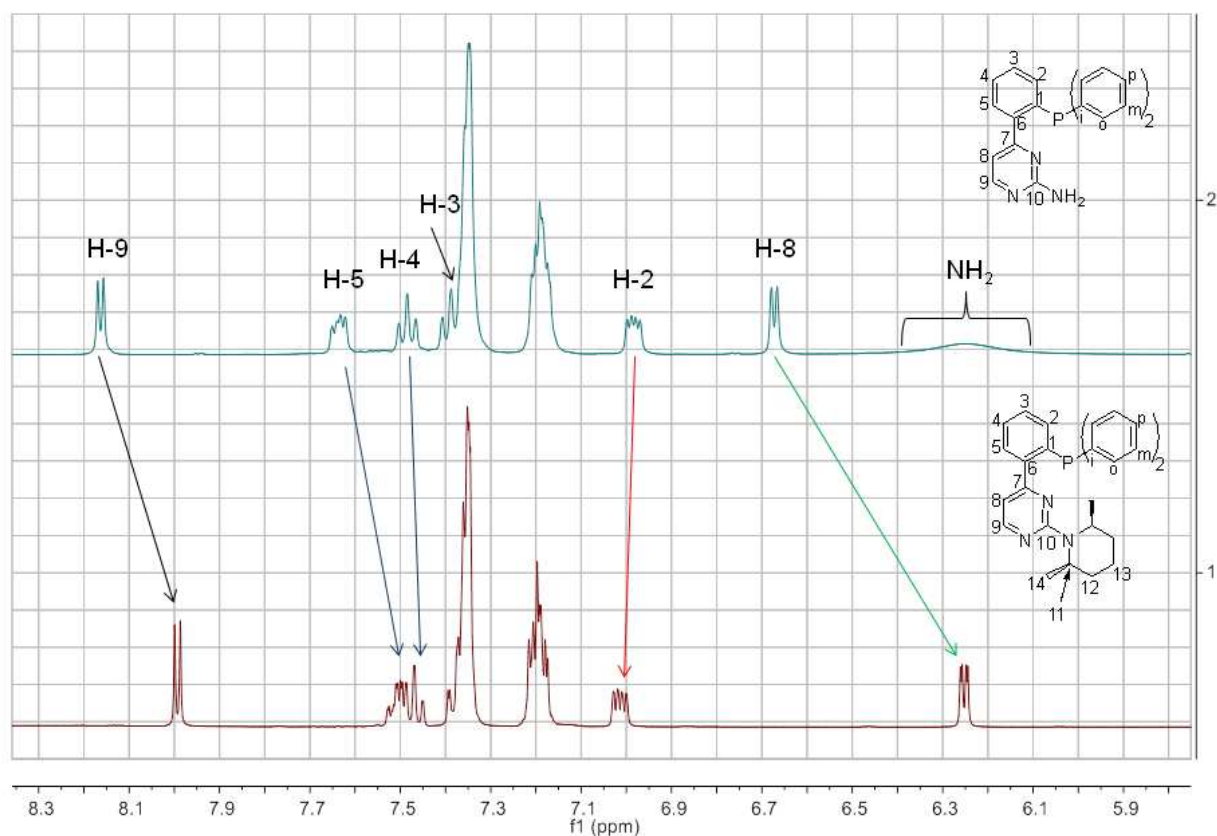
Figure 7. ^{1}H NMR spectra of **4a** (up) and **4g** (bottom) in aromatic region.

Functionalization of the phenyl ring in the *para* position has almost no effect on the resonances of the H-2, H-3, H-4 and H-5 protons of ligands **4h-4j** in ^{1}H NMR spectrum. However, H-8, H-9, H-12 and H-13 have shifted to higher field for **4j** which is functionalized by an electron donating methoxy group. In contrast, functionalizing with an electron withdrawing fluoride group has no effect on the proton's resonances. As expected, the protons of the amino group appear at about 9.37 ppm for **4h**, 9.49 ppm for **4i** and at 9.18 ppm for **4j** (**Table 3**).
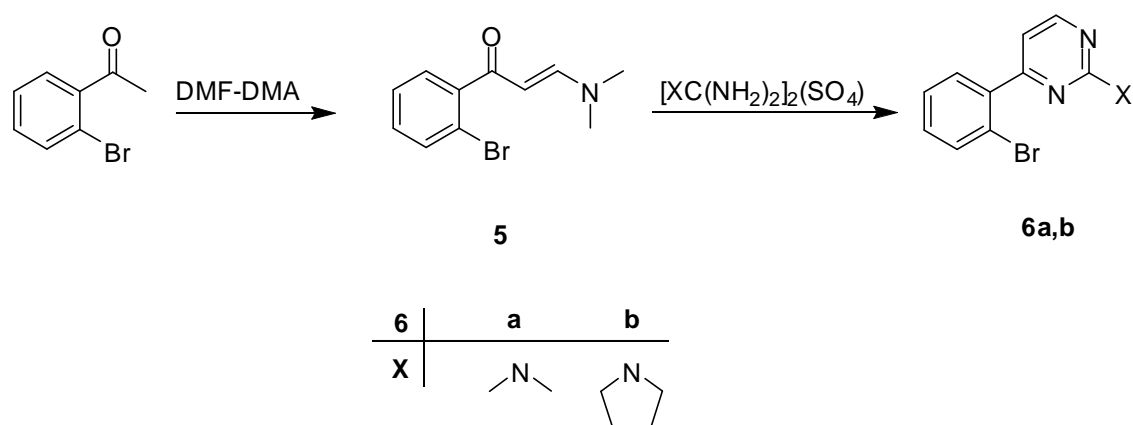
Results and Discussion

Table 3. ^{1}H NMR and ^{31}P NMR data of ligands **4h-4j**.

Ligand↓	H-8	H-9	H-12	H-13	H-14	N-H	[31]P
4h	6.67	8.38	7.71	7.15-7.24	6.90	9.37	–12.82
4i	6.80	8.37	7.70	6.96-7.07	.....	9.49	–12.84
4j	6.71-6.78	8.33	7.55-7.61	6.71-6.79	.....	9.18	–13.00

3.1.1.4.   Synthesis of the Ortho Substituted Bulky Phosphines Based on a 2-Aminopyrimidinyl Group

Starting from 2-bromoacetophenone, 4-(2-bromophenyl)-*N,N*-dialkylpyrimidin-2-amine **6a,b** can be synthesized in three steps. In the first step, refluxing 2-bromoacetophenone and *N,N*-dimethylformamide dimethylacetal for 4 h gave almost quantitatively (*E*)-1-(2-bromophenyl)-3-(dimethylamino)prop-2-en-1-one. Then, a mixture of intermediate **5** and the proper guanidinium sulfate was refluxed for 8 h in the presence of KOH in ethanol. After evaporating the solvent, the product was extracted using dichloromethane (**Scheme 15**). The material was recrystallized from an ethanol-ether solution.


Scheme 15. Synthesis of the 4-(2-bromophenyl)-*N,N*-dialkylpyrimidin-2-amines **6a,b.**

The ^{1}H NMR spectrum of **6a** shows a singlet at about 3.24 ppm which can be assigned

Results and Discussion

to the $N(CH_3)_2$ group and two doublets at about 8.38 and 6.76 ppm with $^3J_{HH} = 5.0$ Hz were assigned to the pyrimidine hydrogen atoms. Slight shifts of the resonances of the protons of **6a** in comparison to **6b** (**Figure 8**) can be explained by the better electron donating property of pyrrolidin compared to dimethylamine. In the ^{13}C NMR spectra, the carbon resonances of **6b** are slightly shifted to higher field in comparison to **6a**, a significant change appeared for the carbon atom in the 1-position of the pyrimidine ring (162.3 ppm and 160.3 ppm for **6a** and **6b**, respectively).
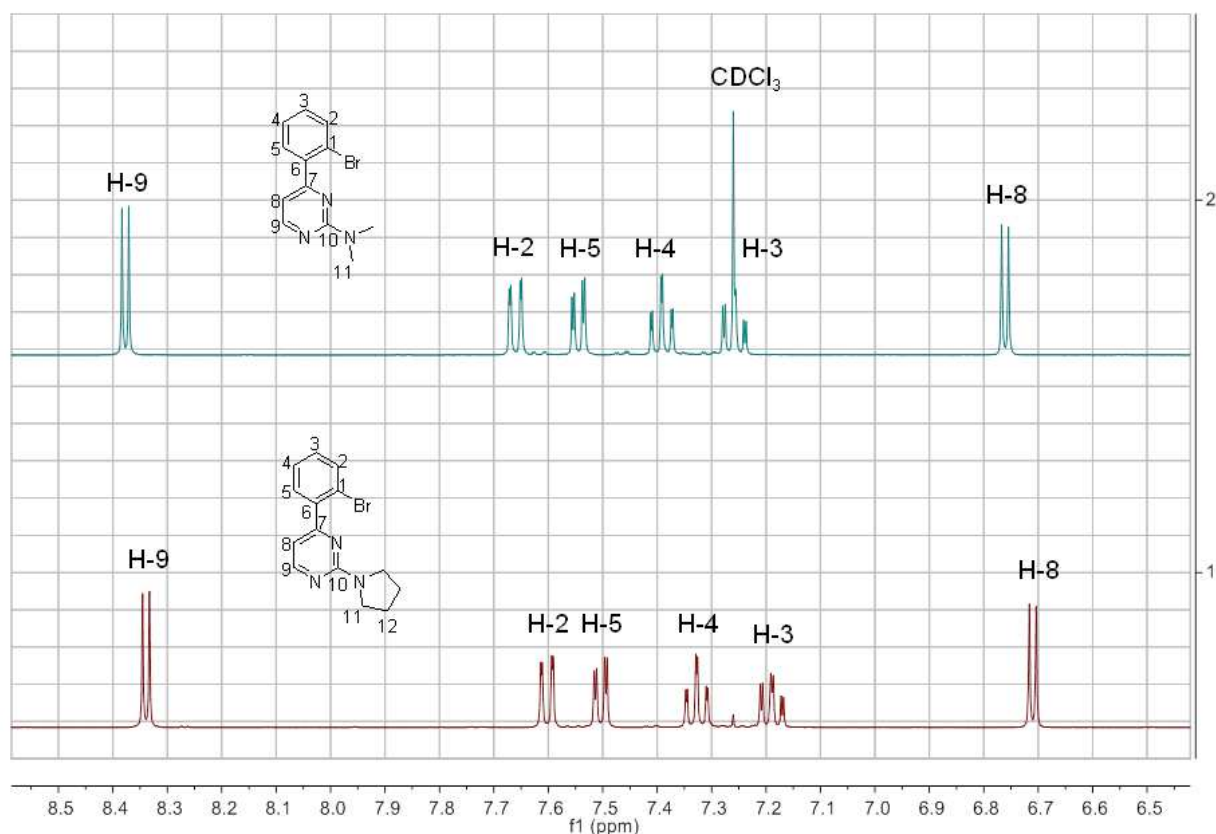

Figure 8. ^1H NMR spectra of **6a** (up) and **6b** (bottom) in aromatic region.

The syntheses of the phosphine ligands **7a-c** were carried out by lithiation of **6a,b** in dry THF at –78 °C and adding the appropriate chlorophosphine. The synthetic route is presented in **Scheme 16**. The reaction conditions were optimized with respect to reaction time,

Results and Discussion

temperatures, stoichiometry of the reactants and the best condition turned out as follows: under a nitrogen atmosphere *n*-butyllithium was added dropwise via syringe over 15 min to a solution of **6a,b** in THF at –78 °C. The resulting mixture was stirred at –78 °C for 60 min for complete lithiation. In the next step, the chlorodialkylphosphine was added dropwise via a syringe. The resulting mixture was stirred at –78 °C for 1 h, then allowed to slowly warm to room temperature. The reaction was monitored by ^{1}H NMR which indicates complete consumption of **6a,b**. After filtration, the solvent was evaporated under reduced pressure to give a pale orange solid.
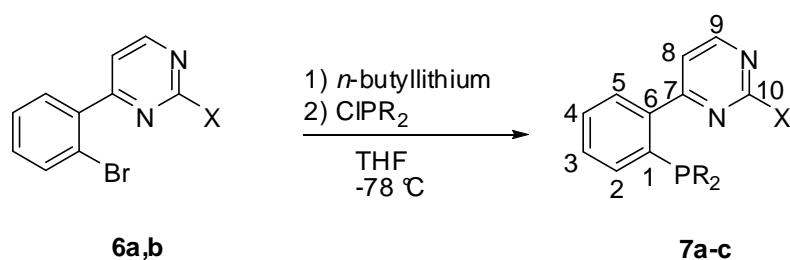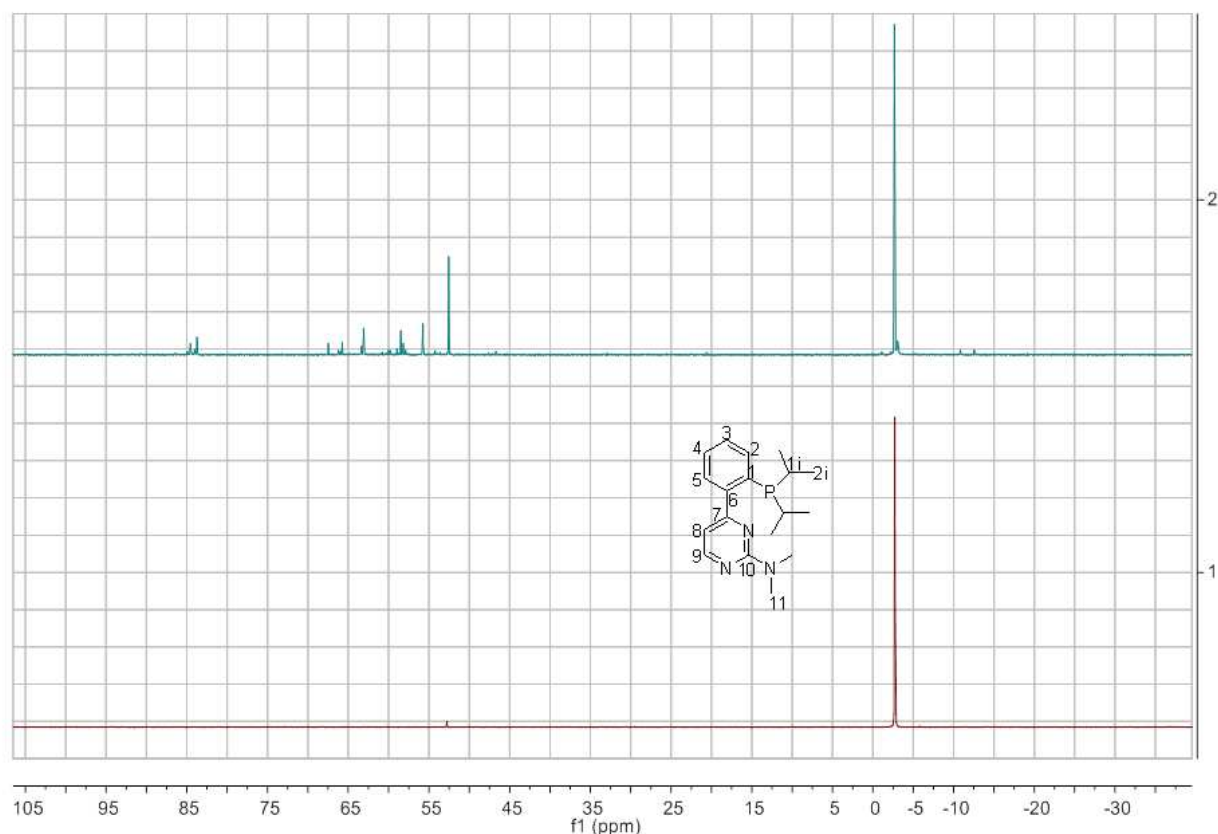

7	a	b	c
X			
R	isopropyl	cyclohexyl	cyclohexyl

Scheme 16. Synthesis of *ortho* substituted bulky phosphines.

Ligands **7a-c** could not be purified by recrystallization. Finally the products were purified by flash chromatography using CombiFlash® Companion personal flash chromatography apparatus from Isco Inc. flash (**Figure 9**).

Results and Discussion

**Figure 9**. ^{31}P NMR spectra of **7a** before (top) and after (bottom) purification.

The NMR data of **7a-c** are summarized in **Table 4**. Significant differences are found in the ^{31}P NMR spectra, showing the phosphorous resonance in **7b,c** being shifted by about 10 ppm to higher field by replacing the isopropyl against a cyclohexyl group. Moreover, comparing the chemical shifts in **7b** and **7c**, it is obvious that functionalizing the pyrimidine ring does not have a big electronic influence. Exemplarily the ^{1}H NMR and ^{13}C NMR spectra of ligand **7a** are shown in **Figure 10** and **Figure 11**.

Results and Discussion

Table 4. ^{1}H NMR, ^{13}C NMR and ^{31}P NMR data for ligands 7a-c.

| Ligand	7a	7b	7c
C-1	134.9	134.2	134.2
H-2	7.60	7.60	7.60
C-2	132.64	133.0	133.0
H-3	7.35-7.42	7.33-7.42	7.34-7.41
C-3	128.6	128.6	128.6
H-4	7.35-7.42	7.33-7.42	7.34-7.41
C-4	129.3	129.3	129.3
H-5	7.35-7.42	7.33-7.42	7.34-7.41
C-5	127.9	127.9	127.8
C-6	148.1	148.5	148.5
C-7	168.9	169.0	169.0
H-8	6.59	6.54	6.54
C-8	110.8	110.8	110.9
H-9	8.31	8.30	8.30
C-9	156.5	156.3	156.6
C-10	161.8	161.8	160.2
[31]P	–2.71	–11.04	–10.99

Results and Discussion
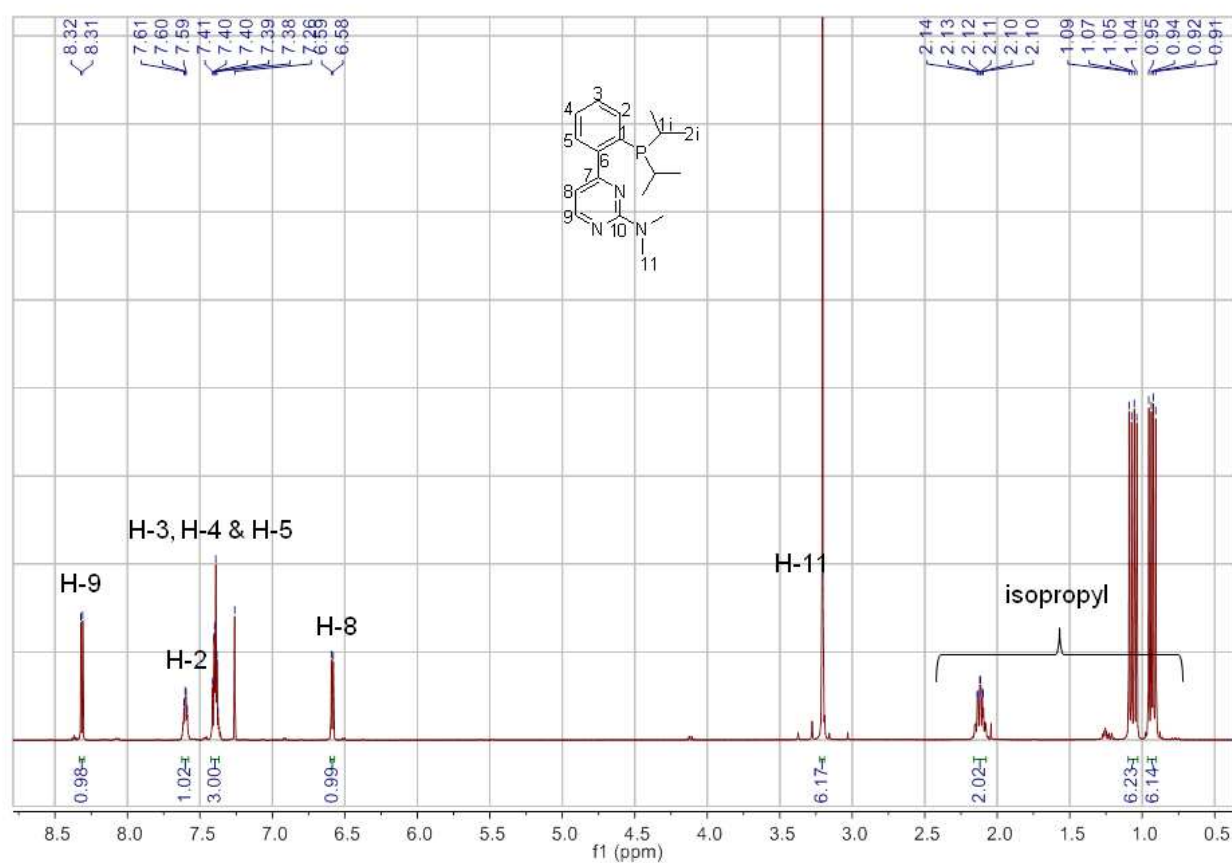
Figure 10. ^{1}H NMR spectrum of ligand **7a**.

Results and Discussion
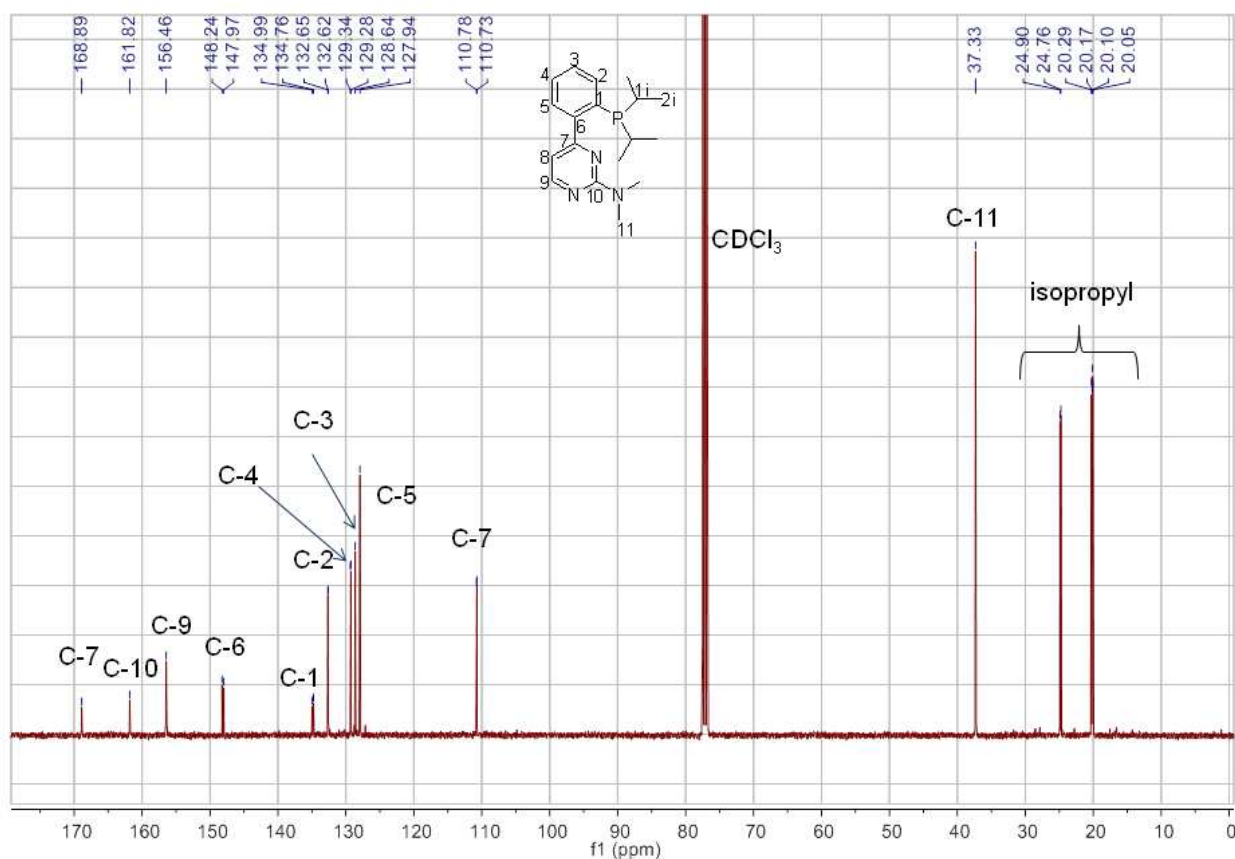
Figure 11. ^{13}C NMR spectrum of ligand **7a**.

The synthesis of [2-(4-(2-pyrrolidino)pyrimidinyl)phenyl]di(*p*-tolyl)phosphine **7d** was carried out as described for **7a-c** (**Scheme 17**).
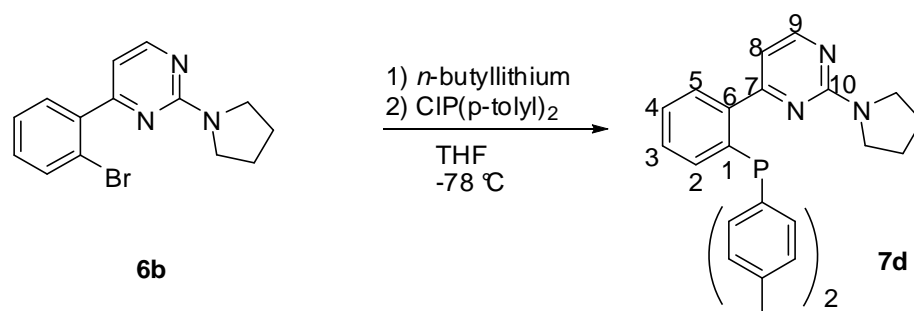

Scheme 17. Synthesis of [2-(4-(2-pyrrolidino)pyrimidinyl)phenyl]di(*p*-tolyl)phosphine.

The ^{31}P NMR resonance of **7d** in DMSO-d_6 is observed at about –13.76 ppm which is slightly shifted to the higher field in comparison to the **4e** (–12.8 ppm) and **7c** (–11.86 ppm)

34

Results and Discussion

and, as it is shown in **Figure 12**, changing the phosphine moiety of the ligands **4d**, **7c** and **7d**, has no significance effect on the ^{1}H NMR shifts.
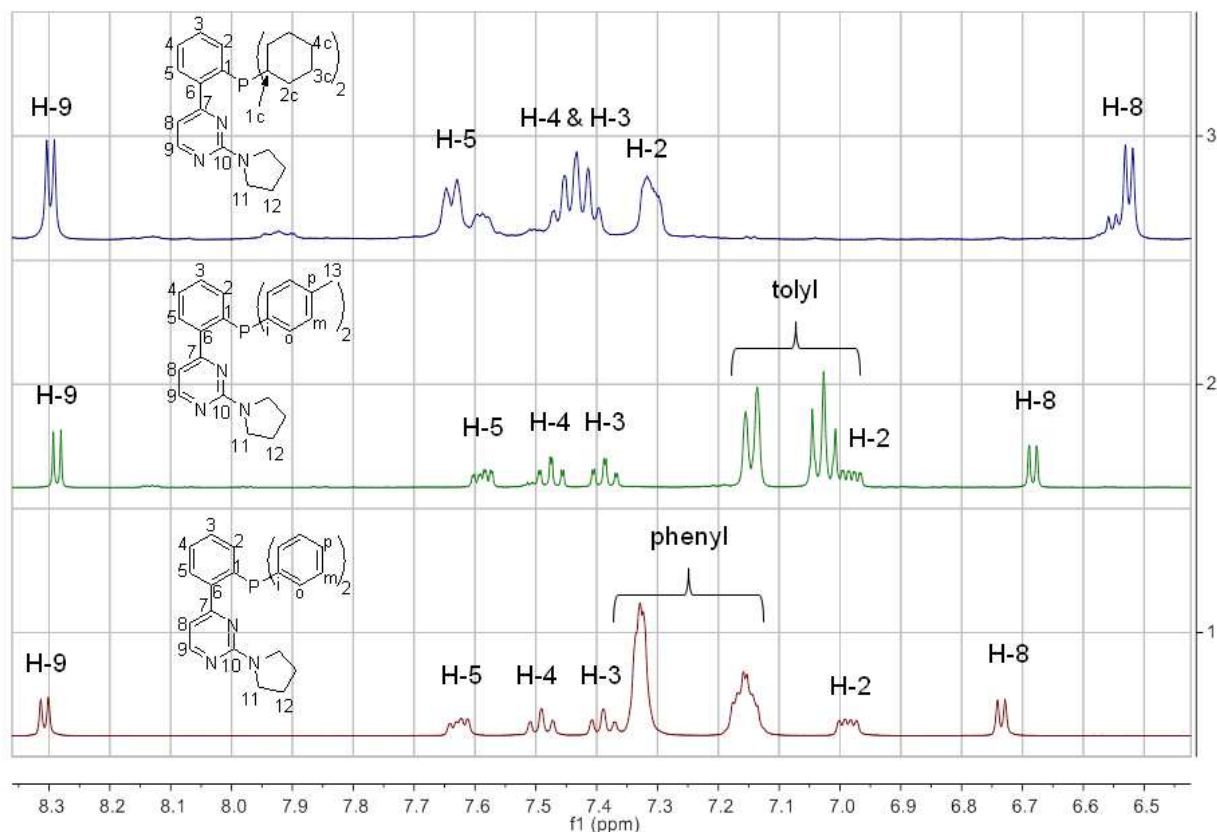
Figure 12. ^{1}H NMR spectra of ligands **4e** (bottom), **7d** (middle) and **7c** (top).

3.1.2. Synthesis of Multidentate Ligands

3.1.2.1. Synthesis of the Precursors

The precursors were synthesized in three steps starting from acetophenone and 2-acetylpyridine (**Scheme 18**). The intermediates **8-10** were synthesized according to published methods.[92,93]

Acetophenone and 2- acetylpyridine are converted to **8** and **9** by refluxing in DMF-DMA. Intermediate **10** was obtained by aldol condensation of 2-acetylpyridine with

Results and Discussion

benzaldehyde. Compounds **8** and **9** were reacted with guanidinium nitrate in refluxing ethanol in presence of KOH as catalyst to give phenylpyrimidine **11a** and pyridylpyrimidine **11b** or, with thiourea under the same conditions, to give the pyridylpyrimidine thiolate **11d**. **11c** was synthesized in the same way by reacting of **10** with proper guanidinium nitrate.
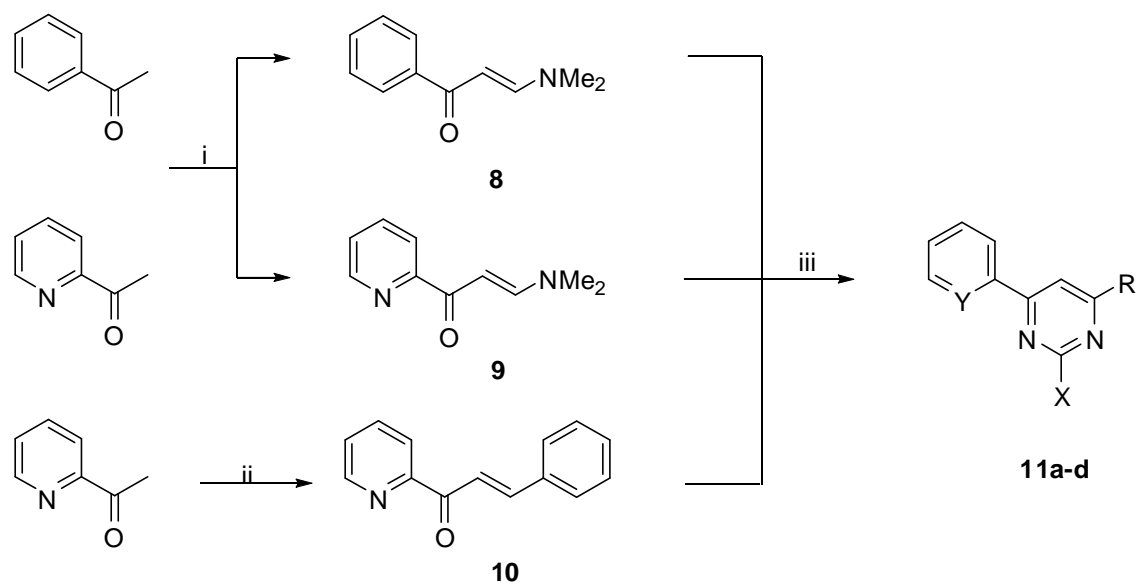

11	a	b	c	d
X	NH_2	NH_2	NH_2	SK
Y	CH	N	N	N
R	H	H	phenyl	H

Scheme 18. Synthesis of **8-10** and **11a-d**; i) $HC(NMe_2)(OMe)_2$, 4 h, reflux; ii) benzaldehyde, NMe_2, isopropanol, 12 h, reflux; iii) thiourea or guanidinium nitrate, KOH, Ethanol, 12-24 h, reflux.

36

Results and Discussion

3.1.2.2. Synthesis of the PNN and PN Ligands

Under an atmosphere of nitrogen, PPh_2Cl was added dropwise to a solution of **11a-d** in dry THF in presence of NEt_3 at 0 °C. The mixture was stirred for several hours at room temperature depending on the nature of precursors to give the ligands **12a-d**. Synthesis of **12d** was completed in 12 h however the other ligands needed longer reaction times, up to 3 days for **12c** (**Scheme 19**). Increasing the temperature to 50-80 °C did not increase the rate of reaction and in most cases no product was obtained. To increase the rate of reaction other solvents were also tested. Toluene as a common solvent for such reactions[94,95] could not increase the rate may be because of the poor solubility of the **11a-d** in toluene. The use of CH_2Cl_2 as an excellent solvent for **11a-d** decreased just a little bit the rate of reaction however the byproduct $NEt_3 \cdot HCl$ is soluble in CH_2Cl_2 which makes the work-up harder than with THF.
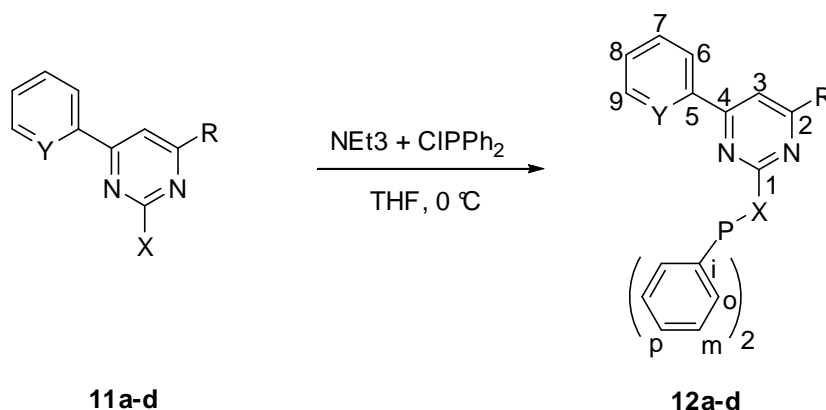

12	a	b	c	d
X	NH	NH	NH	S
Y	CH	N	N	N
R	H	H	phenyl	H

Scheme 19. Synthesis of **12a-d**.

Results and Discussion

For the synthesis of further electron rich and bulky phosphine ligands of this series, **11b,c** were reacted with chlorodiisopropylphosphine in a similar way. Various results were obtained due to different substituents on the 2-position of the pyrimidinyl ring. Reacting **11d** bearing a thiolate with P(*i*-Pr)$_2$Cl gave the expected ligand **13b**. In contrast, the desired reaction did not occur for **11b** bearing an amino group (**Scheme 20**). It means that only thiolate could serve as a nucleophile and attack to the phosphorous center. Attempts to obtain bulkier phosphines e.g. with cyclohexyl and *tert*-butyl groups instead of *iso*-propyl failed. The initial observation indicated that **13b** is significantly more moisture and air sensitive than **12a-d**, therefore glove box techniques are required.


11	b	d
X	NH$_2$	SK
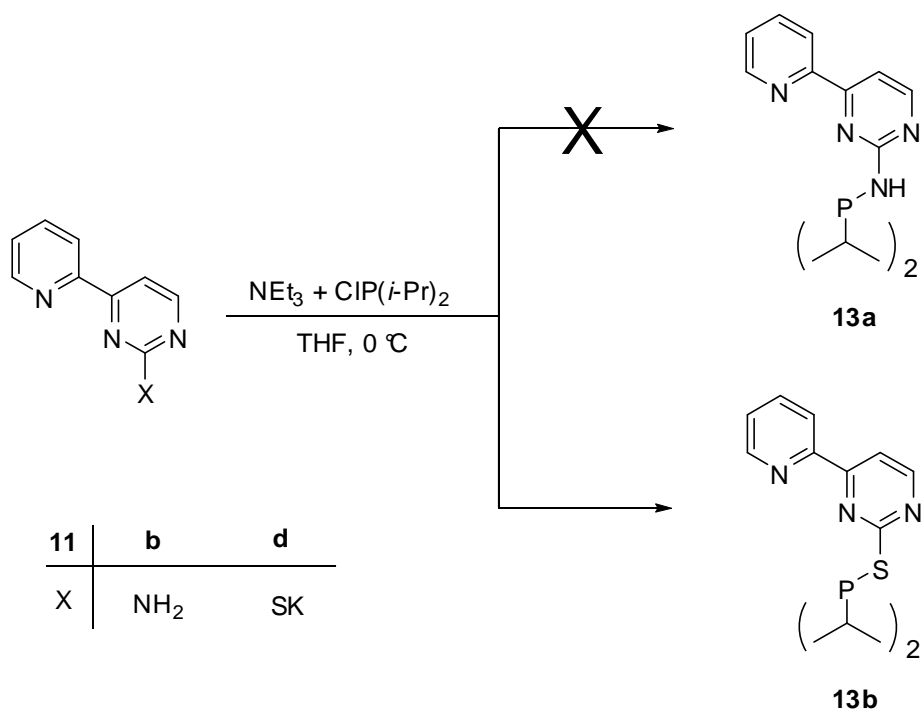
Scheme 20. Synthesis of **13b**.

The ^{31}P NMR spectra of ligands **12a-d** and **13b** are shown in **Figure 13**. Introduction of 2-pyridine (**12b**) against phenyl (**12a**) in the 4-position of the pyrimidyl ring or attaching a phenyl group at the 6-position of the pyrimidinyl ring (**12c**) did not affect the phosphorous chemical shift significantly. An upfield chemical shift observed for **12d** suggests an increase of

38

Results and Discussion

electron density of the phosphorus atom compared to **12b** due to the higher electronegativity of the nitrogen atom compared to sulfur. The chemical shifts are significantly different for **12d** and **13b.**
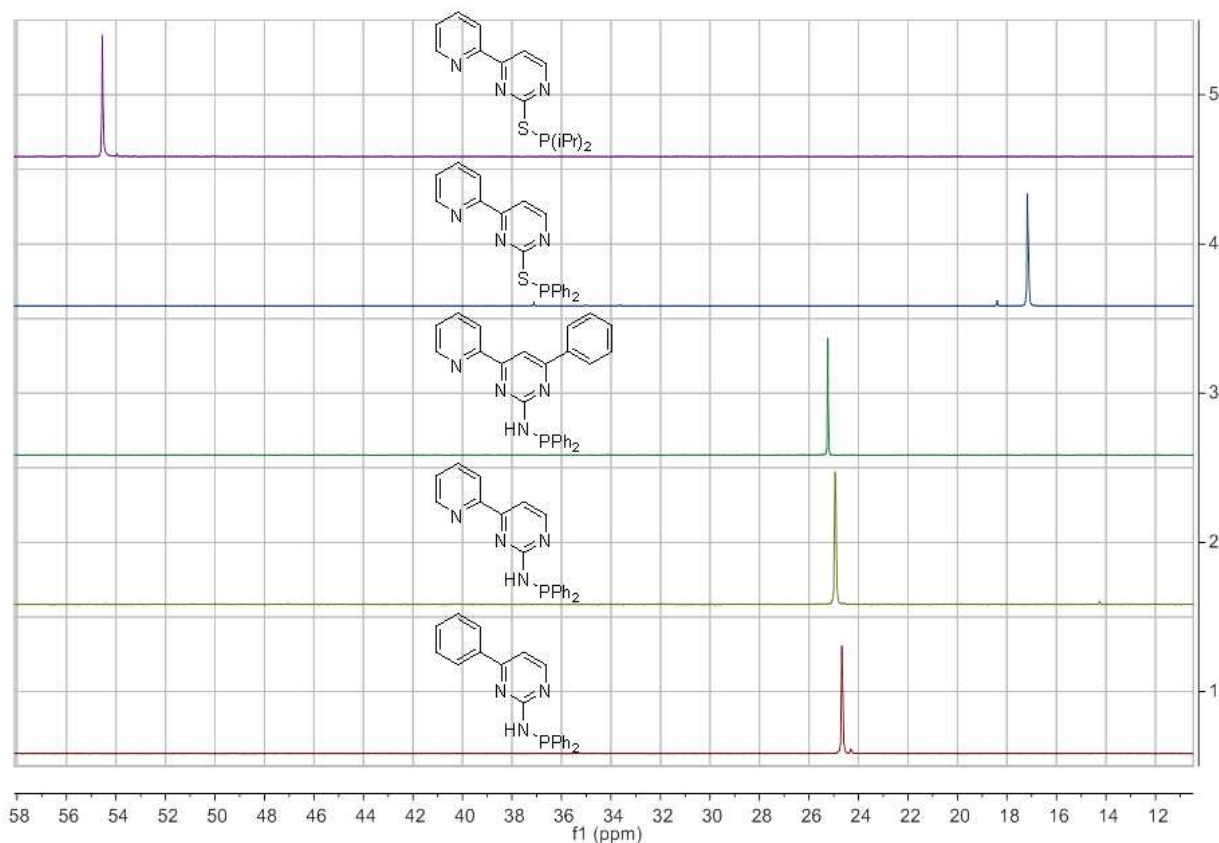
Figure 13. ^{31}P NMR spectra of ligands **12a-d and 13b** recorded in DMSO-d_6.

The ^{1}H NMR and ^{13}C NMR data for ligands **12a-b** and **13b** are listed in **Table 5**. Comparing the NMR data for **12a** and **12b** indicate that the resonances are shifted slightly downfield for **12b**, particularly the resonances of the C-5, C-3, C-2, H-3 and H-2. By introducing a phenyl group at the 6-position of the pyrimidyl ring in **12c**, the resonance of H-2 disappeared and H-3 appears as singlet at about 8.22 ppm and also the resonance of C-2 in ^{13}C NMR is shifted to lower field (**Figure 14**). The resonance of the N-H proton for **12b** is shifted to higher field compared to **12a**, which is in agreement with the increased shielding factor.

39

Results and Discussion
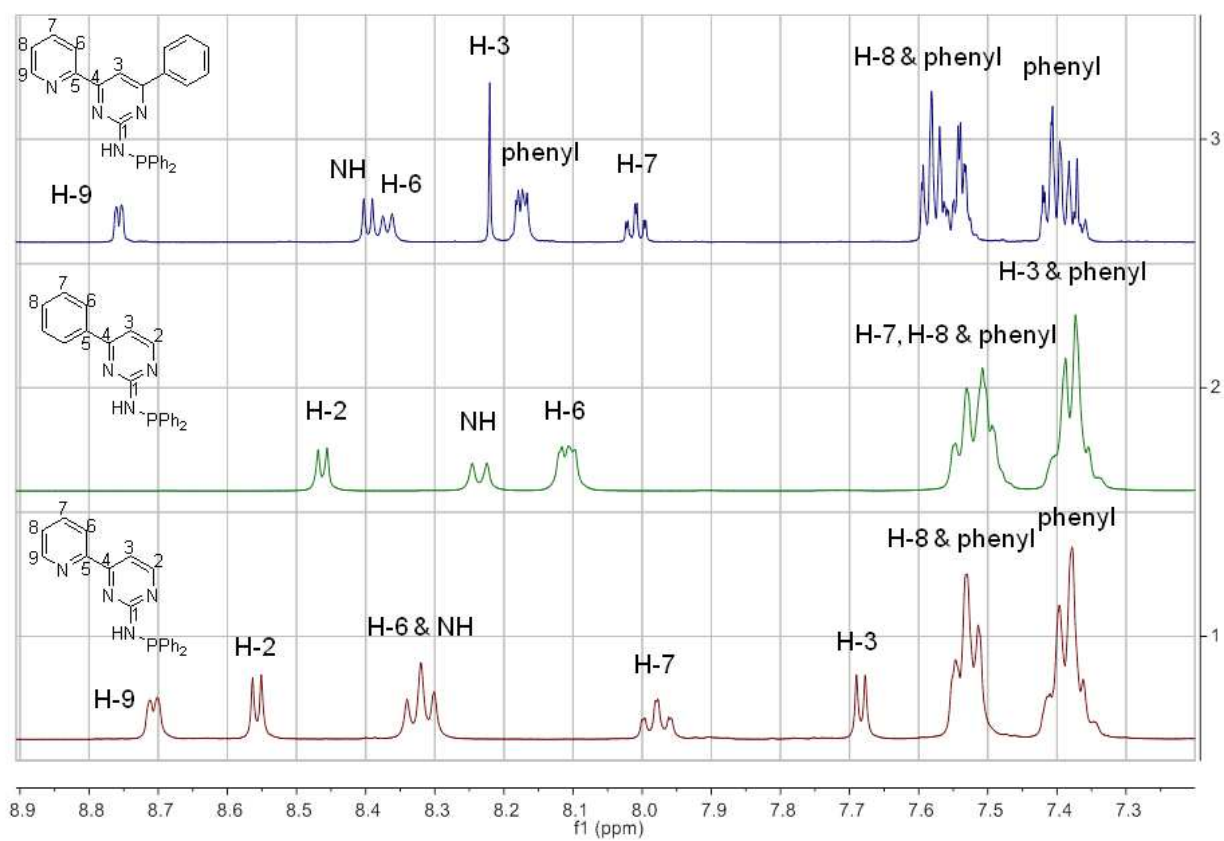
Figure 14. ^{1}H NMR spectra of ligands **12a** (middle), **12b** (bottom) and **12c** (top), recorded in DMSO-d_6.
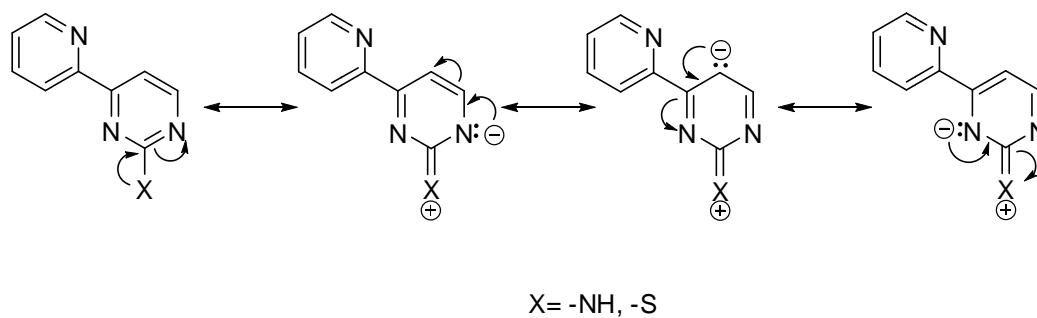
Results and Discussion

Table 5. ^{1}H NMR and ^{13}C NMR data for the backbone of the functionalized pyrimidine part in the ligands **12a-b** and **13b** recorded in DMSO-d_6.

| Ligand	12a	12b	12c	12d	13a
C-1	163.2	163.3	163.5	169.4	171.0
H-2	8.46	8.56	······	8.78	8.71-8.76
C-2	159.2	159.6	164.0	159.5	159.1
H-3	7.32-7.42	7.68	8.22	8.07-8.12	8.02-8.08
C-3	107.9	108.0	103.4	113.5	113.8
C-4	163.5	162.8	165.1	162.5	162.3
C-5	136.4	153.5	153.7	152.3	152.7
H-6	8.10	8.29-8.34	8.37	8.07-8.12	8.46
C-6	126.9	121.0	121.2	121.4	121.3
H-7	7.47-7.58	7.98	8.01	7.93	8.02-8.08
C-7	128.9	137.4	137.4	137.6	137.7
H-8	7.47-7.58	7.49-7.56	7.51-7.60	7.54	7.58
C-8	130.8	125.6	125.8	126.3	126.2
H-9	······	8.70	8.76	8.72	8.71-8.76
C-9	······	149.5	149.5	149.9	149.8
N-H	8.24	8.29-8.34	8.40	······	······

Investigation of the ^{1}H NMR and ^{13}C NMR spectra of **12b,d** and **13b** indicate that the resonances for **13a** and **12d** are shifted to lower field compared to **12b** (**Figure 15** and **Figure 16**). Among them, the most pronounced differences were found for H-3 and C-3 with downfield shift about 13 ppm for **13a** and **12d** towards **12b**. Since -NH and -S groups shield the *ortho* and *para* positions, the resonance forms shown below will make significant contributions to the ground state structure of the molecules (**Scheme 21**). By the NMR data in hand it is obvious that -NH is a better electron-donating group than -S and this is in agreement with the increasing order of electrondonating abilities.
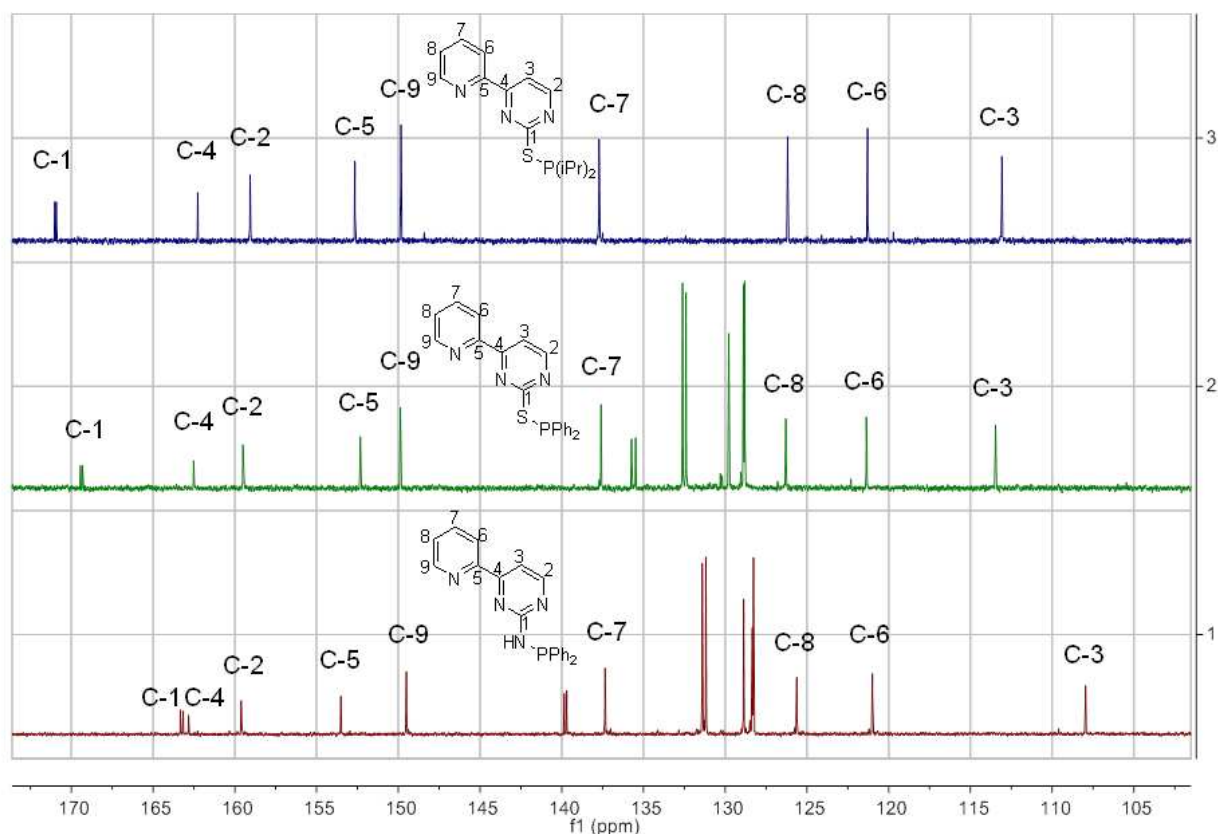
Results and Discussion

X= -NH, -S

Scheme 21. Possible resonances of pyrimidyl pyridine structurs.
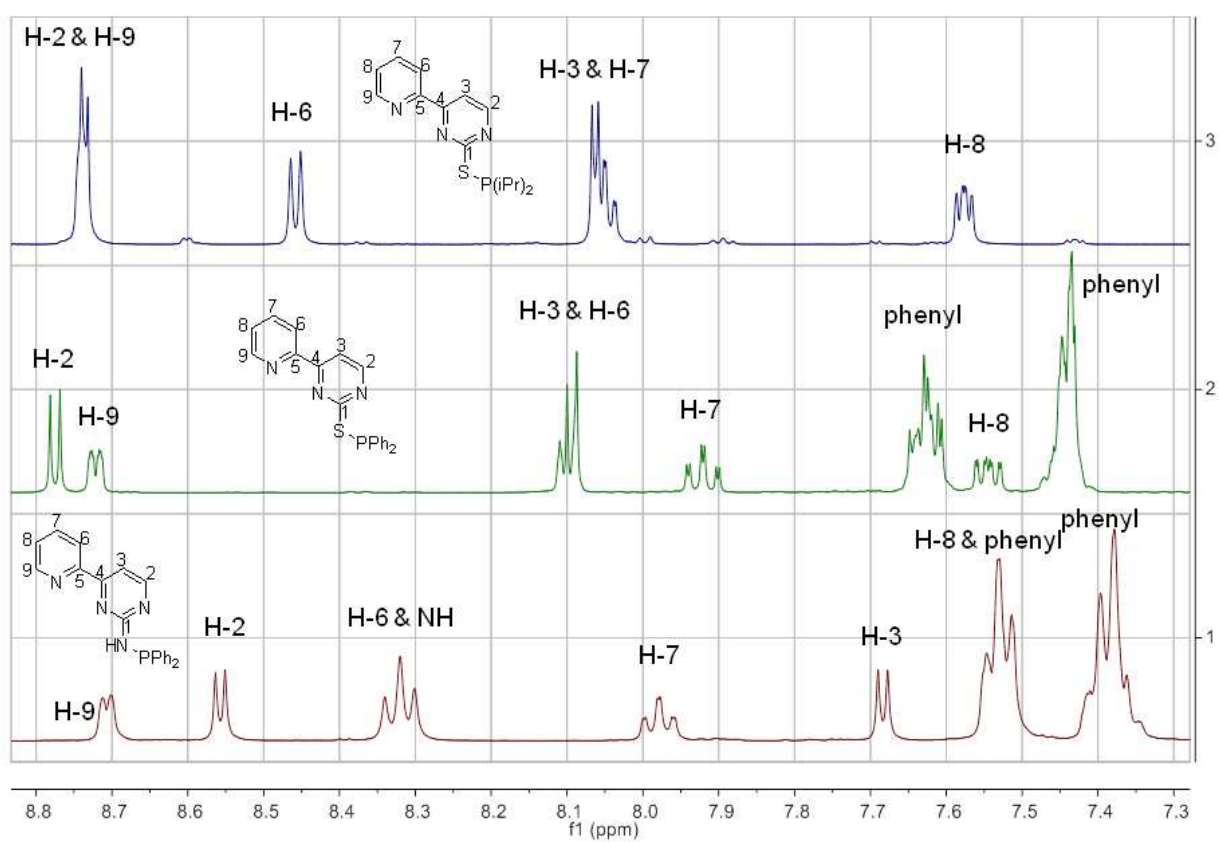
Figure 15. ^{1}H NMR spectra of ligands **12b** (bottom), **12d** (middle) and **13b** (top), recorded in

DMSO-d_6.

Results and Discussion

Figure 16. ^{13}C NMR spectra of ligands **12b** (bottom), **12d** (middle) and **13b** (top), recorded in DMSO-d_6.

Slow evaporation of a concentrated ethanol solution of ligand **12a** gave single crystals suitable for X-ray analysis (**Figure 17**). The molecular structure shows the planar geometry for the P1–N1–C1–N2 backbone with a dihedral angle 1.02°. Furthermore, the crystal structure of **12a** also shows that the molecule dimerizes in the solid state via intermolecular hydrogen bonding between molecules as follow: The HN1 proton as hydrogen donor of the first molecule is shared with the pyrimidinyl nitrogen (N3A) as hydrogen acceptor of a second and the HN1A proton of the second as mutual manner with the pyrimidinyl nitrogen (N3) of the first molecule. The P1-N1, HN2···N3A and N2···N3A distances are 1.72 Å, 2.187 Å and 3.038 Å respectively with angle of 175.48° for N2-HN2···N3A.
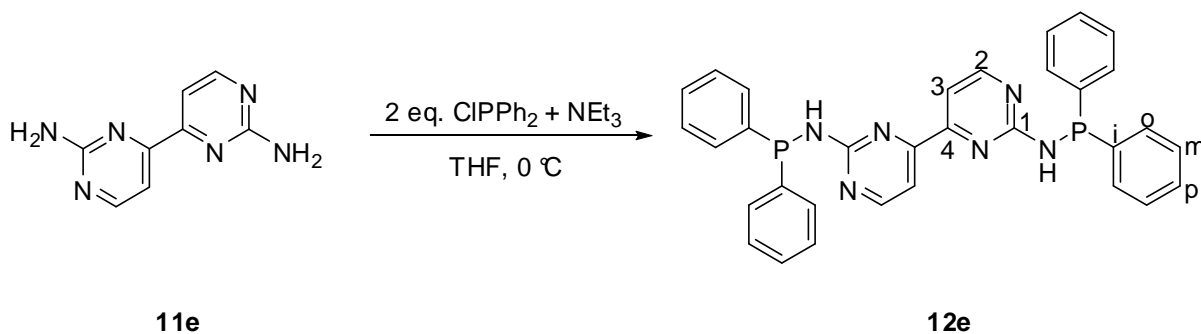
Results and Discussion
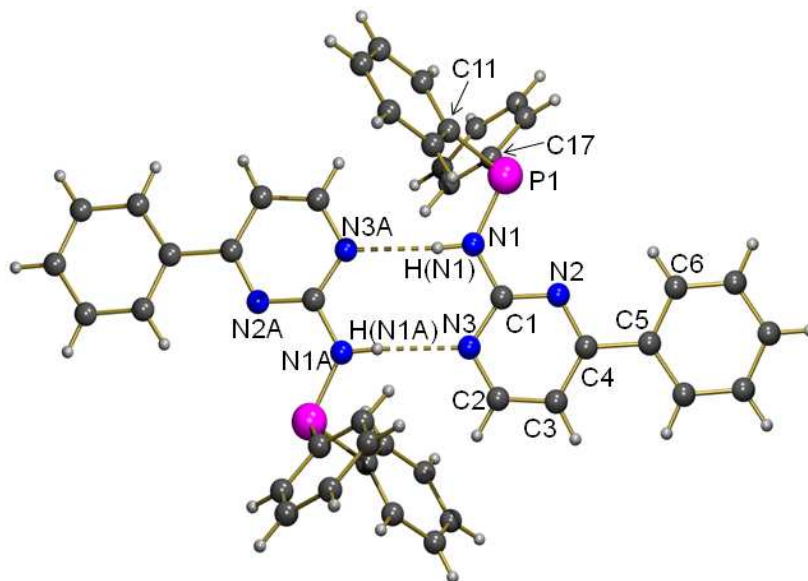
Figure 17. Molecular structure of **12a** in the solid state. Selected bond lengths [Å] and angels [°]: C1–N11.3668(17) , C1–N2 1.3364(16), C1–N3 1.3491(17), C4–C5 1.4866(18), P1–C11 1.8404(14), P1–C17 1.8363(14), N1–C1–N2 117.82(11), N1–C1–N3 115.77(11), N2–C1–N3 126.41(11), C11–P1–N1 96.52(6), C17–P1–N1 102.70(6), N2–C4–C5–C6 –158.

3.1.2.3.   Synthesis of PNNP Ligands

4,4'-Bipyrimidine-2.2'-diamine **11e** was synthesized according to a published method.[96] The desired doublet bidentate pyrimidinylphosphine ligand **12e** was obtained in good yield (**Scheme 22**) by reacting the intermediate **11e** with two equivalents of PPh$_2$Cl in presence of NEt$_3$.

Scheme 22. Synthesis of **12e**.

Results and Discussion

The ^{31}P NMR resonance of **12e** in DMSO-d_6 is observed as singlet at about 25.17 ppm (**Figure 18**) which slightly shifted to the lower field in comparison to **12a,b**.
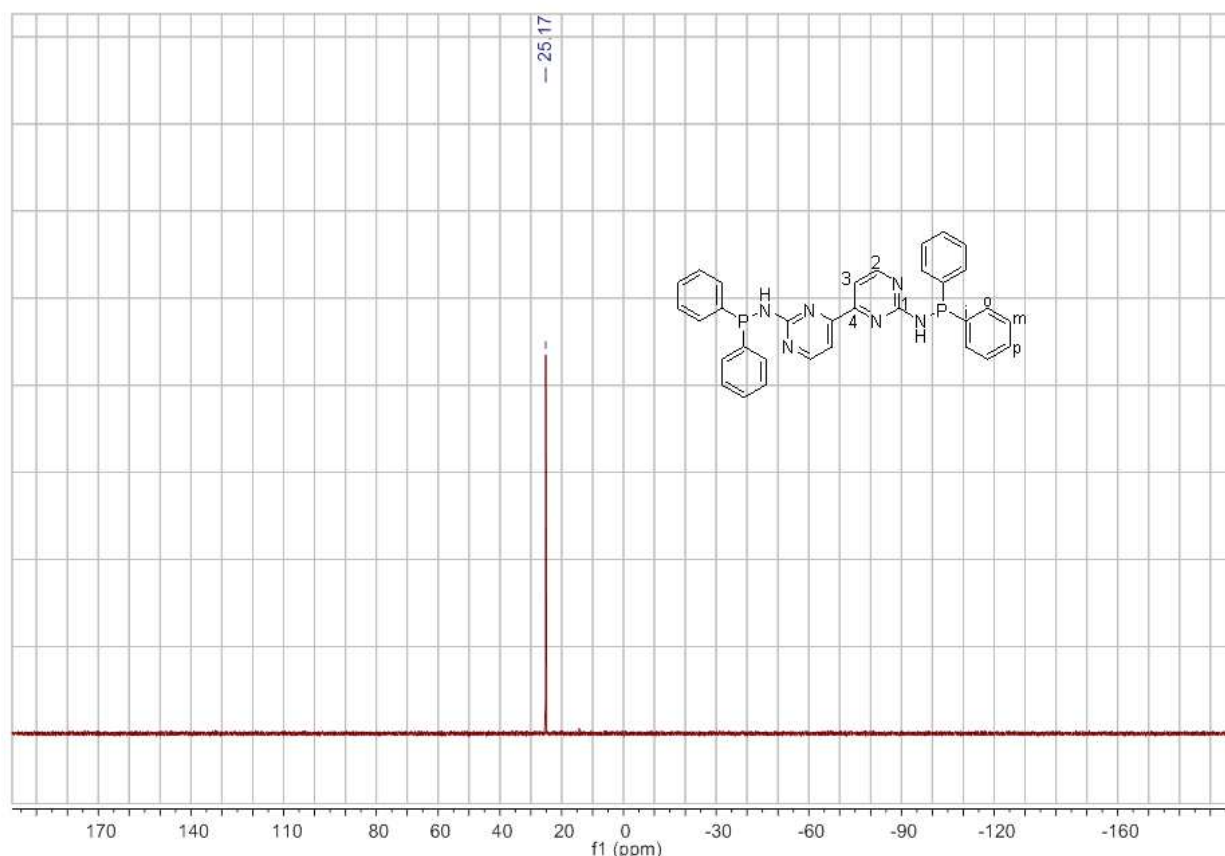
Figure 18. ^{31}P NMR spectrum of ligand **12e** recorded in DMSO-d_6.

In the ^{1}H NMR spectrum, two doublets at about 8.60 and 7.56 ppm with a coupling constant of J_{HH} = 5.0 Hz were assigned to the hydrogen atoms H-2 and H-3, respectively and a doublet at about 8.44 ppm was assigned to the hydrogen atom of the NH group (**Figure 19**). In ^{13}C NMR spectrum eight distinguished signals at about 108.25, 128.4, 129.0, 131.4, 139.6, 160.1, 161.5 and 163.3 were observed.

Results and Discussion
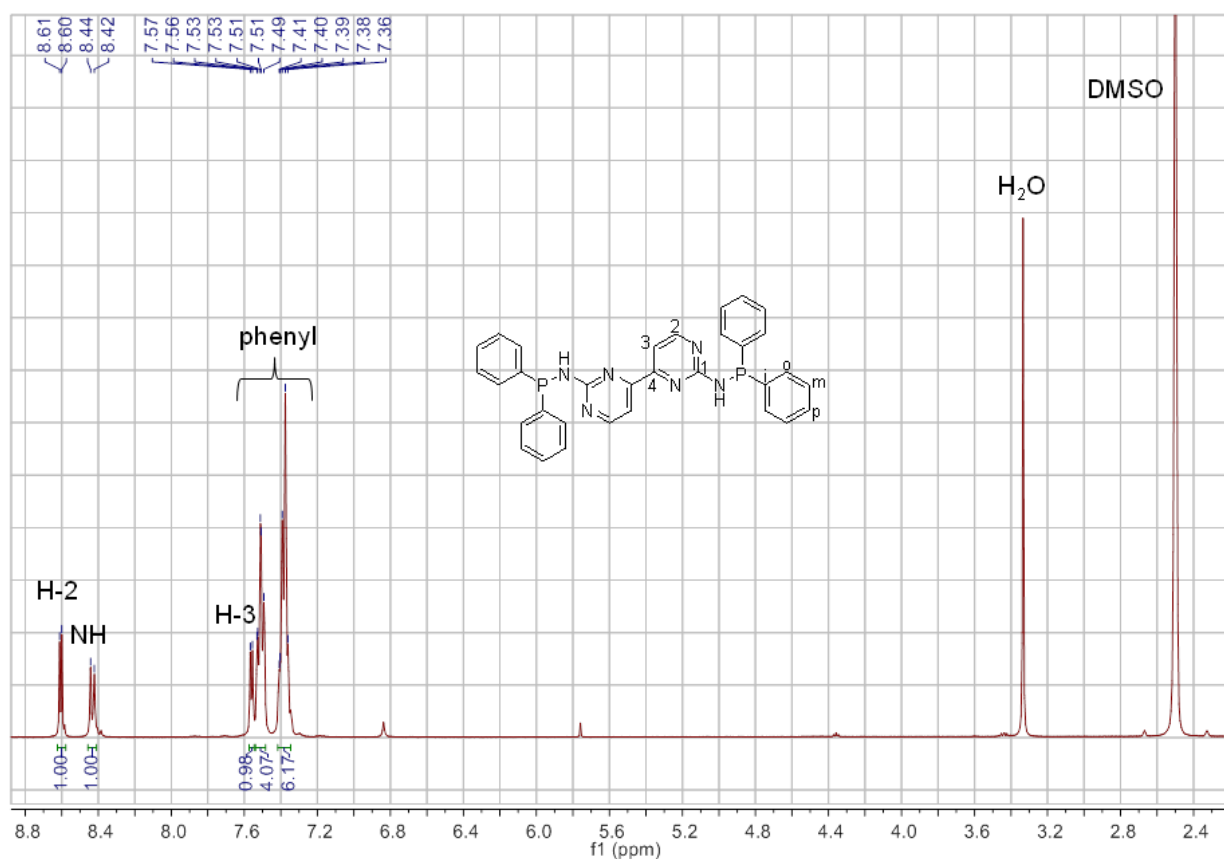
Figure 19. ^{1}H NMR spectrum of ligand **12e** recorded in DMSO-d_6.

3.2. Complex Synthesis

Bidentate *P,N* ligands containing phosphorus as a soft donor, exhibiting weak π-acceptor properties and thus stabilizing metal centers in low oxidation states and nitrogen as a hard donor atom exhibiting σ-donor properties and stabilizing electron-poor metals have been used widely in the synthesis of complexes. The major part of the investigations in metal complexes containing *P,N* hybrid ligands have focused on phosphino pyrazoles (**L1**), phosphino oxazolines (**L2**), phosphine imines (**L3**), phosphine pyridine combinations (**L4-L5**) and phosphine amines (**Scheme 23**).
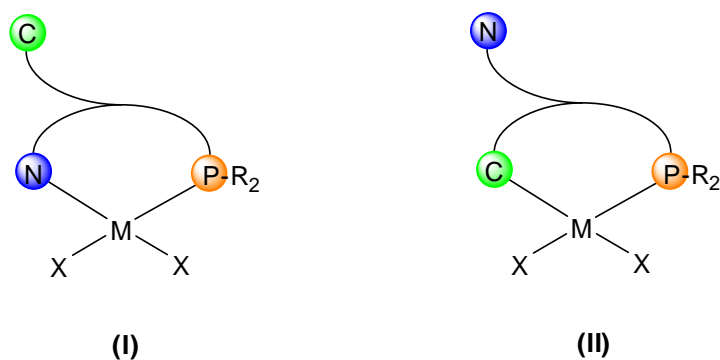
46

Results and Discussion

L1

L2

L3

L4

L5

L6 n n=0-3

L7 | **a** | **b**
R | Ph | Cy

L8

L9
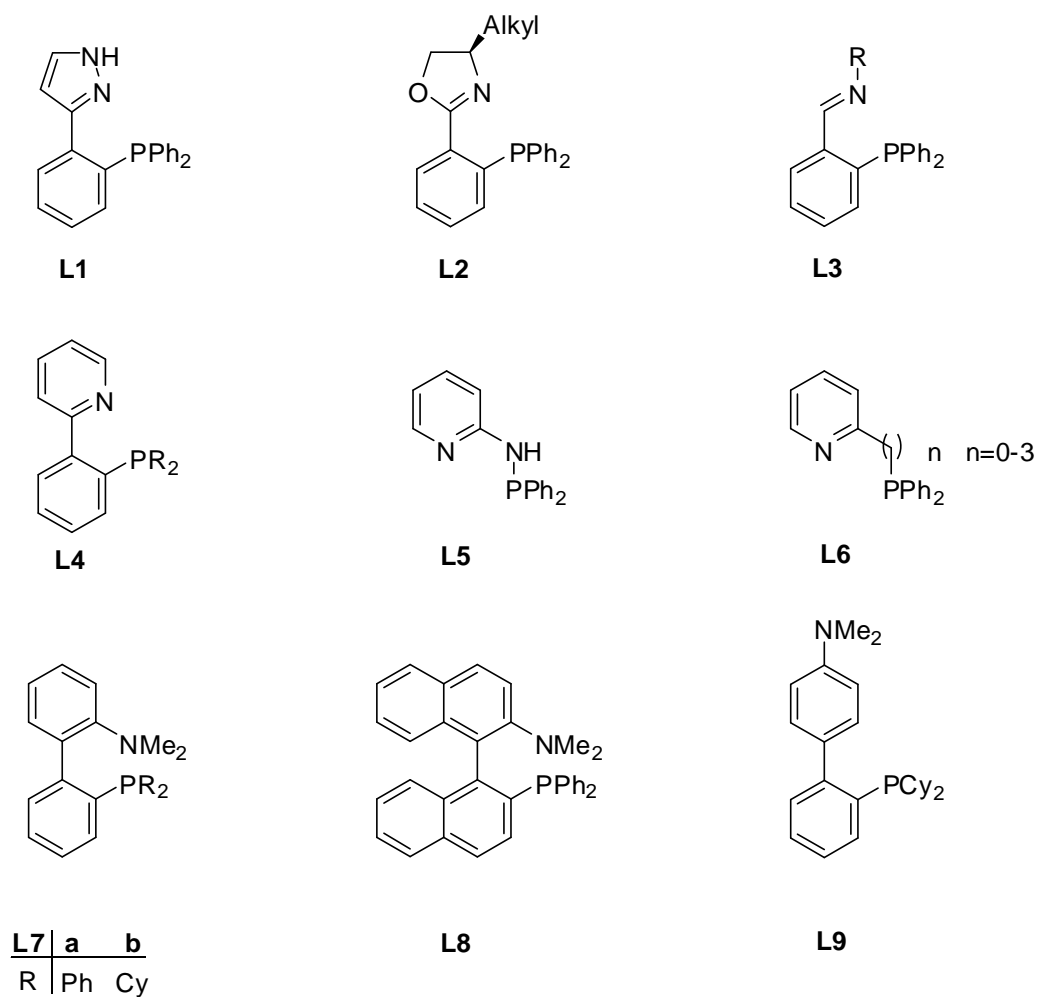
Scheme 23. Different types of *P,N* ligands.

The coordination chemistry of ligands types **L1**[97], **L2**[98], **L3**[99], **L4**[100], **L5**[101] and **L6**[102] towards metal ions has shown solely the *P,N* coordination mode (Form (**I**), **Scheme 24**).


(I)

(II)

Scheme 24. Bonding modes of *P,N* based ligands.

Results and Discussion

Kocovsky et al. were able to prove by X-ray crystal structural analysis that **L8** (MAP) coordinates to palladium (II) through an unusual *P,Cσ*- chelation rather than by a *P,N*-binding mode.[103] Faller et al. prepared and characterized two allyl palladium complexes of **L7** type ligands. They demonstrated that the preference for *P,N*- versus *P,C*-binding is controlled by subtle electronic and steric effects: *P,N*-binding is preferred in the Ph$_2$P case, whereas *P*,η^2(C1´-C6´)-binding is preferred for the Cy$_2$P analogue.[104] Vilar et al. reported that in the palladium complex of **L7b**[105] the ligand undergoes *P,Cσ*-chelation as **L8**. Lakshman et al. obtained single crystals of a 1:1 complex of **L9** and Pd(OAc)$_2$ and found that C-H activation of the arene ring in the *ortho* position gives a cyclometallated product.[106]

3.2.1. Palladium Complexes with Pyrimidinylphosphine Ligands with Primary and Secondary Amino Groups

Treatment of **4a-c** with one equivalent of the palladium(II) precursor (C$_6$H$_5$CN)$_2$PdCl$_2$ in dichloromethane at room temperature leads to the formation of the expected *P,N*-coordinated dichloropalladium(II) complexes **14a-c** as orange colored solids in almost quantitative yields (**Scheme 25**). All compounds are stable in both the solid state and solution.

X	14a	14b	14c
X	NH$_2$	NHEt	NHOct
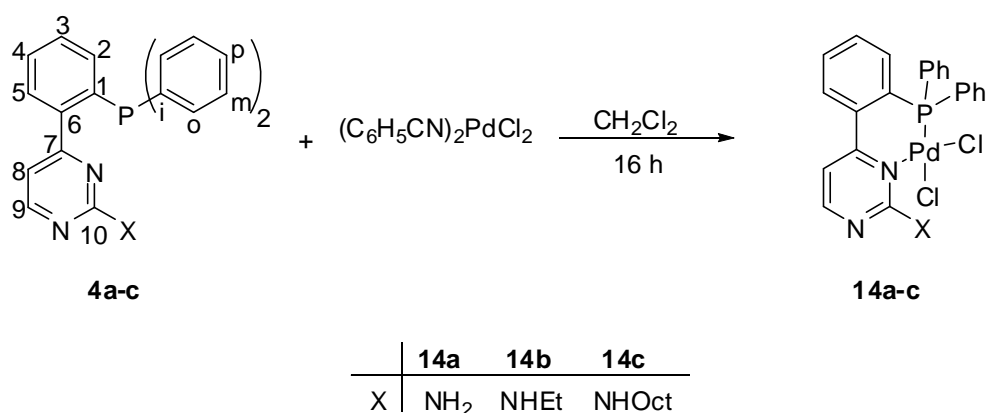
Scheme 25. Synthesis of palladium(II) complexes.

Results and Discussion

According to the NMR data of **14a,b** the different amino groups indicat no significant effect. The resonances in the ^{31}P NMR spectra of **14a,b** are observed at about 31.27 and 30.71 ppm. The resonances of hydrogen atoms in the ^{1}H NMR spectra of **14a,b** were assigned on the basis of ^{1}H–^{1}H correlation experiments (**Figure 20**). Two doublets for the H-8 and H-9 protons which couple with each other are observed at about 6.88 and 8.16 ppm, respectively. In the ^{1}H NMR spectrum of **14b** a broad signal at about 8.50 ppm was assigned to the N-H proton however the NH$_2$ protons of **14a** were not detected.
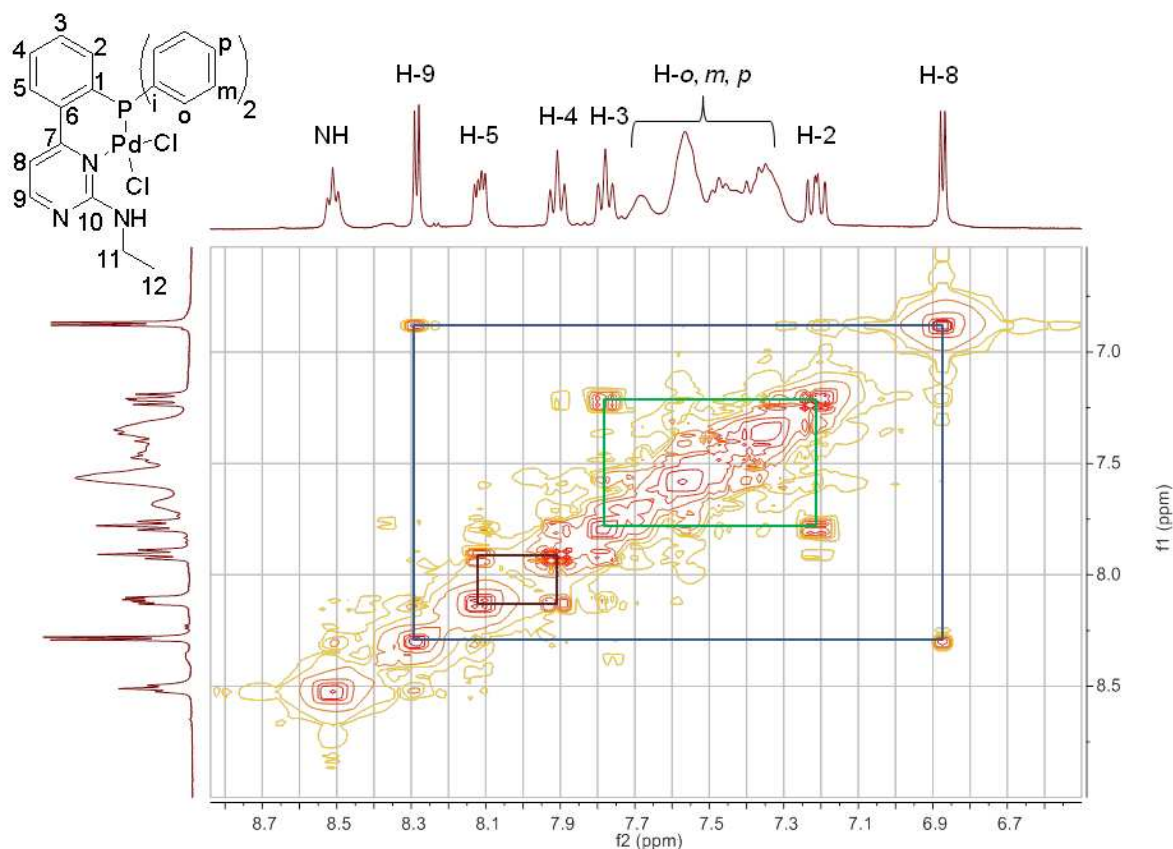

Figure 20. ^{1}H–^{1}H COSY spectrum (aromatic region) of complex **14b** in DMSO-d_6.

Coordination of ligands **4a,b** to the palladium(II) centre causes a down field shift for the resonances of the protons with respect to the free ligands **4a,b**. As shown in **Figure 21**, H-5 is the most influenced proton and is shifted by about 0.6 ppm towards lower field and H-9 is

Results and Discussion

the least influenced proton with a shifted less than 0.1 ppm to lower field.
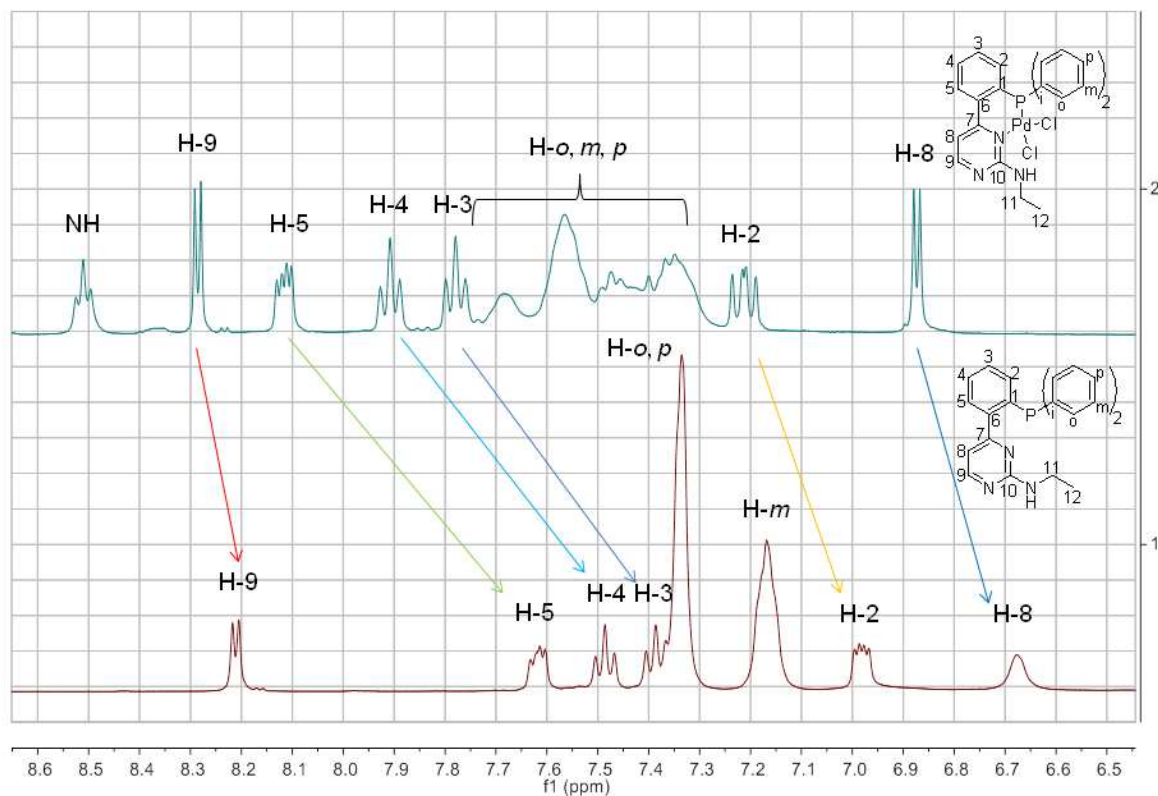
Figure 21. ^{1}H NMR spectra of **4b** (bottom), **14b** (top).

Recrystallization of compounds **14a** by diffusion of *n*-hexane in to a CHCl$_3$ solution gave crystals suitable for single-crystal X-ray diffraction analysis (**Figure 22**). The palladium centre is coordinated in a distorted square-planar geometry and undergoes intra- (N3–H3A···Cl1) and intermolecular hydrogen bonding (N3–H3B···Cl2a) leading to dimers in the solid state.

Results and Discussion
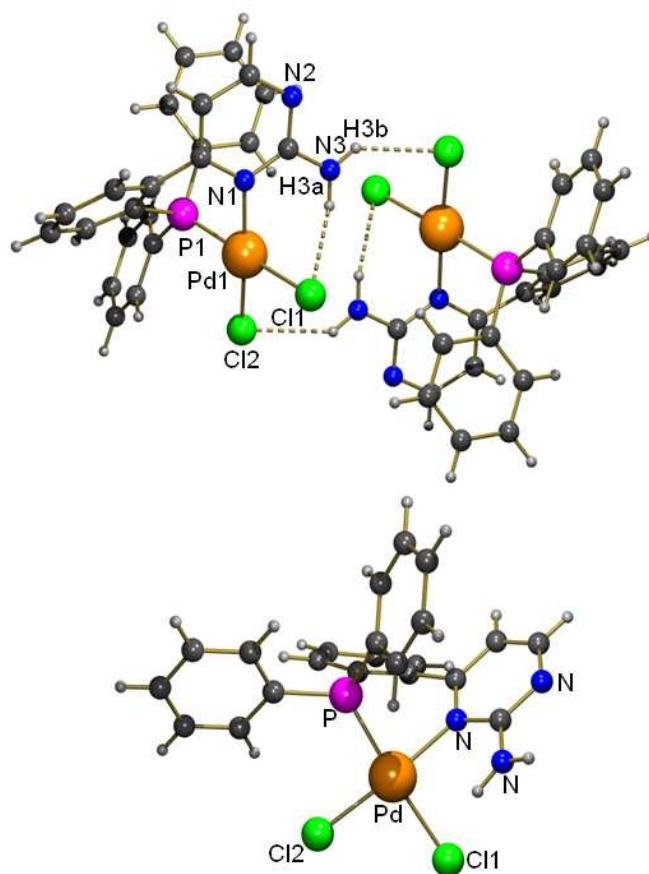
Figure 22. Molecular structure of the palladium complex **14a** in the solid state; Characteristic bond lengths [Å] and angles [°]: Pd1–Cl1 2.3913(7), Pd1–Cl2 2.2915(7), Pd1–P1 2.2184(6), Pd1–N1 2.083(2), N3–H3A 0.90(2), H3A···Cl1 2.48(3), N3···Cl1 3.201(4), Cl1–Pd1–Cl2 90.98(3), Cl1–Pd1–P1 174.29(3), Cl1–Pd1–N1 93.35(6), Cl2–Pd1–P1 93.63(2), Cl2–Pd1–N1 175.52(6), P1–Pd1–N1 82.11(6), N3–H3A···Cl1 137(3).

3.2.2. Palladium Complexes of Pyrimidinylphosphine Ligands with a Tertiary Amino Group

The syntheses of the **15a-c** were carried out according to the same procedure as for **14a,** but the results were completely different. Ligands **4d-f** – all bearing a tertiary amino group – led to C–H activation and thus to the cyclometallated products **15a-c** (**Scheme 26**).
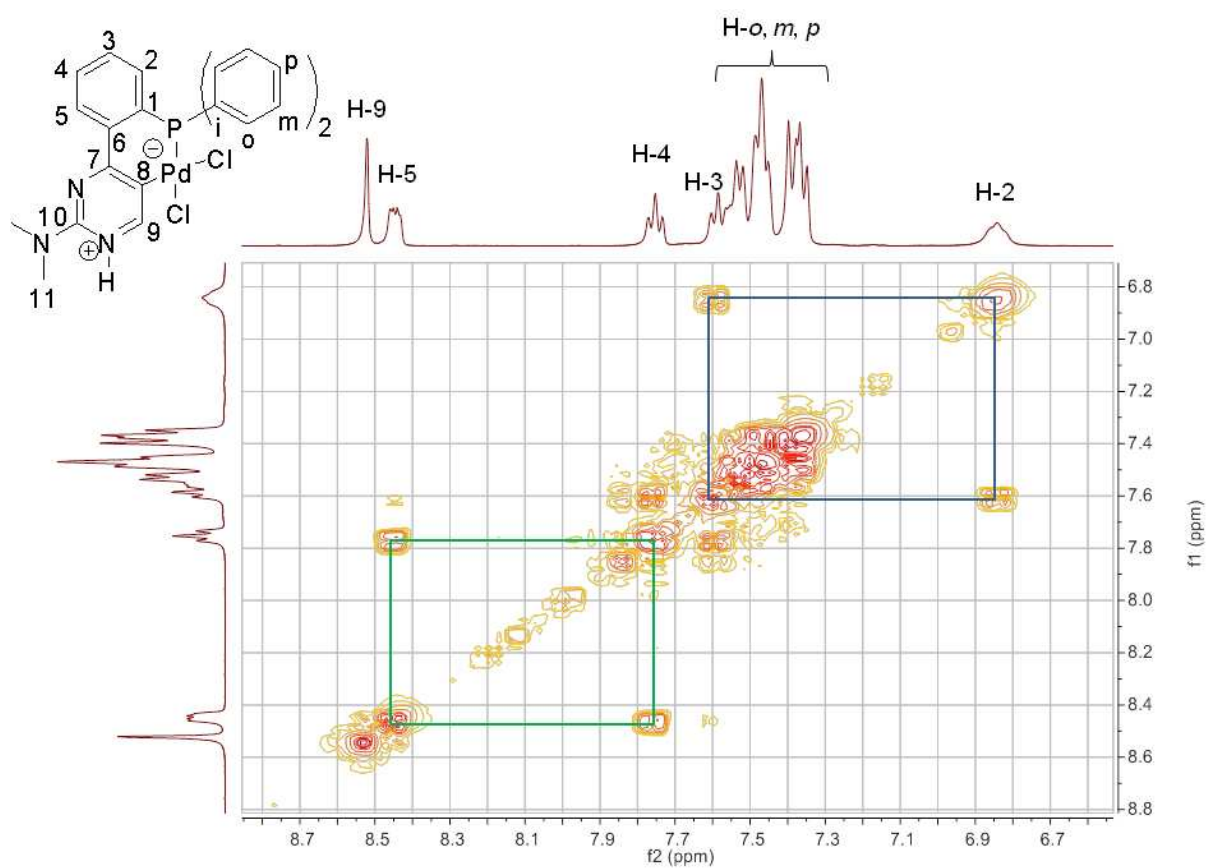
Results and Discussion
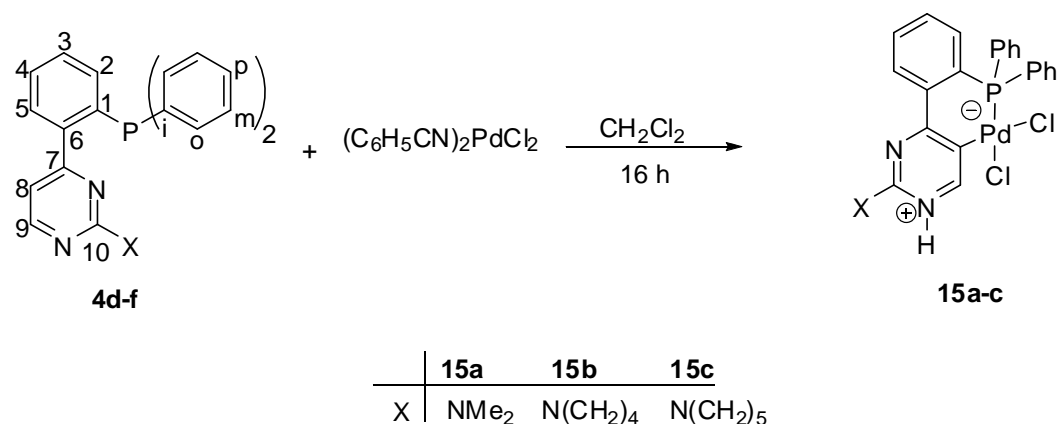
Scheme 26. Synthesis of the palladium(II) complexes **15a-c**.

X	15a	15b	15c
	NMe_2	$N(CH_2)_4$	$N(CH_2)_5$

^{1}H NMR spectroscopy clearly proves the cleavage of the C-H bond. H-9 appears as a singlet at about 8.52 ppm, and there is no correlation for it (**Figure 23**), since the resonance of H-8 disappeared for the C–H-activated complexes **15a-c** which was also proved by means of integration of the NMR signals. As shown in **Figure 24**, the resonances of the protons are slightly shifted downfield after complexation and the signal of H-5 indicated the major change.

The ^{31}P NMR resonances of **15a-c** are observed at about 29.69, 29.67 and 29.60 ppm respectively which are shifted by about 1.0–1.5 ppm towards higher field with respect to **14a,b** indicating an increase of electron density at the palladium(II) centers due to the coordination of a carbanion in the *cis*-position to the phosphine donor.

Results and Discussion

Figure 23. ^{1}H–^{1}H COSY spectrum (aromatic region) of complex **15a** in DMSO-d_6.

Results and Discussion
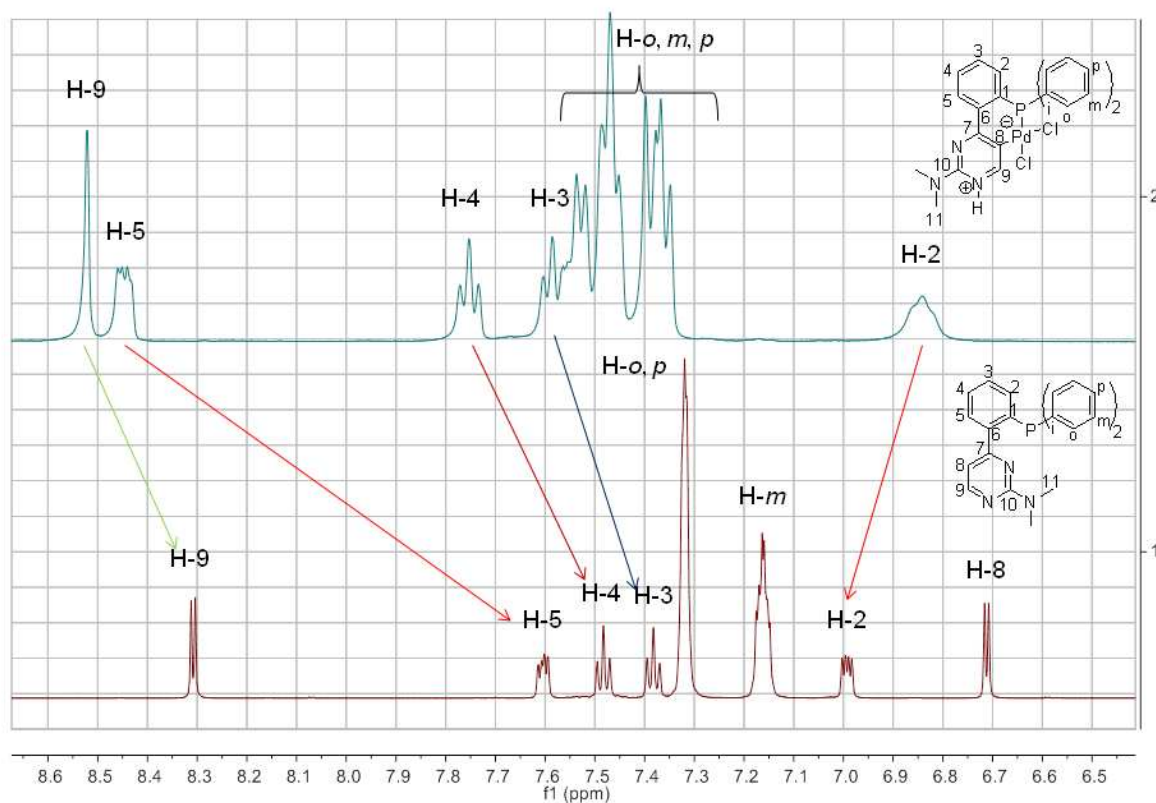
Figure 24. ^{1}H NMR spectra of **4d** (bottom), **15a** (top).

Recrystallization of **15a** by vapor diffusion of diethyl ether into a solution of the compound in DMSO/CHCl$_3$ gave crystals suitable for single-crystal X-ray diffraction analysis (**Figure 25**). Palladacycle **15a** crystallizes as a zwitterion in the solid state. The palladium centre is coordinated in a distorted square-planar geometry. There is intermolecular hydrogen bonding (N2–HN2···Cl1a) leading to dimers in the solid state. The formation of dimers is probably the reason for the pronounced bending of the Cl1–Pd1–C8 axis (165.91°) in compound **15a**. Although there is only a slight difference in the Pd–P distances between the complexes, the Pd–C distance in **15a** (2.016 Å) is significantly shorter than the Pd–N distance in **14a** (2.083 Å), expressing increased covalency.

54

Results and Discussion
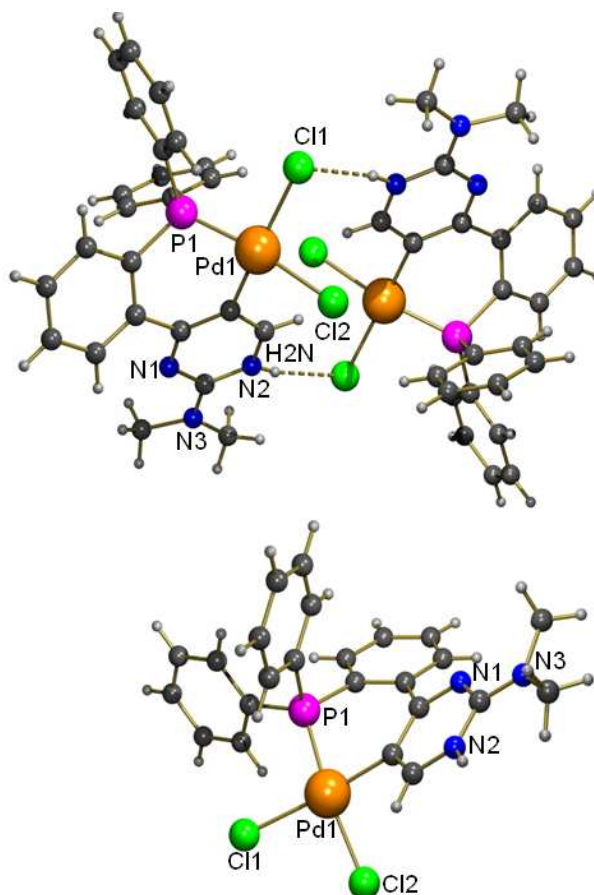
Figure 25. Molecular structure of the palladium complex **15a** in the solid state; Characteristic bond lengths [Å] and angles [°] : Pd1–Cl1 2.3885(9), Pd1–Cl2 2.3696(10), Pd1–P1 2.2118(9), Pd1–C8 2.016(4), N2–H2N 0.87(3), Cl1–Pd1–Cl2 90.14(3), Cl1–Pd1–P1 95.93(3), Cl1–Pd1–C8 165.91(10), Cl2–Pd1–P1 171.34(3), Cl2–Pd1–C8 91.56(10), P1–Pd1–C8 84.06(10).

Often C–H activation in the *ortho*-position of aromatic ligands requires basic reaction conditions [e.g., Pd(OAc)$_2$ as the Pd source]. For **15a-c**, the much less reactive PdCl$_2$ fragment alone is capable of performing this reaction since the pyrimidine moiety acts as an internal base.

Attempts to deprotonate **15a** and to split one of the Pd–Cl bonds with different bases such as NEt$_3$, (Bu)$_4$NOH, DBU and also KOH in different solvents were unsuccessful (**Scheme 27**).

Results and Discussion
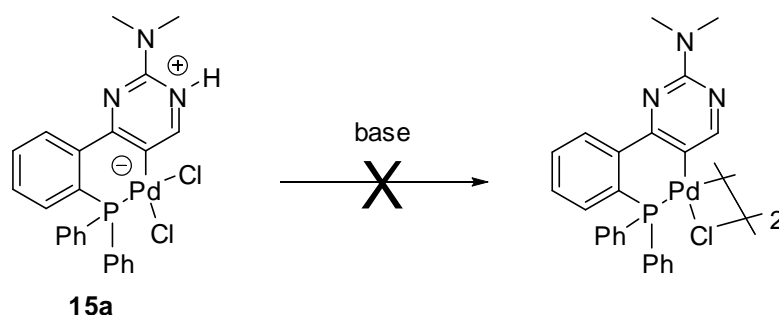
Scheme 27. Failed elimination of HCl at **15a** under basic condition.

Reacting the ligand **4d** with the palladium(II) precursor $Pd(CH_3COO)_2$ directly gave the red colored palladium complex **16** (**Scheme 28**).
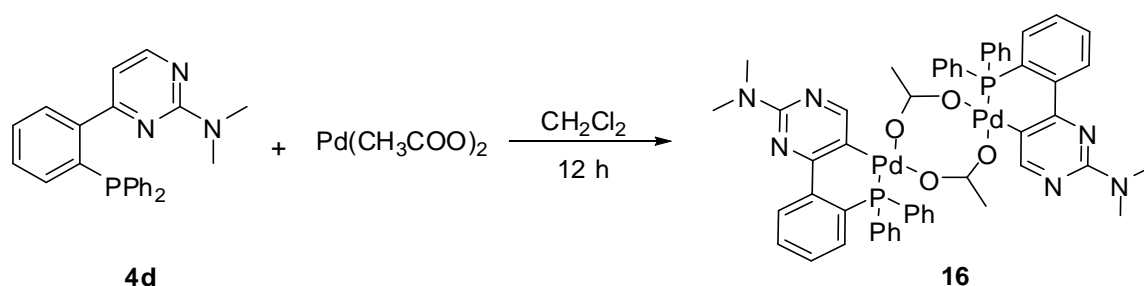
Scheme 28. Synthesis of the dimeric palladacycle **16**.

Suitable crystals of **16** for X-ray crystallographic studies were obtained by the slow diffusion of ether into a $CHCl_3$ solution. The structure of **16** reveals a dimeric species with two bridging acetate ligands (**Figure 26**). Both palladium atoms show distorted square planar geometry, the largest angles are 95.30(5)° and 94.62(6)°, belonging to O3–Pd1–P1 and O2–Pd2–P2 respectively, while the smallest angles are 84.04(6)° and 83.80 (7)°, belonging to C8-Pd1–P1 and C32–Pd2–P2 respectively.

The Pd⋯Pd distance is 3.1506(3) Å, typical for two Pd atoms bridged by acetate.[106] The smallest torsion angles were found for Pd1–O1–O2–Pd2 (0.61°) and Pd1–O3–O4–Pd2

Results and Discussion

(0.13°) which points out that the plane of the carboxylate groups is almost in line with the Pd1–Pd2 bond. Each palladium center is part of a cyclometalated six-membered ring. The distance between Pd1–C8 and Pd2–C32 are 2.007(2) Å and 1.995(2) Å respectively which are significantly shorter than the Pd–C distance in **15a**.
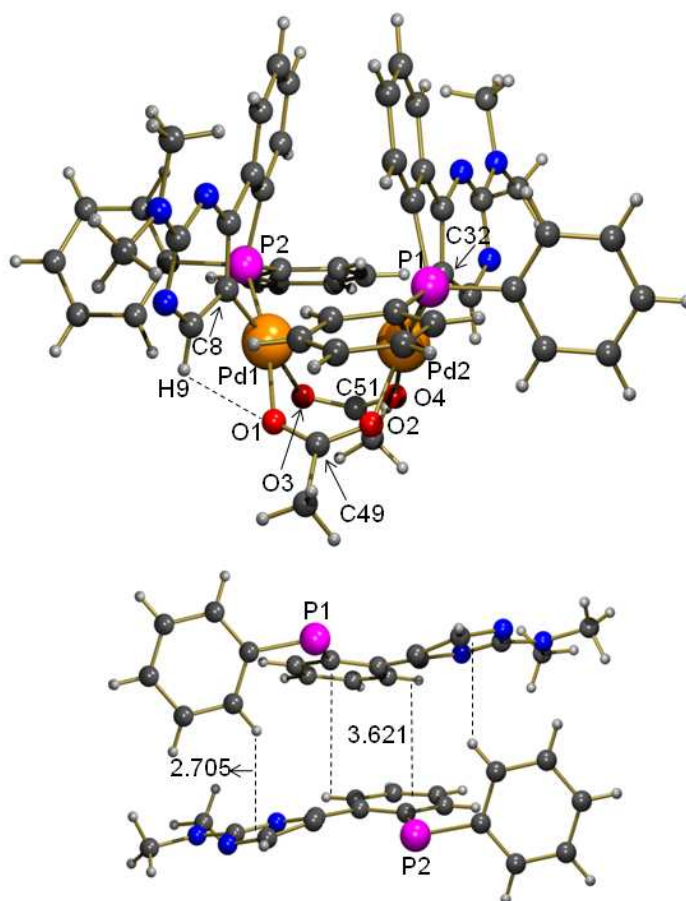
Figure 26. Molecular structure of the cyclopalladated complex **16** in the solid state (top), representation of π-stacking in some parts of cyclopalladated complex **16** (bottom); Characteristic bond lengths [Å] and angles [°] : Pd1–P1 2.1749(6) (2), Pd2–P2 2.1751(7), Pd1–C8 2.007(2), Pd1–C32 1.995(2), Pd1–O1 2.1192(15), Pd1–O3 2.0976(17), Pd2–O2 2.1206(18), Pd2–O4 2.1265(18), P1–Pd1–C8 84.04(6), P2–Pd2–C32 83.80(7), O1–C49–O2 125.7(2), O3–C51–O4 126.1(2).

Results and Discussion

The ^{31}P NMR resonance of **16** was observed at 32.86 ppm (**Figure 27**) which is slightly shifted towards lower field with respect to **15a**. ^{1}H NMR spectroscopy clearly proves the cleavage of the C–H bond. H-9 appears as a singlet at about 8.74 ppm which is slightly shifted towards lower field with respect to **15a** (**Figure 28**). This is probably due to hydrogen bonding between H-9 of the ligand and closest oxygen of the acetate ligand (H-9···O1, **Figure 26**).
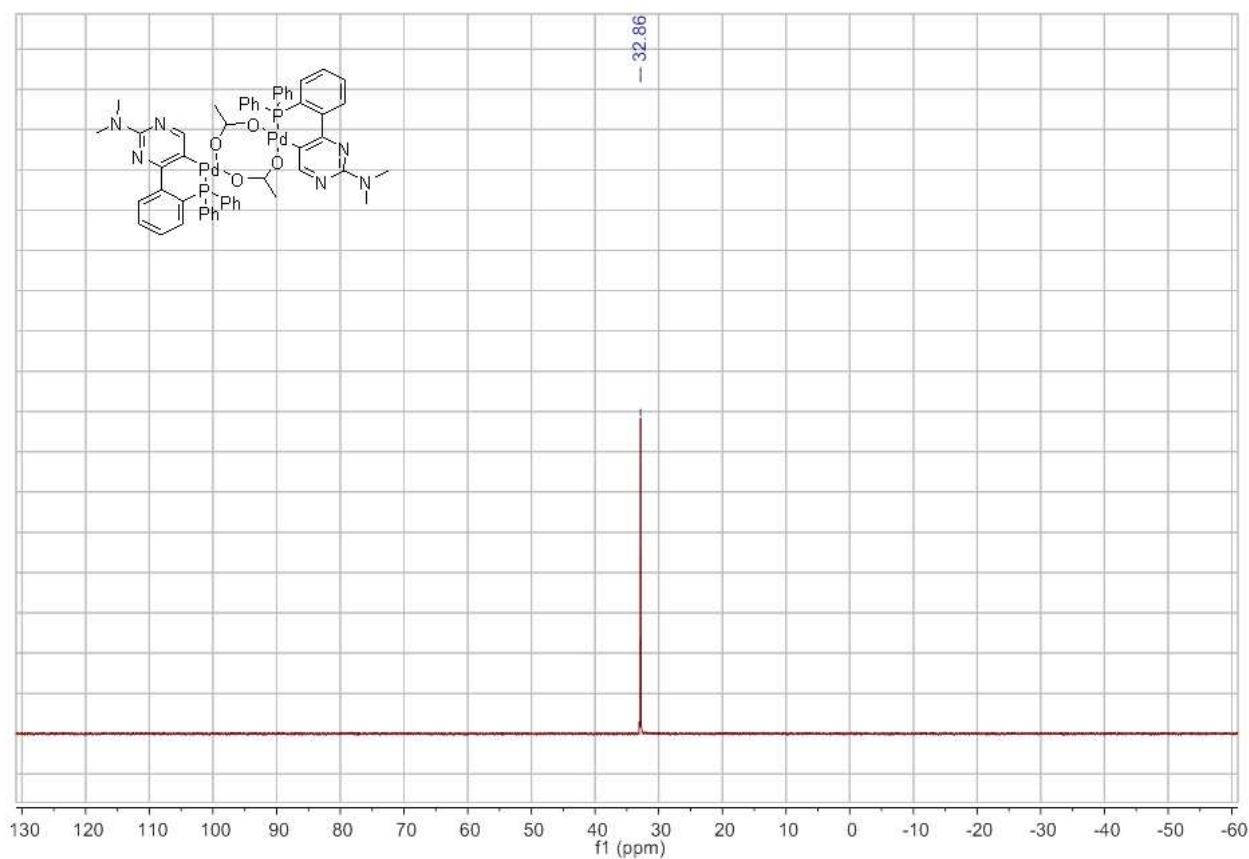
Figure 27. ^{31}P NMR spectrum of **16**.

Results and Discussion
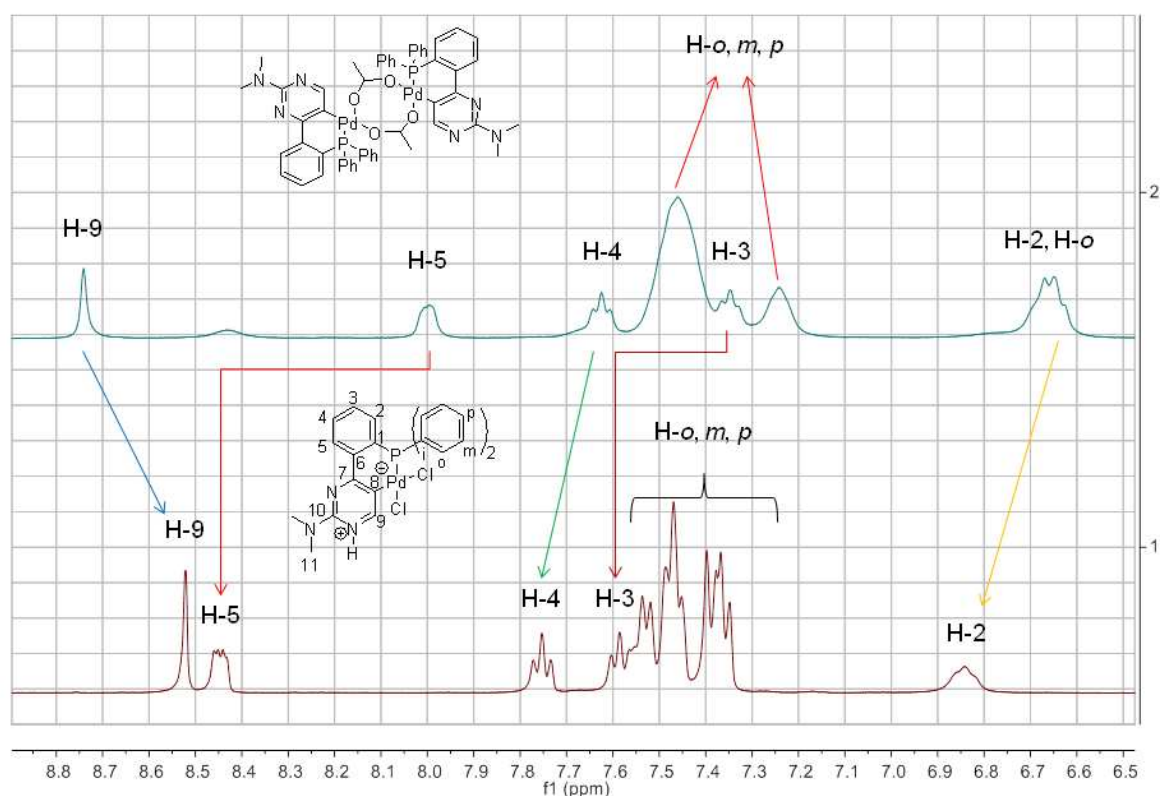
Figure 28. ^{1}H NMR spectra (aromatic region) of **15a** (bottom), **16** (top).

As shown in **Figure 28**, the ^{1}H NMR resonances of **16** shifted to higher field in comparison to **15a** with the exception of H-9. Among them H-5 and one of the *ortho* protons have a pronounced upfield shift (about 0.45 and 0.76 ppm, respectively), which can be explained by the molecular structure of **16** (**Figure 26**).

3.2.3. DFT Calculations

DFT calculations (B3LYP//6-31G*/LANL2DZ*) on compounds **14a** (APT charge on Pd: 0.437) and **15a** (APT charge on Pd: 0.228) support the interpretation of increased covalency. These calculations also corroborate an increased stability of the *P,C* coordination for the dimethylaminofunctionalized compound (see index). There may be various reasons for the different behavior of the -NHR/-NH$_2$ and the -NR$_2$ functionalized systems:

1) The NH moiety allows intramolecular hydrogen bonding to one of the chlorido ligands,

Results and Discussion

preventing decoordination of the pyrimidine ligand.

2) The bulky $-NR_2$ group undergoes repulsive interaction with one of the chlorido ligands, facilitating decoordination of the pyrimidine ligand.

3) The strongly electron donating $-NR_2$ group stabilizes the C–H activated product more efficiently than a $-NHR/-NH_2$ group.

The latter reason should not play a key role since the calculated APT charges of the carbon atoms in the 5-position of the pyrimidine ring (*trans* to the amino group) for the *P,N*-coordinated compounds **14a** (–0.190) and **15a** (–0.212) do not differ largely. With the above mentioned results in hand, I therefore assigned the favored C–H activation of the $-NR_2$ functionalized systems to a destabilization of the *P,N*-coordination due to steric reasons and the missing hydrogen bond.

3.2.4. Synthesis of a Palladium Complex with a *Para* Substituted Pyrimidinylphosophine Ligand.

Reacting two equivalents of ligand **2b** with the palladium(II) precursor $(C_6H_5CN)_2PdCl_2$ at room temperature in dichloromethane solution gave the orange colored neutral diphosphine dichloropalladium(II) complex **17** in almost quantitative yields (**Scheme 29**).

Results and Discussion
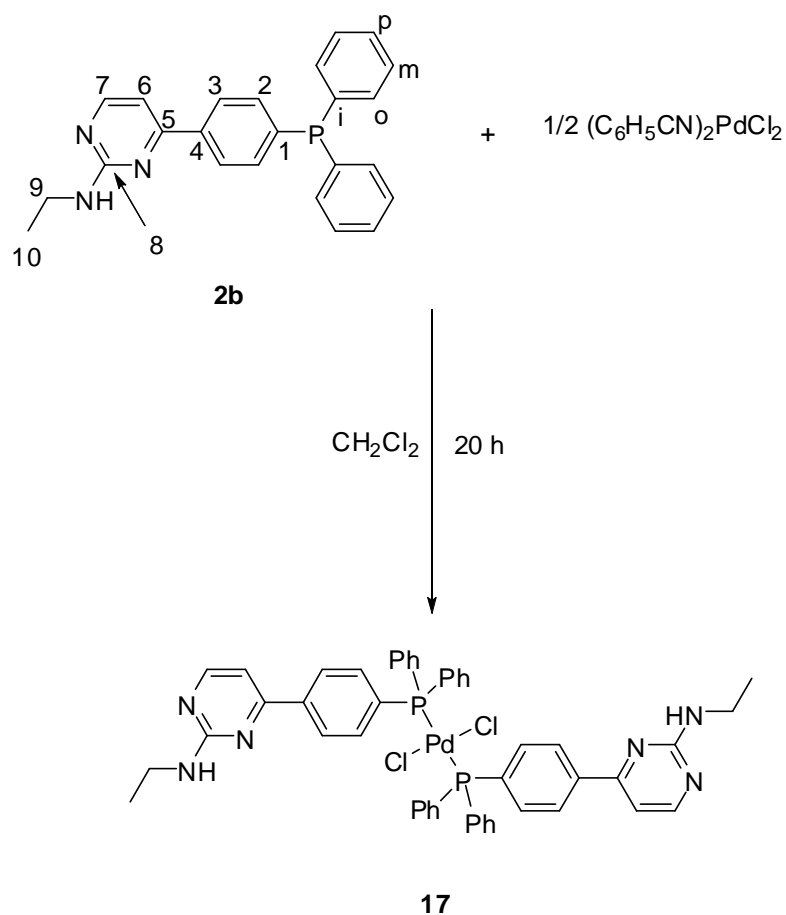
Scheme 29. Synthesis of the palladium(II) complex **17**.

The ^{31}P NMR resonance of **17** is observed as singlet at about 23.08 ppm in CDCl$_3$, and indicates no equilibrium mixture of the *cis* and *trans* isomers (**Figure 29**). In the ^{1}H NMR spectrum of **17**, the resonances of H-3, H-6, H-7, H-9, H-10 and N–H are observed at almost the same chemical shift as in the free ligand **2b**, while the H-2, H-*o*, H-*m* and H-*p* are slightly shifted to lower field (**Figure 30**).

Results and Discussion
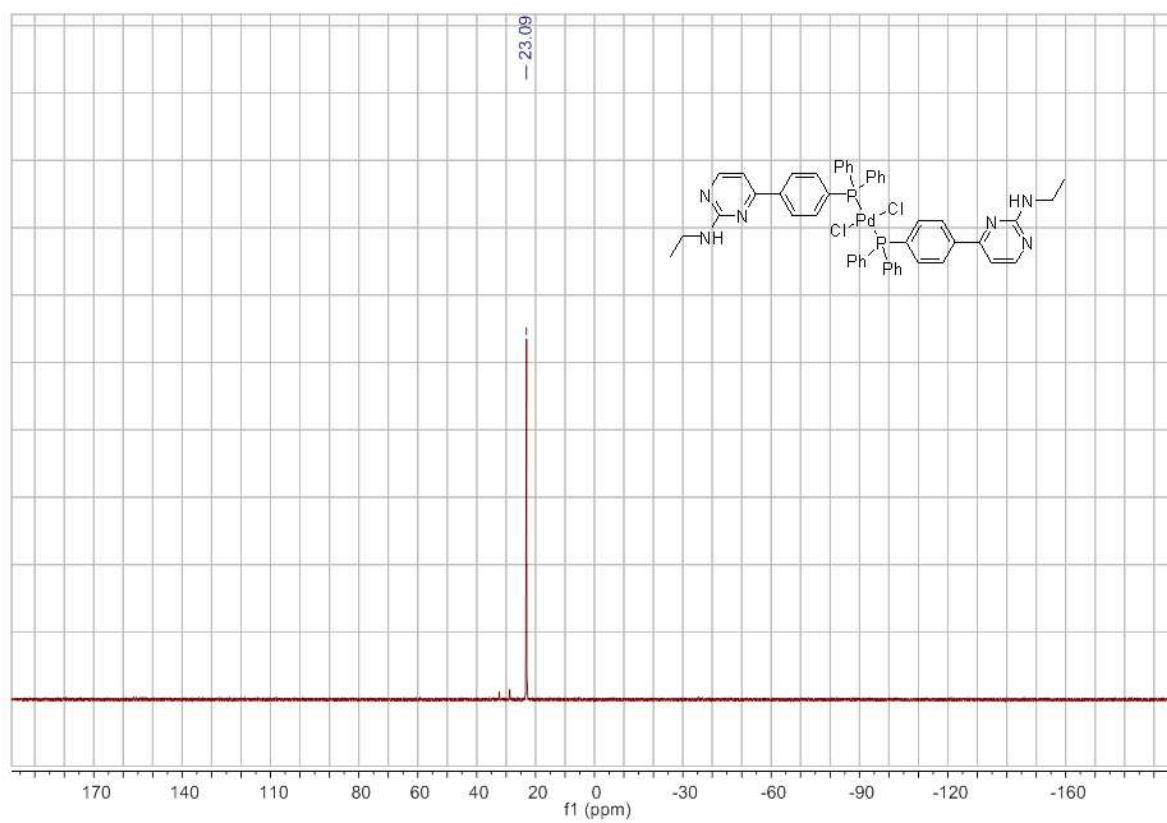
Figure 29. ^{31}P NMR spectra of **17.**

Results and Discussion
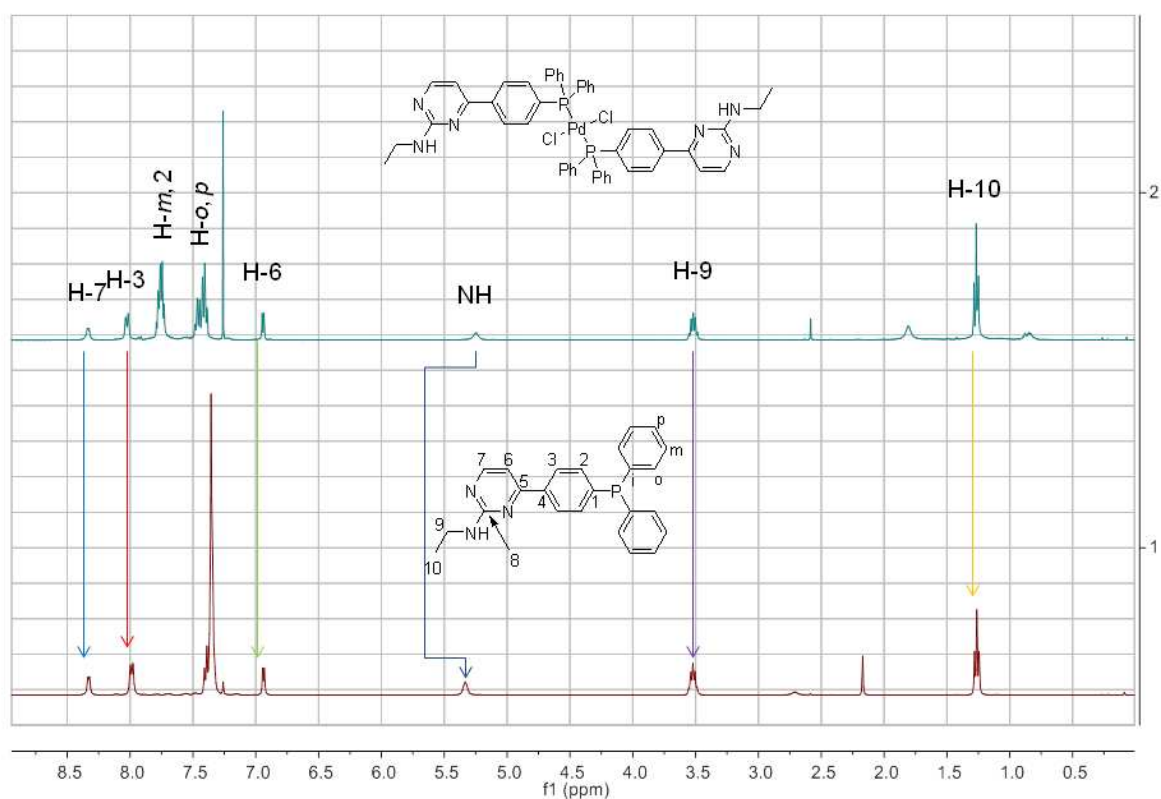
Figure 30. ^{1}H NMR spectra of **2b** (bottom), **17** (top).

Crystals of **17** suitable for X-ray crystallographic study were obtained from slow diffusion of ether into a CHCl$_3$ solution (**Figure 31**). The palladium complex **17** displays a *trans* configuration with respect to the pyrimidinylphosphine ligands and the coordination sphere is square-planar, with small distortion of bond angles P–Pd–Cl (92.13(3) and 87.87(3)).

63

Results and Discussion
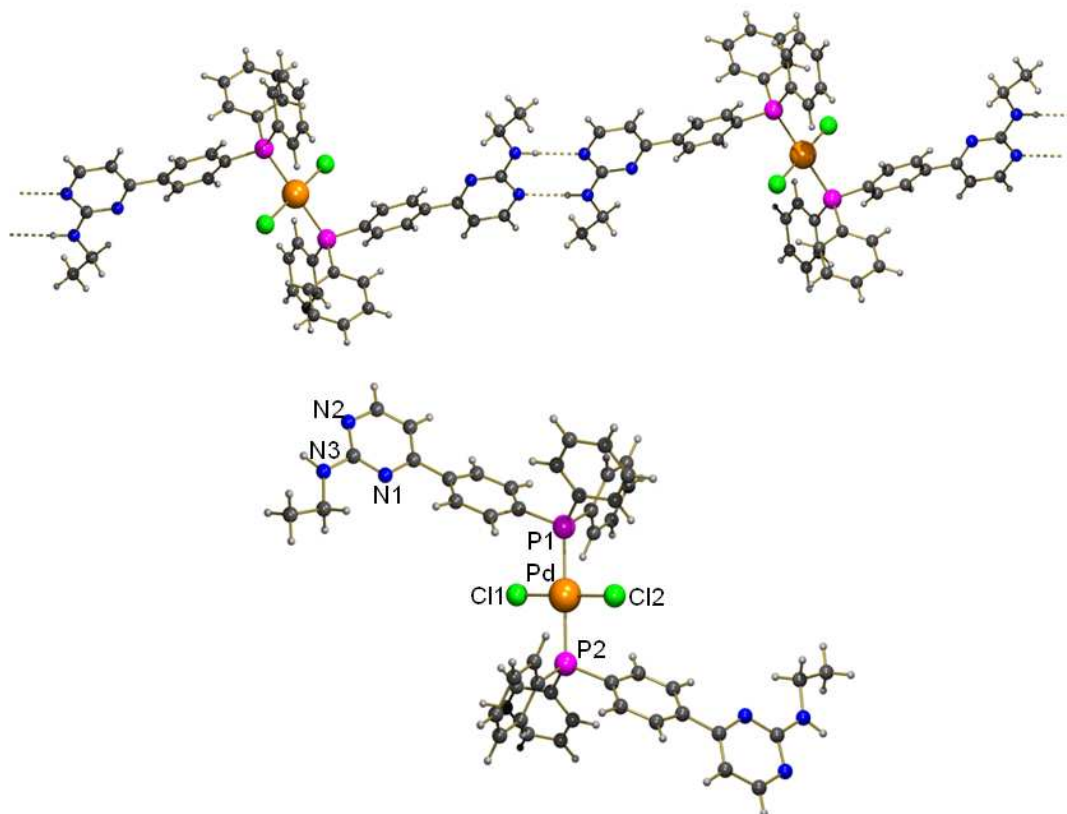
Figure 31. Molecular structures of the palladium complexes **17** in the solid state; Characteristic bond lengths [Å] and angles [°]: Pd1–Cl1 2.2865(9), Pd1–Cl2 2.2865(9), Pd–P1 2.3568(8), Pd–P2 2.3568(8), Cl1–Pd–Cl2 180.000(1), P1–Pd–P2 180.0.

3.2.5. Palladium Complexes with Pincer-Type *PNN* and *PN* Ligands Based on 3-Aminopyrimidyl pyridine

Pincer ligands are a specific type of chelating ligand with three coordination sites abbreviated to EYE in which E are usually NR_2, PR_2, SR, and SeR sides which strongly influenced the electronic properties of the metal center. The first pincer ligands with typical ECE arrangement and their corresponding metal complexes were reported by Shaw and co-workers[107] in 1976. Here the metal atom (Pd, Ni, Pt, Rd, Ir) is hold in place by a monoanionic, terdentate symmetric PCP ligand. This pioneering work has been followed by a large number of reports on synthesis and application of a wide variety of pincer complexes.

Results and Discussion

The replacement of a carbon atom in the ECE skeletal system by other elements such as silicon, phosphorus and in some cases, a neutral aromatic nitrogen atom (Y = N) has been used to further promote this type of ligands. In addition, nonsymmetrical pincer ligands containing two different donors (EYE) exhibited superior catalytic activity. Among them phosphorus-containing pincer-type ligands are particularly well defined. As examples of palladium complexes of phosphine-based PCN pincer ligands (Form (**I**), **Scheme 30**), Song et al. prepared and characterized complexes of **L10** and **L11**.[108] Motoyama and co-workers prepared a palladacycle of **L12** in order to use it as a catalyst in stereoselective transformations.[109] Raul SanMartin and his group reported the synthesis and the most relevant catalytic properties of palladacycles containing ligand **L13** in Suzuki, Sonogashira, and Hiyama cross-coupling reactions.[110]
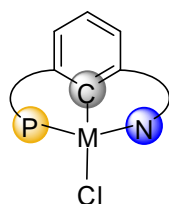
(I)
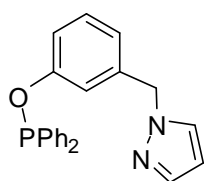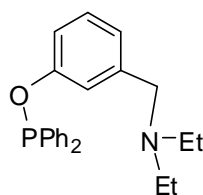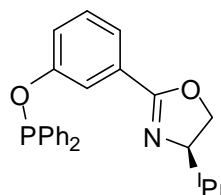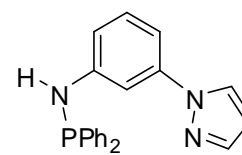
L10   **L11**   **L12**   **L13**

Scheme 30. Pincer frameworks (I) and PCN ligands **L10-L13**.

Metal (Pd(II) and Ru(II)) complexes of phosphine-based PNN pincer ligands (Form (**II**), **Scheme 31**) have been developed over the last decade. Vrieze and his group have described the ligand **L14**, showing the P-sp^3, N-sp^2 (imine), N-sp^2 (pyridinyl) donor sequence,

Results and Discussion

and several different transition metal complexes bearing **L14**.[111,112] Later on Del Zotto and his group investigated the coordination chemistry of **L14** towards group 10 metal halides.[113] Ruthenium pincer complexes of PNN ligands **L15** and **L16** (Form (**III**), **Scheme 31**) have been investigated by Milstein and co-workers.[114] These ruthenium complexes, well-known as Milstein catalysts, have been studied in multifarious catalytic applications, for instance direct synthesis of amides from alcohols and primary amines,[115] hydrogenation of esters in high yields under mild conditions,[116] dehydrogenative coupling of alcohols to form esters,[117] hydrogenation of CO_2 derived carbonates, carbamates, and formates.[118]
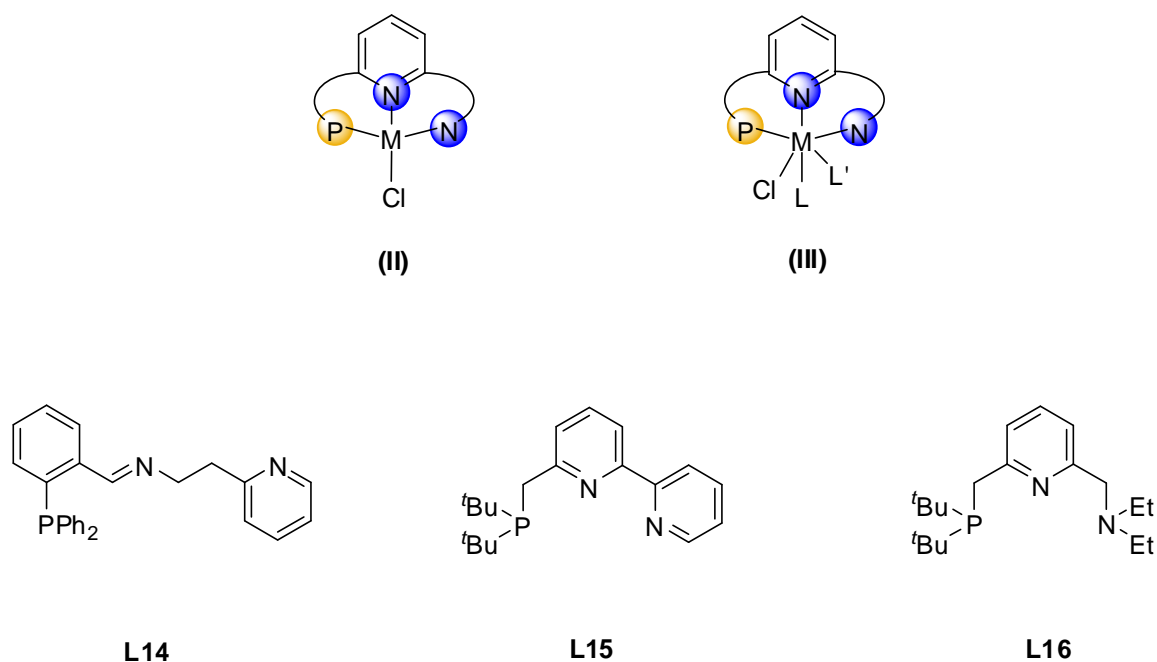
Scheme 31. Pincer frameworks (II), (III) and PNN ligands **L14-L16**.

Reacting ligand **12b** with the palladium (II) precursor $(C_6H_5CN)_2PdCl_2$ at room temperature in dichloromethane for 24 h gave an orange colored solid (**Scheme 32**). Two different products were detected by means of NMR spectroscopy (**Figure 32** and **Figure 33**). Using $CHCl_3$ as the solvent and heating to gain just one product was as well unsuccessful. Attempts to separate the products by crystallization also failed.

Results and Discussion
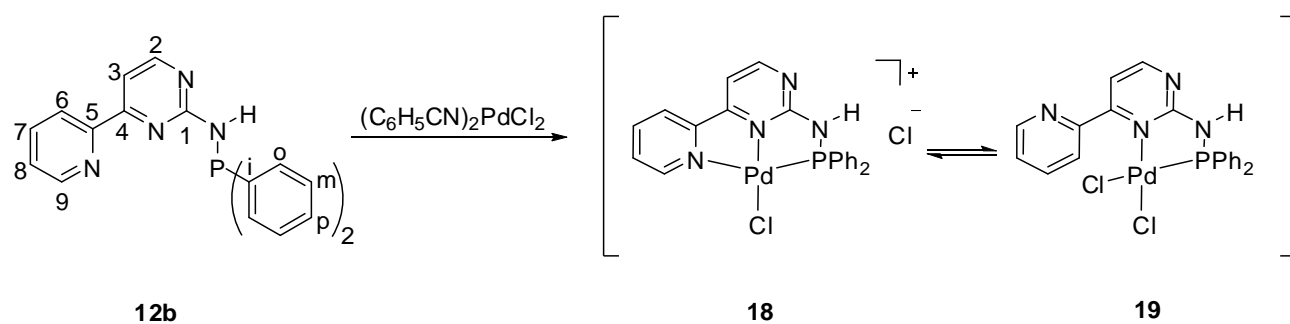
Scheme 32. Synthesis of a palladium pincer complex from ligand **12b**.
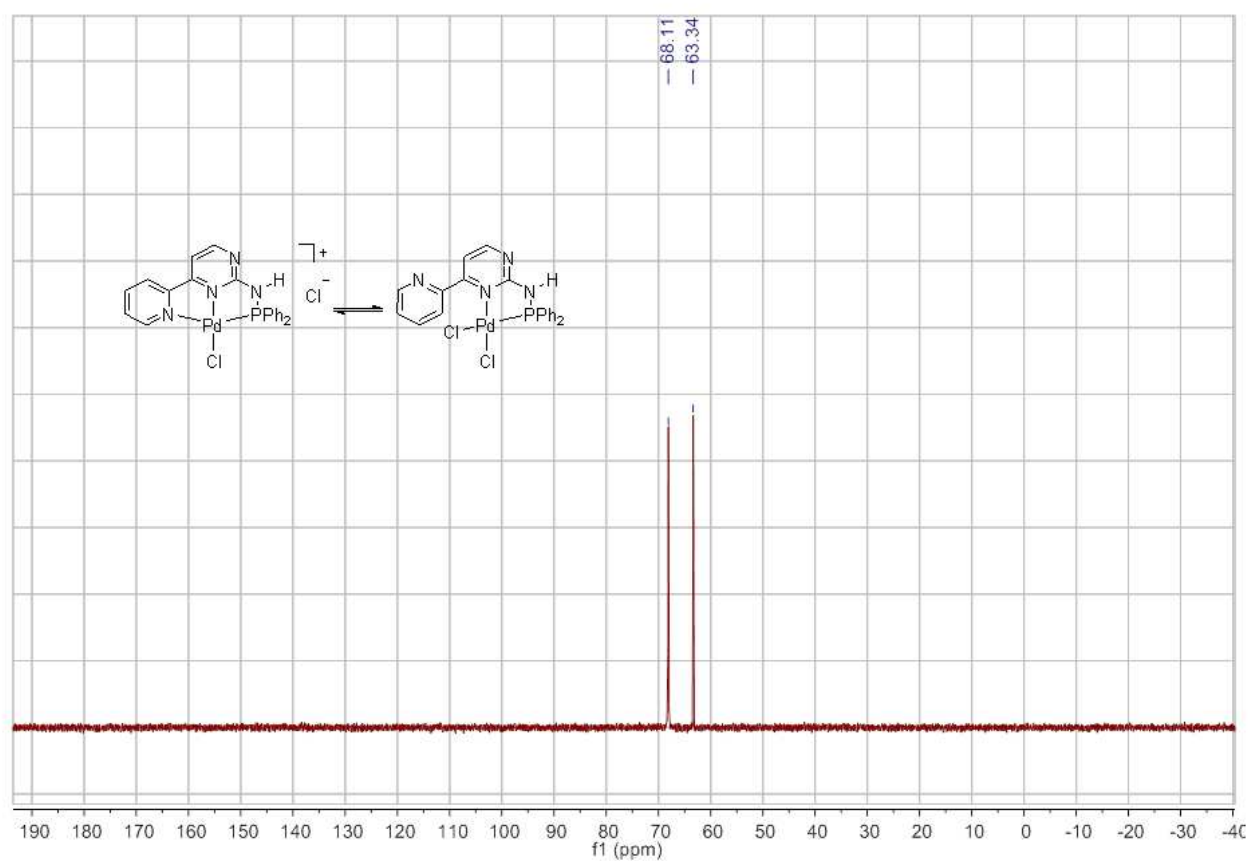
Figure 32. ^{31}P NMR spectrum of the product mixture in DMSO-d$_6$.

Results and Discussion
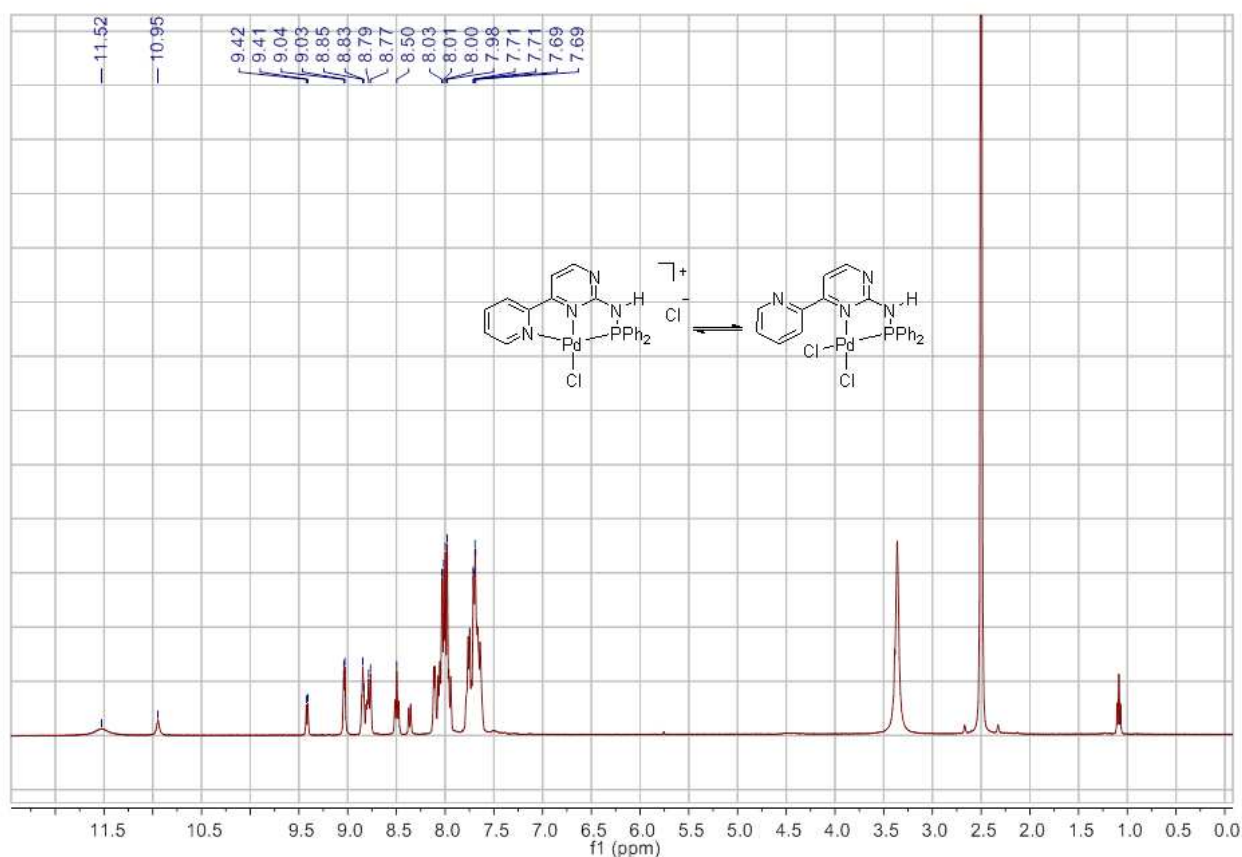
Figure 33. ^{1}H NMR spectrum of the product mixture in DMSO-d_6.

In order to find out the composition of the mixture in the solid state, an inert-atmosphere MALDI-TOF study of the mixture was carried out using, 4-hydroxy-α-cyanocinnamic acid (HCCA) as the matrix. MALDI characterization of the sample showed just the complex **18** which was clearly observed in the MALDI-TOF spectrum at m/z = 498.27 (M, Calcd. for $C_{21}H_{16}ClN_4PPd$for the signal w: m/z = 497.98 ith highest intensity). The peak (at m/z = 498.27) can be generated by the elimination of one molecule of HCl (chloride counter anion and probably a proton from the N-H group) from complex (**Figure 34**). According to these results complex **18** should be the single component in the solid state. To find out the effect of the solvent, NMR spectra of the sample in CD$_3$CN, and also CDCl$_3$ as non coordinating solvent were measured (**Figure 35**). In both cases two different complexes were observed as in DMSO-d_6.

68

Results and Discussion
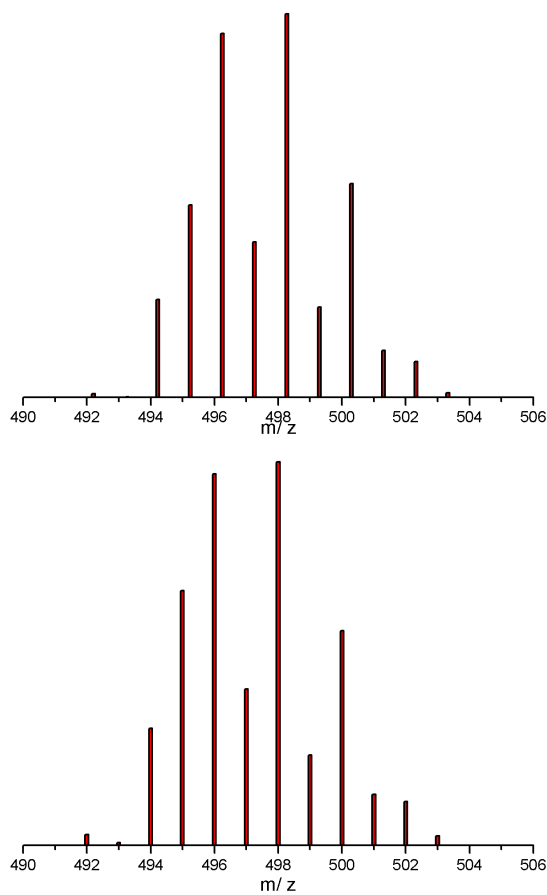
Figure 34. Inert-atmosphere MALDI-MS spectra (HCCA matrix) showing observed (top) and simulated (bottom) isotope patterns for compound **18**.

Results and Discussion

^{31}P NMR spectra measured in a range of 218 K to 328 K (**Figure 35**) showed that by varying the temperature, the proportion of mixture changes.
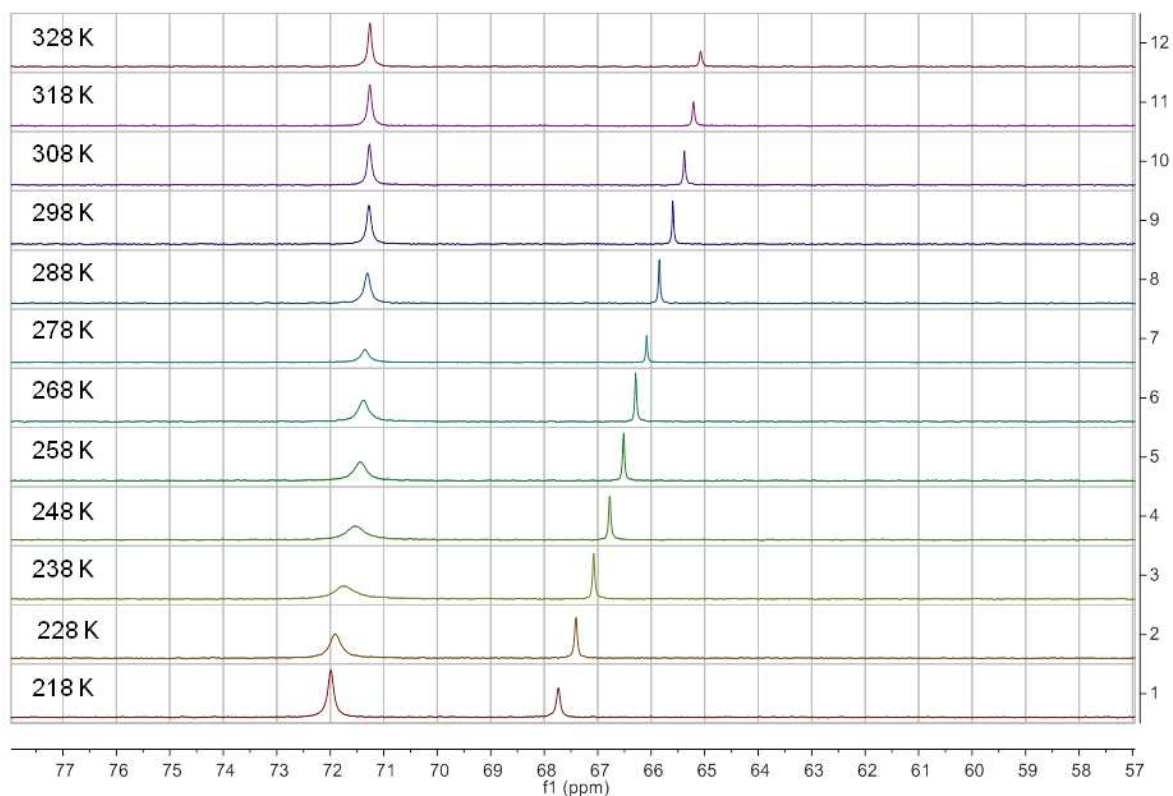
Figure 35. Variable temperature ^{31}P NMR spectra of the mixture **18** and **19**.

Finally palladium complex **20** was obtained as a pale orange solid by adding an excess amount of KF_6 to the reaction mixture (**Scheme 33**). The reaction mixture was stirred over night and the precipitated yellow solid was filtered and KCl as well as excess of KF_6 was washed with water.

Results and Discussion
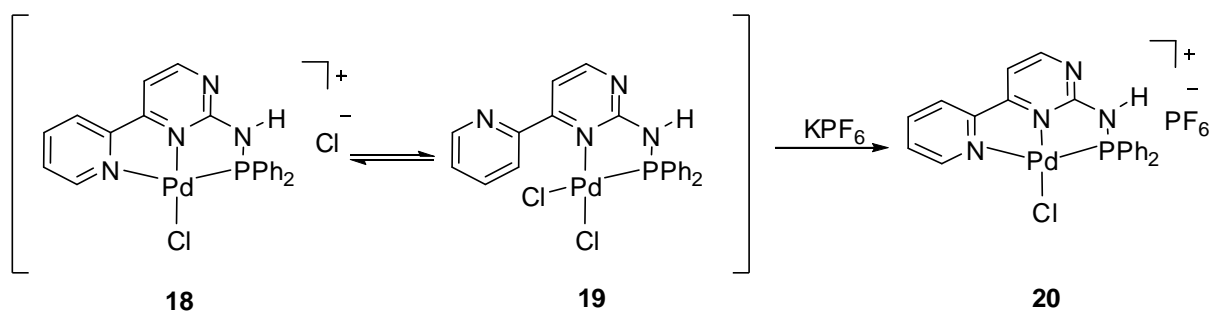
Scheme 33. Synthesis of complex **20**.

The ^{31}P NMR spectrum of **20** recorded in DMSO-*d6* indicates two resonances at about 65.64 ppm and –144.2 ppm (septet) which belongs to the counter anion (**Figure 36**). The ^{1}H NMR spectrum of **20** shows that, after coordination to palladium, the resonance of all hydrogen atoms shifted to lower field in comparison to the free ligand (**Figure 37**). Among them, the resonance of the hydrogen atom of the amino group dramatically shifted to lower field by about 3 ppm.

Results and Discussion
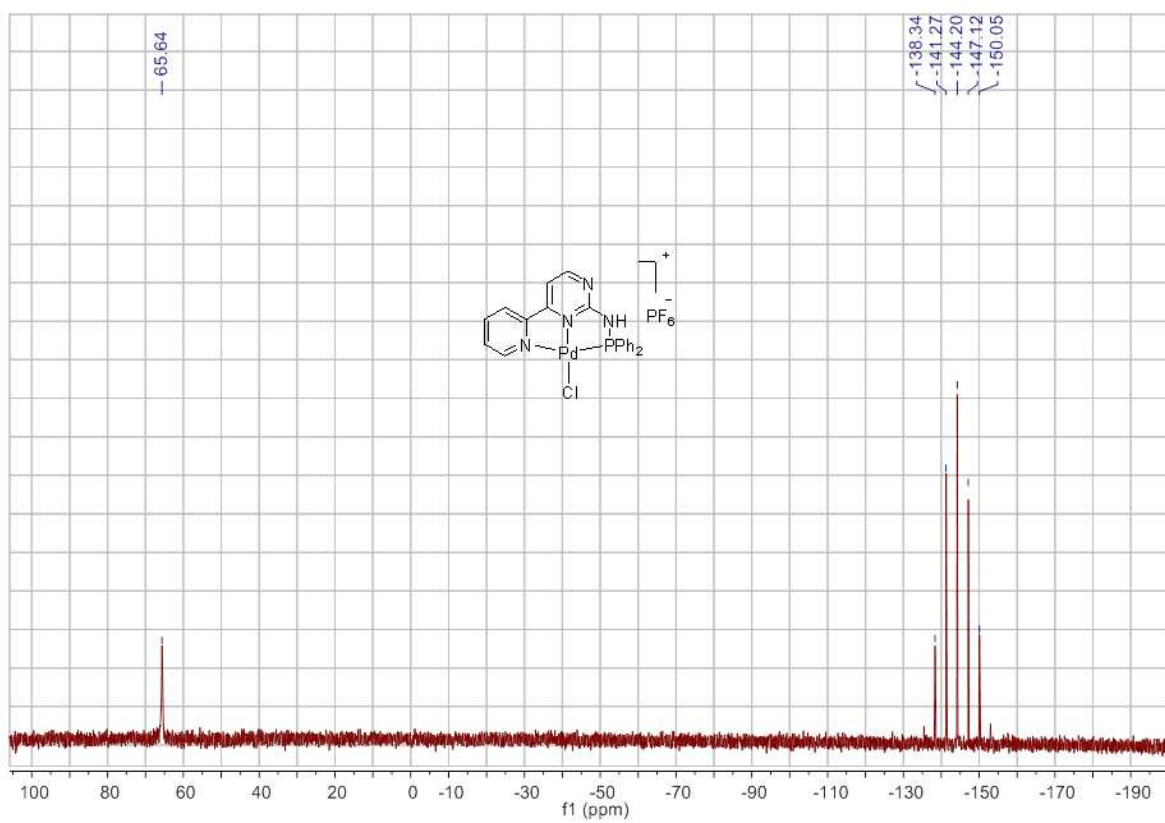
Figure 36. [31]H NMR spectrum of **20**.

Results and Discussion
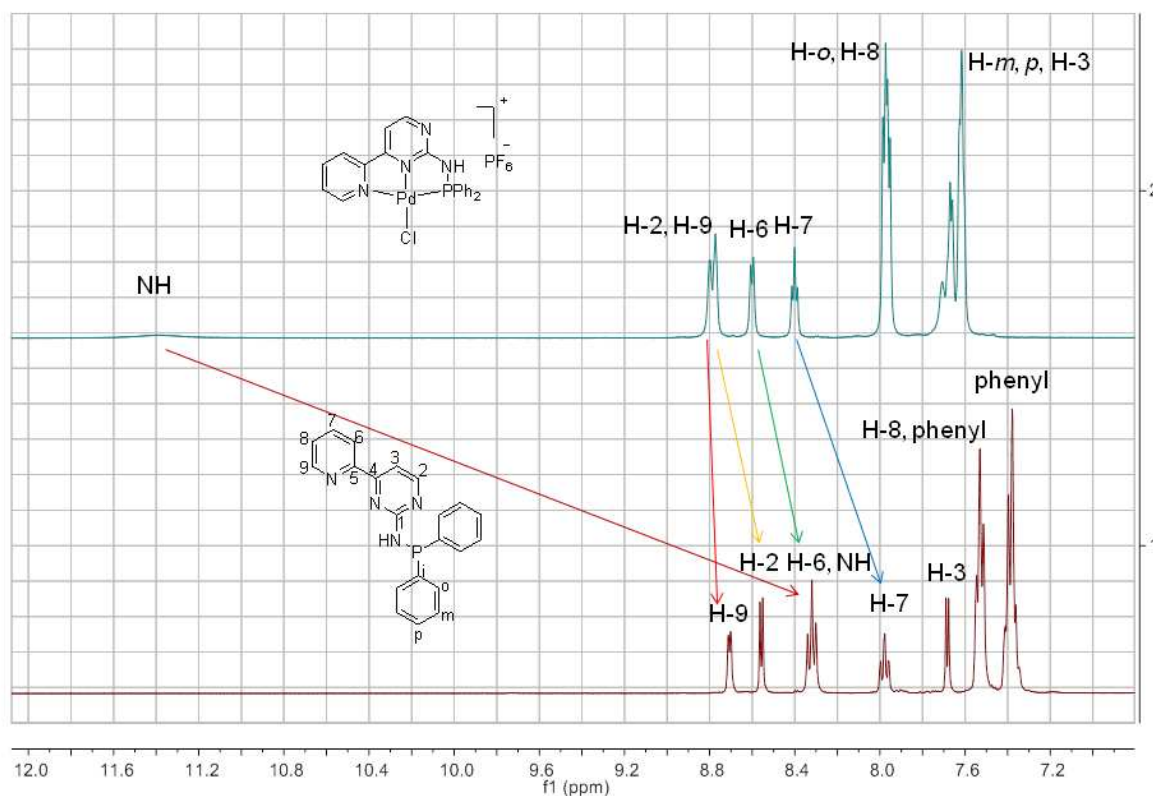
Figure 37. ^{1}H NMR spectra (aromatic region) of **12b** (bottom) and **20** (top).

Vapor diffusion of ether in to the solution of **20** in DMSO/Ethanol/CHCl$_3$ provided suitable crystals for X-ray analysis in which complex **20** crystallized with one molecule of DMSO hydrogen-bonded with the NH group (**Figure 38**). The X-ray structure analysis of **20** shows that the ligand is coordinated to the palladium(II) center via the nitrogen atom of the pyridine ring (N-4), the nitrogen atom of the pyrimidine ring (N-2), and the phosphorous atom of the phosphine in a tridentate manner (**Figure 38**). The Pd–P (2.2143(4) Å) bond length is comparable to those in a related PCN pincer palladium complex,[118,119] but slightly shorter than the Pd–P distance found in related symmetrical PCP-bis(phosphinite) pincer palladium complexes (2.26–2.29 Å).[120,121,122] The Pd–N$_{pyrimidinyl}$ distance (1.9690(13) Å) is shorter than Pd–N$_{imine}$ in related PNN palladium complex[113] (2.037(4) Å) as well as the Pd–N$_{pyridin}$ distance in SNS palladium complex[123] (1.993(16) Å). The strongly distorted square planar geometry

Results and Discussion

around the palladium atom is also remarkable, as shown by the Cl–Pd–C9 and P–Pd–N1 bond angles. The small (162.52(4)°) P1–Pd–N4 bond angle is in agreement with a pincer consisting of two five-membered ring palladacycles[118,120,121,124,] and indicates a relatively strong steric strain in the closely planar (see torsion angles in **Figure 38**) tetracyclic core.
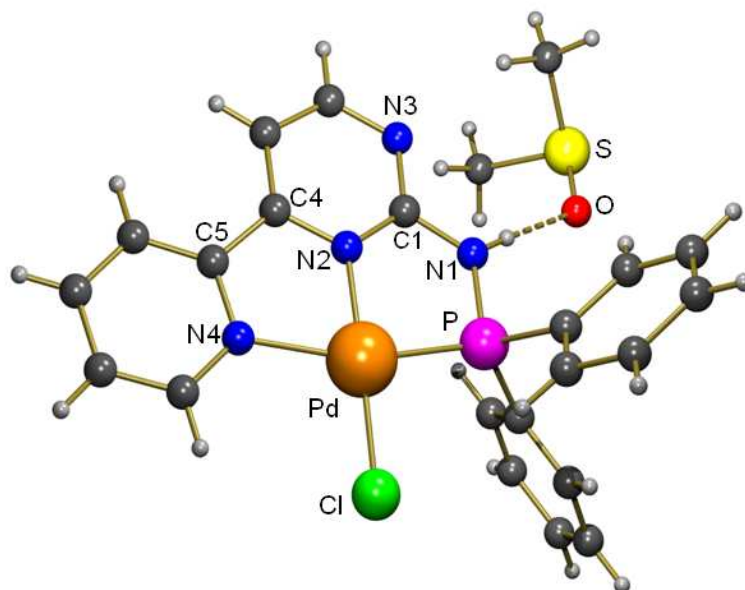
Figure 38. Molecular structure of the cation of the palladium complex **20** in the solid state. Selected bond lengths [Å] and angels [°] for complex **20**. Pd–P1 2.2143(4), Pd–N2 1.9690(13), Pd–N4 2.1074(14), Pd–Cl 2.2897(4), N1–P1 1.6875(15), C1–N1 1.361(2), C1–N2 1.344(2), C1–N3 1.335(2), C4–C5 1.472(2). N4–Pd–P1 162.52(4), N2–Pd–Cl 178.44(4), P1–N1–C1 118.86(12), C1–N2–C4 120.12(13), C4–C5–N4 115.30(14), P1–N1–C1–N3 173.03, N4–C5–C4–C3 178.90, Pd–P1–N1–C1 7.29, Pd–N4–C5–C4 –0.85.

Reacting ligand **12c** (containing a phenyl group at the 5-position of pyrimidyl ring) with the palladium(II) precursor $(C_6H_5CN)_2PdCl_2$ at room temperature in dichloromethane solution gave the orange colored ionic palladium(II) complex **21** in almost quantitative yield.

74

Results and Discussion
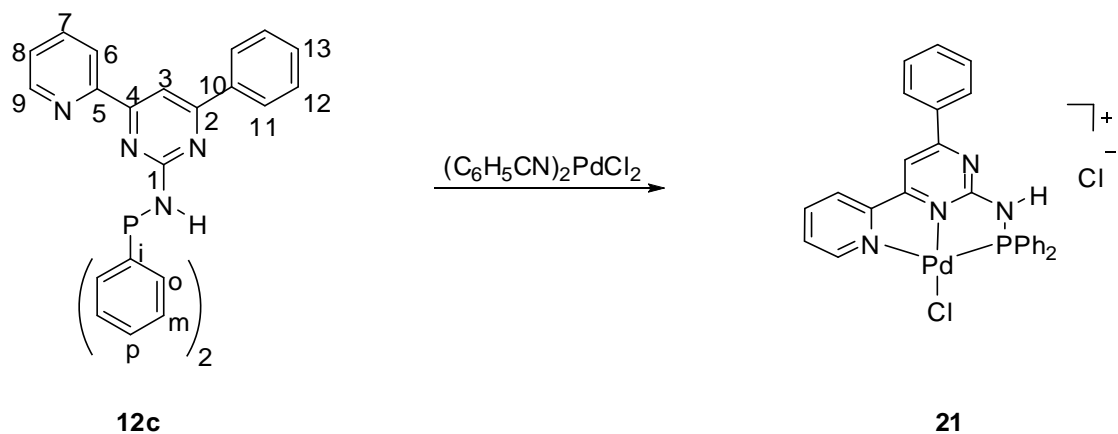
Scheme 34. Synthesis of complex **21**.

^{31}P NMR and ^{1}H NMR spectra of **21** are shown in **Figure 39**, and **Figure 40** respectively and both spectra clearly prove a single complex in solution- in contrast to the formation of **18** and **19** from **12b**- which has a PNN coordination mode.

Results and Discussion
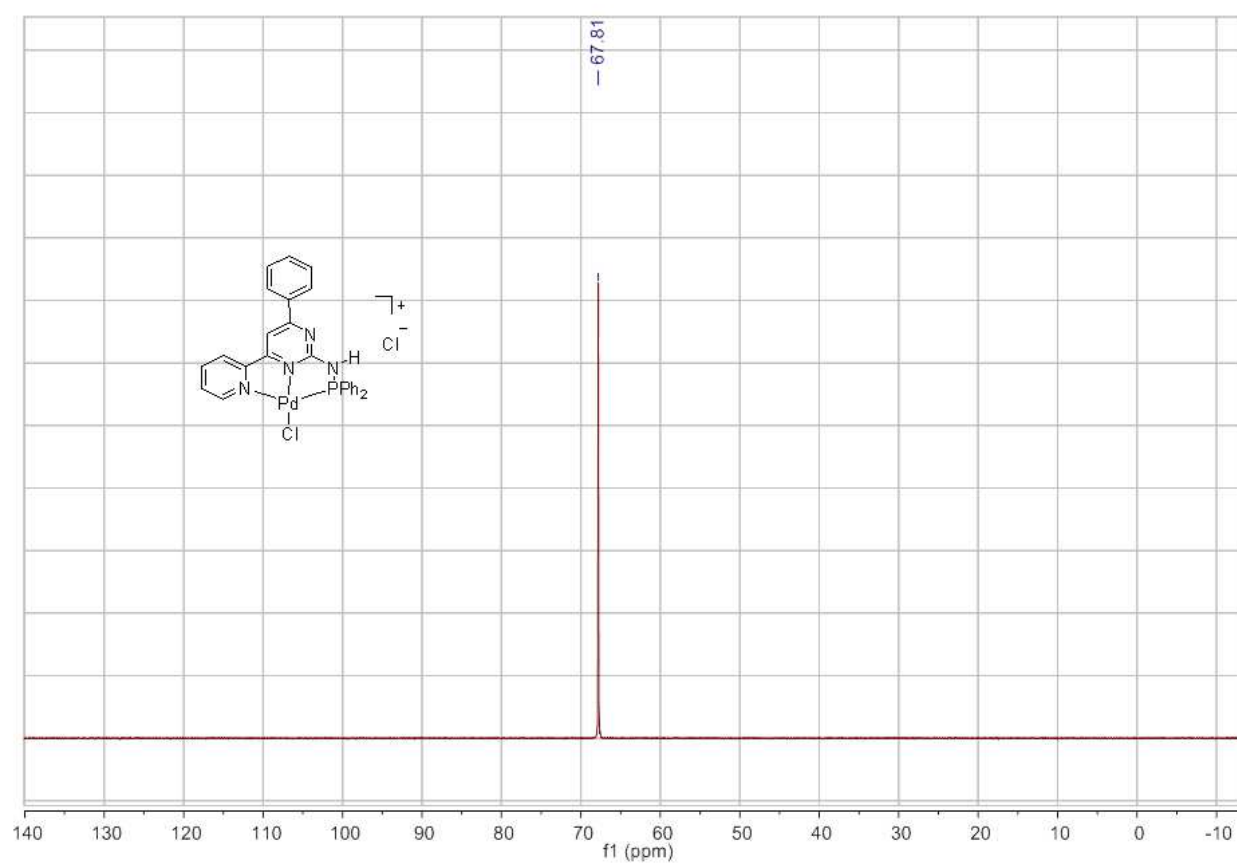
Figure 39. ^{31}P NMR spectrum of complex **21**.

Results and Discussion
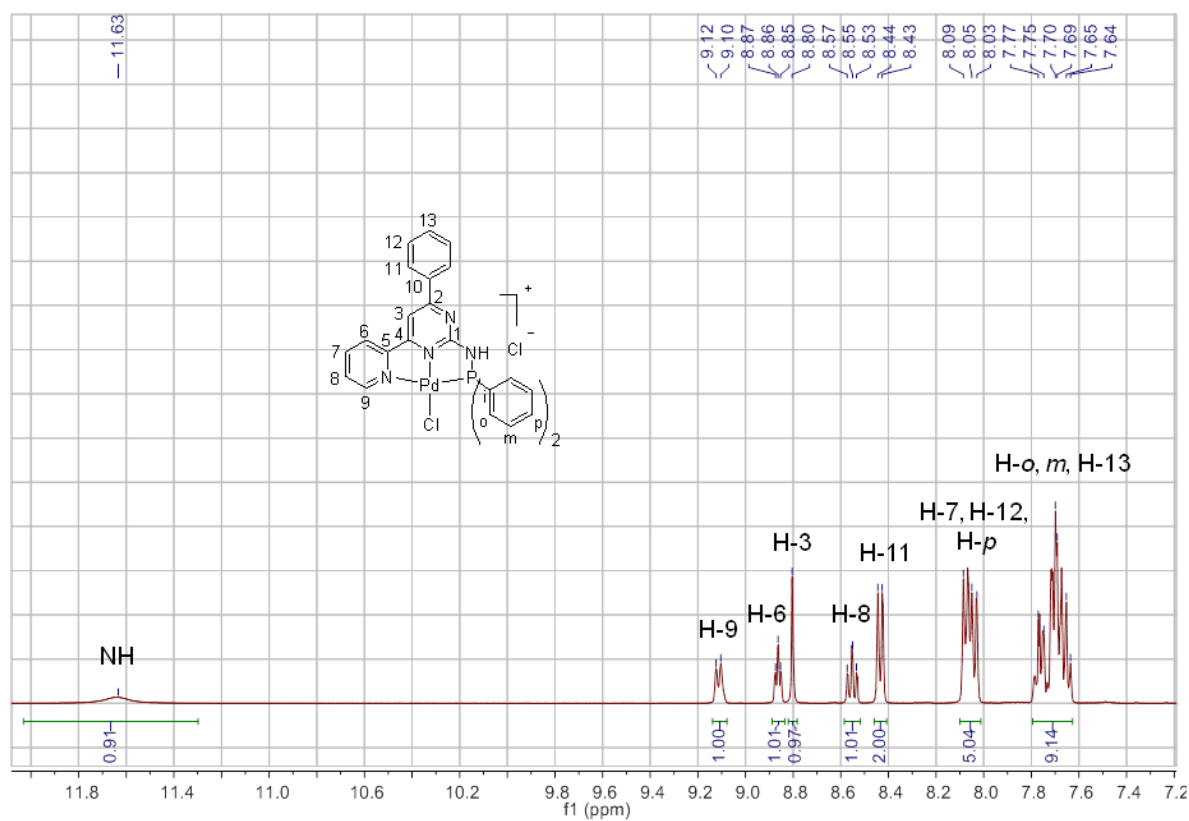
Figure 40. ^{1}H NMR spectrum (aromatic region) of complex **21**.

Reacting the ligand **12a** with the palladium(II) precursor (C$_6$H$_5$CN)$_2$PdCl$_2$ at room temperature in dichloromethane solution gave the orange colored neutral palladium(II) complex **23** in almost quantitative yield (**Scheme 35**).

Results and Discussion
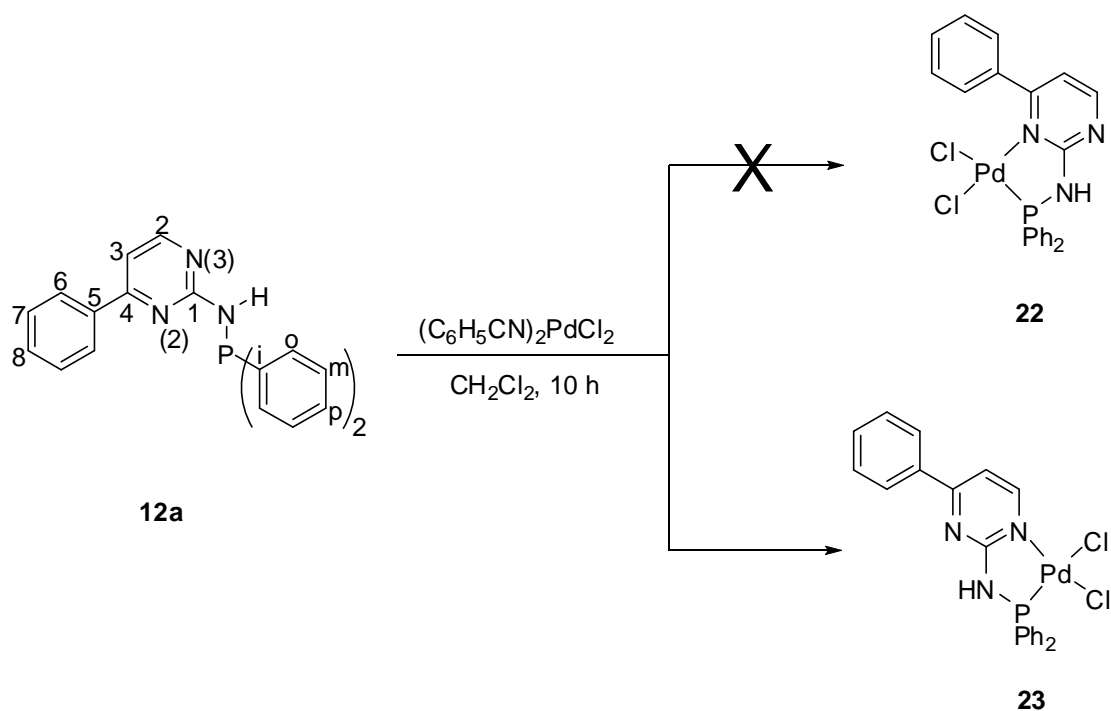
Scheme 35. Synthesis of complex **23**.

The ^{1}H NMR spectrum of the product in comparison to the free ligand **12a** indicates that the resonances of all C-H hydrogen atoms are shifted to lower field (**Figure 41**). The resonance of the N-H proton of the 2-aminopyrimidinyl group is also shifted towards lower field compared to the free ligand and is observed at 10.84 ppm. The ^{1}H NMR spectroscopic data also confirm the coordination mode of **12a** through N-3 of the pyrimidinyl ring. Coordination of the pyrimidinyl nitrogen atom (N-3) to the metal centre causes the signal for H-2 of the pyrimidinyl ring to be shifted downfield with respect to the free ligand **12a** ($\Delta\delta$ = 0.82 ppm). According to the literature, a downfield shift for the α protons of the coordinated pyridine moieties offers a proof for coordination of the nitrogen atom.[125,126] As expected, the ^{31}P resonance of **23** (63.4 ppm) is shifted to lower field compared to the free ligand **12a**.

Results and Discussion
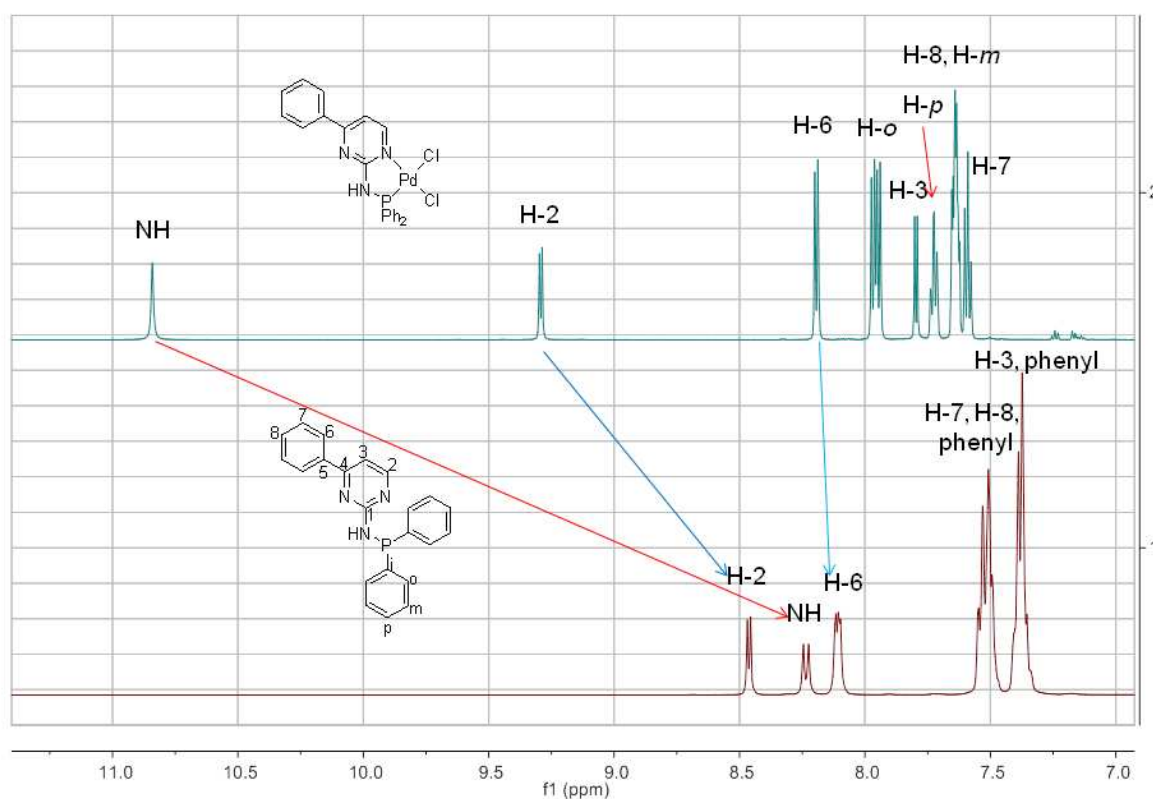
Figure 41. ^{1}H NMR spectra (aromatic region) of **12a** (bottom) and **23** (top).

Orange crystals of **23** suitable for X-ray diffraction measurement were obtained from vapor diffusion of ether in to the DMSO/CHCl$_3$ solution of **23** (

Figure 42). **23** crystallizes in the monoclinic space group P2$_1$/c with four molecules and four DMSO units in the unit cell, forming intermolecular hydrogen bonding between the N-H proton of one molecule and the oxygen atom of DMSO (**Figure 42**). The crystal structure confirmed the chelating coordination mode of the ligand, in which the *P,N* units together with the chloride ligands form a distorted square-planar coordination sphere around the palladium. The largest angle is 94.13(6)° belongs to N2–Pd–Cl1 while the smallest angle is 83.76(6)° belonging to N2–Pd–P1. The Pd–Cl1 bond length *trans* to the phosphorus atom (2.3601(6) Å) is longer than the Pd–Cl2 bond length *trans* to the nitrogen atom (2.2977(6) Å) which can be explained due to the larger trans influence of the phosphorus donor over the nitrogen donors

Results and Discussion

(imine and pyri dine).[127]
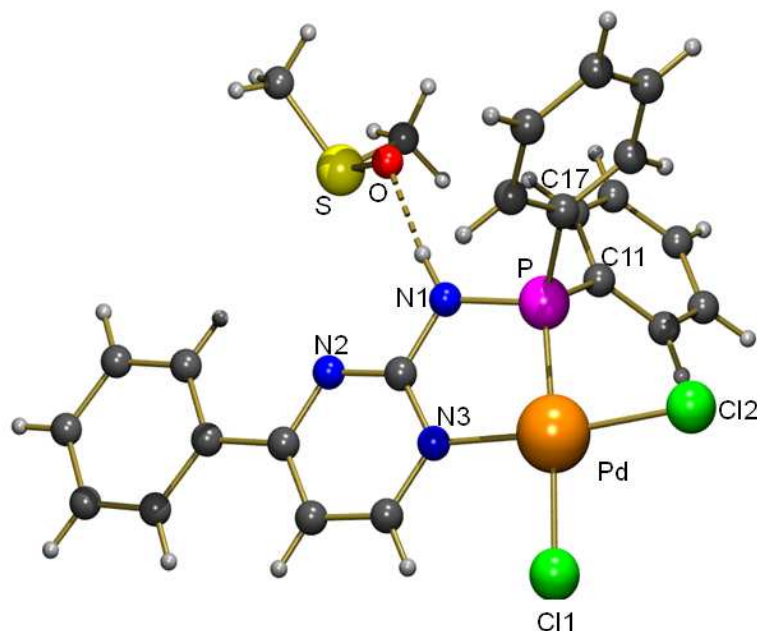
Figure 42. Molecular structure of the palladium complex **23** in the solid state. bond lengths [Å] and angels [°] for complex **23** :Pd–P 2.1914(6), Pd–N3 2.0452(19), Pd–Cl1 2.3601(6), Pd–Cl2 2.2977(6), N1–P1 1.682(2), C1–N1 1.370(3), C1–N2 1.330(3), C1–N3 1.357(3), P–C11 1.802(2). N3–Pd–Cl2 172.64(6), P–Pd–Cl1 174.69(2), P1–N1–C1 118.79(17), P–Pd–N(3) 83.76(6), C11–P–C17 106.00(11), C11–P–Pd 119.69(8), C17–P–Pd 115.40(8), P1–N1–C1–N3 11.81, N2–C4–C5–C6 –0.03.

3.3. Homogeneous Catalytic Experiments

The synthesized palladium complexes were tested as catalysts for the Suzuki coupling reaction. The discovery of palladium complexes as catalysts for C–C bond formation turned out to be one of the fundamental advances in organic synthesis during the last years.[128] In 2010, it was highlighted by awarding the Nobel Prize to Heck,[129,130,131] Negishi[132,133,134] and

Results and Discussion

Suzuki. In 1979 Suzuki and his group reported that organoboron compounds can be used as coupling partners in palladium-catalyzed cross couplings with aryl- or vinyl -halides in the presence of a base (**Equation 1**).[135,136]

$$RBY_2 \; + \; R'X \quad \xrightarrow[\text{base}]{\text{palladium catalyst}} \quad RR' \; + \; \text{Inorganic Salts} \qquad (1)$$
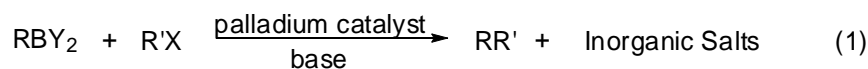
R, R' = aryl, vinyl and alkyl
X = halide, triflate, etc.
Y = alkyl, OH, O-alkyl

Equation 1. Suzuki cross coupling reaction.

Several advantages of Suzuki reaction are summarized below:

1. Organoboron compounds made this reaction readily applicable due to their stability and low nucleophilicity.

2. The reaction tolerates a wide range of functional groups reflecting the high chemoselectivity.

3. Many kind of organoborons compounds (especially boronic acids) are commercially available.

4. The inorganic by-products are easily removed from the reaction mixture, making the reaction suitable for industrial processes.

5. Dry solvents are generally not required.

These advantages have highlighted the reaction as an industrial powerful and convenient synthetic method for the preparation of biaryl derivatives that are structural components of natural products,[137] pharmaceuticals,[138,139,140,141,142] ligands,[143,144] polymers[145] and various materials.[146] The catalytic cycle of the palladium-catalyzed Suzuki reaction is thought to follow a sequence involving oxidative addition of the aryl halide to Pd(0) to give an

Results and Discussion

arylpalladium(II) halide intermediate. In the second step, called transmetalation, the organic

group, R on boron, is transferred to palladium. Finally two aryl groups couple together to give

a new carbon-carbon single bond and the corresponding biaryl is released from palladium. In

this process Pd(II) is reduced to Pd(0) and therefore the final step is called a reductive

elimination (**Scheme 36**). The role of the base in this reaction can be explained by two

proposed mechanisms:

The base initially reacts with the boronic acid to form a more reactive boronate species, and the

latter species are responsible for the transmetalation process with the palladium center (path A,

Scheme 36).[147] Alternatively, it has also been proposed that the halide is directly substituted by

the base in the coordination sphere of the catalyst (path B, **Scheme 36**).[148]
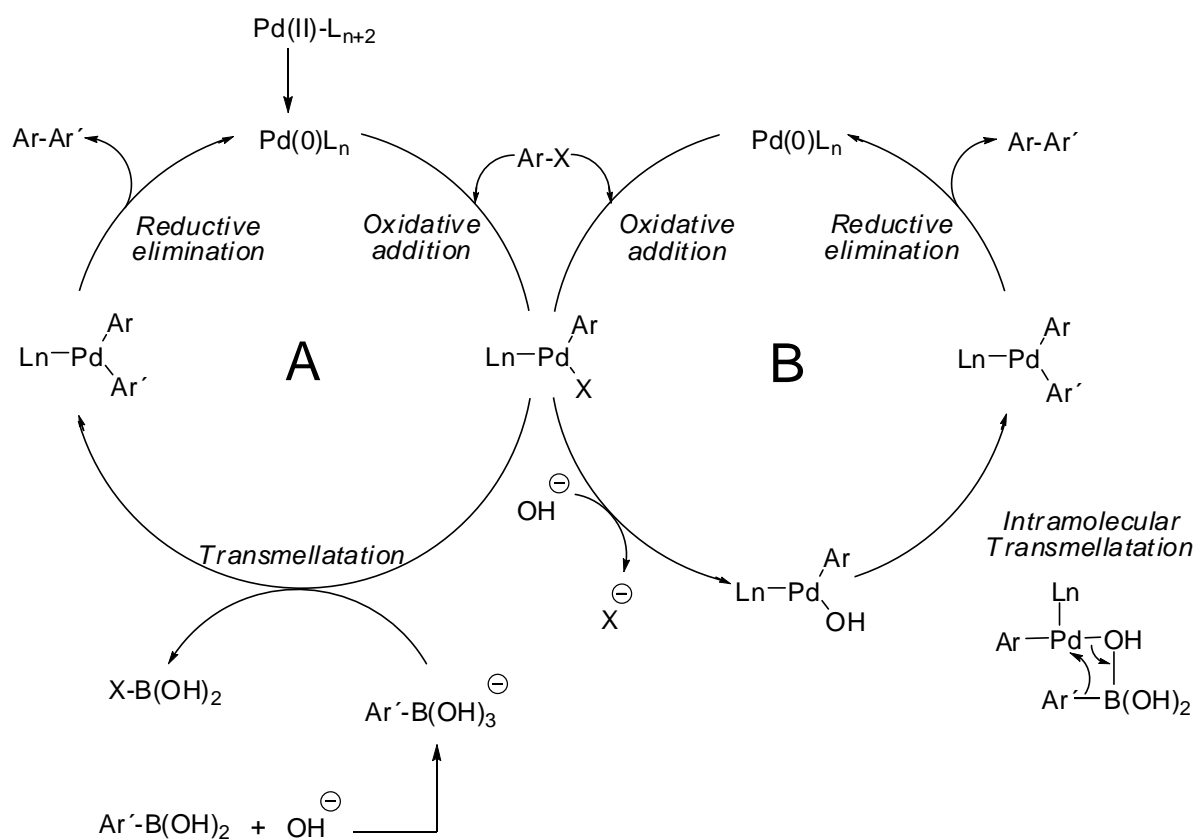
Scheme 36. General catalytic cycles for Suzuki couplings.[149]

Challenges associated with Suzuki reactions have focused on the use of unreactive

arylchlorides as coupling partners[150,151] and in developing catalysts that efficiently perform

Results and Discussion

under mild reaction conditions in combination with low catalyst loadings.[152,153,154,155,156] A remaining task is to achieve cross couplings under these mild conditions for highly hindered biaryl junctions.[157,158,159]

Palladium phosphine complexes such as Pd(PPh$_3$)$_4$ with strong phosphorus donors have been the most commonly employed as catalysts for this reaction.[160,161,162,163,164,165] Among them electron-rich and sterically bulky monophosphines exhibited considerably more activity in this reaction.[166,167]

As alternative ligand to tertiary phosphines, *N*-heterocyclic carbenes have been introduced in Suzuki reactions by Nolan and his coworkers.[168,169,170,171,172,173] These ligands have better donating properties than tertiary phosphines, but with restricted flexibility. Therefore, by attaching a donation group to at least one of the phenyl rings of PPh$_3$, bidentate hybride PX (X = N[174,175,176,177,178], O[179,180,181] and C[182]) ligands with difunctional properties and the flexibility of the backbone have been found to be catalytically active in a range of reactions. The use of these bidentate ligands in Suzuki reactions was reviewed by Hor and co-workers in 2008.[183]

3.3.1. Catalytic Activities

The palladium (II) complexes **14a,b** and **15a-c**, were investigated as catalysts for the Suzuki–Miyaura coupling reaction. To optimize the reaction conditions, we initially examined the coupling reaction of bromobenzene and phenylboronic acid with **14a** at 70 °C (**Table 6**). The reaction is strongly dependent on the used base and solvent. A combination of Cs$_2$CO$_3$ and EtOH gave the best results; 93% conversion of bromobenzene was achieved at 70 °C in 45 min with just 0.1 mol-% of **14a** (TOF: 1240 mol·mol^{-1}h^{-1}).

Results and Discussion

Table 6. Coupling of PhBr and PhB(OH)$_2$ with **14a**.[a]

Entry	Solvent	Cat.loading (mol-%)	Base	Time (h)	% Conversion [b]
1	1,4-dioxane	1	Na$_2$OAc	4	5
2	1,4-dioxane	1	Na$_2$CO$_3$	4	22
3	1,4-dioxane	1	K$_2$CO$_3$	4	38
4	1,4-dioxane	1	K$_3$PO$_4$	4	64
5	1,4-dioxane	1	Cs$_2$CO$_3$	4	69
6	toluene	1	Cs$_2$CO$_3$	4	41
7	DMF	1	Cs$_2$CO$_3$	4	2
8	DMF/H$_2$O	1	Cs$_2$CO$_3$	1	82
9	EtOH	1	Cs$_2$CO$_3$	0.75	94
10	EtOH	0.1	Cs$_2$CO$_3$	0.75	93
11	EtOH	0.01	Cs$_2$CO$_3$	0.75	73
12	EtOH	0.001	Cs$_2$CO$_3$	0.75	47

[a] PhBr (1 mmol), PhB(OH)2 (1.2mmol), base (1.2 mmol), solvent (5 mL), 70 °C. [b]

Determined by GC based on PhBr.

Then I explored the influence of the amino substituent with catalysts **14a,b** and **15a** (**Table 6**). Whereas at 70 °C the activities of **14a,b** and **15a** differ solely by a factor of two, a decrease in the reaction temperature to 60 °C makes catalyst **14a** fail completely. Even going down to lower temperatures (40 °C) the differences between catalytic activity of **15a** (90%) and **14b** (12 %) become more pronounced. Investigations at room temperature showed that **14b** and **15a** are still active; **15a** gave 87% conversion of bromobenzene after 240 min. Encouraged by these results the reaction conditions were optimized again for **15a**. It was found that the best results were obtained with a 1:1 mixture of DMF/H$_2$O and Cs$_2$CO$_3$ as the base; 0.1 mol-% of the catalyst gave 80% conversion of bromobenzene in 45 min at room temperature.

Results and Discussion

14a

14b

15a

15b

15c

16
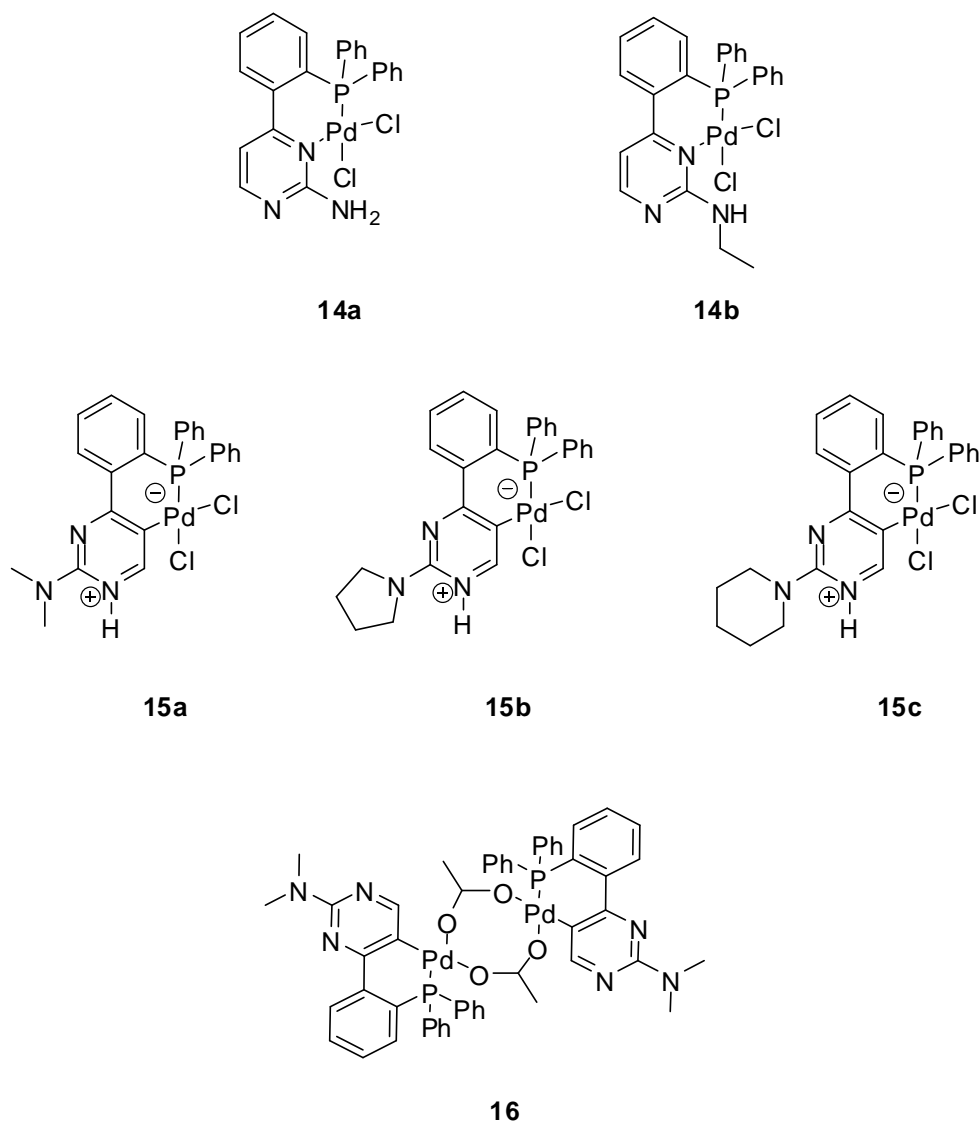
Scheme 37. Palladium catalysts **16**, **14a,b** and **15a-c**.

Results and Discussion

Table 7. Coupling reactions of PhBr and PhB(OH)$_2$ with **14a,b** and **15a** at variable temperatures.[a]

Entry	Cat.	T [°C]	Time (min)	% conversion [b]
1	**14a**	70	15	49
2	**14b**	70	15	96
3	**15a**	70	15	75
4	**14a**	60	45	traces
5	**14b**	60	45	97
6	**15a**	60	45	83
7	**14a**	40	45	0
8	**14b**	40	45	12
9	**15a**	40	45	90
10	**14a**	r.t.	45	0
11	**14a**	r.t.	240	0
12	**14b**	r.t.	45	traces
13	**14b**	r.t.	240	23
14	**15a**	r.t.	45	46
15	**15a**	r.t.	240	87

[a] PhBr (1 mmol), PhB(OH)$_2$ (1.2 mmol), Cs$_2$CO$_3$ (1.2 mmol), catalyst (0.1 mol %), EtOH (5 mL). [b] Determined by GC based on PhBr.
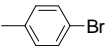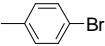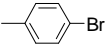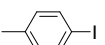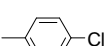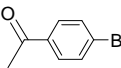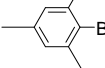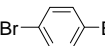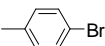
To elucidate the influence of the amine substituents, the pyrrolidinyl and piperidinyl functionalized catalysts **15b** and **15c** (**Scheme 37**) were included in the study. The bulky piperidinyl group gave even better results than **15a** for the coupling of 4-bromotoluene with phenylboronic acid (**Table 8**, entries 1–3). Whereas 4-iodotoluene underwent coupling with phenylboronic acid (entry 4), the catalyst failed with the coupling of 4-chlorotoluene (entry 5). Reacting 4-bromoacetophenone as an electron deficient substrate gave the coupled product in 93% yield after 1 h with 0.1 mol-% and after 10 h with 0.01 mol-% of catalyst (entries 6 and 7). Sterically hindered substrates bearing one *ortho*-substituent could also be coupled efficiently at room temperature with 0.1 mol-% of catalyst **15c** in just 1 h (entries 9 and 10). However, 2-bromomesitylene bearing two methyl substituents in the *ortho*-position to bromine

Results and Discussion

required a higher catalyst loading (1 mol-%, entry 12). On the other hand, 0.1 mol-% of **15c** resulted in the almost quantitative coupling of 1,4-dibromobenzene with 2.5 equiv. of phenylboronic acid at room temperature in 1 h (entry 13). The use of dimeric palladacycle **16** as a non zwitterionic complex gave conversions almost similar to **15a** (entry 14 vs. 1).

Table 8. Coupling reactions of a variety of aryl halides with phenylboronic acid at room temperature using the palladium catalysts **15a-c** and **16**.[a]

Entry	Aryl halide	Cat.	Cat. loading (mol-%)	Yield[b] (%)[b]
1	(benzene)–Br	**15a**	0.1	77
2	(benzene)–Br	**15b**	0.1	59
3	(benzene)–Br	**15c**	0.1	88
4	(benzene)–I	**15c**	0.1	61
5	(benzene)–Cl	**15c**	0.1	0
6	(acetyl)(benzene)–Br		0.1	93
7[c]		**15c**	0.01	93
8[c]			0.001	6
9	(o-methyl)(benzene)–Br	**15c**	0.1	41
10	(o-acetyl)(benzene)–Br	**15c**	0.1	8
11	(dimethyl)(benzene)–Br		0.1	traces
12[c]		**15c**	1	48
13[d]	Br–(benzene)–Br	**15c**	0.1	95[e]
14	(benzene)–Br	**16**	0.1	80

[a] Aryl halide (1 mmol), phenylboronic acid (1.2 mmol), Cs_2CO_3 (1.2 mmol), reaction time: 1 h, DMF/H2O (v/v = 1:1, 5 mL), room temperature. [b] NMR yield. [c] 10 h. [d] Phenylboronic acid (2.5 mmol). [e] Isolated yield.

Results and Discussion

In the commonly accepted mechanism of palladium-catalyzed coupling reactions, palladium(0) species, either introduced directly or formed in-situ, undergo oxidative addition of the aryl halide. Amatore et al. proved for the Heck olefination and other coupling reactions, that the formation of anionic palladium(0) species such as $[XPdL_2]^-$ (X = halide, acetate, etc.) strongly facilitates the oxidative addition of the substrate.[184] It can be assumed that, in the presence of a base such as Cs_2CO_3, C–H activation of the pyrimidine site will lead to anionic palladium(II) compounds, which, after in-situ reduction, will give anionic palladium(0) species.

3.4. Covalently Supported Pyrimidinylphosphine Palladacycles as a Heterogenized Catalysts for the Suzuki–Miyaura Cross Coupling.

3.4.1. Introduction

As I already mentioned in Section 1.3, homogeneous palladium catalysts have proved to be highly active and selective for coupling reactions. However difficulties in recovering the palladium catalysts produce metal contamination in the products and additionally hamper the reuse of the expensive noble metal. Therefore, a facile and efficient separation of expensive noble-metal catalysts and their consecutive reuse remains a challenge in terms of economic and environmental considerations. Along with Thiel's group efforts to develop heterogenization of homogeneous catalysts on supports, I came up with the idea to immobilize the pyrimidinylphosphine palladacycles.

During the last decade, a series of silica-supported palladium catalysts have been developed using sol-gel processes or anchoring strategies. Among them, systems with chelating palladium complexes, such as oximecarbapalladacycles (**I**[185], **Scheme 38**), iminepalladacycles (**II**[186], **Scheme 38**) and palladium(II) complexes with N–N (**III**[187], **IV**[188],

Results and Discussion

V[189], **VI**[190], **VII**[191,192], **VIII**[193], **Scheme 38**), N–O (**IX**[193] and **XII**[193], **X**[194] **Scheme 38**) or N–S (**XI**[193]) donors, were described in the literature and their activities in the cross-coupling reactions of aryl iodides or bromides with arylboronic acids were examined. Generally, high palladium loadings and harsh reaction conditions (80-110 °C) were required for reasonable catalytic conversions.

Results and Discussion

(I)

(II)

(III), SiO2, X= Cl
(IV), SiO2, X= OAc
(V), FSM-16, X= Cl

(VI)

8d

(VII)

(VIII), X= NH
(IX), X= O

(X)

(XI), X= S
(XII), X= O
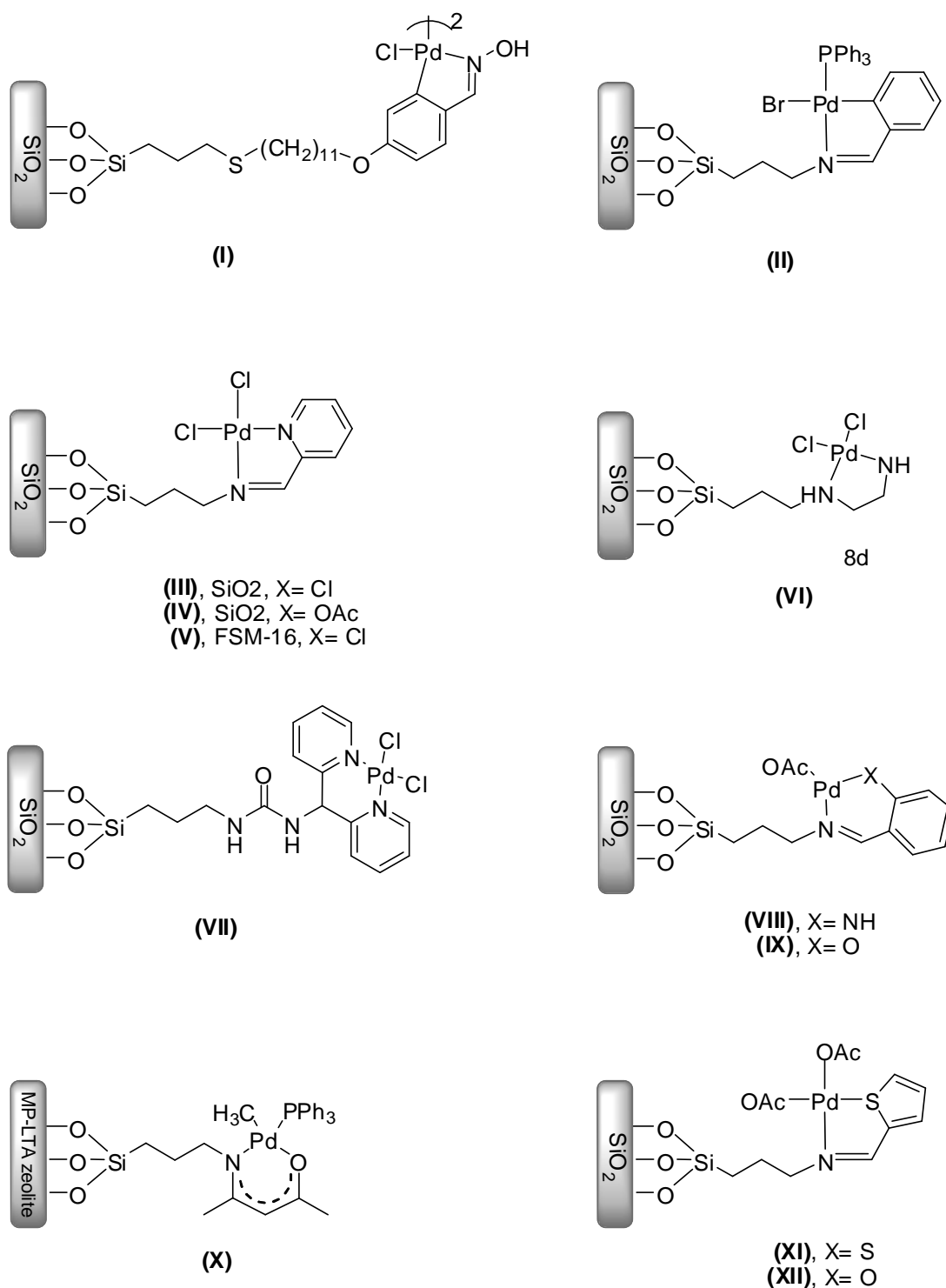
Scheme 38. Different chelating palladium complexes immobilized on mesoporous materials.

For the grafting process with SiO_2-based supports a ligand bearing -$Si(OR)_3$ function is required. It therefore seemed reasonable that the amino group in **4a** opens up a possibility for a simple immobilization over solid supports. According to previous works,[195,196,197] I found two

90

Results and Discussion

commercially available precursors having a -Si(OR)$_3$ group that could be reacted with the amino group of the pyrimidine site. Unfortunately all attempts to synthesize ligand **24** by reacting (3-chloropropyl)triethoxysilane and **4a** were unsuccessful. Changing the starting material to 3-triethoxysilylpropyl-1-isocyanate was expected to provide a solution to this problem.

The reaction of **4a** with an excess of 3-triethoxysilylpropyl-1-isocyanate is carried out under reflux conditions in presence of NEt$_3$ as a base in THF. Removing the solvent followed by purification gave **25** as a yellow solid but in only about 20% yields. Using toluene allows the reaction to be carried out at higher temperatures but improved the yield up to about 35%. Finally, I found that, using a fusing method, the yield of the reaction can be further improved: Heating a 1:1 mixture of **4a** and 3-triethoxysilylpropyl-1-isocyanate to 200 °C for 1 h results in the formation of the triethoxysilyl-modified ligand **25** possessing a stable urea linker unit in about 72% yields (**Scheme 39**).
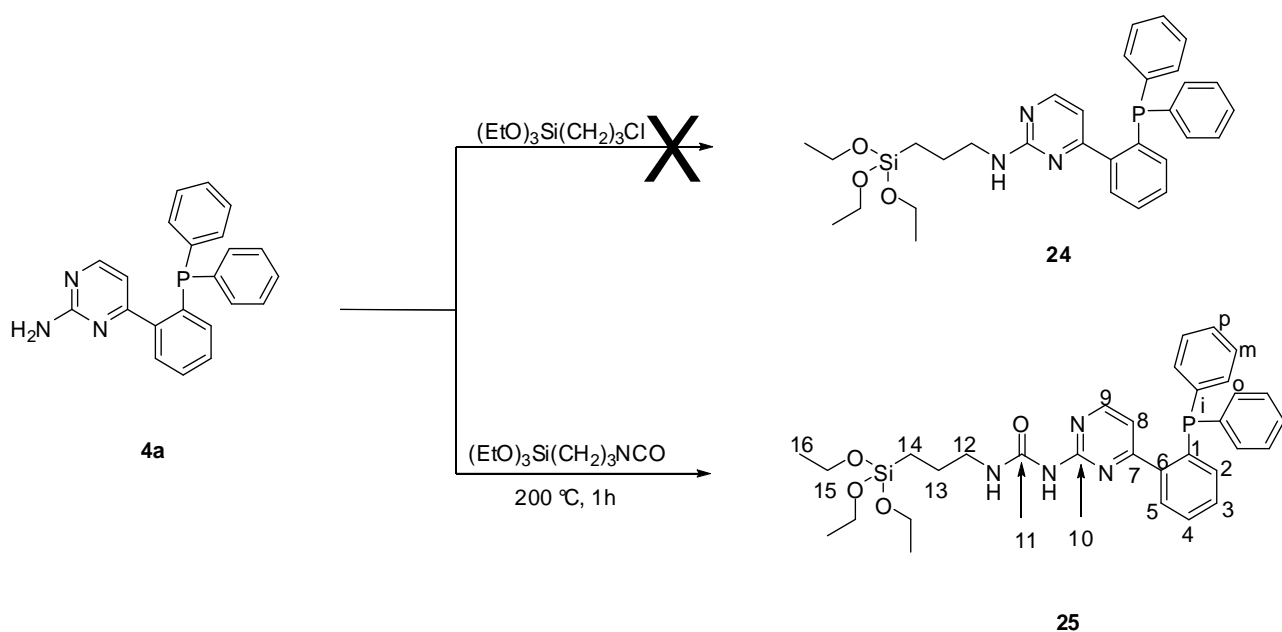
Scheme 39. Synthesis of the triethoxysilyl-modified ligand **25**.

Results and Discussion

The formation of **25** is confirmed by means of NMR spectroscopy: Five novel sets of resonances appear in the high-field region of the ^{1}H NMR spectrum: three of them (at 3.21, 1.57, and 0.57 ppm) are typical of the propylene chain and the other two (at 3.67 and 1.07 ppm) are assigned to the Si(OEt)$_3$ group (**Figure 43**). Compared to the intermediate **4a**, the ^{1}H NMR resonances of the pyrimidine ring of **25** (at 8.42 (H-9) and 7.00 ppm (H-8)) are shifted slightly to higher field, which is consistent with the shift of the phosphorous atom's resonance in the ^{31}P NMR spectrum from –12.05 (**4a**) to –9.51 ppm (**25**). Two different N-H resonances appeared at 9.09 and 9.27 ppm, the HH-COSY spectrum shows a correlationship between NHb (at about 9.09 ppm) and H-12 (**Figure 44**).
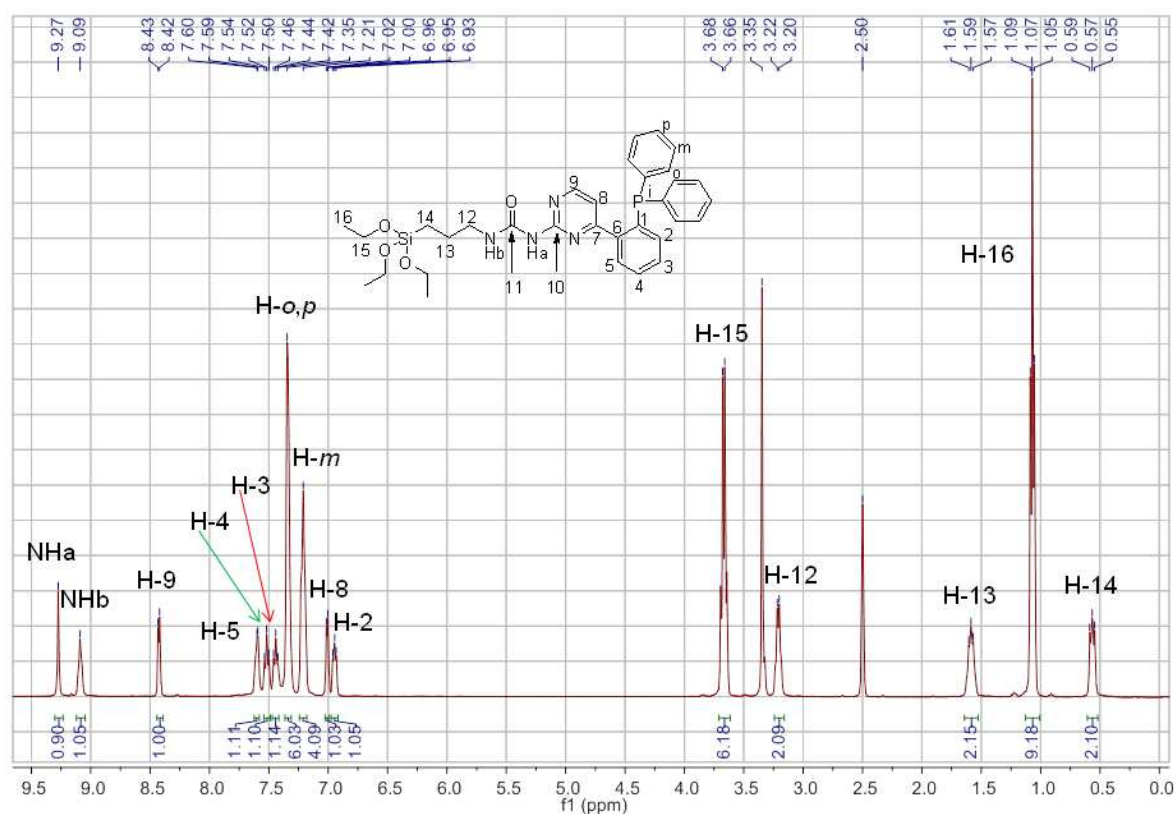
Figure 43. ^{1}H NMR spectrum of **25** in DMSO-d_6.

Results and Discussion
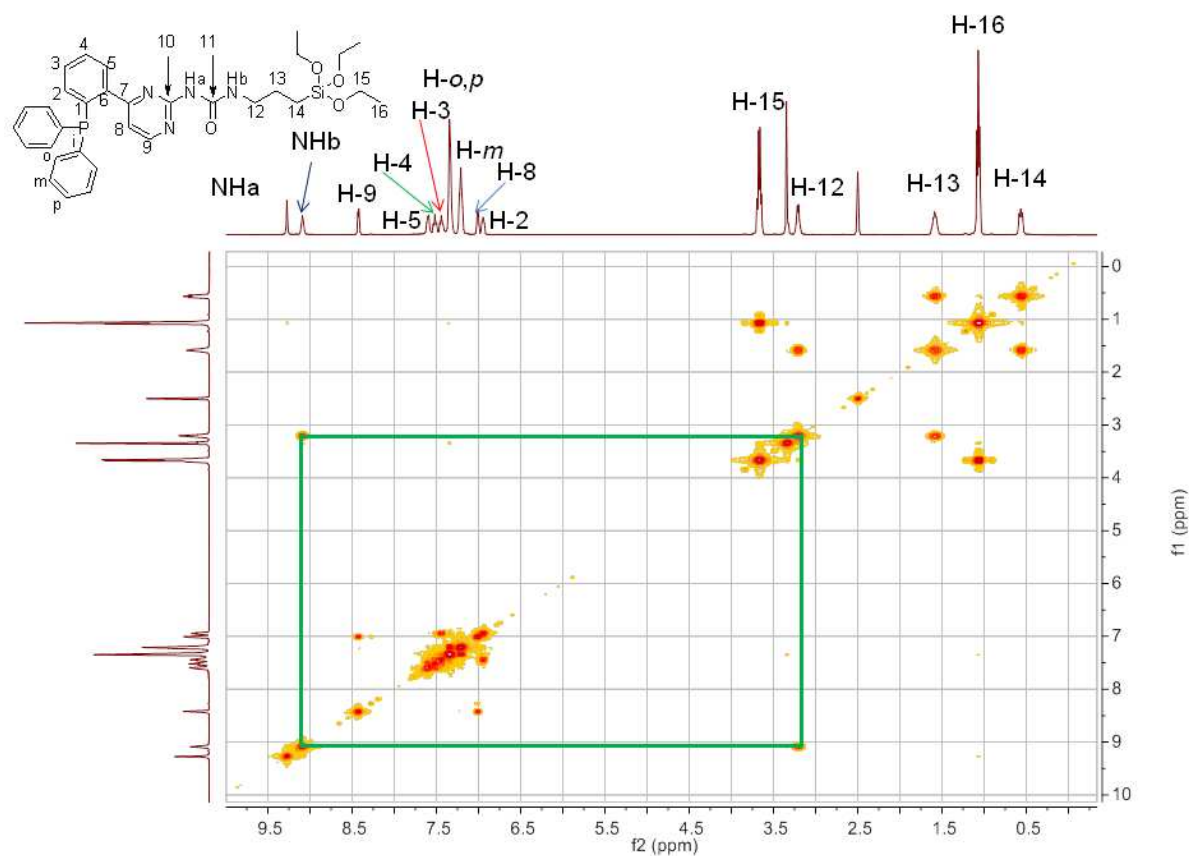
Figure 44. ^{1}H-^{1}H COSY spectrum of **25** in DMSO-d_6.

Reacting ligand **25** with $(C_6H_5CN)_2PdCl_2$ in CH_2Cl_2 at room temperature for 1 h directly gives the cyclometalated zwitterionic product **26** (**Scheme 40**).

Results and Discussion
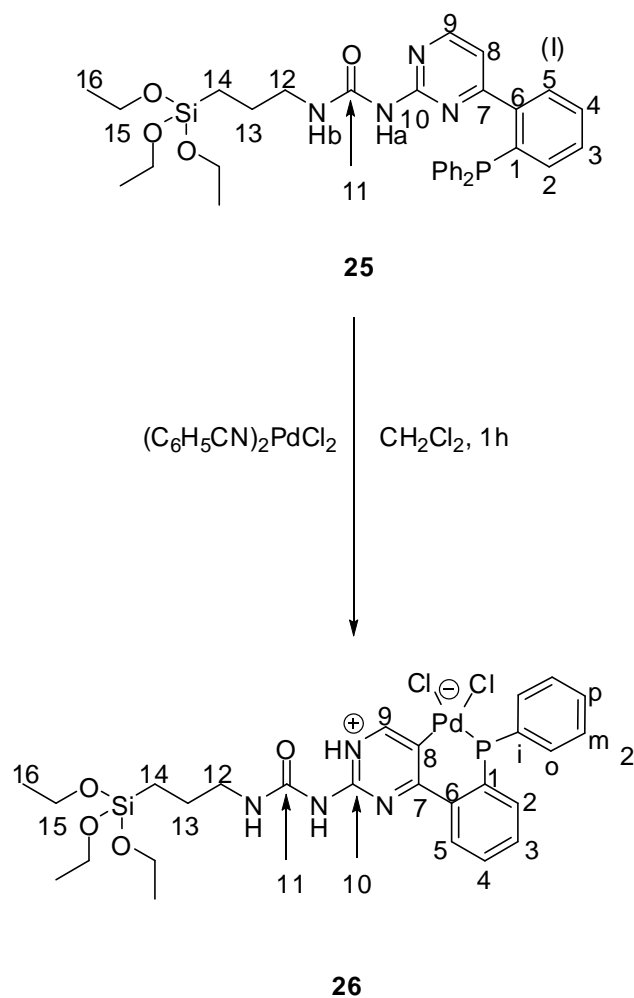
Scheme 40. Synthesis of complex **26**.

^{1}H NMR spectroscopy proves clearly the activation of the pyrimidinyl C-H bond in the *trans* position to the urea unit. Obviously, the resonance of one of the pyrimidinyl protons is missing, and the resonance of the phenylene *ortho* proton is shifted to lower field, owing to an interaction with one of the pyrimidinyl nitrogen atoms.

Results and Discussion
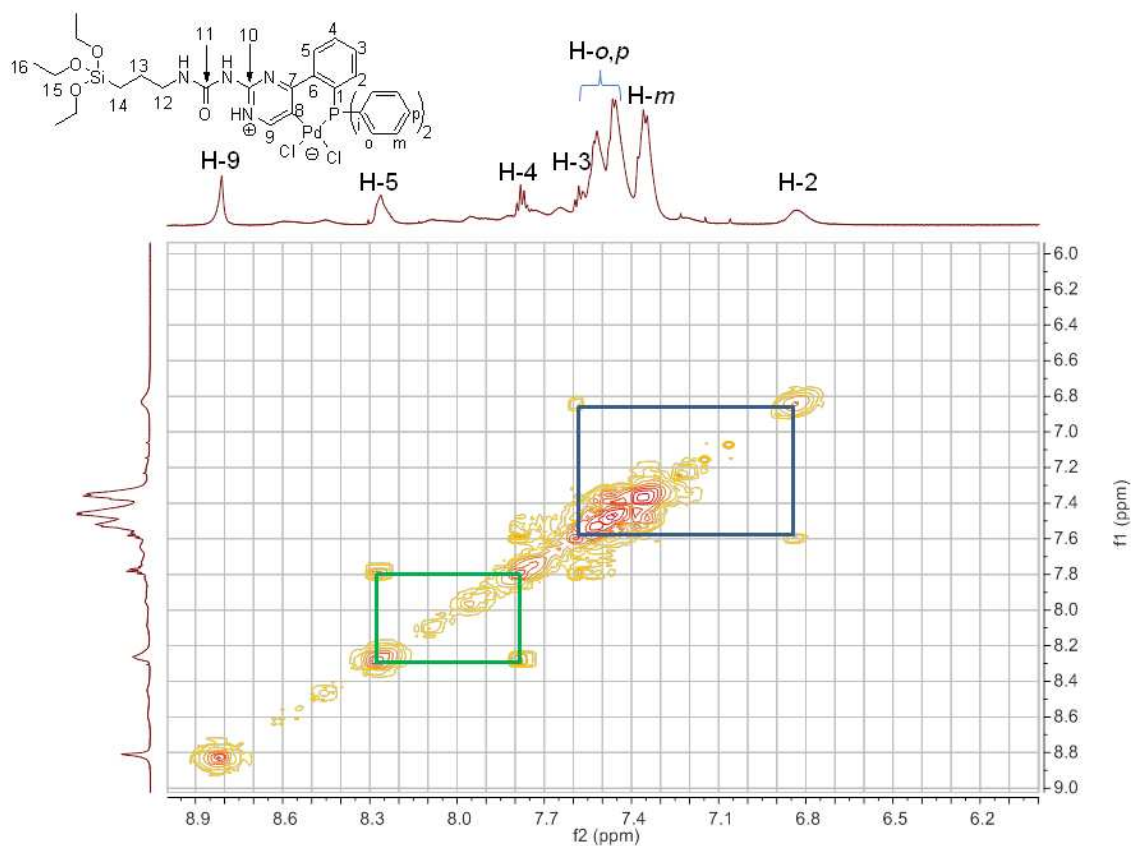
Figure 45. ^{1}H-^{1}H COSY spectrum of **26** in DMSO-d_6.

The ^{13}C NMR spectra of ligand **25** and complex **26** are shown in **Figure 46**. Comparing the spectra, it is obvious that complexation of the ligand has a big influence on C-8 which is shifted more than 10 ppm towards lower field with respect to the free ligand. This is probably due to a deshielding effect of the Lewis-acidic palladium(II) centre.

Results and Discussion
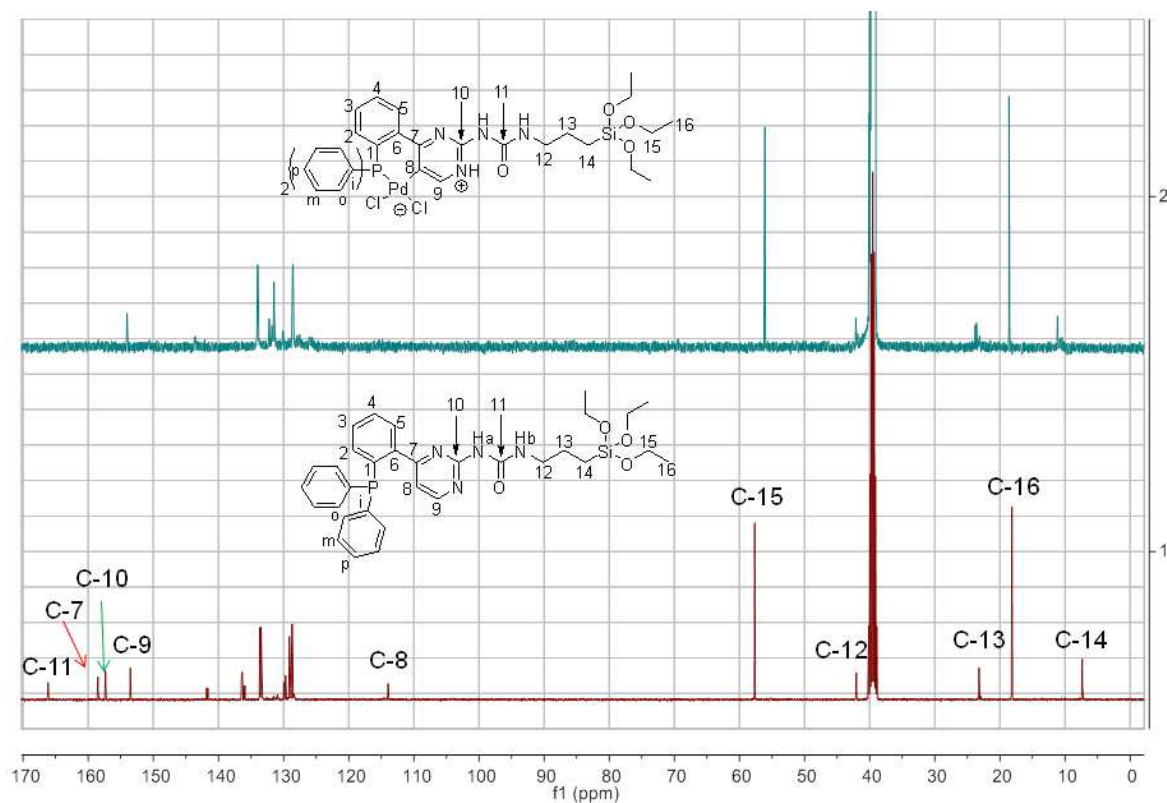
Figure 46. ^{13}C NMR spectra of ligand **25** (bottom) and complex **26** (up) in DMSO-d_6.

The ^{31}P NMR spectrum of complex **26** is shown in **Figure 47**. As expected, the ^{31}P resonance of **26** (29.38) is shifted towards lower field compared to the free ligand **25** and is almost the same as for compounds **15a-c**.

Results and Discussion
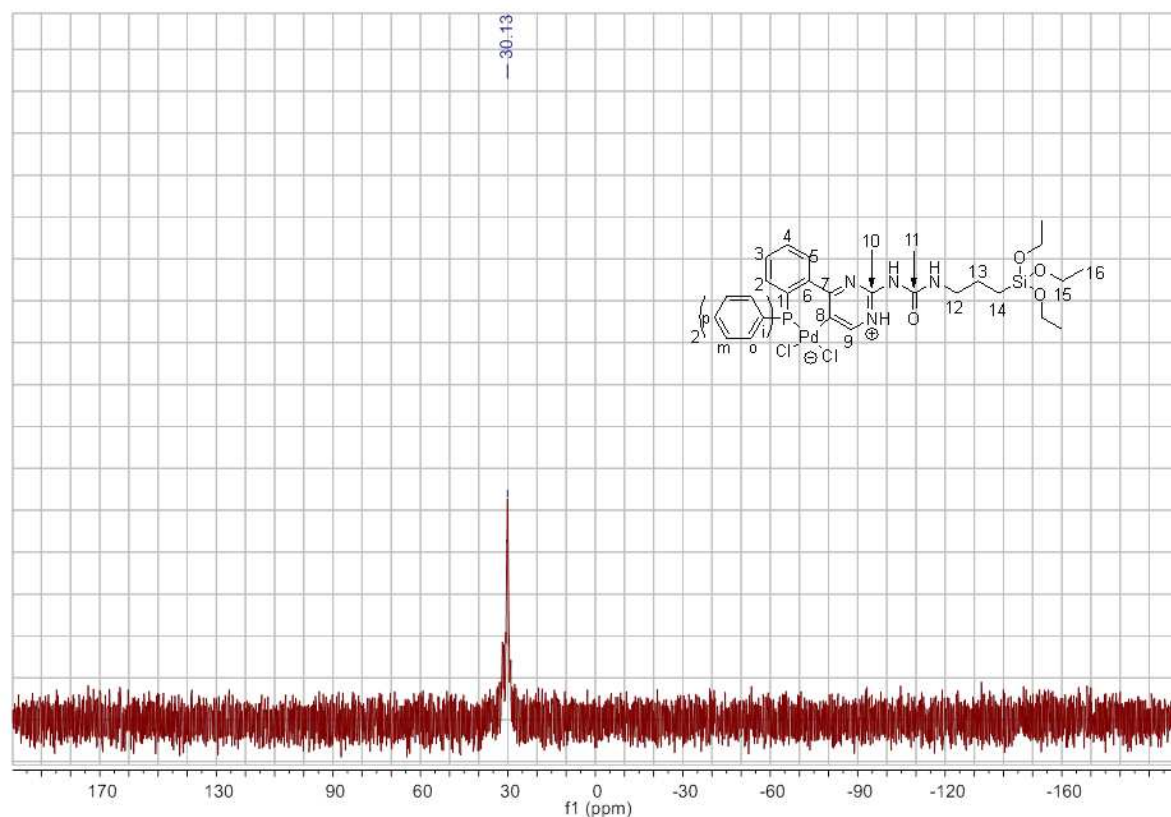
Figure 47. ^{31}P NMR spectrum of **26** in DMSO-d_6.

3.4.2. Preparation of the Heterogeneous Catalysts 26@MCM-41 and 26@SiO$_2$

Finally, complex **26** was covalently grafted onto the ordered mesoporous silica MCM-41 and on a commercial amorphous SiO$_2$. For better comparison, the same procedure (reactant and solvent amount, reaction temperature and reaction time) was applied for both heterogeneous catalysts **26@MCM-41** and **26@SiO$_2$** as follows: A solution of **26** in dry CHCl$_3$ was added to a suspension of MCM-41 or SiO$_2$ in dry toluene. The mixture was stirred for 18 h at 100 °C. The solid part was filtered off and washed with CH$_2$Cl$_2$ in a soxhlet apparatus for 24 h. Finally, the solid was dried in vacuum at 50 °C for 5 h to obtain **26@MCM-41** and **26@SiO$_2$**, respectively.

Results and Discussion

26

Toluene/CHCl₃ | MCM-41 or SiO₂
18 h, 100 °C
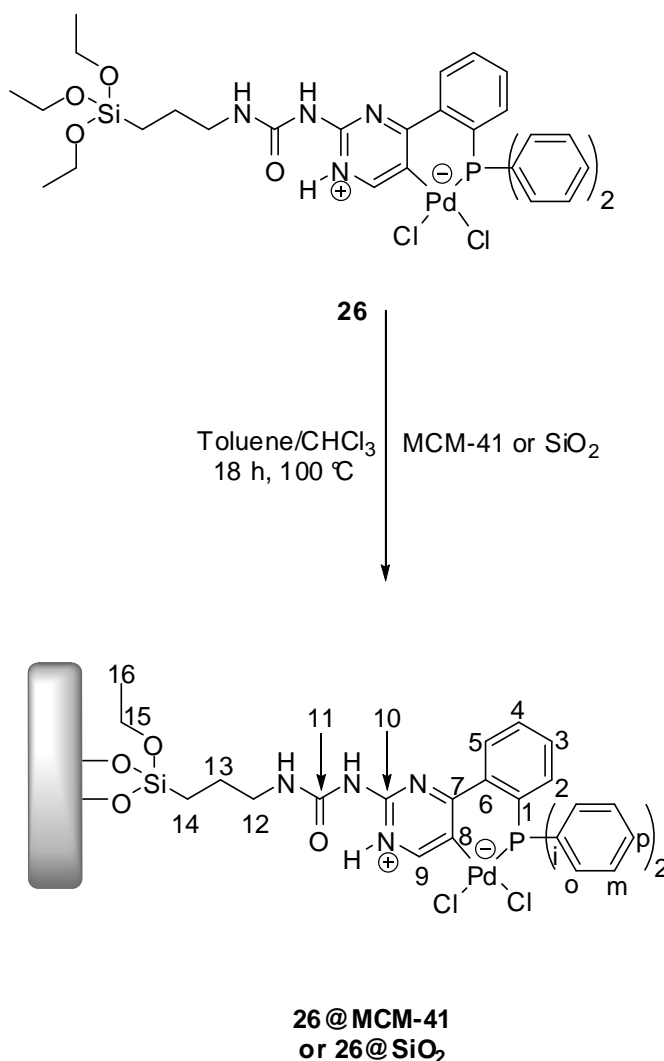
26@MCM-41
or 26@SiO₂

Scheme 41. Synthesis of the heterogeneous catalysts **26@MCM-41** and **26@SiO₂**.

3.4.3. Characterization of the Heterogeneous Catalysts 26@MCM-41 and 26@SiO₂

The success of the immobilization is proved by ^{29}Si CP-MAS NMR spectra of the hybrid materials **26@MCM-41** and **26@SiO₂** (**Figure 48**). Resonances at about –110, –101, and –92 ppm correspond to the framework siloxane units $Si(OSi)_4$ (Q^4), $HOSi(OSi)_3$ (Q^3), and $(HO)_2Si(OSi)_2$ (Q^2), and overlapping resonances at about –48, –53, and –66 ppm can be assigned to $RSi(RO)_2(OSi)$ (T^1), $RSi(RO)(OSi)_2$ (T^2), and $RSi(OSi)_3$ (T^3) organosiloxane species.[198,199] The difference in the intensities of the signals in **26@MCM-41** ($T^2>T^1>>T3$) and **26@SiO₂** (T1>T2>>T3) owes to the different numbers of silanol groups in the silica precursors.

98

Results and Discussion
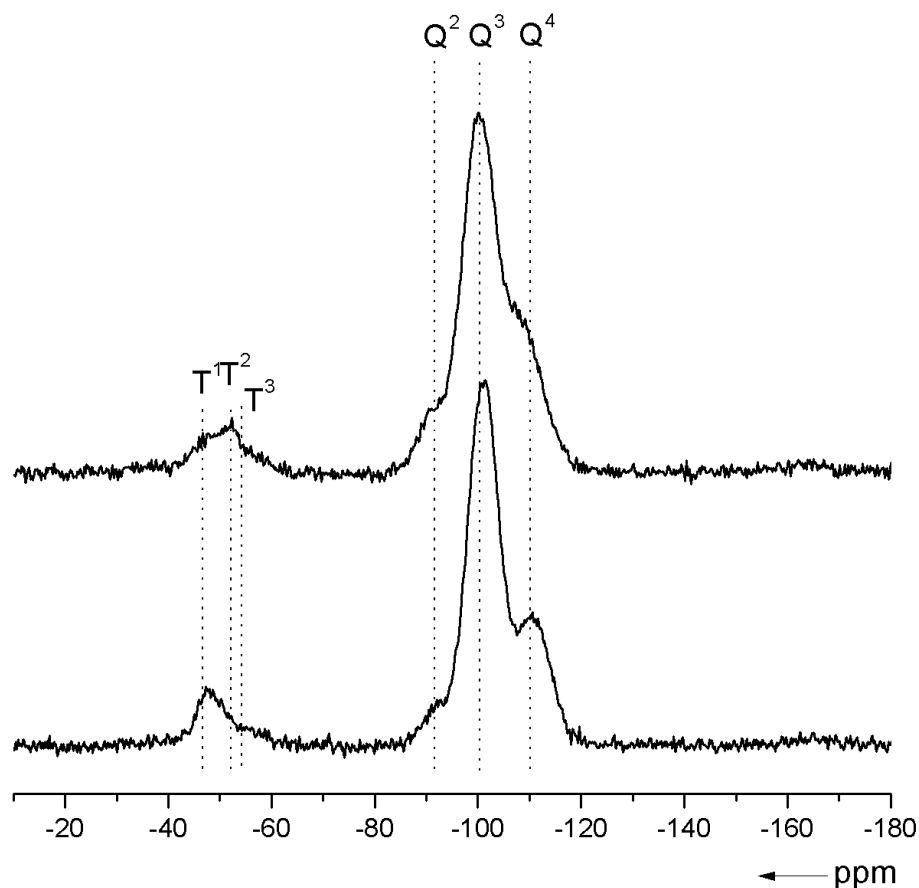
Figure 48. Solid-state ^{29}Si CP-MAS NMR spectra of **26@MCM-41** (top line) and **26@SiO$_2$** (bottom line).

Both hybrid materials present ^{13}C CP-MAS NMR spectra similar to those of ligand **25** in solution. Two distinct resonances between 167 and 152 ppm can be assigned to pyrimidinyl carbon atoms and to the urea carbonyl group. A broad signal between 145 and 113 ppm owes to all other aromatic carbon atoms. The only difference is that the resonance of the pyrimidinyl carbon atom that underwent C–H activation (at about 113.9 ppm in ligand **25**) is shifted to lower field.[200] Three resonances at about 43.3, 22.8, and 9.3 ppm can be correlated with the resonances of the propylene linker, and the dominant resonances at about 58.3 and 16.5 ppm can be assigned to ethoxysilyl (SiOCH$_2$CH$_3$) units. The weak resonance arising at about 72

Results and Discussion

ppm in **26@MCM-41** owes to residual $CHCl_3$ in the material (**Figure 49**).
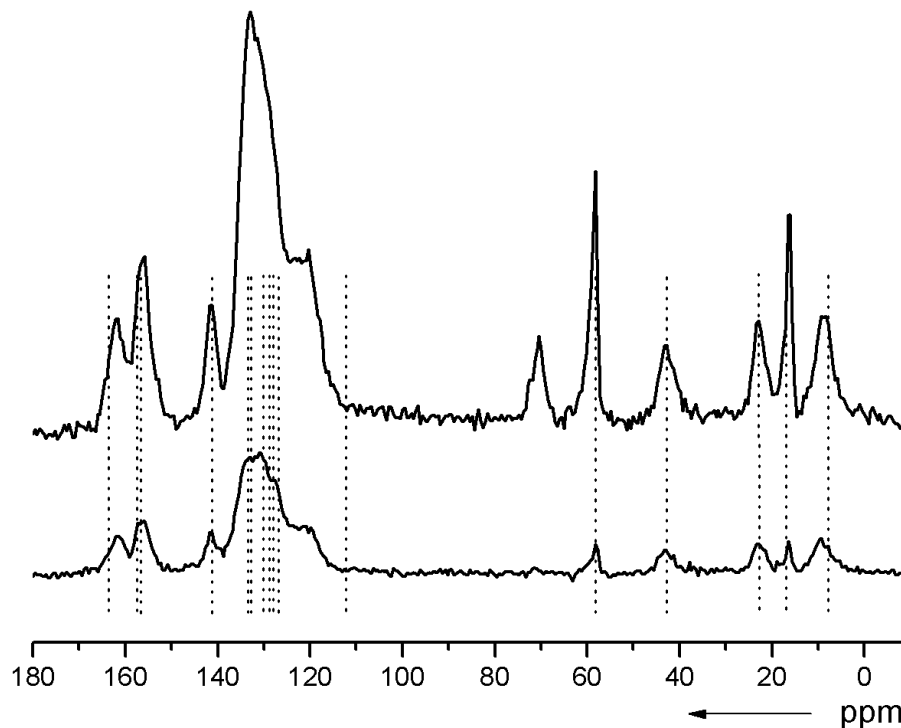
Figure 49. Solid-state ^{13}C CP-MAS NMR spectra of **26@MCM-41** (top line) and **26@SiO$_2$** (bottom line); the dashed lines assign the resonances of the ^{13}C NMR spectrum of the free ligand **25** in solution.

The ^{31}P MAS NMR spectra of the hybrid materials **26@MCM- 41** and **26@SiO$_2$** show an intense resonance at about 36.9 ppm and a weak signal at about 15.5 ppm (**Figure 50**). Compared to the ^{31}P NMR spectrum of compound **26** in solution, the solid-state NMR resonances are shifted about 6 ppm to lower field, probably owing to some interactions between the grafted complex and support's surface (e.g., Si–OH···Cl–Pd). No signals for the free ligands or for phosphine oxide (expected at about 26 ppm) are observed, which confirms no anchoring of the palladium complex on the solid supports without decomposition.

100

Results and Discussion
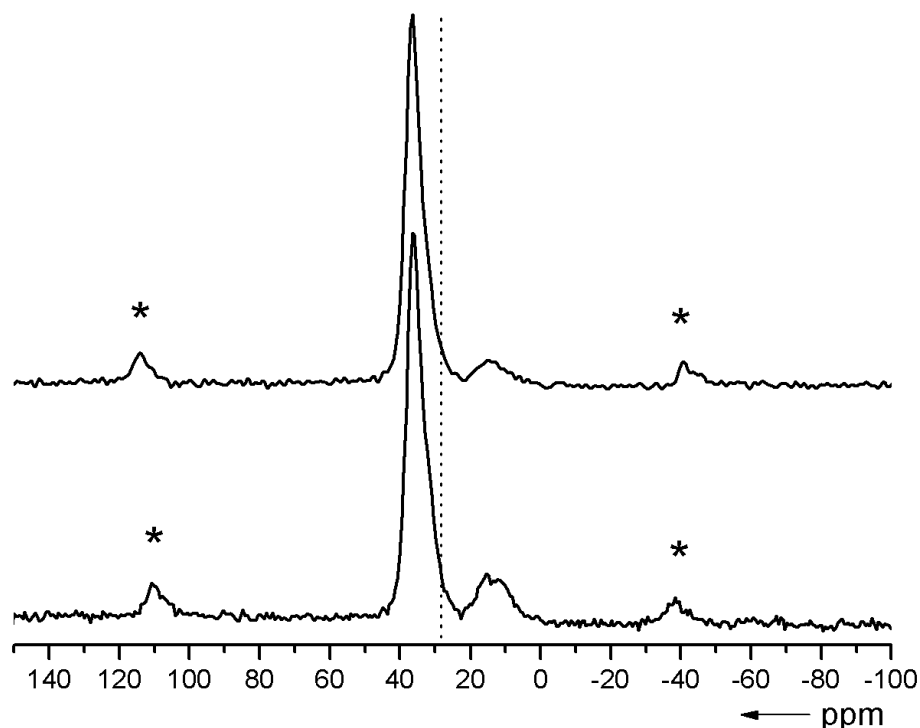
Figure 50. ^{31}P MAS NMR spectrum of **26@MCM-41** (top line) and **26@SiO₂** (bottom line); the dashed line signs the ^{31}P NMR resonance of the palladium(II) complex **26** in solution.

Further characterizations by means of IR spectroscopy are in complete agreement with the NMR results (**Figure 51**). The aminopyrimidinylphosphane **4a** shows N–H stretching absorptions ($\tilde{v}$ = 3317 and 3160 cm^{-1}), which are no longer present in the urea derivative **25**. A sole broad band at $\tilde{v} \approx 3450$ cm^{-1} could be observed containing NH and OH absorptions (from residual water in KBr). It is well known that urea motifs form strong hydrogen bonds with each other and with other proton donors and acceptors (such as the KBr matrix), which leads to broad signatures of the N–H absorptions.[201] There is one unexpected absorption at $\tilde{v}$ = 1747 cm^{-1}, which is out of the range of urea C=O stretching absorptions. I assign this to the imine tautomer of the urea unit, which is stabilized by an O–H···N hydrogen bond with one of the pyrimidinyl nitrogen atoms in a six-membered cycle. There is another signal at $\tilde{v}$ = 1681 cm^{-1} that can be assigned to the amide I absorption of the urea group. The amide II absorption is not

Results and Discussion

clearly distinguishable from other signals. The situation changes after C–H activation and coordination of the palladium(II) center: In the resulting palladium(II) complex **26**, one of the pyrimidine nitrogen atoms is protonated and may be involved in a N^+–H$\cdots$O hydrogen bond. Two bands at $\tilde{v} = 1697$ and 1668 cm^{-1} can be assigned to amide I absorptions and one band at $\tilde{v} = 1587$ cm^{-1} to an amide II absorption. In the corresponding heterogenized systems **26@MCM-41** and **26@SiO$_2$**, two well-separated bands at $\tilde{v} = 1668$ and 1593 cm^{-1} are typical for the urea fragment. In these materials, further intense bands at $\tilde{v} \approx 3450$ cm^{-1} ($\tilde{v}_{OH}$ from Si–OH), 1070 cm^{-1} ($\tilde{v}_{asym}$ from Si–O–Si), and 790 cm^{-1} ($\tilde{v}_{sym}$ from Si–O–Si) are found.[202,203]
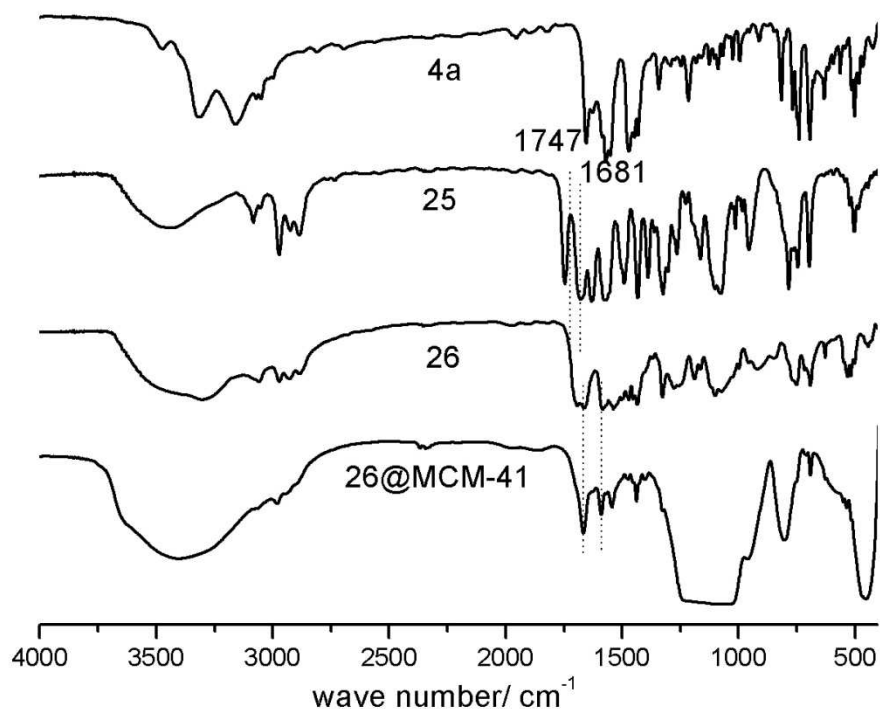
Figure 51. FTIR spectra (KBr) of compounds **4a**, **25**, **26**, and **26@MCM-41**.

Powder XRD patterns of the parent MCM-41 and the hybrid material **26@MCM-41** are presented in **Figure 52**. MCM-41 can be characterized clearly by four reflections at 2θ angles of 2–6°, which includes a very strong d_{100} reflection at 2.12° and three other weaker reflections at 3.74° (d_{110}), 4.39° (d_{200}), and 5.85° (d_{210}) indexed to a highly ordered hexagonal

Results and Discussion

pore arrangement possessing a two-dimensional *p6mm* symmetry. **26@MCM-41** also demonstrates a strong d_{100} reflection and two other weaker reflections assigned to d_{110} and d_{200}. The decrease in the intensity of the reflections of **26@MCM-41** compared with that of MCM-41 can be attributed to the contrast matching between the silica walls and organic moieties located inside the channels after functionalization.[204,205,206,207]
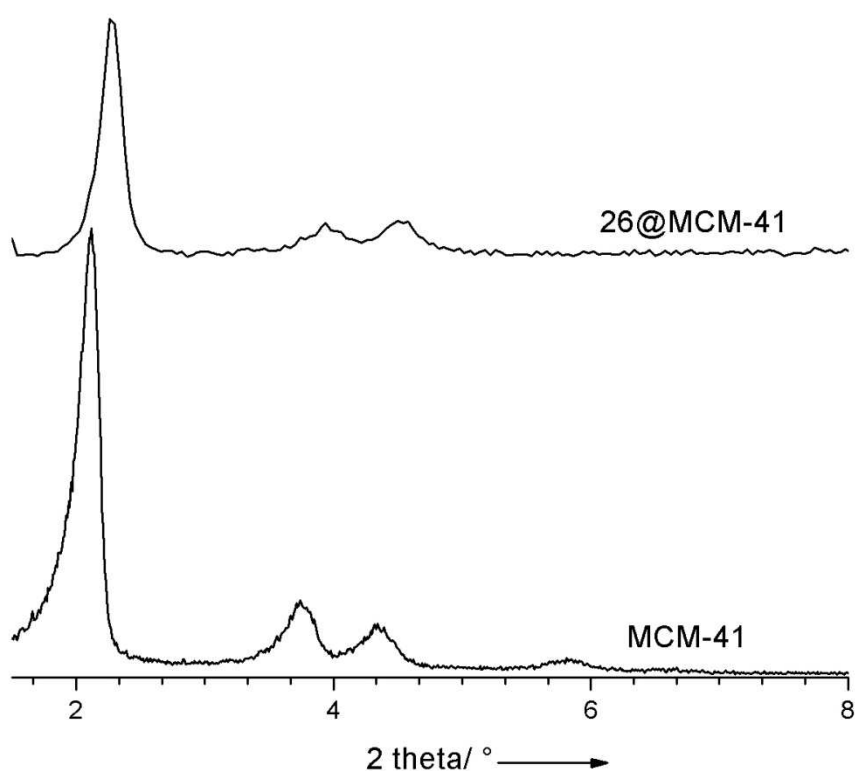
Figure 52. Powder XRD patterns of MCM-41 and **26@MCM-41**.

The morphologies and microstructure of the **26@MCM-41** was further investigated by scanning electron microscopy (SEM). The image presented in **Figure 53** clearly reveals that obtained hybrid material **26@MCM-41** has hexagonal morphologies and is monodispersed. However, a deeper focus on the state of the grafted palladium species is not possible according

Results and Discussion

to the resolution limit of SEM.
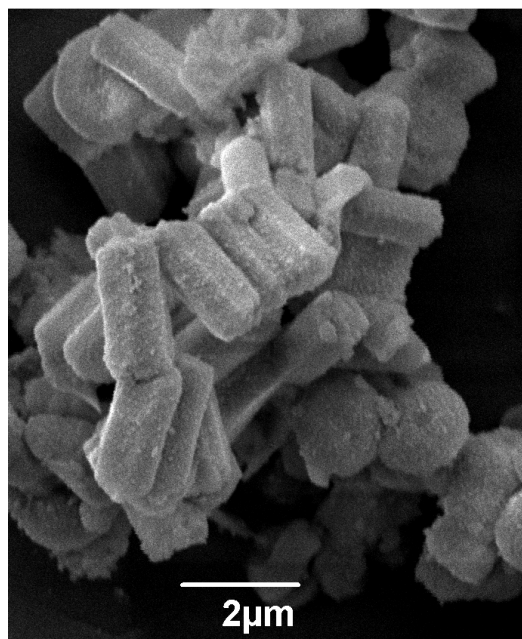
Figure 53. SEM image of the freshly prepared **26@MCM-41**.

Figure 54 shows the spectrum of an energy-dispersive X-ray analysis (EDX analysis) of **26@MCM-41**. This analysis indicates that the major composition in the scanned area is silicon and also confirms the presence of palladium on the mesoporous silica matrix.

Results and Discussion
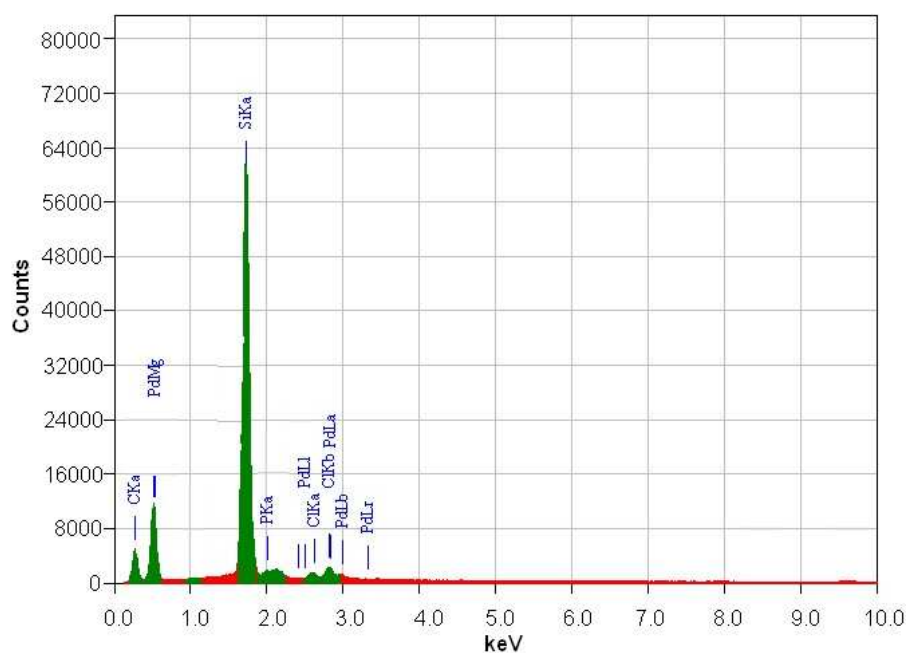
Figure 54. *EDX* analysis of **26@MCM-41**.

The surface areas, pore volumes, and pore size distributions of MCM-41, SiO_2, and the hybrid materials **26@MCM-41** and **26@SiO$_2$** were determined by N_2 adsorption–desorption experiments. All corresponding data are listed in **Table 9**. Owing to the presence of the bulky catalyst moieties, the modified samples **26@MCM-41** and **26@SiO$_2$** demonstrate a decrease in pore size, pore volume, and surface area compared to the parent mesoporous MCM-41 and SiO_2 supports. N_2 adsorption–desorption measurements of all samples demonstrated typical type IV isotherms (definition by IUPAC) with a hysteresis characteristic for mesoporous materials possessing pore diameters between 2 and 50 nm.[208] The sharp capillary condensation steps at P/P_o= 0.2–0.4 for MCM-41 and **26@MCM-41** (**Figure 55**) is related to the ordered pore structure with narrow pore size distributions and are thus consistent with the XRD patterns.

Results and Discussion

Table 9. Textural parameters of parent MCM-41 and SiO₂ supports and of the hybrid materials **26@MCM-41** and **26@SiO₂**.

Sample	S_{BET}[a] [m^2g^{-1}]	Pore size [Å]	Pore volume [m^3g^{-1}]	Pd content[b] [$mmolg^{-1}$]
MCM-41	1374	27.08	1.014	-
26@MCM-41	710	21.03	0.533	0.31
SiO₂	510	60	0.75	-
26@SiO₂	321	55	0.549	0.28

[a] S_{BET}= Brunauer–Emmett–Teller surface area. [b] Calculated according to the nitrogen content of the elemental analysis.
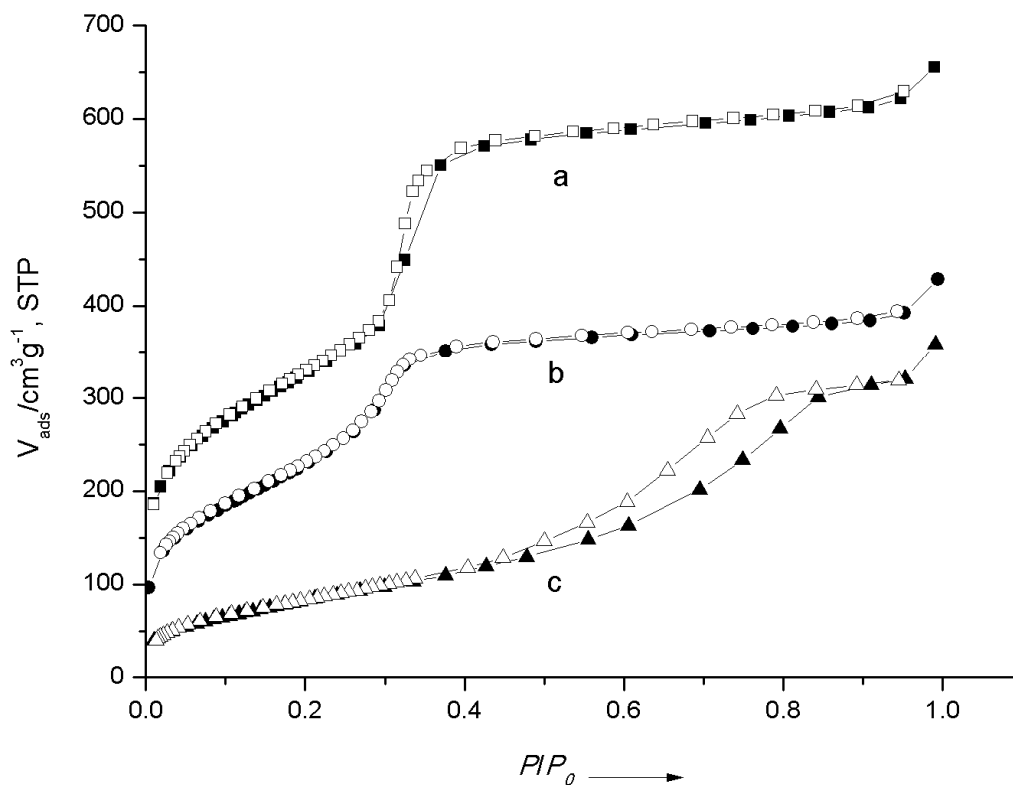
Figure 55. Nitrogen adsorption–desorption isotherms of a) MCM-41, b) **26@MCM-41**, and c) **26@SiO₂**. ■, ●, ▲ adsorption; □, ○, Δ desorption.

The thermal stabilities of the obtained catalyst **26@MCM-41** and **26@SiO₂** were evaluated with thermogravimetric and differential thermogravimetric (TG-DTG) analysis

106

Results and Discussion

(**Figure 56** and **Figure 57**). The DTA curves for both catalysts show significant endothermic peaks bellow 120 °C indicating the thermodesorption of physically adsorbed water. The analyses also indicate that both catalysts have almost the same thermal stability up to 200 °C.
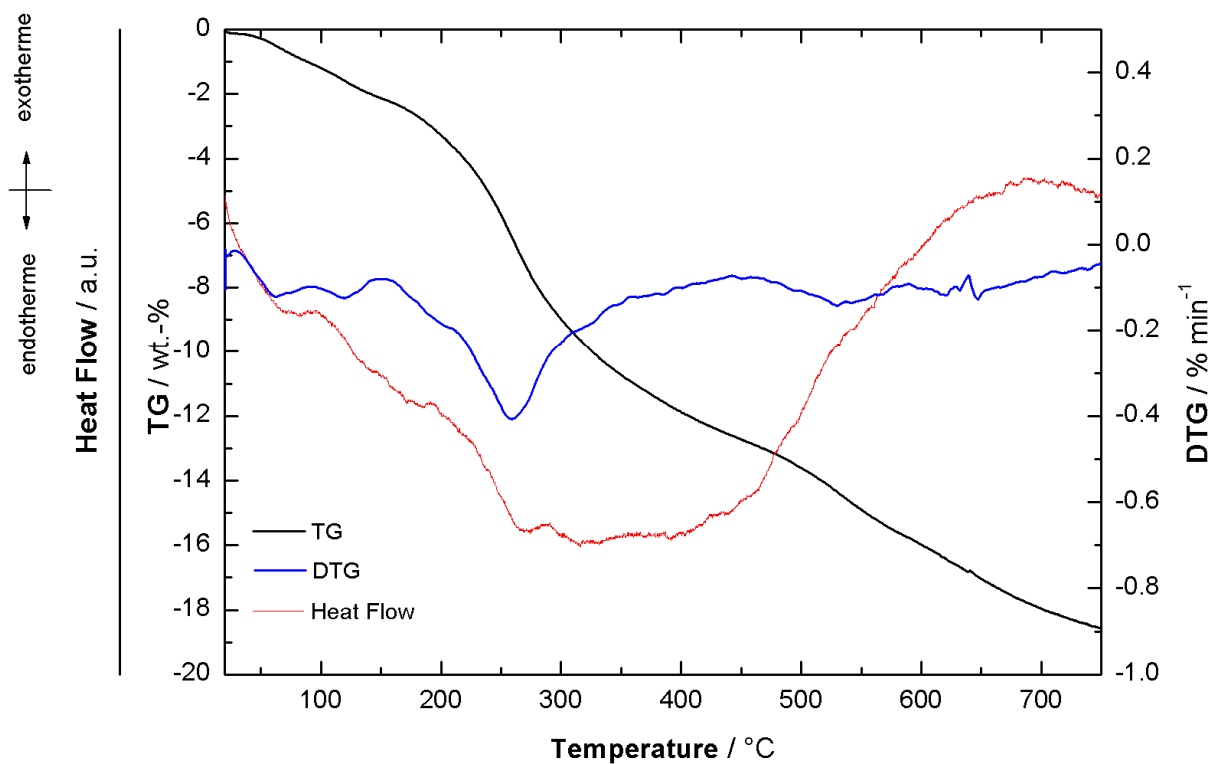
Figure 56. Thermogravimetric and differential thermogravimetric (TG–DTG) analyses of **26@MCM-41**.

Results and Discussion
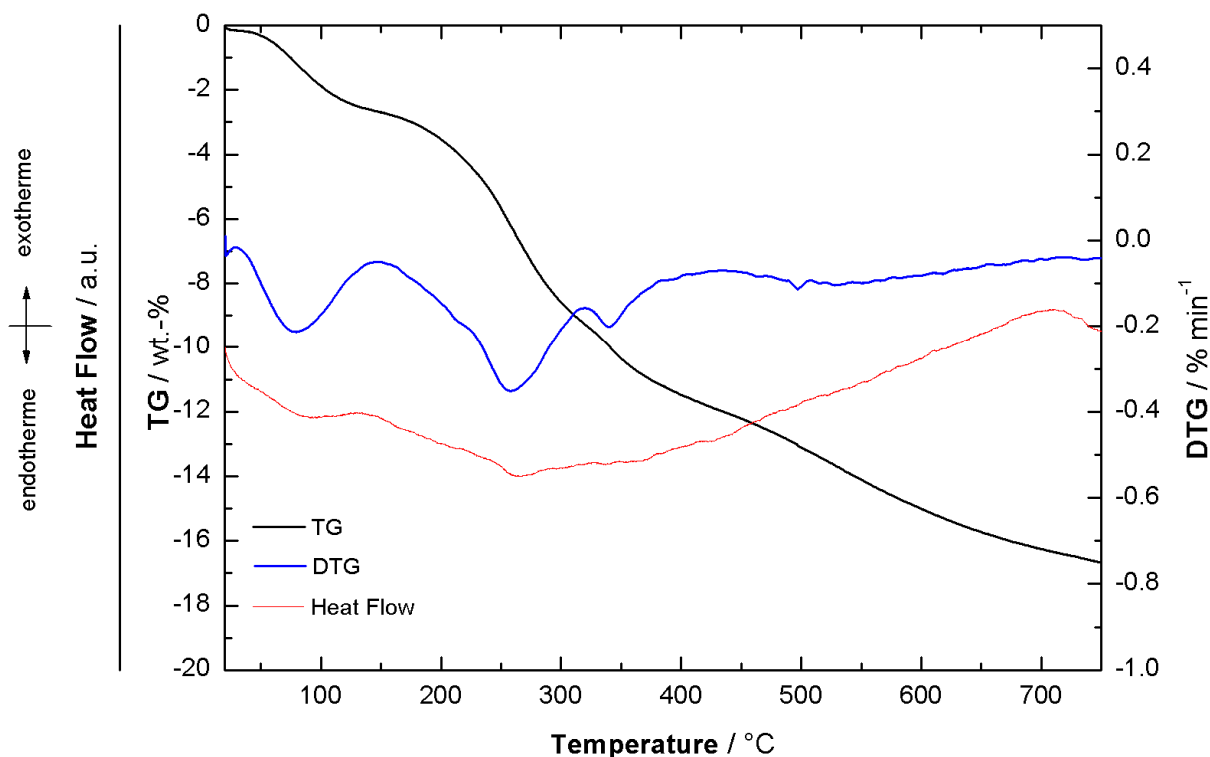
Figure 57. Thermogravimetric and differential thermogravimetric (TG–DTG) analyses of **26@SiO$_2$**.

3.4.4. Catalysis

The hybrid materials **26@MCM-41** and **26@SiO$_2$** were used as catalysts for the Suzuki–Miyaura cross-coupling of phenyl halides and phenylboronic acid. Reaction conditions, such as solvent, base, and reaction temperature, were tested initially. Control experiments performed in the absence of the palladium catalyst confirmed the crucial role of palladium (0% of conversion after 24 h). In the presence of 0.1–1.0 mol% of the appropriate catalyst, the cross-coupling reaction of bromobenzene with phenylboronic acid was investigated in commonly used solvents (**Table 10**). When the reaction was tested at room temperature with 0.1 mol% of the catalyst in DMF/H$_2$O, it gave 33% conversion after 20 h, whereas at higher temperatures, nearly complete conversion was observed after 2 h (**Table 10**,

Results and Discussion

entries 1–4). An examination of different solvents at 50 °C proved that use of ethanol as the protic solvent gave satisfactory results (**Table 10**, entry 9), whereas the use of unaccompanied pure H_2O and aprotic polar solvents such as DMF or dioxane gave poor results (**Table 10**, entries 5–8). Nonpolar solvents such as toluene, however, led to 0% conversion even at high temperatures (**Table 10**, entries 10 and 11). The reactions proceeded with different bases. The best results were obtained with potassium carbonate in ethanol even at room temperature with 1.0 mol% of catalyst loading (**Table 10**, entries 14 and 15).

Results and Discussion

Table 10. Coupling of PhBr with PhB(OH)$_2$ with **26@SiO$_2$**.[a]
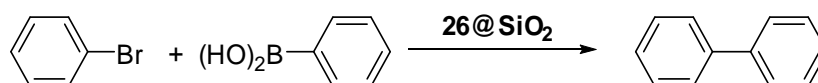
Entry	Solvent	Catalyst Loading [mol%][b]	Base	T [°C]	Yield[c] [%] 1 h	2 h	20 h
1	DMF/H$_2$O	0.1	Cs$_2$CO$_3$	RT	trace	-	33
2	DMF/H$_2$O	0.1	Cs$_2$CO$_3$	40	18	35	-
3	DMF/H$_2$O	0.1	Cs$_2$CO$_3$	50	29	56	-
4	DMF/H$_2$O	0.1	Cs$_2$CO$_3$	60	51	82	-
5	H$_2$O	0.1	Cs$_2$CO$_3$	50	0	0	trace
6	DMF	0.1	Cs$_2$CO$_3$	0	0	0	trace
7	1, 4-dioxane	0.1	Cs$_2$CO$_3$	50	0	0	-
8	1, 4-dioxane	0.1	Cs$_2$CO$_3$	80	-	-	21
9	EtOH	0.1	Cs$_2$CO$_3$	50	64	80	-
10	toluene	0.1	Cs$_2$CO$_3$	50	-	-	0
11	toluene	0.1	Cs$_2$CO$_3$	100	-	-	0
12	EtOH	0.1	NaOAc	50	trace	trace	-
13	EtOH	0.1	Na$_2$CO$_3$	50	7	12	-
14	EtOH	0.1	K$_2$CO$_3$	50	80	92	-
15	EtOH	1	K$_2$CO$_3$	RT	-	-	77[d]
16	EtOH	0.1	K$_3$PO$_4$	50	57	61	-

[a] PhBr (1 mmol), PhB(OH)$_2$ (1.5 mmol), base (1.2 mmol), and solvent (5 mL). [b] Catalyst loading: mol% of palladium with respect to PhBr. [c] Determined by using GC based on PhBr. [d] Yield after 4 h.

With optimized reaction conditions, I examined the scope of the palladium-catalyzed Suzuki–Miyaura coupling on a series of different substrates (**Table 11**). For the electron deficient substrate 4-bromoacetophenone the product was obtained in 100% yield after 1 h with 0.1 mol% at 50 °C and 95% yield after 20 h with 1 mol% at room temperature (entry 1). 4-Iodoacetophenone gave the desired product in 82% yield (entry 2). Bromotoluene, iodotoluene,

110

Results and Discussion

and 2-bromoanisol gave 89, 61, and 82% of the products, respectively (entries 3–5), which

shows that the reaction rate is clearly influenced by the electronic impact of the substituents on

the aryl halide: Electron withdrawing groups increase the rate, whereas electron-donating

groups decrease it (entries 1 and 2 vs. 3 and 4). Attempts to couple *ortho*-substituted aryls gave

the desired products in only low yields, probably owing to steric hindrance (entry 6). The

catalyst is not able to activate aryl chlorides.

Table 11. Suzuki reactions of aryl halides in the presence of **26@SiO₂** as catalyst.[a]
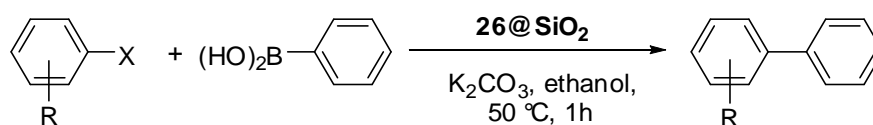
Entry	Aryl halide	Product	Yield [%]
1	Br—C₆H₄—C(O)CH₃	Ph—C₆H₄—C(O)CH₃	100 / 95[b]
2	I—C₆H₄—C(O)CH₃	Ph—C₆H₄—C(O)CH₃	82
3	Br—C₆H₄—CH₃	Ph—C₆H₄—CH₃	89
4	I—C₆H₄—CH₃	Ph—C₆H₄—CH₃	61
5	Br—C₆H₄—O	Ph—C₆H₄—O	82
6	o-Br—C₆H₄—CH₃	Ph—C₆H₄—CH₃	33

[a] Reaction conditions: aryl bromide (1 mmol), phenylboronic acid (1.2 mmol), K₂CO₃ (1.2

mmol), catalyst (0.1 mol%), 60 min reaction time, ethanol, 50 °C, conversions determined by

using GC. [b] Catalyst (1 mol%) at RT, 20 h.

3.4.5. Reusability of the Catalysts 26@MCM-41 and 26@SiO₂

The reusability of both hybrid catalysts was examined for the coupling of

Results and Discussion

bromobenzene and phenylboronic acid at room temperature. To ensure that the high activity of **26@MCM-41** and **26@SiO$_2$** arises from the palladium sites on the surface and not from the leached palladium species, the heterogeneity of **26@MCM-41** and **26@SiO$_2$** was tested by reusing the catalyst. After the first cycle of the reaction, the catalyst was recovered by centrifugation and then washed thoroughly with ethanol and water to remove the base. Finally, the recovered catalyst was washed with dichloromethane and dried under vacuum at 60 °C for 10 h. The activity of the recovered catalyst remained high for the next four subsequent reactions. **26@MCM-41** demonstrated slightly better results than **26@SiO$_2$** (**Table 12**).

Table 12. Catalyst recycling experiments.[a]
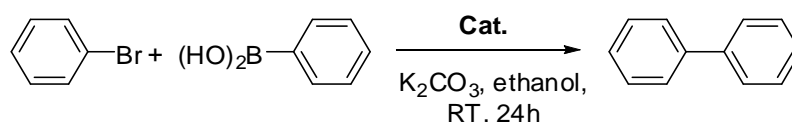
Run	Yield [%]	
	26@MCM-41	**26@SiO$_2$**
1	100	100
2	96	92
3	94	86
4	91	80

[a] Reaction conditions: bromobenzene (1 mmol), phenylboronic acid (1.2 mmol), K$_2$CO$_3$ (1.2 mmol), catalyst (1 mol%), 24 h reaction time, ethanol, RT, conversions determined by using GC.

The high stability and reusability of the catalysts is assigned to the chelating nature of the bidendate PC ligand and to the linkage of the palladium complex to the silica surface by mainly T^2 sites (**Figure 48**). MCM-41 as the support leads to a more stable catalyst than the SiO$_2$ (higher content of T^1 sites). After using the catalyst, there was no color change in the catalysts (**Figure 58**). The heterogeneity of palladium-derived catalysts for C–C coupling

Results and Discussion

reactions is still under discussion.[209,210,211] There are reports in the literature that clearly show that leached palladium species from, for example, deposited palladium nanoparticles can catalyze such couplings especially with aryl bromides or iodides as the substrate and at elevated temperatures.[212,213,214,215] There are, however, reports on the usage of palladium catalysts for C–C couplings under continuous flow conditions, which argue for heterogenized active species.[216] These contrasting results make it difficult to label a catalytically active species as heterogeneous or homogeneous. The heterogeneity of **26@MCM-41** was tested first by performing a hot filtration experiment. No further reaction was observed in the filtrate after the addition of another 1.2 equivalents of the base. The palladium content in the filtrate, determined by means of atomic absorption spectroscopy (AAS), was, however, found to be 1.3% for **26@MCM-41** and 6.2% for **26@SiO$_2$** relative to the original palladium loading of the catalysts. Firstly, this result shows that the degree of palladium leaching is strongly dependent on the nature of the support. Secondly, it implies that if the leached species were responsible for the catalytic activity, there should be a large difference in activity between **26@MCM-41** and **26@SiO$_2$**, which is not the case. On the other hand, there is a stronger decrease in activity over four recycling experiments for **26@SiO$_2$** than for **26@MCM-41**, which correlates overall to the loss of palladium determined by AAS. Furthermore, the applied reaction temperature and the solvent that was used provide reaction conditions untypical of a dominant palladium leaching. The results lead me to conclude, that the observed activities can be attributed to heterogenized rather than leached palladium species.

Results and Discussion
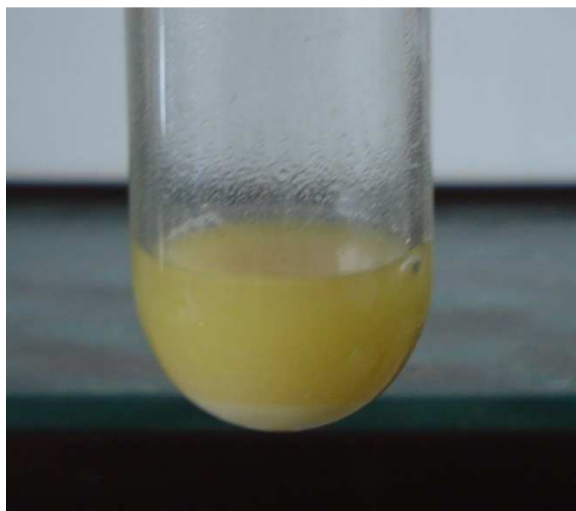
Figure 58. Reaction vessel containing **26@MCM-41** at the end of the second run.

3.5. A Covalently Supported Palladium Complex Bearing a 4-(2-Amino)pyrimidinyl Functionalized Triphenylphosphine Ligand.

3.5.1. Introduction

Triphenylphosphine (TPP) is one of the most important and widely used ligands for transition metal based homogeneous catalysts. Thiel's group was recently looking for a method to immobilize TPP or related ligands and derived complexes on mesoporous silica materials. In a first attempt a functionalized triphenylphosphine palladium complex (**Scheme 42**, **I**)[83] could successfully be immobilized onto neat silica by applying a covalent grafting method. Its catalytic properties were studied for the Suzuki reaction. It showed good activity and efficient reusability. To have a better recycling process, the functionalized triphenylphosphine palladium complex was covalently grafted on silica coated magnetic nanoparticles (SMNP) by a 'bottom-up' approach (**Scheme 42**, **II**).[87] In continuing these efforts to develop heterogenization of TPP in Thiel's group, a functionalized triphenylphosphine palladium complex with a phosphonic acid functionalized linker recently was covalently grafted on TiO_2 (**Scheme 42**, **III**) and ZrO_2 (**Scheme 42**, **IV**)[91] and the catalytic activity of these hybrid

Results and Discussion

materials as well as reusability of the catalysts were studied for the Suzuki reaction.

X Y	P=O	Si-OMe
SiO$_2$	-	I
SMNP	-	II
TiO$_2$	III	-
ZrO$_2$	IV	-
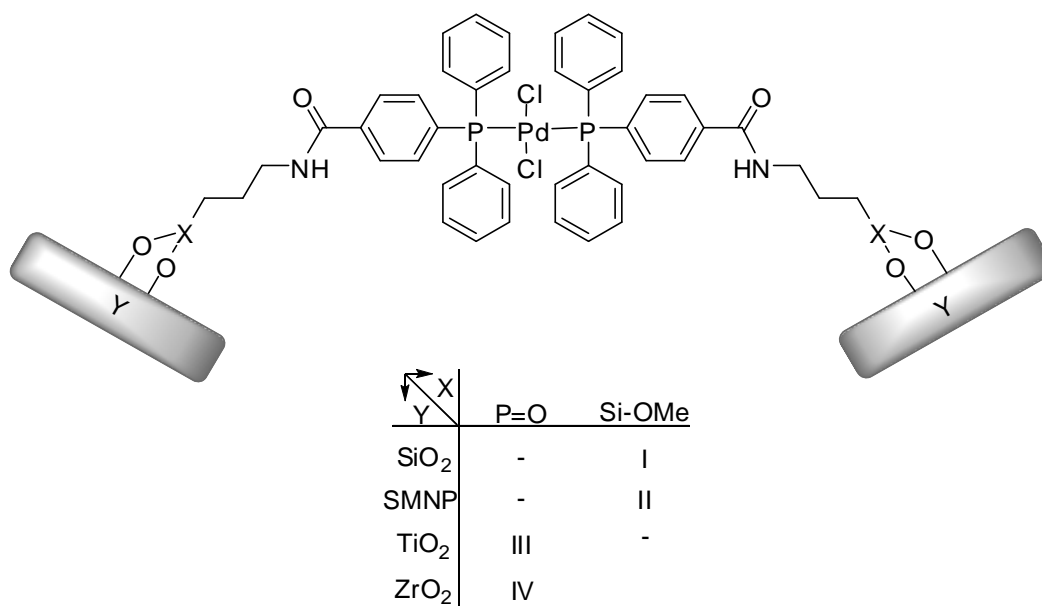
Scheme 42. Immobilized triphenylphosphine palladium complexes **I-IV**.

As mentioned in the previous part, the amino moiety of an *ortho*-functionalized aminopyrimidinyl phosphine allows a rapid functionalization of the ligand with a silylated side chain containing a urea linker for catalyst heterogenization. By applying the same procedure and using a *para*-functionalized aminopyrimidinyl phosphine, ''single-site'' TPP type catalysts grafted onto inorganic supports will be accessible. Recently, it has been shown in Thiel's group that (*E*)-[4-{(3'-*N,N*-dimethylamino)prop-2-en-1-onyl}phenyl]diphenylphosphine (**Scheme 43**) gives access to aminopyrimidinyl-functionalized arylphosphines in large scales and excellent yields by ring closure with an excess of guanidinium salt and KOH in refluxing EtOH.[91] Heating a 1:1 mixture of **2a** and commercially available 3-triethoxysilylpropyl-1-isocyanate to 200 °C results in the formation of the triethoxysilyl-modified ligand **27**. As I presented earlier in section 3.1.1.2, fusing just the guanidinium carbonate and the precursor will result in the *ortho*-functionalized aminopyrimidinyl phosphine in high yield. With this idea the process can be simplified as follow: the phosphine precursor is mixed with guanidinium

Results and Discussion

carbonate and heated to 220 °C until all dimethylamine is released. Then 3-triethoxysilylpropyl-1-isocyanate was added directly to the Schlenk tube. Heating the mixture to 200 °C results in the formation of the triethoxysilyl-modified ligand **27** possessing a stable urea group just in one step.
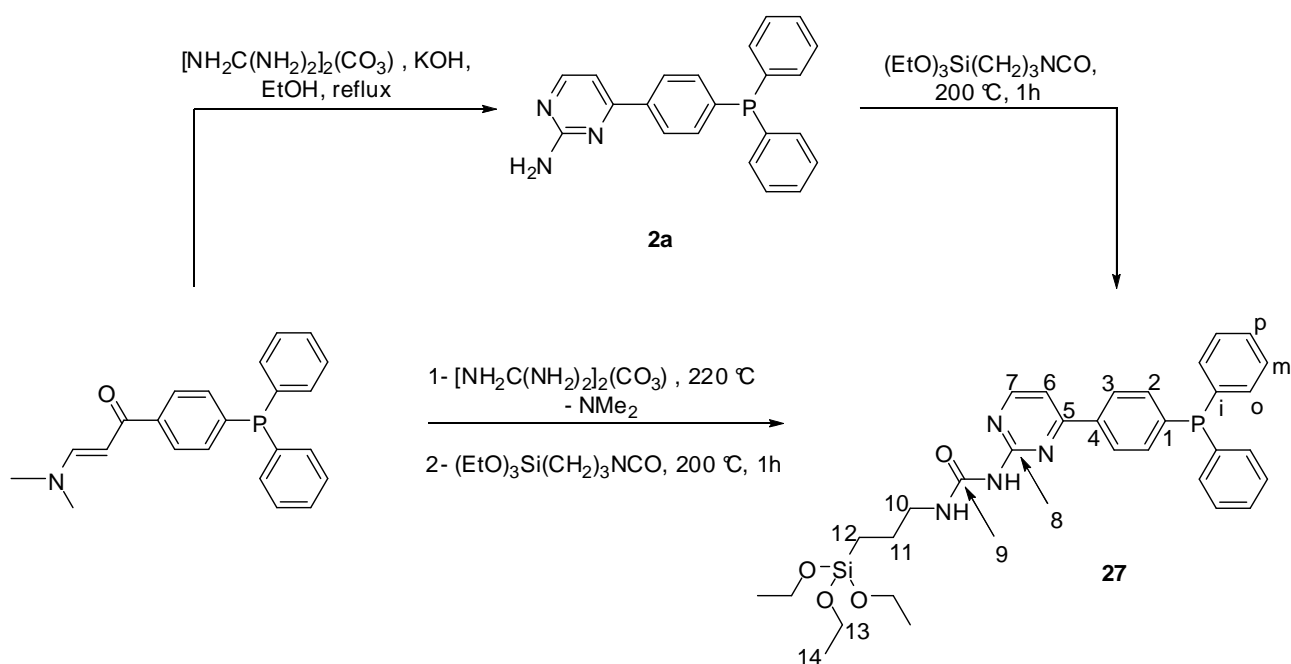
Scheme 43. Synthesis of **27**.

The pale yellow colored solid product **27** was characterized by NMR spectroscopy: three sets of signals in the high-field region of the ^{1}H NMR spectrum (at 4.05, 1.86, 0.70 ppm), are typical for the propylene chain. Two sharp signals (at 3.81 and 1.21 ppm) are assigned to the Si(OEt)$_3$ group (**Figure 59**). The ^{31}P NMR spectrum shows one sharp resonance at –4.18 ppm. In comparison to the **2a** the resonance is shifted by 7.87 ppm to lower field (**Figure 60**).

Results and Discussion
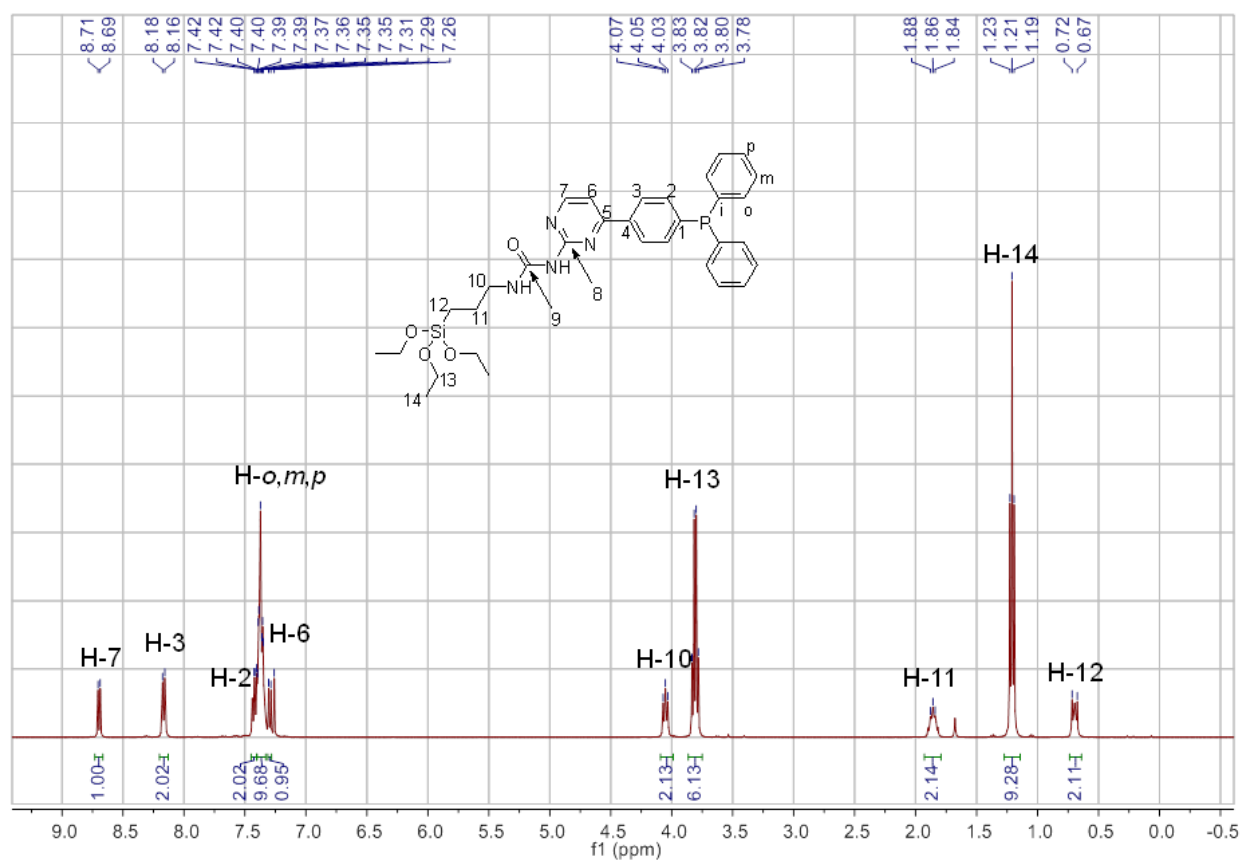
Figure 59. ^{1}H NMR spectrum of **27** in CDCl$_3$.

Results and Discussion
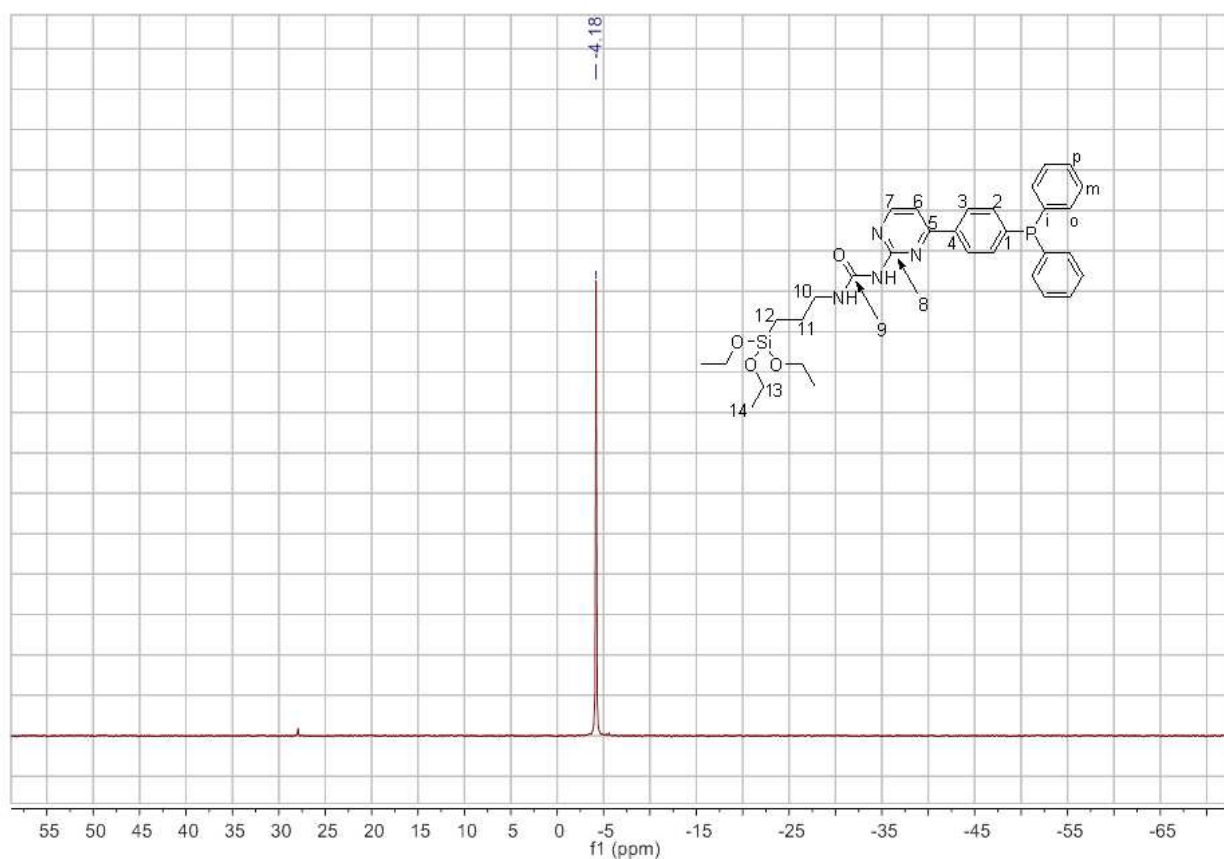
Figure 60. ^{31}P NMR spectrum of **27** in CDCl$_3$.

In the ^{13}C NMR spectrum (**Figure 61**), the three resonances of the propylene linker are observed at 46.0, 21.0, 7.9 ppm. The resonances at 58.6 and 18.4 ppm can be assigned to the organosilica -Si(OCH$_2$CH$_3$)$_3$ group. The signals for the aryl groups appear in the range from 128.7 to 146.9 ppm. The two resonances at 148.0 and 106.7 can be assigned to C-7 and C-6 respectively and the signal at 172.2 ppm to the C=O group of the linker.

Results and Discussion
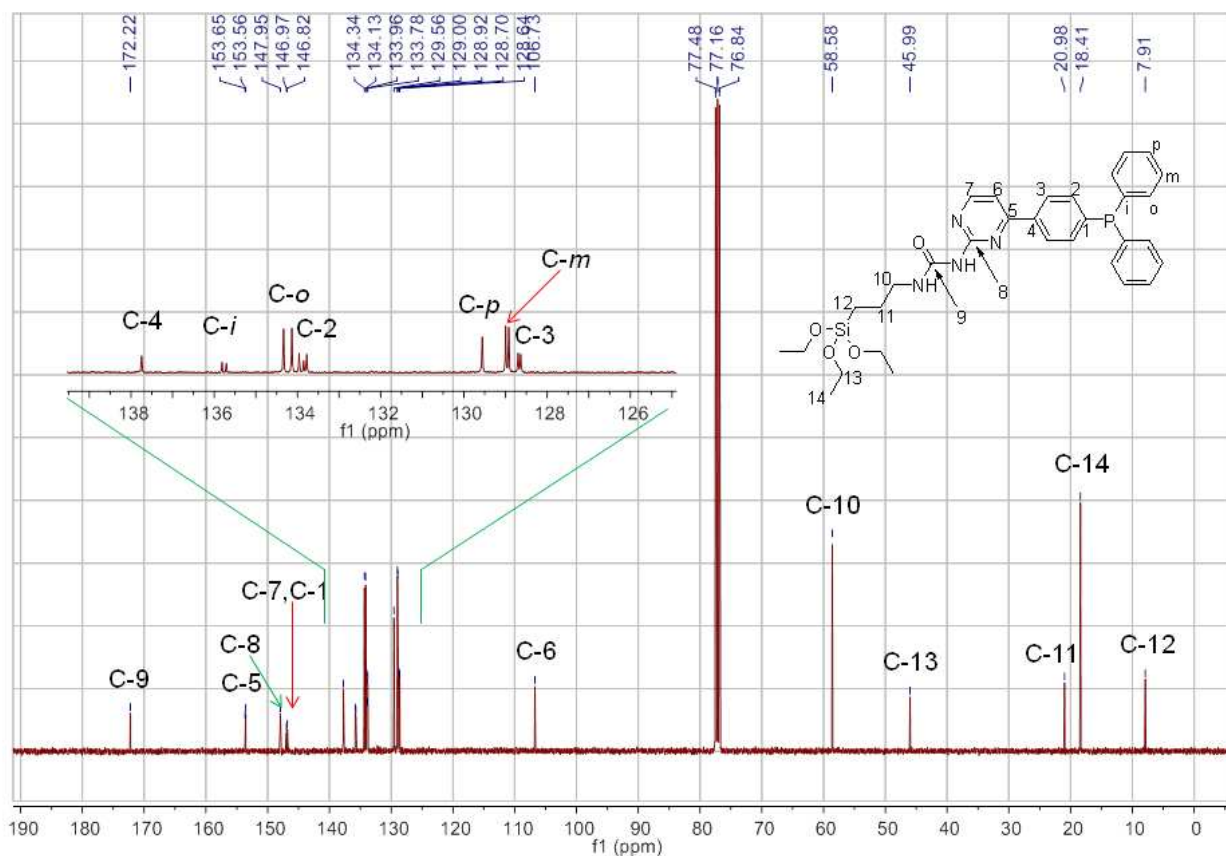
Figure 61. ^{13}C NMR spectrum of **27** in CDCl$_3$.

Reacting ligand **27** with half an equivalent of (C$_6$H$_5$CN)$_2$PdCl$_2$ in CH$_2$Cl$_2$ gives the desired palladium complex **28** in almost quantitative yields (**Scheme 44**). The formation of complex **28** was proved by ^{31}P NMR spectroscopy (**Figure 62**). The phosphorus resonance appeared at 23.90 ppm which is shifted to lower field in comparison to the free ligand **27**.

Results and Discussion

27

$(C_6H_5CN)_2PdCl_2$ | CH_2Cl_2, 1 h

28
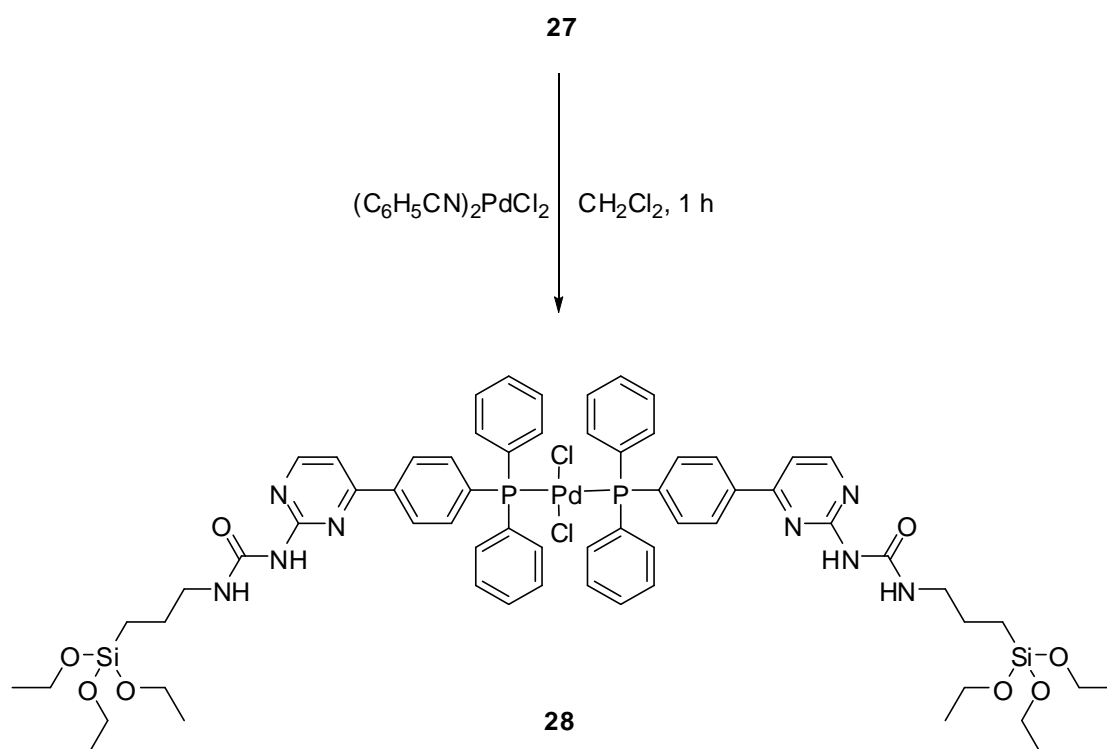
Scheme 44. Synthesis of complex **28**.

Results and Discussion
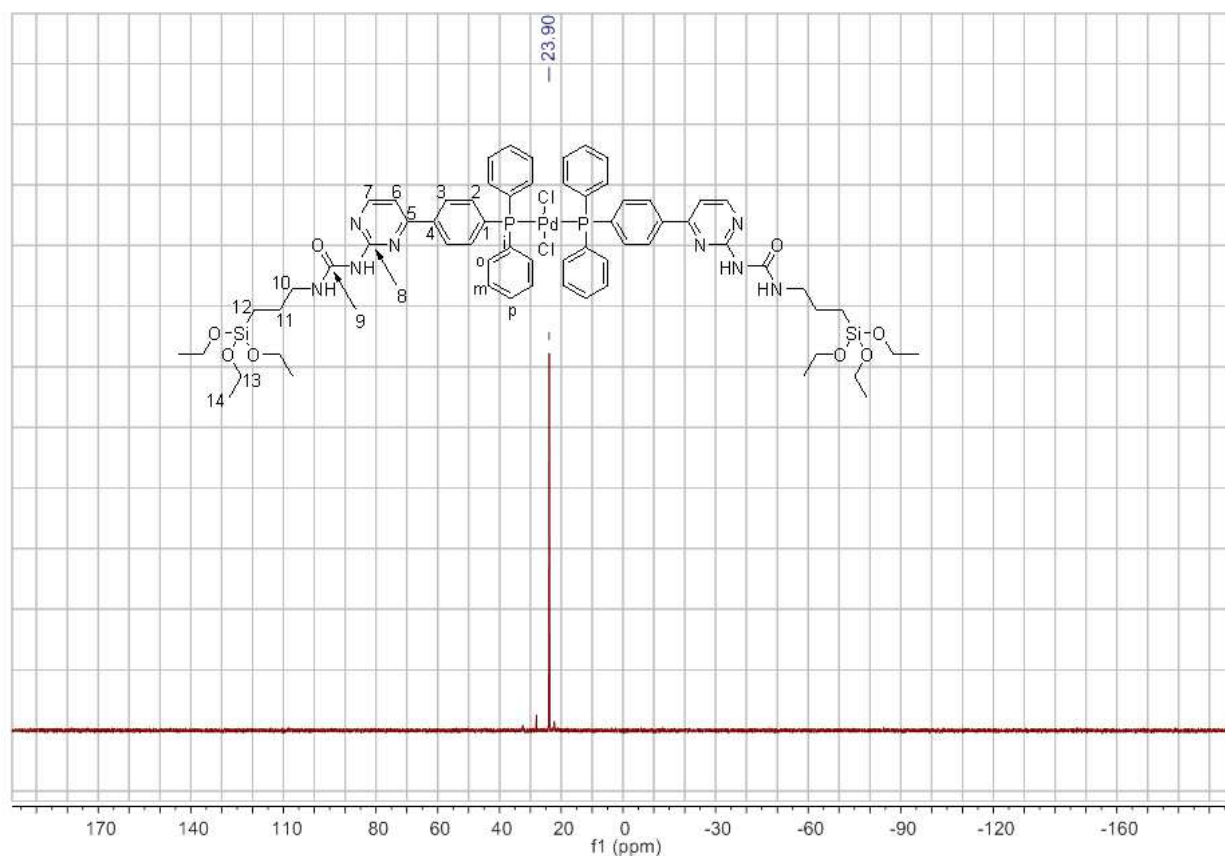
Figure 62. ^{31}P NMR spectrum of palladium complex **28** in CDCl$_3$.

The ^{1}H NMR and ^{13}C NMR spectra of the palladium complex **28** are shown in **Figure 63** and **Figure 64**. In both case ^{1}H NMR and ^{13}C NMR data are in accordance to the spectroscopic features of ligand **27**.

Results and Discussion
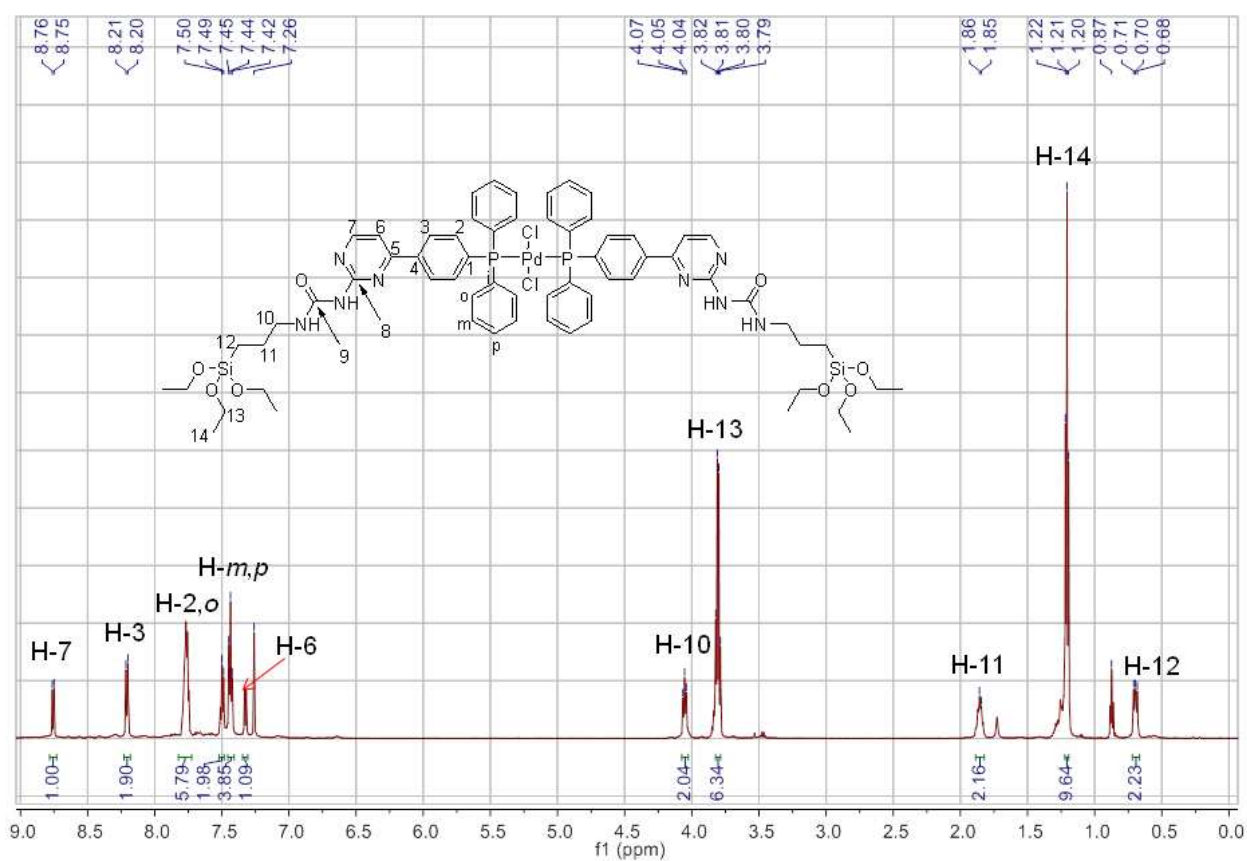
Figure 63. ^{1}H NMR spectrum of palladium complex **28** in CDCl$_3$.

Results and Discussion
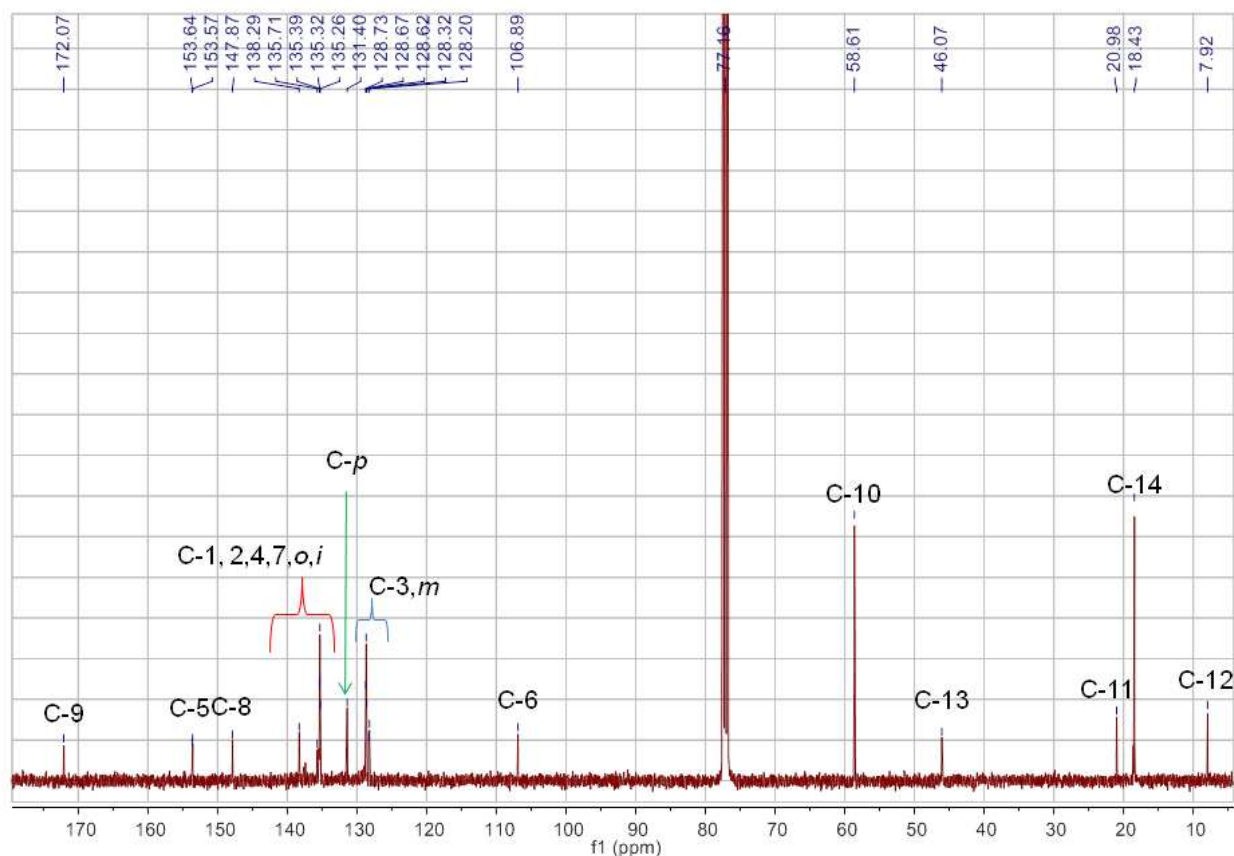
Figure 64. ^{13}C NMR spectrum of palladium complex **28** in CDCl$_3$.

3.5.2. Preparation of the Heterogeneous Catalysts 28@MCM-41 and 28@SiO$_2$

Finally, complex **28** was covalently grafted onto the ordered mesoporous silica MCM-41 and on commercial amorphous SiO$_2$ (**Scheme 45**). For both heterogeneous catalysts **28@MCM-41** and **28@SiO$_2$**, the same reaction conditions (reactant and solvent amount, reaction temperature and reaction time) were applied. A solution of complex **28** in dry CH$_2$Cl$_2$ was added to a suspension of MCM-41 or SiO$_2$ in dry toluene. The mixture was stirred for 12 h at 100 °C. The solid was filtered off and washed with CH$_2$Cl$_2$ in a Soxhlet apparatus for 24 h. Finally, the solid was dried in vacuum at 50 °C for 5 h to obtain **28@MCM-41** or **28@SiO$_2$**.

Results and Discussion

28
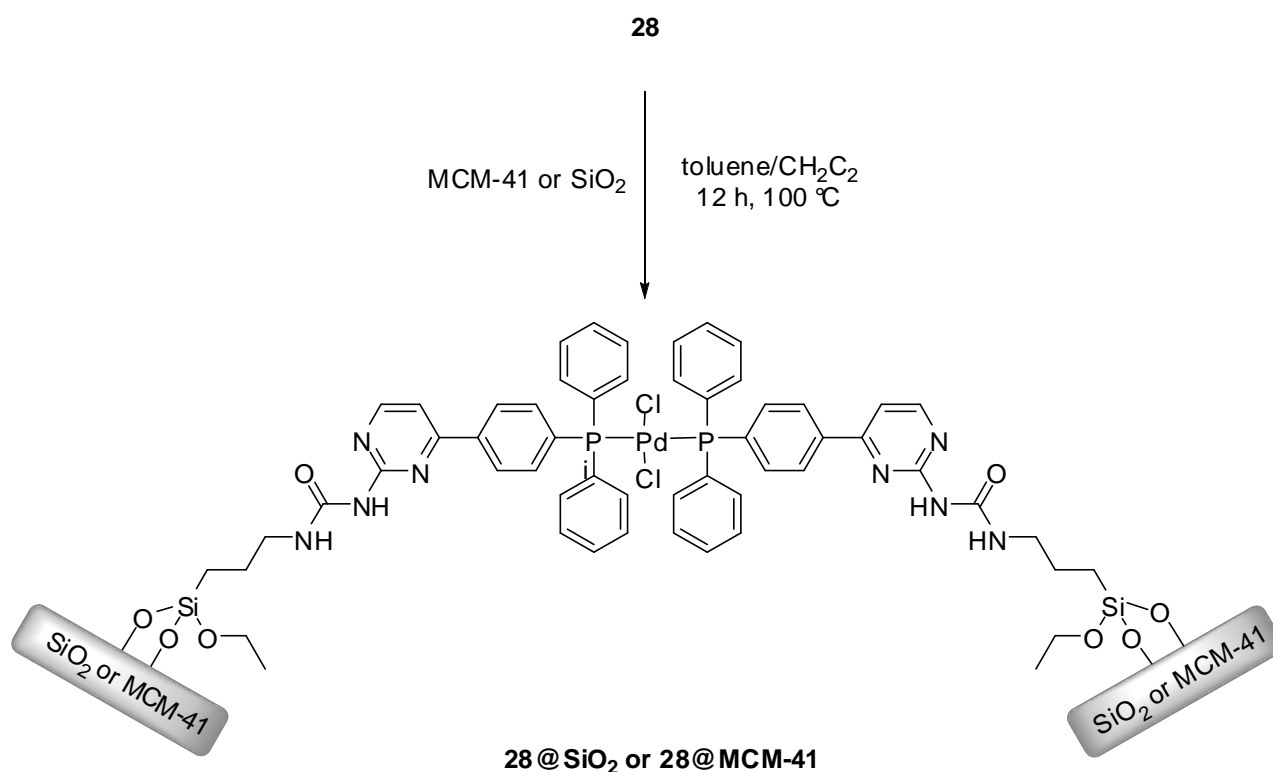
Scheme 45. Synthesis of the heterogeneous catalysts **28@MCM-41** and **28@SiO$_2$**.

The loading of the palladium complex was determined by measuring the nitrogen content of the material. Although 0.28 mmol of complex **28** per gram of SiO$_2$ and MCM-41 were applied in the grafting procedure, elemental analysis shows that only 0.15 mmol g^{-1} and 0.09 mmol g^{-1} of palladium complex **28** were finally immobilized on the surface of **28@SiO$_2$** and **28@MCM-41,** respectively. As mentioned in previous section, the palladium complex content of **26@MCM-41** (0.31 mmol g^{-1}) is higher than in **26@SiO$_2$** (0.28 mmol g^{-1}) which is attributed to the larger surface area of **26@MCM-41** (710 m^{2}g^{-1}) versus **26@SiO$_2$** (321 m^{2}g^{-1}). However, for **28@MCM-41** the palladium content is dramatically decreased which could not be expected according to the surface area (**Table 13**). This reduction can be explained by a blockage of the pore entrance by the large complexes **28** which can cause a low mobility of the free complexes inside the pore system.

At first, information about the silicon environment and the degree of organic

Results and Discussion

functionlization of both catalysts **28@SiO$_2$** and **28@MCM-41** were obtained from solid state ^{29}Si CP MAS NMR. As shown in **Figure 65**, a similar type of pattern is observed for both hybrid materials. The low-intensity peaks at about –92 ppm correspond to silicon atoms with two siloxane bonds and two silanol groups (Q^2). The peaks with high intensity at about –101 ppm is attributed to silicon atoms with three siloxane bonds and one silanol group (Q^3), and the resonance at about –110 ppm is attributed to the four siloxane bond silicon atoms (Q^4). The signals from –45 ppm to –70 ppm are belonging to organo silicon species. Among them a broad band having a center at about –49 ppm can be observed, which confirmed the existence of R-Si(HO)$_2$(OSi) species (T^1), as major species in both hybrid materials.
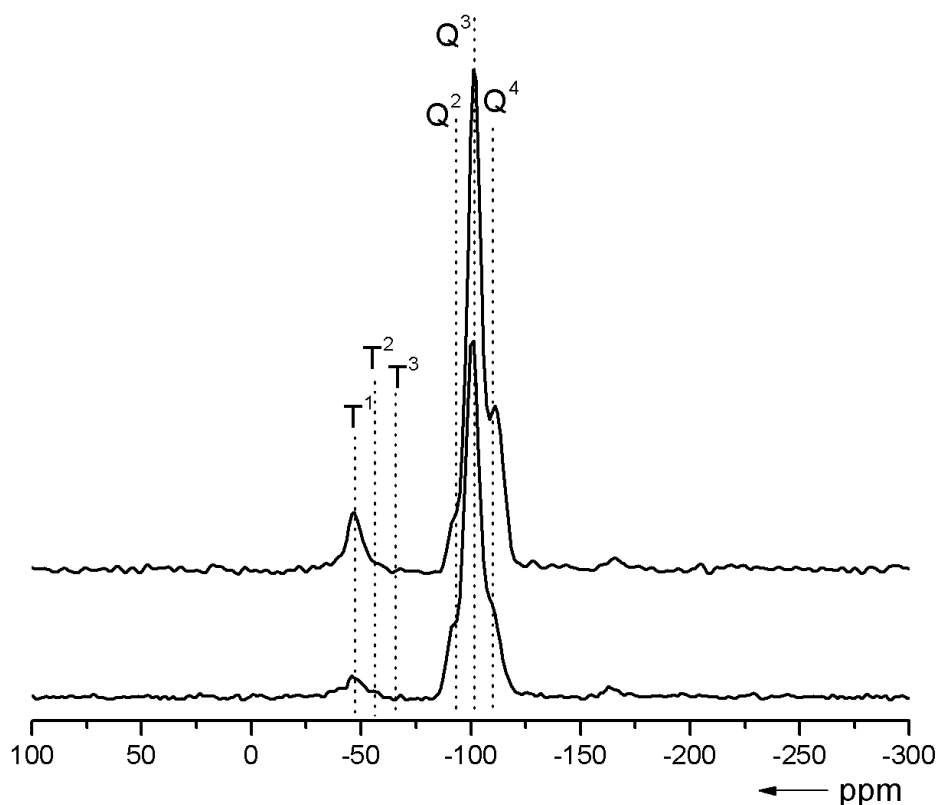
Figure 65. Solid-state ^{29}Si CP-MAS NMR spectra of **28@MCM-41** (bottom line) and **28@SiO$_2$** (top line).

Results and Discussion

The ^{31}P CP-MAS NMR of **28@MCM-41** and **28@SiO$_2$** are shown in **Figure 66**. The ^{31}P NMR signals of both hybrid materials correspond well with the chemical shifts of the palladium complex in solution. There is no signal of uncoordinated phosphine and phosphineoxide present in **28@SiO$_2$**, which means that the complex can survive in the grafting process even under harsh reaction conditions. However a weak signal at about –5 ppm is observed in **28@MCM-41** which is attributed to the free ligand and confirms decomposition of a small amount of the palladium complex **28** during the anchoring on the solid support. The unsymmetrical phosphorus resonance in both hybrid materials are probably caused by differences in the chemical environment of the phosphine and the palladium sites which are located in close proximity to the surface. These unsymmetrical phosphorus resonances also were reported for other immobilized functionalized triphenylphosphine palladium complexes on silica in Thiel's group.[83]

Results and Discussion
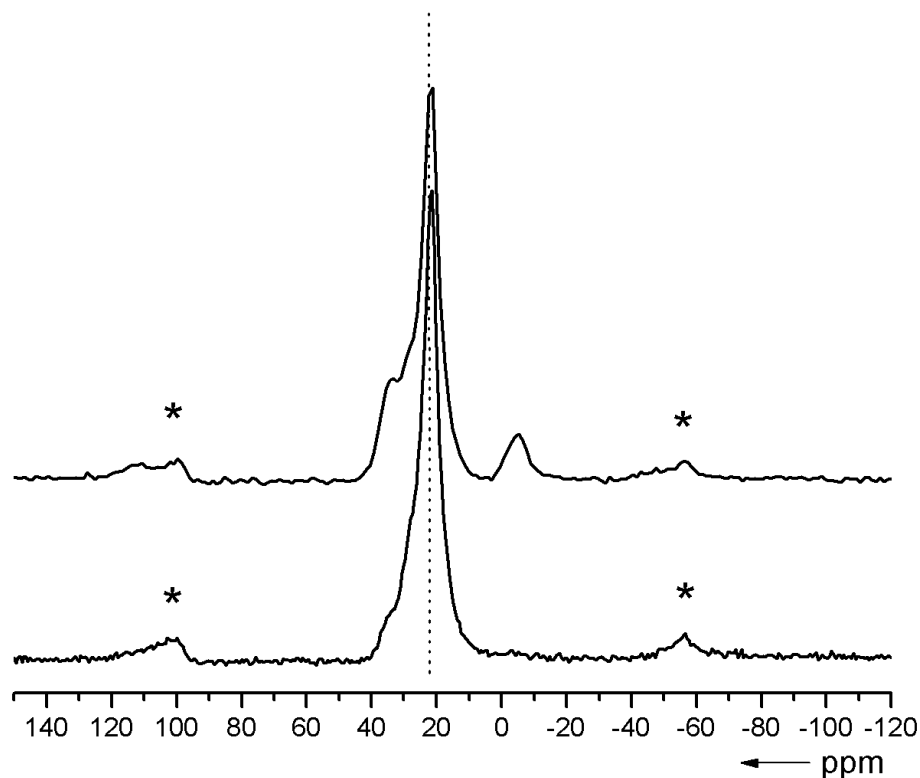
Figure 66. ^{31}P MAS NMR spectrum of **28@MCM-41** (top line) and **28@SiO$_2$** (bottom line); the dashed line signs the ^{31}P NMR resonance of the palladium(II) complex **28** in solution. The asterisks denote rotational sidebands.

For both hybrid materials **28@MCM-41** and **28@SiO$_2$**, ^{13}C CP-MAS NMR spectra are presented in **Figure 67**. The spectra of the hybrid materials are similar to the spectrum of complex **28** in CDCl$_3$. The resonance at about 173 ppm was assigned to the urea carbonyl group. The resonances between 148 and 142 ppm can be assigned to pyrimidinyl carbon atoms, a broad signal between 140 and 120 ppm belongs to all other aromatic carbon atoms. The resonances of the propylene linker appear at about 46.0, 21.1, and 8.0 ppm and the dominant resonances at about 58.7 and 18.3 ppm can be assigned to ethoxysilyl (SiOCH$_2$CH$_3$) units.

Results and Discussion
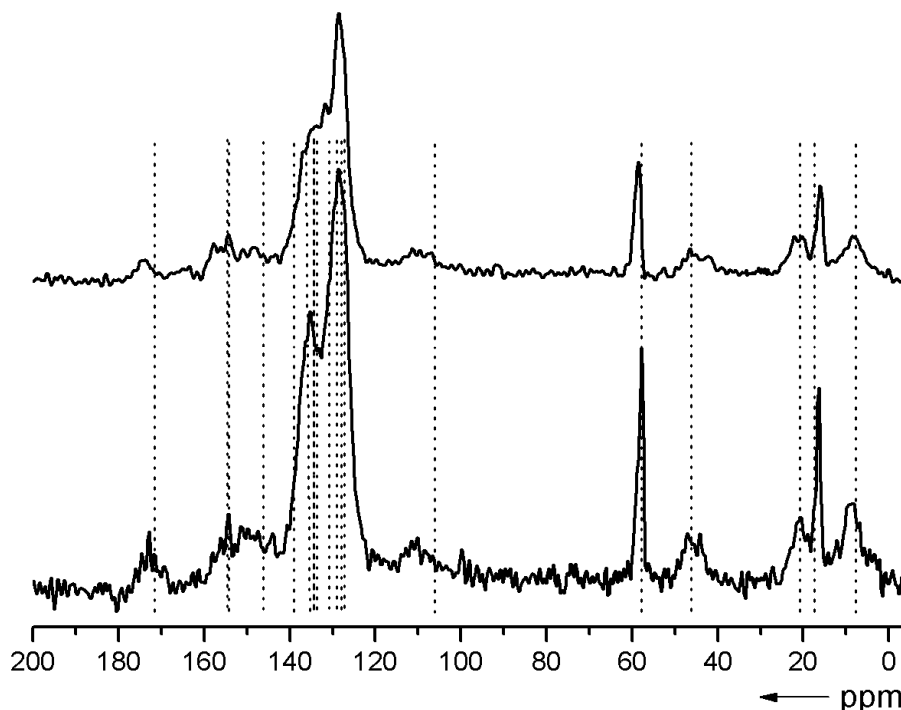
Figure 67. ^{13}C MAS NMR spectra of **28@MCM-41** (top line) and **28@SiO$_2$** (bottom line); the dashed lines assign the ^{13}C NMR resonances of the palladium(II) complex **28** in CDCl$_3$.

The infrared spectrum of ligand **2a** is shown in **Figure 68**. A broad band at about $\tilde{v} \approx$ 3460 cm^{-1} can be assigned to NH and OH groups (from residual water in KBr). The sharp signals of urea I and urea II vibration can be observed at $\tilde{v} \approx$ 1745 cm^{-1} and 1671 cm^{-1}, which are out of the range of urea stretching absorptions. A similar signal was observed for **25**. This unusual difference is assigned to the imine tautomer of the urea unit, which is stabilized by an O–H$\cdots$N hydrogen bond with one of the pyrimidinyl nitrogen atoms in a six-membered cycle. In the IR spectrum of complex **28**, the urea I and II peaks are slightly shifted to higher frequencies (1751 and 1680 cm^{-1}, respectively) due to the electron withdraw of the Lewis acidic palladium(II), which is in agreement with the ^{31}P NMR spectra of ligand **27** and complex **28**. The infrared spectra of the corresponding heterogenized systems and **28@SiO$_2$** clearly show the success of immobilization. However the low loading in **28@MCM-41** leads to a low intensity of the spectrum. In these materials, the bands in the range of $\tilde{v}$ = 1550-1700

Results and Discussion

are typical for the urea fragment and broad band in the range of $\tilde{v}$ = 3700-3200 cm^{-1} is attributed to the hydroxyl stretching vibrations of hydrogen bonded internal silanol groups ($\tilde{v}_{OH}$ from Si–OH). The asymmetric Si-O-Si vibration appears at about $\tilde{v}$ = 1070 cm^{-1} ($\tilde{v}_{asym}$ from Si–O–Si), while the peak at about $\tilde{v}$ = 790 cm^{-1} can be assigned to the symmetric Si-O-Si vibration ($\tilde{v}_{sym}$ from Si–O–Si).
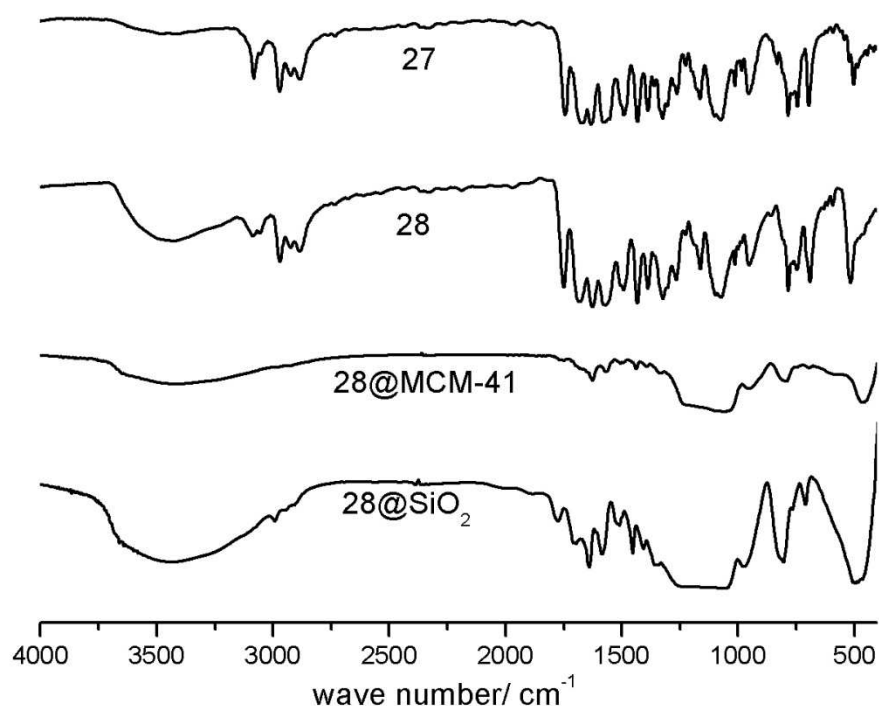
Figure 68. FT-IR spectra (KBr) of compounds **27**, **28**, and **28@MCM-41** and **28@SiO₂**.

The surface areas, pore volumes, and pore size distributions of materials **28@MCM-41** and **28@SiO₂** were determined by N_2 adsorption–desorption experiments. All the corresponding data are listed in **Table 13**. N_2 adsorption–desorption measurements of all samples demonstrated typical type IV isotherms (definition by IUPAC) with a hysteresis characteristic for mesoporous materials possessing pore diameters between 2 and 50 nm.[208] The sharp capillary condensation steps at P/P_o= 0.2–0.4 for **28@MCM-41** (**Figure 69**) is related to the ordered pore structure with narrow pore size distributions and is thus consistent

Results and Discussion

Table 13. Textural parameters of **28@MCM-41** and **28@SiO$_2$**.

Sample	S_{BET}[a] [m^{2}g^{-1}]	Pore size [Å]	Pore volume [m^{3}g^{-1}]	Pd content[b] [mmolg^{-1}]
28@MCM-41	901	27.5	0.663	0.09
28@SiO$_2$	306	57	0.555	0.15

[a] S_{BET}= Brunauer–Emmett–Teller surface area. [b] Calculated according to the nitrogen content of the elemental analysis.
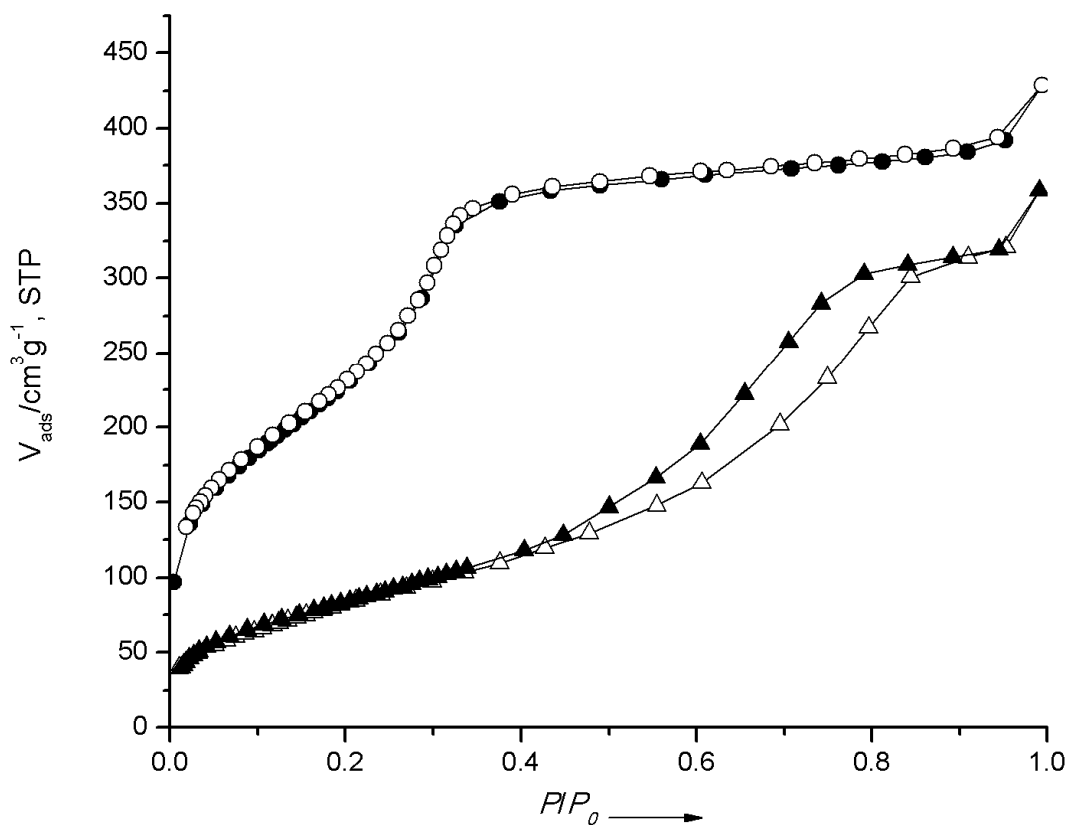
Figure 69. Nitrogen adsorption–desorption isotherms of **28@MCM-41** (top line) and **28@SiO$_2$** (bottom line); ■, ●, ▲ adsorption; □, ○, Δ desorption.

As expected, the surface area, the pore volume and pore size of the hybrid material are

Results and Discussion

decreased compared to the neat silica support (**Table 9** and **Table 13**). These results indicate that the palladium complex was grafted in the pores of the support.

The powder XRD pattern of the hybrid material **28@MCM-41** (**Figure 70**) exhibits a strong d_{100} reflection and two other weaker reflections assigned to d_{110} and d_{200}, suggesting that the two-dimensional hexagonal pore structure is remained after the immobilization of complex **28**.
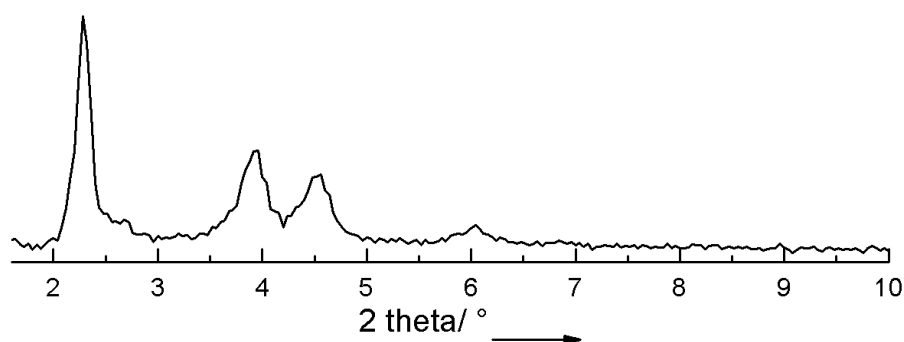
Figure 70. Powder XRD patterns of **28@MCM-41**.

The morphologies and microstructure of the **28@MCM-41** were further investigated by scanning electron microscopy (SEM). The image presented in **Figure 71** clearly reveals that obtained hybrid material **28@MCM-41** has a hexagonal morphology and is quite monodisperse. However, a deeper focus to the state of the grafted palladium species is not possible due to the resolution limit of SEM. For **28@MCM-41** energy-dispersive X-ray analysis (EDX analysis) also was carried out and the spectrum is shown in **Figure 72**. This analysis indicates that the major composition in the scanned area is silicon and also confirms the presence of palladium on the mesoporous silica matrix.

Results and Discussion
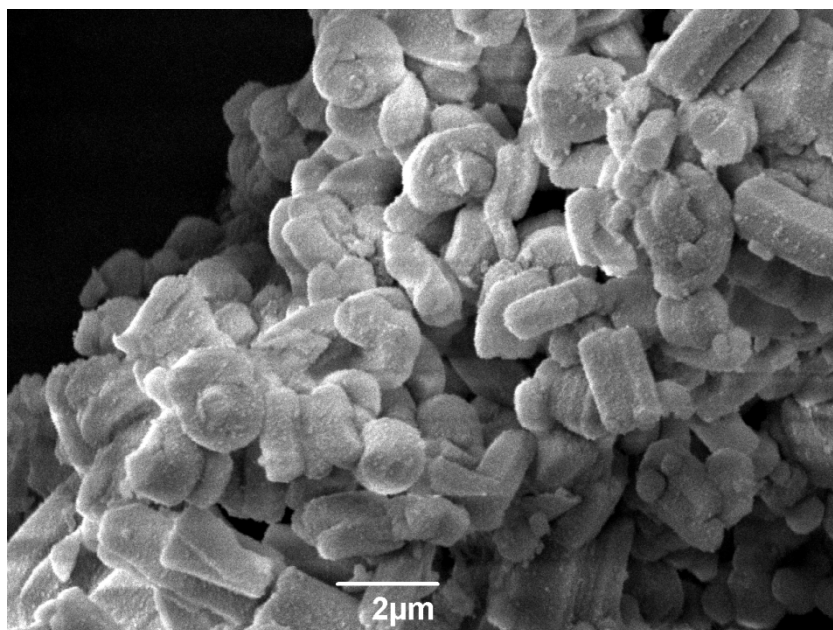
Figure 71. SEM image of the freshly prepared **28@MCM-41**.
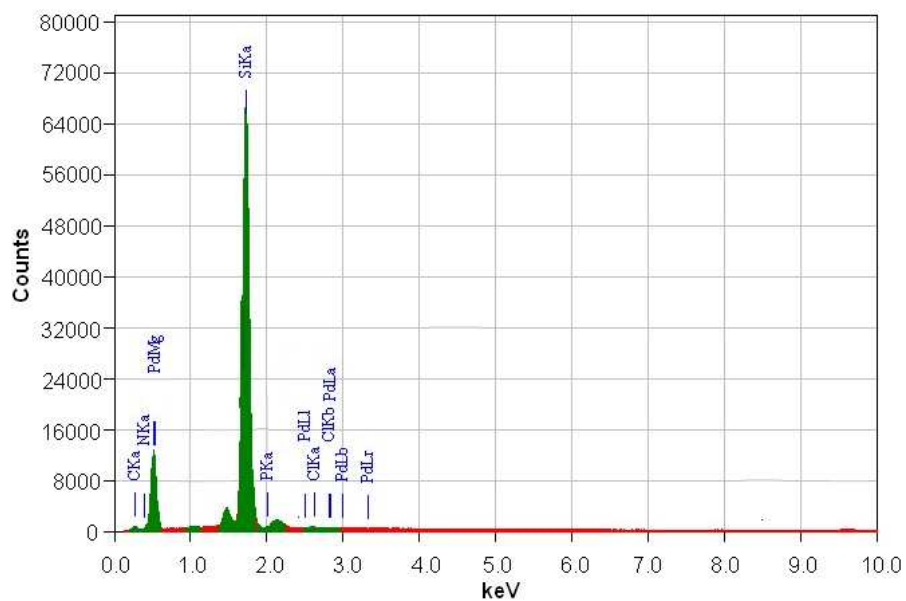
Figure 72. *EDX* analysis of **28@MCM-41**.

The thermal stability of obtained catalysts **28@MCM-41** and **28@SiO$_2$** were evaluated with thermogravimetric and differential thermogravimetric (TG-DTG) analysis (**Figure 73** and **Figure 74**). The DTA curves for both catalysts show a significant endothermic peak below 120

Results and Discussion

°C, which can be attributed to the desorption of physically adsorbed water. The decomposition of the organic compound begins at about 170 °C. In the case of **28@SiO₂** a larger weight loss is observed, which confirms the high loading of immobilized complexes in **28@SiO₂** in comparison to **28@MCM-41**. These analyses also indicate that both catalysts have almost same thermal stability up to 170 °C.
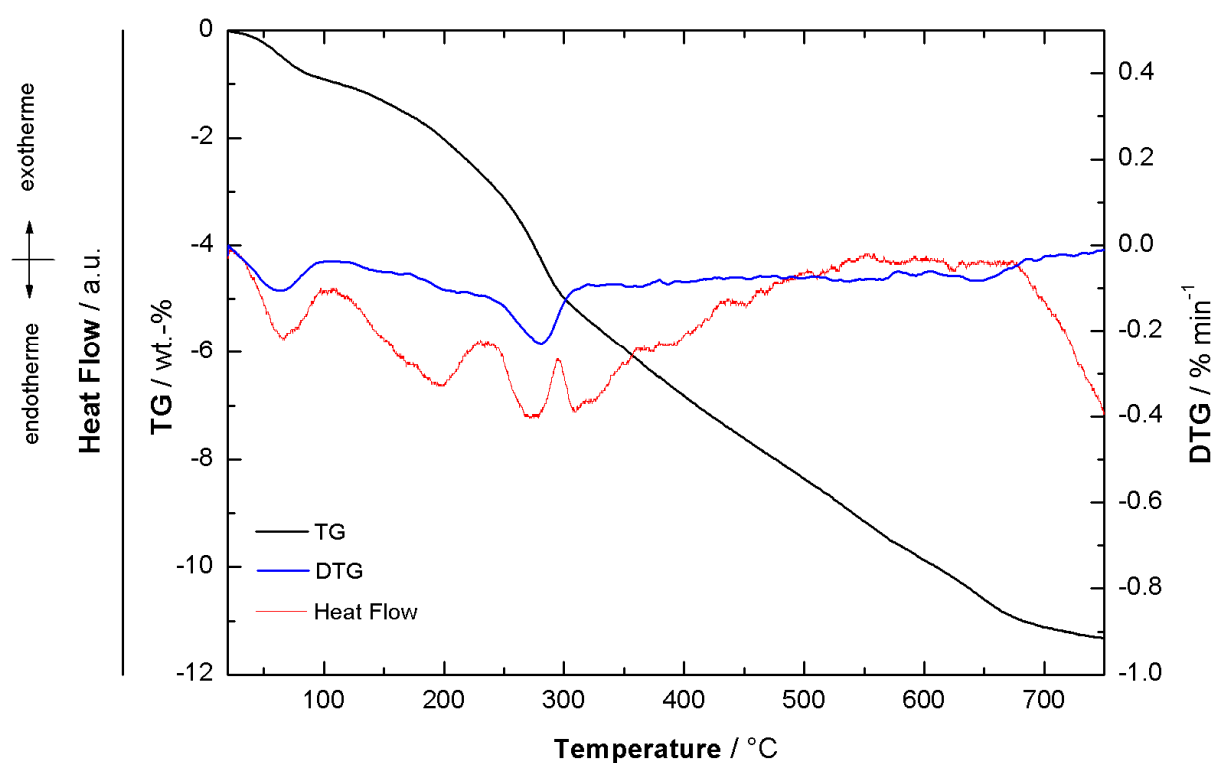
Figure 73. Thermogravimetric and differential thermogravimetric (TG–DTG) analyses of **28@MCM-41**.

Results and Discussion
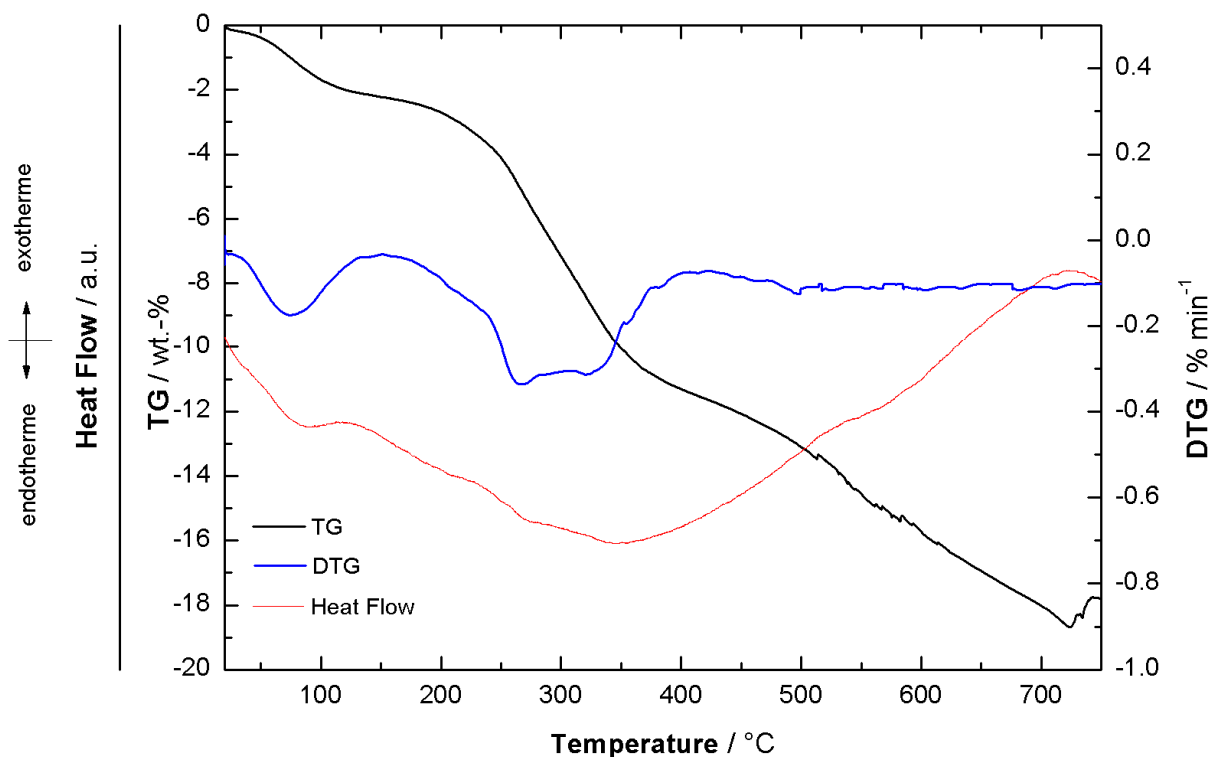
Figure 74. Thermogravimetric and differential thermogravimetric (TG–DTG) analyses of **28@SiO$_2$**.

3.5.3. Catalysis

The hybrid materials **28@MCM-41** and **28@SiO$_2$** were used as catalysts for the Suzuki–Miyaura cross-coupling of phenyl halides and phenylboronic acid. Optimization studies have been done by using the high loaded **28@SiO$_2$** and it revealed that Cs$_2$CO$_3$ and 1,4-dioxane gave the best conversions compared to other bases like CH$_3$COON, K$_3$PO$_3$, K$_2$CO$_3$, and other solvents like toluene, ethanol, and DMF (**Table 14**). On the other hand, the use of the **28@MCM-41** catalyst under these optimized condition gave a poor repeatability.

134

Results and Discussion

Table 14. Coupling of PhBr with PhB(OH)$_2$ with **28@SiO$_2$**.[a]
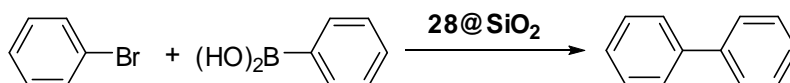
Entry	Solvent	Base	Yield^c [%]
1	DMF	Cs$_2$CO$_3$	10
2	1,4-dioxane	Cs$_2$CO$_3$	92
3	EtOH	Cs$_2$CO$_3$	46
4	toluene	Cs$_2$CO$_3$	trace
5	1,4-dioxane	NaOAc	trace
6	1,4-dioxane	K$_3$PO$_4$	88
7	1,4-dioxane	K$_2$CO$_3$	60

[a] PhBr (1 mmol), PhB(OH)$_2$ (1.5 mmol), base (1.2 mmol), 1, 4-dioxane (5 mL), 80 °C. Catalyst loading: 1 mol% of palladium with respect to PhBr. [b] Determined by using GC based on PhBr.

Under the optimized reaction conditions, the scope of the palladium-catalyzed Suzuki coupling on a series of substrates was tested in the presence of catalyst **28@SiO$_2$**. The coupling of 4-bromoacetophenone and 4-iodoacetophenone with phenylboronic acid afforded the formation of biphenyl in >90% yield after 24 h (**Table 15**, entries 1 and 2). However, for the less reactive 4-chloroacetophenone, a pronounced reduction in activity was observed (**Table 15**, entry 3). Similarly, 4-bromotoluene and 4-iodotoluene also led to coupled products (**Table 15**, entries 4, 5). Additionally the coupling of 2-bromoacetophenone with phenylboronic acid afforded the formation of the desired product (**Table 15**, entry 6).

Results and Discussion

Table 15. Suzuki reactions of aryl halides in the presence of **28@SiO₂** as the catalyst.[a]

Entry	Aryl halide	Product	Yield[b] [%]
1	Br–(4-acetylphenyl)	phenyl-(4-acetylphenyl)	> 99
2	I–(4-acetylphenyl)	phenyl-(4-acetylphenyl)	92
3	Cl–(4-acetylphenyl)	phenyl-(4-acetylphenyl)	14
4	Br–(4-methylphenyl)	phenyl-(4-methylphenyl)	> 99
5	I–(4-methylphenyl)	phenyl-(4-methylphenyl)	> 99
6	Br–(2-acetylphenyl)	phenyl-(2-acetylphenyl)	75

[a] Reaction conditions: aryl bromide (1 mmol), phenylboronic acid (1.2 mmol), Cs₂CO₃ (1.2 mmol), catalyst (1 mol%), 24 h reaction time, 1,4-dioxane, 80 °C. [b] Conversions determined by using GC.

3.5.4. Reusability of the Catalysts 28@MCM-41 and 28@SiO₂

The reusability of the hybrid catalyst **28@SiO₂** for the coupling of bromobenzene with phenylboronic acid at 80 °C was examined. To ensure that the high activity of **28@SiO₂** arises from the palladium sites on the surface and not from the leached palladium species, the heterogeneity of **28@SiO₂** was tested by reusing the catalyst. After the first cycle of the reaction, the catalyst was recovered and the recovered catalyst was washed with dichloromethane and dried under vacuum at 60 °C for 10 h. The activity of the recovered catalyst remained high for the next four subsequent reactions (**Table 16**). However in

136

Results and Discussion

comparison to the **26@MCM-41** and or **26@SiO₂** which was discussed in the previous part, yellow colored catalyst **28@SiO₂** turned to grey after the first run and the color became darker during consequent recycling which is possibly due to the formation of palladium nanoparticles. A similar observation was reported with similar systems (**I, III, V**, mentioned above) in Thiel's group. With the help of TEM imaging, they confirmed that the real active centers of the Suzuki reaction are palladium nanoparticles which are formed in the reaction process.

Table 16. Catalyst recycling experiments.[a]
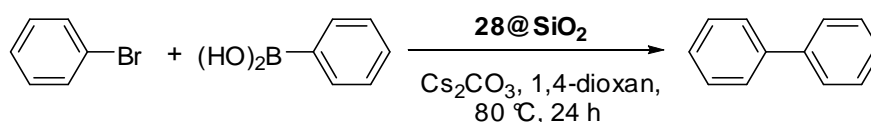
Recycle	Yield[b] [%]
1st	100
2nd	96
3rd	92
4th	89

[a] Reaction conditions: bromobenzene (1 mmol), phenylboronic acid (1.2 mmol), K_3PO_4 (1.2 mmol), catalyst (1 mol%), 24 h reaction time, 1,4-dioxane, 80 °C. [b] Conversions determined by using GC.

The heterogeneity of **28@MCM-41** was tested first by performing a hot filtration experiment as follows: The coupling reaction was done for 1 h, and then the catalyst was removed by filtration at the reaction temperature. 1.2 equivalents of base were added to the filtrate which was heated for additional 23 h to 80 °C. No further reaction was observed. The palladium content in the filtrate after first cycle, also determined by means of atomic absorption spectroscopy (AAS), and palladium contamination of about 0.6% was found relative to the original Pd loading of **28@SiO₂**. The results lead us to conclude, that

Results and Discussion

heterogenized particles are responsible to the observed activities rather than leached palladium

species.

Conclusion and Outlook

4. Conclusion and Outlook

The scientific aim of this work was to synthesize and characterize new bidentate and tridentate phosphine ligands and corresponding palladium complexes and to examine their application as homogenous catalysts. Later on, a part of the obtained palladium catalysts was immobilized and used as heterogonous catalyst.

Pyrimidinyl functionalized diphenyl phosphine ligands were synthesized by ring closure of [2-(3-dimethylamino-1-oxoprop-2-en-yl)phenyl]diphenylphosphine with an excess of substituted guanidinium salts (**Scheme 46**).
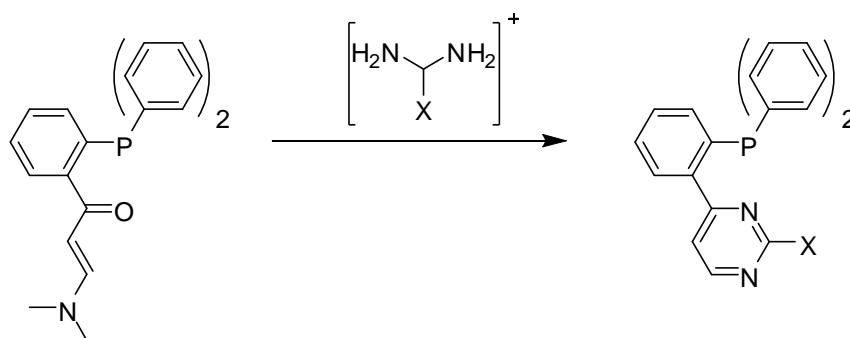
Scheme 46. Synthesis of pyrimidinyl functionalized diphenyl phosphine ligands.

Furthermore to increase the electron density at phosphorous centre the two aryl substituents on the phosphanyl group were exchanged against two alkyl substituents. Electron rich pyrimidinyl functionalized dialkyl phosphine ligands were synthesized from pyrimidinyl functionalized bromobenzene in a process involving lithiation followed by reaction with a chlorodialkylphosphine (**Scheme 47**).

Conclusion and Outlook
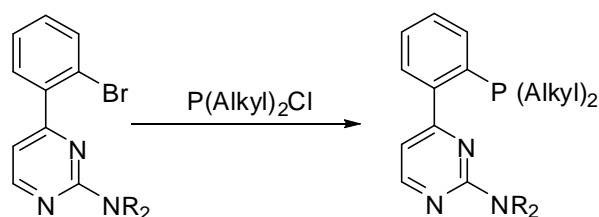
Scheme 47. Synthesis of pyrimidinyl functionalized dialkyl phosphine ligands.

Starting from the new synthesized diaryl phosphine ligands, their corresponding palladium complexes were synthesized. I was able to show that slight changes at the amino group of [(2-aminopyrimidin-4-yl)aryl]phosphines lead to pronounced differences in the stability and catalytic activity of the corresponding palladium(II) complexes (**Scheme 48**). Having a *P,C* coordination mode, the palladium complex can catalyze rapidly the Suzuki coupling reaction of phenylbronic acid with arylbromides even at room temperature with a low loading.
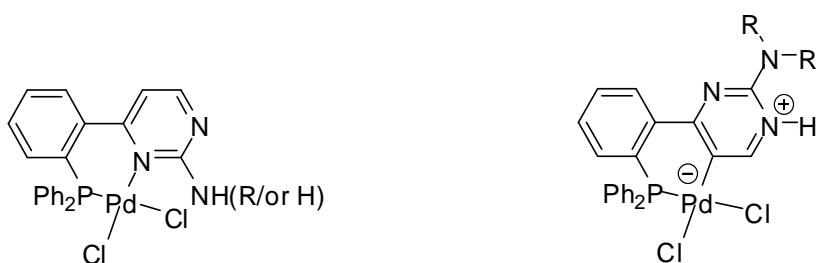
Scheme 48. Different coordination modes in palladium complexes.

Since it is known that bulkier phosphines are potentially better ligands for catalysts, the palladium complexes as well as other complexes of bulky dialkyl phosphine ligands should be synthesized and their potential as catalysts for different reactions shall be investigated in the future.

Using the NH$_2$ group of the aminopyrimidine as a potential site for the introduction of an other substituent, bidentate and tridentate ligands containing phosphorous atoms connected

Conclusion and Outlook

to the aminopyrimidine group and their corresponding palladium complexes were synthesized and characterized (**Scheme 49**). These ligands, are also matter of interest in the SFB/TRR-88 (3MET) at the TU Kaiserslautern. Having pyrimidine groups as relatively soft donors for late transition metals and simultaneously possessing a binding position for another metal, these ligands could be used for synthesizing bimetallic complexes.
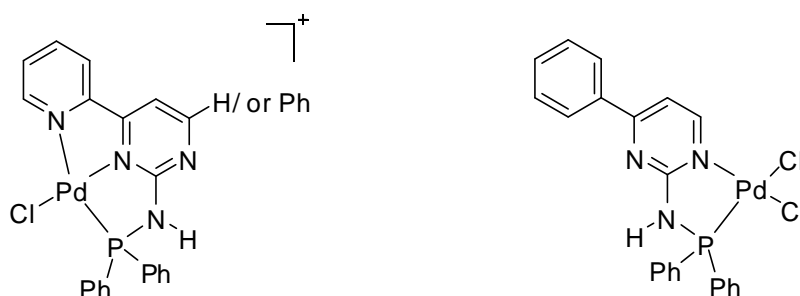
Scheme 49. *PNN* and *PN* palladium complexes.

Two ligands [2- and 4-(4-(2-amino)pyrimidinyl)phenyl]diphenylphosphine (**4a** and **2a**) functionalized with a ethoxysilane group were synthesized (**Scheme 50**). The palladium complexes based on these ligands were prepared and immobilized on commercial silica and MCM-41. Using elemental analysis, FT-IR, solid state ^{31}P, ^{13}C and ^{29}Si CP–MAS NMR spectroscopy, XRD and N_2 adsorption the success of the immobilization was confirmed and the structure of the heterogenized catalyst was investigated.

Conclusion and Outlook
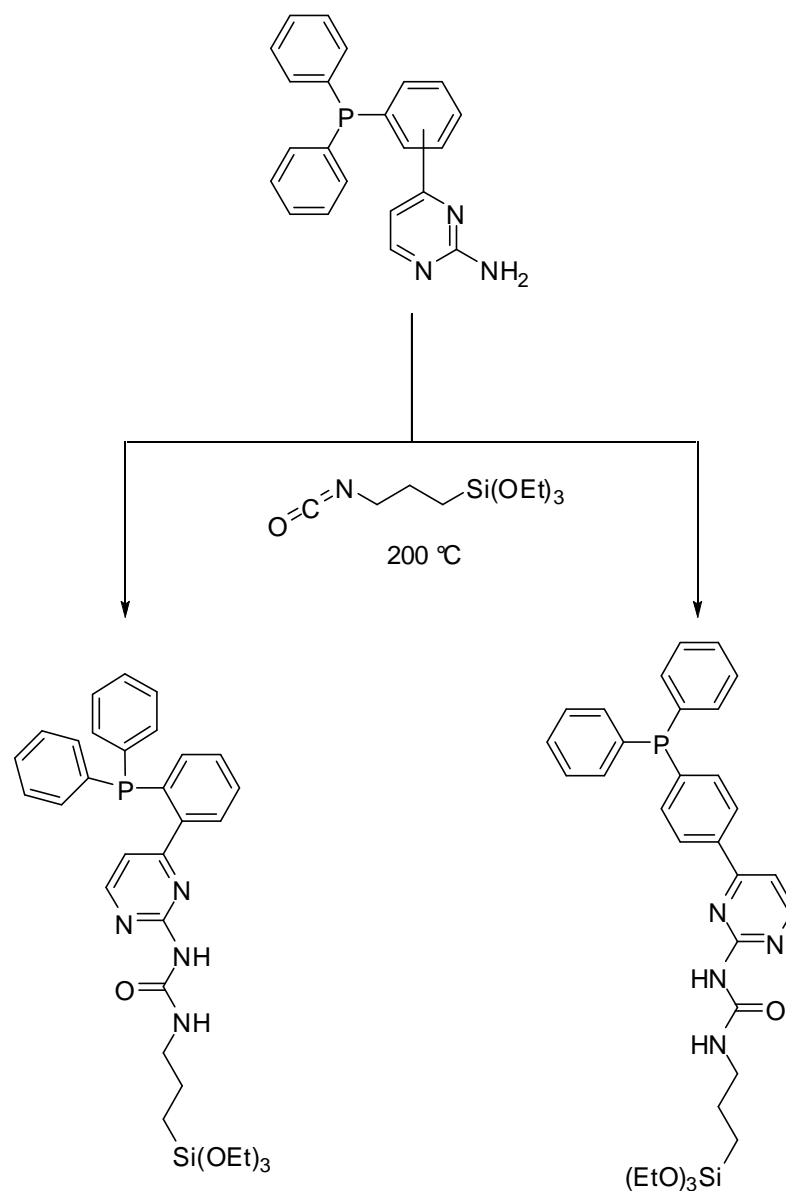
Scheme 50. Functionalization of a [2- and 4-(4-(2-amino)pyrimidinyl)phenyl]diphenyl-phosphine ligands with [(3-Triethoxysilyl)prop-1-yl]isocyanate.

The resulting heterogeneous catalysts were applied for the Suzuki reaction and exhibited excellent activity, selectivity and reusability. These heterogenized catalysts shall be tested as catalysts for other coupling reactions in future.

Experimental

5. Experimental

5.1. Materials

Some solvents such as THF, toluene, diethylether, pentane and dichloromethane were used directly from a MBraun MB-SPS solvent drier without further drying, the other solvents were dried and distilled according to standard methods.[217] Reagents were purchased from ACROS, Aldrich, Fluka, Merck and used without further purification. The silica gel used for the heterogenization was obtained from Aldrich (TLC standard grade, without binder, catalogue no. 28 850-0).

5.2. Characterization of Precursors, Ligands and Complexes

➢ NMR spectroscopy: NMR spectra were recorded on the following devices:

- Bruker DPX 400 (^{1}H: 400.1 MHz, ^{13}C: 100.6 MHz, ^{31}P: 162.0 MHz)
- Bruker AVANCE 600 (^{1}H: 600.1 MHz, ^{13}C: 150.9 MHz)

The chemical shifts are given in δ-values [ppm]; abbreviations: s = singlet, d = doublet, t = triplet, m = multiplet, br. = broad.

➢ Solid state structure analysis: The measurements of the crystal structures were carried out by Dr. Yu Sun on a Stoe-IPDS X-ray diffractometer and an Oxford Diffraction Gemini S Ultra.

➢ Gaschromatography/mass spectrometry: GC/MS measurements were done on a Varian 3900 gaschromatograph in combination with a Varian GC/MS Saturn 2100T mass spectrometer.

➢ CombiFlashR Companion personal flash chromatography: By this apparatus relatively sensitive bulky phosphines were purified.

Experimental

5.3. Characterization of Hybrid Materials

In general, the characterization of solid material requires deeply focusing to the distribution of elements within the solid material and their interactions. To gain this goal all hybrid materials were characterized using the following techniques and instruments:

- CHN-Elemental analyses were performed with a Perkin-Elmer Elemental Analyzer EA 2400 CHN.

- Infrared spectra (KBr) were recorded using a Jasco FT-IR- 6100 spectrometer in a frequency range of 4000–400 cm^{-1}. Intensities are abbreviated as s (strong), m (medium) and b (broad).

- Nitrogen adsorption-desorption isotherms were measured at 77 K, using a Quantachrome Autosorb 1 sorption analyzer. The specific surface areas were calculated using the Brunauer–Emmett–Teller (BET) equation at a relative pressure of 1.0 (P/P_0), and the pore size distribution curves were analyzed with the desorption branch by the BJH method.

- ^{13}C CP-MAS, ^{31}P CP-MAS and ^{29}Si CP-MAS NMR spectra were obtained on a Bruker DSX Avance spectrometer at resonance frequencies of 100.6, 162.0 and 79.5 MHz, respectively.

- X-ray powder diffraction (XRD) patterns were obtained on a Siemens D5005 diffractometer with Cu K$_\alpha$ radiation (30 kV, 30 mA).

- Scanning electron microscopy (SEM) with a K$_\alpha$ JSM-6490LA device and energy dispersive X-ray analysis (EDX) were used to analyze the catalysts surfaces before or after the reaction.

- Atomic adsorption spectra (AAS) were measured with a Perkin Elmer AAnalyst 300 to determine the degree of leached metal from the heterogeneous catalyst.

Experimental

5.4. Ligand Synthesis

[2-(3-Dimethylamino-1-oxoprop-2-en-yl)phenyl]diphenylphosphine (1a). In a flame-dried, nitrogen flushed three-necked flask 176.00 g (1.16 mol) of CsF were suspended in dry DMF (700 ml) and 178 g (921.23 mmol) of (*E*)-3-(*N,N*-dimethylamino)-1-(2'-fluorophenyl)prop-2-en-1-one were added. Then 238 ml (929.45 mmol) of diphenyl(trimethylsilyl)phosphine were added dropwise, the reaction mixture was stirred for 48 h at room temperature. The mixture was diluted with H_2O (800 ml) and CH_2Cl_2 (800 ml), the layers were separated and the aqueous layer was extracted with CH_2Cl_2 (3 × 200 ml). The combined organic layers were washed with H_2O (3 × 400 ml), dried over $MgSO_4$. Removing the solvent in vacuum gave the desired product **1a**, yield: 314.0 g (95%, yellow solid). ^{1}H NMR (CDCl$_3$, 400.1 MHz, 20 °C): δ = 2.69 + 2.94 (2 s, 6 H, H-10, H-11), 5.40 (d, $^3J_{HH}$ = 12.6 Hz, 1 H, H-8), 7.04 (dd, $^3J_{HP}$ = 3.3 Hz, $^3J_{HH}$ = 7.0 Hz, 1 H, H-2), 7.26-7.34 (m, 12 H, H-2, H-*m*, H-*p*, H-3, H-4), 7.38 (ddd, $^4J_{HP}$ = 1.2 Hz, $^3J_{HH}$ = 7.4 Hz, $^3J_{HH}$ = 7.5, 1 H, H-5), 7.64 (m, 1 H, H-9) ppm. ^{13}C NMR (CDCl$_3$, 100.62 MHz, 20 °C): δ = 36.51 + 44.38 (s, C-10, C-11), 95.89 (s, C-8), 127.10 (d, $^3J_{CP}$ = 5.5 Hz, C-5), 127.76 (s, C-*p*), 127.82 (d, $^3J_{CP}$ = 6.5 Hz, C-*m*), 128.03 (s, C-4), 128.83 (s, C-3), 133.15 (d, $^2J_{CP}$ = 19.4 Hz, C-*o*), 134.17 (s, C-1), 135.55 (d, $^2J_{CP}$ = 19.4 Hz, C-2), 138.40 (d, $^1J_{CP}$ = 11.1 Hz, C-*i*), 146.94 (d, $^2J_{CP}$ = 25.9 Hz, C-6), 154.28 (s, 1 C, C-9), 190.91 (s, 1 C, C-7) ppm. ^{31}P NMR (CDCl$_3$, 161.98 MHz, 20 °C): δ = –8.8 (s) ppm.
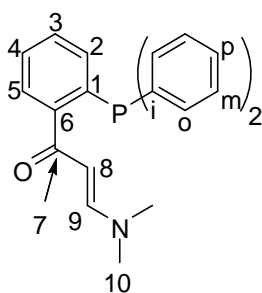
[4-(3-Dimethylamino-1-oxoprop-2-en-yl)phenyl]diphenylphosphine (1c). In an analogous

Experimental

procedure a described for **1a**, phosphine **1c** was synthesized from 593 g (3.07 mol) of (*E*)-3-(*N,N*-dimethylamino)-1-(4'-fluorophenyl)prop-2-en-1-one, 789 ml (3.08 mol) of diphenyl(trimethylsilyl)phosphine (**1a**) and 94.80 g (624.09 mmol) of CsF in dry DMF (600 ml). The reaction mixture was stirred for 60 min at 80 °C. The work-up corresponds to procedure **1c**, yeild: 1036 g (94%, yellow solid). ^{1}H NMR (CDCl$_3$, 400.13 MHz, 20 °C): δ = 2.90 + 3.13 (s, 3 H, H-8, H-9), 5.69 (d, $^3J_{HH}$ = 12.3 Hz, 1 H, H-6), 7.31-7.40 (m, 12 H, H-2, H-*o*, H-*m*, H-*p*), 7.81 (d, $^3J_{HH}$ = 12.4 Hz, 1 H, H-7), 7.84 (dd, $^4J_{HP}$ = 1.3 Hz, $^3J_{HH}$ = 8.2 Hz, 2 H, H-3) ppm. ^{13}C NMR (CDCl$_3$, 100.61 MHz, 20 °C): δ = 37.3 + 45.0 (s, C-8, C-9), 92.3 (s, C-6), 127.3 (d, $^3J_{CP}$ = 6.7 Hz, C-3), 128.5 (d, $^3J_{CP}$ = 6.9 Hz, C-*m*), 128.8 (d, $^4J_{CP}$ = 6.7 Hz, C-*p*), 133.3 (d, $^2J_{CP}$ = 19.0 Hz, C-2), 133.8 (d, $^2J_{CP}$ = 19.7 Hz, C-*o*), 136.8 (d, $^1J_{CP}$ = 10.9 Hz, C-*i*), 140.7 (s, C-4), 140.8 (d, $^1J_{CP}$ = 12.5 Hz, C-1), 154.3 (s, C-7), 188.2 (s, C-5) ppm. ^{31}P NMR (CDCl$_3$, 161.98 MHz, 20 °C): δ = –3.9 (s) ppm.
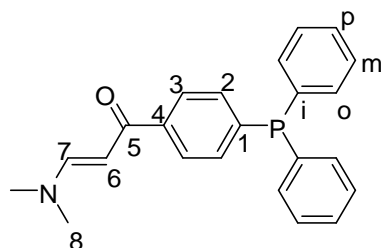
[4-(4-(2-Amino)pyrimidinyl)phenyl]diphenylphosphine (2a). This compound was synthesized by two different methods.

Solvent free synthesis:

Under an atmosphere of nitrogen 4.00 g (11.13 mmol) of **1c** and 1.80 g (10.00 mmol) of guanidinium carbonate were heated to 220 °C until the evolution of dimethylamine and carbon dioxide ceased. After cooling to RT, the residue was dissolved in CH$_2$Cl$_2$, solids were separated by filtration, and the solvent was removed to afford **2a** as a pale yellow powder,

Experimental

yield: 3.6 g (92%).

Solvent based synthesis:

7.50 g (20.87 mmol) of **1c** and 3.25 g (30.00 mmol) of guanidinium sulfate were suspended in dry EtOH (100 ml). After the addition of 1.68 g (30.00 mmol) KOH, the mixture was refluxed for 5 h. Removing the solvent in vacuum, the residue was dissolved in CH_2Cl_2 and filtered. After removing the solvent in vacuum, the crude material was crystallized from ethanol to afford the desired ligand, yield: 6.3g (85%). $C_{22}H_{18}N_3P$ (355.38): calcd. C, 74.35; H, 5.11; N, 11.82; found C, 73.05; H, 5.19; N, 11.61. ^{1}H NMR (CDCl$_3$, 400.13 MHz, 20 °C): δ = 5.16 (br., 2 H, NH2), 7.01 (d, $^3J_{HH}$ = 5.2 Hz, 1 H, H-6), 7.30-7.41 (m, 12 H, H-o, -H-m, H-p, H-2), 7.94 (d, $^3J_{HH}$ = 8.2 Hz, 2 H, H-3), 8.35 (d, $^3J_{HH}$ = 5.2 Hz, 1 H, H-7) ppm. ^{13}C NMR (CDCl$_3$, 100.61 MHz, 20 °C): δ = 107.8 (s, C-6), 127.1 (d, $^3J_{CP}$ = 6.7 Hz, C- 3), 128.7 (d, $^3J_{CP}$ = 7.1 Hz, C-m), 129.1 (s, C-p), 133.9 (d, $^2J_{CP}$ = 22.4 Hz, C-o), 134.0 (d, $^2J_{CP}$ = 18.9 Hz, C-2), 136.7 (d, $^1J_{CP}$ = 10.6 Hz, C- i), 137.4 (s, C-4), 140.9 (d, $^1J_{CP}$ = 12.9 Hz, C-1), 158.9 (s, C-7), 163.4 (s, C-8), 165.2 (s, C-5) ppm. ^{31}P NMR (CDCl$_3$, 161.98 MHz): δ = –5.58(s) ppm.
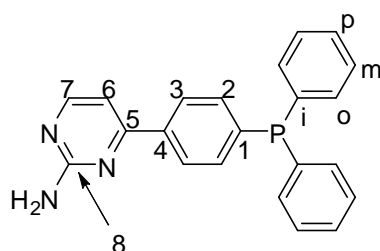
[4-(4-(2-Ethylamino)pyrimidinyl)phenyl]diphenylphosphine (2b). The reaction was carried out in a 2-L round bottomed, three-necked flask, equipped with a reflux condenser, a nitrogen inlet, and a stirring bar. To a suspension of 51.08 g (945.58 mmol) sodium methoxide in (800 ml) dry ethanol 80.40 g (590.48 mmol) 1-ethylguanidium sulfate were added and the mixture was refluxed for 3 h, then 139.34 g (387.70 mmol) of **1c** were added, and the resulting mixture

Experimental

was refluxed for another 3 h. After cooling to room temperature, mixture was strred for 18 h, and then the solvent was removed under reduced pressure, producing an orange solid. The residue was dissolved in ether (700 ml) and the organic phase was washed with water (3× 300 ml) till pH reaches 5-5.5. The aqueous layer was washed with ether (100 ml) and then the combined organic phase was dried over magnesium sulfate and concentrated under vacuum to give a red solid as desired product, yield: 124.0g (83%). $C_{24}H_{22}N_3P$ (383.43): calcd. C, 75.18; H, 5.78; N, 10.96; found: C, 74.58; H, 5.66; N, 10.78. ^{1}H NMR (CDCl$_3$, 400.1 MHz, 20 °C): 1.27 (t, 3 H, H-10), 3.4-3.6 (m, 2 H, H-9), 5.15 (br., 1 H, N-H), 6.94 (d, $^3J_{HH}$ = 5.2 Hz, 1 H, H-6), 7.28-7.48 (m, 12 H, H-o, H-m, H-p, H-2), 7.98 (d, $^3J_{HH}$ = 7.7 Hz, 2 H, H-3), 8.32 (d, $^3J_{HH}$ = 5.2 Hz, 1 H, H-7). ^{13}C NMR (CDCl$_3$, 100.61 MHz, 20 °C): δ = 15.1 (s, C-10), 36.4 (s, C-9), 106.4 (s, C-6), 127.0 (d, $^3J_{CP}$ = 6.7 Hz, C-3), 128.7 (d, $^3J_{CP}$ = 7.1 Hz, C-m), 129.0 (s, C-p), 133.8 (d, $^2J_{CP}$ = 18.9 Hz, C-2), 133.9 (d, $^2J_{CP}$ = 22.4 Hz, C-o), 137.0 (d, $^1J_{CP}$ = 11.1 Hz, C-i), 138.0 (s, C-4), 140.5 (d, $^1J_{CP}$ = 12.9 Hz, C-1), 158.7 (s, C-7), 162.9 (s, C-8), 164.3 (s, C-5) ppm. ^{31}P NMR (CDCl$_3$, 161.98 MHz, 20 °C): δ = –4.18 (s) ppm. IR (KBr, cm^{-1}): 3251s, 3055m, 2972m, 1683w, 1578s, 1556s, 1433m, 1417s, 1340m, 1186w, 1154w, 1090m, 851w, 801s, 747s, 694s, 667s, 514s.

[2-(4-(2-Amino)pyrimidinyl)phenyl]diphenylphosphine (4a). This compound was synthesized by two different methods.

Solvent free synthesis:

148

Experimental

In an analogous procedure a described for **2a**, **4a** was synthesized from 4.00 g (11.13 mmol) of **1a** and and 1.80 g (10.00 mmol) of guanidinium carbonate as a powder, yield: 3.4 g (85%).
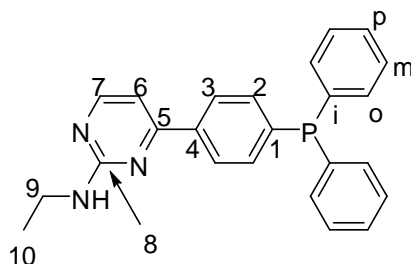
Solvent based synthesis:

Under an atmosphere of nitrogen 3.01 g (8.35 mmol) of **1a** and 1.30 g (12.00 mmol) guanidinium sulfate were suspended in dry ethanol (40 ml). After the addition of 0.67 g (12.00 mmol) KOH, the mixture was refluxed for 20 h. Removing the solvent in vacuum, the residue was dissolved in a mixture of water and CH_2Cl_2. The layers were separated and the aqueous layer was extracted with CH_2Cl_2 (10 ml). The combined organic layers were dried over anhydrous magnesium sulfate and magnesium sulfate was filtered. After removing the solvent in vacuum, the crude material was crystallized from ethanol to afford the desired ligand, yield: 2.8 g (96%). $C_{22}H_{18}N_3P$ (355.38): calcd. C, 74.35; H, 5.11; N, 11.82; found C, 74.01; H, 5.25; N, 11.75. ^1H NMR ([D_6]DMSO, 400.13 MHz, 20 °C): δ = 6.25 (br., 2 H, NH2), 6.67 (d, $^3J_{HH}$ = 4.8 Hz, 1 H, H-8), 6.98 (m, 1 H, H-2), 7.12-7.23 (m, 4 H, H-*m*), 7.30-7.36 (m, 6 H, H-*o*, H-*p*), 7.38 (t, $^3J_{HH}$ = 7.8 Hz, 1 H, H-3), 7.47 (t, $^3J_{HH}$ = 7.3 Hz, 1 H, H-4), 7.63 (m, 1 H, H-5), 8.16 (d, 1 H, H-9) ppm. ^{13}C NMR ([D_6]DMSO, 100.61 MHz, 20 °C): δ = 109.7 (d, $^4J_{CP}$ = 4.6 Hz, C-8), 128.6 (s, C-*m*), 128.6 (s, C-*p*), 128.8 (d, $^3J_{CP}$ = 28.5 Hz, C-2), 129.2 (br., C-3, C-4), 133.2 (d, $^2J_{CP}$ = 20.4 Hz, C-*o*), 134.3 (s, C-5), 135.4 (d, $^1J_{CP}$ = 20.4 Hz, C-1), 138.0 (d, $^1J_{CP}$ = 11.1 Hz, C-*i*), 143.6 (d, $^2J_{CP}$ = 24.0 Hz, C-6), 157.8 (s, C-9), 162.6 (s, C-10), 165.8 (d, $^3J_{CP}$ = 2.8 Hz, C-7) ppm. ^{31}P NMR ([D_6]DMSO, 161.98 MHz, 20 °C): δ = –12.05(s) ppm.
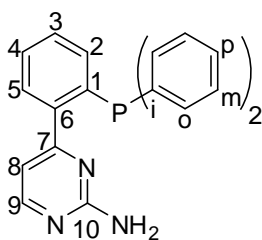
[2-(4-(2-Ethylamino)pyrimidinyl)phenyl]diphenylphosphine (4b). **4b** was synthesized with

Experimental

the same procedure as described for **2b** from *N*-ethylguanidinium sulfate, yield: 3.01 g (94 %).

$C_{24}H_{22}N_3P$ (383.43): calcd. C, 75.18; H, 5.78; N, 10.95; found C, 74.61; H, 5.82; N, 10.80. ^{1}H NMR ([D$_6$]DMSO, 400.13 MHz, 20 °C): δ = 0.82 (br., 3 H, H-12), 2.75 (br., 2 H, H-11), signal not observed: NH, 6.68 (br., 1 H, 8-H), 6.98 (m, 1 H, 2-H), 7.12-7.23 (m, 4 H, H-*m*), 7.30-7.36 (m, 6 H, H-*o*, H-*p*), 7.39 (t, $^3J_{HH}$ = 7.8 Hz, 1 H, H-3), 7.49 (t, $^3J_{HH}$ = 7.4 Hz, 1 H, H-4), 7.61 (m, 1 H, H-5), 8.21 (d, $^3J_{HH}$ = 5.1 Hz, 1 H, H-9) ppm. ^{13}C NMR ([D$_6$]DMSO, 100.61 MHz, 20 °C): δ = 14.8 (s, C-12), 34.92 (s, C-11), 109.0 (s, C-8), 128.4 (s, C-*m*), 128.5 (s, C-*p*), 128.8 (d, $^3J_{CP}$ = 16.6 Hz, C-2), 129.2, 129.3 (2 × s, C-3, C-4), 133.2 (d, $^2J_{CP}$ = 20.3 Hz, C-*o*), 134.7 (s, C-5), 135.3 (d, $^1J_{CP}$ = 19.6 Hz, C-1), 138.2 (d, $^1J_{CP}$ = 12.0 Hz, C-*i*), 144.5 (br., C-6), 157.9 (s, C-9), 161.5 (s, C-10), 166.2 (s, C-7) ppm. ^{31}P NMR ([D$_6$]DMSO, 161.98 MHz, 20 °C): δ = − 12.05 (s) ppm.
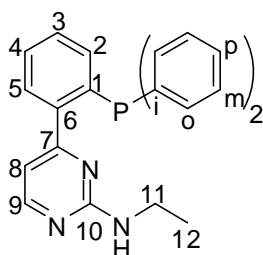
[2-(4-(2-Octylamino)pyrimidinyl)phenyl]diphenylphosphine (4c). 2.35 g (6.50 mmol) of **1a** and 2.73g (13.00 mmol) *N*-octylguanidinium sulfate were suspended in dry EtOH (80 ml). After adding 0.67 g (13.00 mmol) KOH, the mixture was refluxed for 48 h. After removing the solvent in vacuum, the residue was dissolved in a mixture of water and CH$_2$Cl$_2$. The layers were separated and the aqueous layer was extracted with CH$_2$Cl$_2$ (15 ml). The combined organic layers were dried over anhydrous magnesium sulfate and magnesium sulfate was filtered. Removing the solvent in vacuum, the crude material was crystallized from methanol to afford the desired ligand, yield: 2.37 g (78%). $C_{30}H_{34}N_3P$ (467.58): calcd. C 77.06, H 7.33, N

Experimental

8.99; found C 77.08, H 7.71, N 8.74. ^{1}H NMR ([D$_6$]DMSO, 400.13 MHz, 20 °C): δ = 0.82 (br., 3 H, H-18), 1.00-1.50 (br., 14 H, H-12, H-13, H-14, H-15, H-16 and H-17), 2.61-3.00 (br., 2 H, H-11), signal not observed: NH, 6.66 (d, $^3J_{HH}$ = 4.9 Hz, 1 H, H-8), 6.98 (dd, $^3J_{HH}$ = 7.0, 3.9 Hz, 1 H, H-2), 7.12-7.23 (m, 4 H, H-*m*), 7.30-7.35 (m, 6 H, H-*o*, H-*p*), 7.37 (t, $^3J_{HH}$ = 7.6 Hz, 1 H, H-3), 7.48 (t, $^3J_{HH}$ = 7.5 Hz, 1 H, H-4), 7.60 (m, 1 H, H-5), 8.20 (d, $^3J_{HH}$ = 5.0 Hz, 1 H, H-9) ppm. ^{13}C NMR ([D$_6$]DMSO, 100.61 MHz, 20 °C): δ = 13.9+22.0+26.3+28.7+28.8+28.9+31.2 (7 × s, C-12, C-13, C-14, C-15, C-16, C-17, C-18), 40.2 (br., C-11), 108.9 (s, C-8), 128.35 (s, C-*m*), 128.41 (s, C-*p*), 129.0 (d, $^3J_{CP}$ = 16.8 Hz, C-2), 129.09+129.13 (2 × s, C-3, C-4), 133.2 (d, $^2J_{CP}$ = 19.9 Hz, C-*o*), 134.5 (s, C-5), 135.5 (d, $^1J_{CP}$ = 20.3 Hz, C-1), 138.2 (d, $^1J_{CP}$ = 12.3 Hz, C-*i*), 144.5 (br., C-6), 157.9 (s, C-9), 161.5 (s, C-10), 166.1 (s, C-7) ppm. ^{31}P NMR ([D$_6$]DMSO, 161.98 MHz, 20 °C): δ = –12.03 (s) ppm.
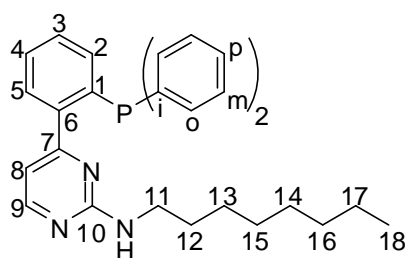
[2-(4-(2-Dimethylamino)pyrimidinyl)phenyl]diphenylphosphine (4d). 4d was synthesized with the same procedure as described for **1a** from *N*,*N*-dimethylguanidinium sulfate, yield: 2.98 g (93 %). C$_{24}$H$_{22}$N$_3$P (383.43): calcd. C, 75.18; H, 5.78; N, 10.95; found C, 75.20; H, 5.88; N, 10.93. ^{1}H NMR ([D$_6$]DMSO, 400.13 MHz, 20 °C): δ = 2.80 [br., 6 H, H-11], 6.71 (d, $^3J_{HH}$ = 4.7 Hz, 1 H, H-8), 6.98 (m, 1 H, H-2), 7.10-7.21 (m, 4 H, H-*m*), 7.22-7.35 (m, 6 H, H-*o*, H-*p*), 7.38 (t, $^3J_{HH}$ = 7.8 Hz, 1 H, H-3), 7.48 (t, $^3J_{HH}$ = 7.4 Hz, 1 H, H-4), 7.61 (m, H-5), 8.31 (d, 1 H, H-9) ppm. ^{13}C NMR ([D$_6$]DMSO, 100.61 MHz, 20 °C): δ = 36.3 [s, C-11], 108.4 (s, C-8), 128.4, 128.4 (2 × s, C-*m*, C-*p*), 129.1 (d, $^3J_{CP}$ = 12.8 Hz, C-2), 129.3, 129.3 (2 × s, C-3,

C-4), 133.2 (d, $^2J_{CP}$ = 19.4 Hz, 4 C, C-*o*), 134.7 (s, C-5), 135.3 (d, $^1J_{CP}$ = 19.4 Hz, C-1), 138.2

(d, $^1J_{CP}$ = 12.9 Hz, C-*i*), 144.6 (d, $^2J_{CP}$ = 24.0 Hz, C-6), 157.8 (s, C-9), 161.1 (s, C-10), 166.4

(s, C-7) ppm. ^{31}P NMR ([D$_6$]DMSO, 161.98 MHz, 20 °C): δ = –12.04 (s) ppm.
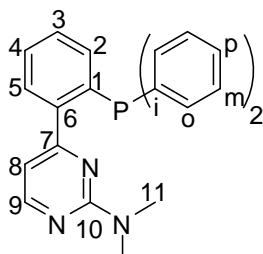
[2-(4-(2-Pyrrolidino)pyrimidinyl)phenyl]diphenylphosphine (4e). 4e was synthesized with

the same procedure as described for **1a** from pyrrolidinylguanidinium sulfate, yield: 3.12 g

(91 %). C$_{26}$H$_{24}$N$_3$P (409.47): calcd. C, 76.27; H, 5.91; N, 10.26; found C, 76.11; H, 5.99; N

10.20. ^{1}H NMR ([D$_6$]DMSO, 400.13 MHz, 20 °C): δ = 1.55-1.80 (br., 4 H, H-12), 2.81+3.36

(2 × br., 4 H, H-11), 6.73 (d, $^3J_{HH}$ = 5.1 Hz, 1 H, H-8), 6.97 (m, 1 H, H-2), 7.12-7.20 (m, 4 H,

H-*m*), 7.30-7.36 (m, 6 H, H-*o*, H-*p*), 7.39 (t, $^3J_{HH}$ = 7.4 Hz, 1 H, H-3), 7.49 (t, $^3J_{HH}$ = 7.4 Hz, 1

H, H-4), 7.63 (m, 1 H, H-5), 8.31 (d, 1 H, H-9) ppm. ^{13}C NMR ([D$_6$]DMSO, 100.61 MHz, 20

°C): δ = 24.8 (s, C-12), 45.7 (br., C-11), 108.3 (s, C-8), 128.3, 128.3 (2 × s, C-*m*, C-*p*), 129.0

(d, $^3J_{CP}$ = 13.9 Hz, C-2), 129.2, 129.2 (2 × s, C-3, C-4), 133.3 (d, $^2J_{CP}$ = 19.4 Hz, C-*o*), 134.8

(s, C-5), 135.3 (d, $^1J_{CP}$ = 20.3 Hz, C-1), 138.4 (d, $^1J_{CP}$ = 13.0 Hz, C-*i*), 144.7 (d, $^2J_{CP}$ = 24.0 Hz,

C-6), 157.8 (s, C-9), 159.3 (s, C-10), 166.3 (d, $^3J_{CP}$ = 1.9 Hz, C-7) ppm. ^{31}P NMR ([D$_6$]DMSO,

161.98 MHz, 20 °C): δ = –12.08 (s) ppm.

Experimental
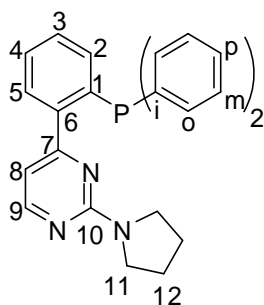
[2-(4-(2-Piperidino)pyrimidinyl)phenyl]diphenylphosphine (4f). 4f was synthesized with the same procedure as described for **1a** from piperidinylguanidinium sulfate, yield: 3.11 g (90 %). $C_{27}H_{26}N_3P$ (423.50): calcd. C, 76.58; H, 6.19; N, 9.92; found C, 76.53; H, 6.30; N, 9.80. ^1H NMR ([D$_6$]DMSO, 400.13 MHz, 20 °C): δ = 1.26 (br., 4 H, H-12), 1.47 (br., 2 H, H-13), 3.34 (br., 4 H, H-11), 6.75 (d, $^3J_{HH}$ = 5.1 Hz, 1 H, H-8), 6.99 (m, 1 H, H-2), 7.13-7.16 (m, 4 H, H-m), 7.20-7.35 (m, 6 H, H-o, H-p), 7.39 (t, $^3J_{HH}$ = 7.8 Hz, 1 H, H-3), 7.49 (t, $^3J_{HH}$ = 7.4 Hz, 1 H, H-4), 7.62 (m, 1 H, H-5), 8.33 (d, 1 H, H-9) ppm. ^{13}C NMR ([D$_6$]DMSO, 100.61 MHz, 20 °C): δ = 24.2 (s, C-13), 25.5 (s, C-12), 43.9 (s, C-11), 108.5 (s, C-8), 128.4, 128.4 (2 × s, C-m, C-p), 129.2 (d, $^3J_{CP}$ = 17.5 Hz, C-2), 129.3, 129.4 (2 × s, C-3, C-4), 133.2 (d, $^2J_{CP}$ = 19.4 Hz, C-o), 134.9 (s, C-5), 135.3 (d, $^1J_{CP}$ = 19.4 Hz, C-1), 138.4 (d, $^1J_{CP}$ = 12.9 Hz, C-i), 144.6 (d, $^2J_{CP}$ = 24.0 Hz, C-6), 158.0 (s, C-9), 160.3 (s, C-10), 166.5 (d, $^3J_{CP}$ = 1.9 Hz, C-7) ppm. ^{31}P NMR ([D$_6$]DMSO, 161.98 MHz, 20 °C): δ = –12.22 (s) ppm.

[2-(4-(2-(2,6-Dimethylpiperidino))pyrimidinyl)phenyl]diphenylphosphine (4g). 2.35 g

Experimental

(6.50 mmol) of **1a** and 2.92g (14.3 mmol) 2,6-dimethylpiperidinylguanidinium sulfate were suspended in dry EtOH (50 ml). After adding 0.76 g (14.3 mmol) KOH, the mixture was refluxed for 30 h. After removing the solvent in vacuum, the residue was dissolved in a mixture of water and CH_2Cl_2. The layers were separated and the aqueous layer was extracted with CH_2Cl_2 (10 ml). The combined organic layers were dried over anhydrous magnesium sulfate and magnesium sulfate was filtered. Removing the solvent, the crude material was recrystallized from ethanol to afford the desired ligand, yield: 2.35 g (80%). $C_{29}H_{30}N_3P \cdot MeOH$: calcd. C, 77.14; H, 6.70; N, 9.30; found C, 74.51; H, 7.09; N 9.80. ^{1}H NMR ([D_6]DMSO, 400.13 MHz, 20 °C): δ = 1.18 (d, $^3J_{HH}$ = 6.5 Hz, 6 H, H-14), 1.22-1.32 (m, 2 H, H-13), 1.35-1.45+1.65-1.76 (2 × m, 4 H, H-12), 3.00-3.11 (m, 2 H, H-11), 6.25 (dd, J_{HH} = 4.9, 1.6 Hz, 1 H, H-8), 7.01 (dd, J_{HH} = 7.2, 3.8 Hz 1 H, H-2), 7.15-7.23 (m, 4 H, H-*m*), 7.32-7.39 (m, 7 H, H-3, H-*o*, H-*p*), 7.45-7.53 (m, 2 H, H-4, H-5), 7.99 (d, $^3J_{HH}$ = 4.9, 1 H, H-9) ppm. ^{13}C NMR ([D_6]DMSO, 100.61 MHz, 20 °C): δ = 19.1 (s, C-14), 22.2 (s, C-13), 29.8 (s, C-12), 52.3 (s, C-11), 109.3 (d, $^1J_{CP}$ = 6.8 Hz, C-8), 128.52, 128.55, 128.59, 128.61 (4 × s, C-*m*, C-*p*), 129.2 (s, C-2), 129.3, 129.4 (2 × s, C-3, C-4), 133.2 (d, $^2J_{CP}$ = 19.8 Hz, C-*o*), 134.1 (s, C-5), 134.7 (d, $^1J_{CP}$ = 18.6 Hz, C-1), 137.7 (d, $^1J_{CP}$ = 13.1 Hz, C-*i*), 145.5 (d, $^2J_{CP}$ = 27.0 Hz, C-6), 156.6 (s, C-9), 166.1 (d, $^3J_{CP}$ = 4.2 Hz, C-7), 168.7 (s, C-10) ppm. ^{31}P NMR ([D_6]DMSO, 161.98 MHz, 20 °C): δ = –14.35 (s) ppm.

Experimental

[2-(4-(2-Anilino)pyrimidinyl)phenyl]diphenylphosphine (4h). 1.00 g (2.78 mmol) of **1a** and 0.73 g (4.00 mmol) *N*-phenylguanidinium sulfate were suspended in dry EtOH (30 ml). After adding of 0.22 g (4.00 mmol) KOH, the mixture was refluxed for 48 h. After removing the solvent in vacuum, the residue was dissolved in a mixture of water and CH_2Cl_2. The layers were separated and the aqueous layer was extracted with CH_2Cl_2 (20 ml). The combined organic layers were dried over anhydrous magnesium sulfate and magnesium sulfate was filtered off. Removing the solvent in vacuum, the crude material was recrystallized from methanol and gave the desired ligand, yield: 1.01 g (85%). $C_{28}H_{22}N_3P$ (431.47): calcd. C, 77.94; H, 5.14; N, 9.74; found C, 77.53; H, 5.25; N 9.72. ^1H NMR ([D_6]DMSO, 400.13 MHz, 20 °C): δ = 6.81 (d, $^3J_{HH}$ = 4.9 Hz, 1 H, H-8), 6.90 (t, $^3J_{HH}$ = 7.3 Hz, 1 H, H-14), 7.04 (dd, $^3J_{HH}$ = 7.3, 4.1 Hz , 1 H, H-2), 7.15-7.24 (m, 6 H, H-m, H-13), 7.32-7.40 (m, 6 H, H-o, H-p), 7.44 (t, $^3J_{HH}$ = 7.1 Hz, 1 H, H-3), 7.53 (t, $^3J_{HH}$ = 7.4 Hz, 1 H, H-4), 7.60 (dd, J_{HH} = 6.9, 3.9 Hz, 1 H, H-5), 7.71 (d, $^3J_{HH}$ = 7.8 Hz, 2 H, H-12), 8.38 (d, $^3J_{HH}$ = 5.0 Hz, 1 H, H-9), 9.35-9.40 (br., NH) ppm. ^{13}C NMR ([D_6]DMSO, 100.61 MHz, 20 °C): δ = 112.5 (s, C8), 118.8(s, C-13), 121.3 (s, C-14), 128.4 (s, C-12), 128.6, 128.5, 128.7 (3 × s, C-m, C-p), 129.2 (d, $^3J_{CP}$ = 14.9 Hz, C-2), 129.5, 129.5 (2 × s, C-3, C-4), 133.3 (d, $^2J_{CP}$ = 20.2 Hz, C-o), 134.1 (s, C-5), 135.2 (d, $^1J_{CP}$ = 19.0 Hz, C-1), 137.2 (d, $^1J_{CP}$ = 12.3 Hz, C-i), 140.2 (s, C-11), 144.2 (d, $^2J_{CP}$ = 24.0 Hz, C-6), 157.6 (s, C-9), 159.4 (s, C-10), 166.7 (d, $^3J_{CP}$ = 3.5 Hz, C-7) ppm. ^{31}P NMR ([D_6]DMSO, 161.98 MHz, 20 °C): δ = –12.82 (s) ppm.
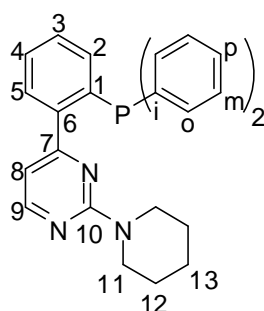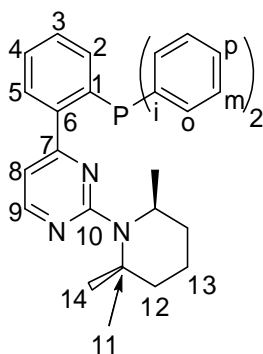
Experimental
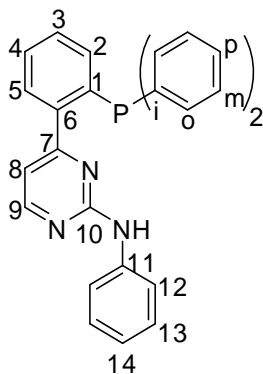
[2-(4-(2-(*p*-Methoxyanilino))pyrimidinyl)phenyl]diphenylphosphine **(4i)**. **4i** was synthesized with the same procedure as described for **4h** from *N*-(4-methoxyphenyl)guanidinium sulfate, yield: 1.05 g (82 %). $C_{29}H_{24}N_3OP$ (461.49): calcd. C, 75.47; H, 5.24; N, 9.11; found C, 75.29; H, 5.30; N 9.07. ^{1}H NMR ([D$_6$]DMSO, 400.13 MHz, 20 °C): δ = 3.69 (s, 3 H, H-15), 6.71-6.79 (m, 3 H, H-8, H-13), 7.04 (dd, $^3J_{HH}$ = 7.3, 3.9 Hz, 1 H, H-2), 7.16-7.23 (m, 4 H, H-*m*), 7.33-7.39 (m, 6 H, H-*o*, H-*p*), 7.43 (t, $^3J_{HH}$ = 7.5 Hz, 1 H, H-3), 7.51 (t, $^3J_{HH}$ = 7.4 Hz, 1 H, H-4), 7.55-7.61 (m, 3 H, H-5, H-12), 8.33 (d, $^3J_{HH}$ = 4.9 Hz, 1 H, H-9), 9.13-9.26 (br., NH) ppm. ^{13}C NMR ([D$_6$]DMSO, 100.61 MHz, 20 °C): δ = 55.12 (s, C-15), 111.9 (d, $^4J_{CP}$ = 5.1 Hz, C8), 113.6 (s, C-13), 120.5 (s, C-14), 120.6 (s, C-12), 128.7, 128.7, 128.8 (3 × s, C-*m*, C-*p*), 129.2 (d, $^3J_{CP}$ = 8.0 Hz, C-2), 129.4, 129.4 (2 × s, C-3, C-4), 133.3 (d, $^2J_{CP}$ = 20.1 Hz, C-*o*), 134.2 (s, C-5), 135.2 (d, $^1J_{CP}$ = 18.9 Hz, C-1), 137.3 (d, $^1J_{CP}$ = 12.4 Hz, C-*i*), 144.4 (d, $^2J_{CP}$ = 25.8 Hz, C-6), 154.1 (s, C-11), 157.6 (s, C-9), 159.6 (s, C-10), 166.6 (d, $^3J_{CP}$ = 3.5 Hz, C-7) ppm. ^{31}P NMR ([D$_6$]DMSO, 161.98 MHz, 20 °C): δ = –13.00 (s) ppm.

Experimental
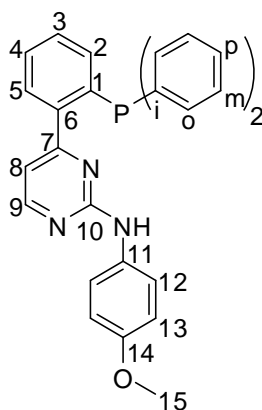
[2-(4-(2-(*p*-Fluoranilino))pyrimidinyl)phenyl]diphenylphosphine (4j). 4j was synthesized with the same procedure as described for **4h** from *N*-(4-fluorophenyl)guanidinium sulfate, yield: 1.11 g (89 %). $C_{28}H_{21}FN_3P$ (449.46): calcd. C, 74.82; H, 4.71; N, 9.35; found C, 74.38; H, 4.77; N 9.24. ^{1}H NMR ([D$_6$]DMSO, 400.13 MHz, 20 °C): δ = 6.80 (d, $^3J_{HH}$ = 4.6 Hz, 1 H, H-8), 6.96-7.07 (m, 3 H, H-2, H-13), 7.15-7.23 (m, 4 H, H-*m*), 7.32-7.38 (m, 6 H, H-*o*, H-*p*), 7.43 (t, $^3J_{HH}$ = 7.4 Hz, 1 H, H-3), 7.52 (t, $^3J_{HH}$ = 7.3 Hz, 1 H, H-4), 7.56-7.60 (m, 1 H, H-5), 7.70 (m, 2 H, H-12), 8.37 (d, $^3J_{HH}$ = 4.8 Hz, 1 H, H-9), 9.46-9.52 (br., NH) ppm. ^{13}C NMR ([D$_6$]DMSO, 100.61 MHz, 20 °C): δ = 112.5 (d, $^4J_{CP}$ = 5.2 Hz, C8), 114.8 (d, $^2J_{CF}$ = 22.0 Hz, C-13), 120.4 (d, $^3J_{CF}$ = 7.6 Hz, C-12), 128.5, 128.6, 128.8 (3 × s, C-*m*, C-*p*), 129.2 (d, $^3J_{CP}$ = 13.2 Hz, C-2), 129.4, 129.4 (2 × s, C-3, C-4), 133.3 (d, $^2J_{CP}$ = 20.2 Hz, C-*o*), 134.1 (s, C-5), 135.2 (d, $^1J_{CP}$ = 18.9 Hz, C-1), 136.6 (s, C-11), 137.1 (d, $^1J_{CP}$ = 12.4 Hz, C-*i*), 144.3 (d, $^2J_{CP}$ = 25.1 Hz, C-6), 157.3 (d, $^1J_{CF}$ = 179.2 Hz, C-14), 157.6 (s, C-9), 159.4 (s, C-10), 166.7 (d, $^3J_{CP}$ = 3.3 Hz, C-7) ppm. ^{31}P NMR ([D$_6$]DMSO, 161.98 MHz, 20 °C): δ = –12.84 (s) ppm.

Experimental
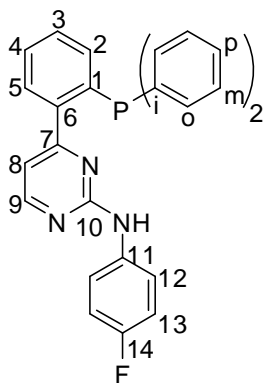
(*E*)-1-(2-Bromophenyl)-3-(dimethylamino)prop-2-en-1-one (5). The mixture of 25.41 g (127.7 mmol) 2-bromoacetophenone and 22.20 ml (167.1 mmol) of DMF-DMA were refluxed for 4 h and then excesses of DMF-DMA were removed under vacuum. Distillation of the orange oily compound under vacuum at 100 °C gave the pure product, yield: 27.3 g (84%). $C_{11}H_{12}BrNO$ (254.12): calcd. C, 51.99; H, 4.76; N, 5.51; found C, 51.91; H, 4.75; N, 5.46. ^{1}H NMR (CDCl$_3$, 400.13 MHz, 20 °C): δ = 2.87+3.07 (2 × br., 6 H, 10-H), 5.31 (d, $^3J_{HH}$ = 12.7 Hz, 1 H, 8-H), 7.25-7.35 (m, 4 H, 2-H, 3-H, 4-H & 5-H), 7.56 (d, $^3J_{HH}$ = 8.0 Hz, 1 H, 9-H) ppm. ^{13}C NMR (CDCl$_3$, 100.61 MHz, 20 °C): δ = 37.3+45.2 (2 × s, C-10), 97.5 (br., C-8), 119.2 (s, C-1), 127.0 (s, C-5), 128.6 (s, C-2), 129.8 (C-4), 133.0 (s, C-3), 143.4 (br., C-6), 153.2 (br., C-9), 191.7 (br., C-7) ppm.
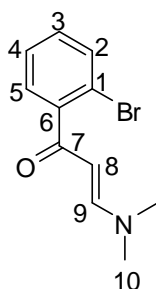
4-(2-Bromophenyl)-*N*,*N*-dimethylpyrimidin-2-amine (6a). 10.50 g (41.00 mmol) of **5** and 9.00g (61.50 mmol) *N*,*N*-dimethylguanidinium sulfate were suspended in EtOH (50 ml). After

Experimental

adding 3.44 g (61.50 mmol) of KOH, the mixture was refluxed for 8 h. Removing the solvent by rotary evaporator, the residue was dissolved in a mixture of water and CH_2Cl_2. The layers were separated and the aqueous layer was extracted with CH_2Cl_2 (30 ml). The combined organic layers were dried over anhydrous magnesium sulfate and magnesium sulfate were filtered off. Removing the solvent in vacuum, the crude material was recrystallized from ethanol-ether, yield: 90%. $C_{12}H_{12}BrN_3$ (278.15): calcd. C, 51.82; H, 4.35; N, 15.11; found C, 51.69; H, 4.25; N, 14.49. ^{1}H NMR (CDCl$_3$, 400.13 MHz, 20 °C): δ = 3.24 (s, 6 H, H-11), 6.76 (d, $^3J_{HH}$ = 5.0 Hz, 1 H, H-8), 7.26 (m, 1 H, H-3), 7.39 (m, 1 H, H-4), 7.54 (dd, J_{HH} = 5.0 Hz, 2 H, H-5), 7.66 (dd, J_{HH} = 8.0, 1.1 Hz, 1 H, H-2), 8.38 (d, $^3J_{HH}$ = 5.0 Hz, 1 H, H-9) ppm. ^{13}C NMR (CDCl$_3$, 100.61 MHz, 20 °C): δ = 37.2 (s, C-11), 109.3 (s, C-8), 121.5 (s, C-1), 127.5 (s, C-4), 130.2 (s, C-3), 131.2 (C-5), 133.7 (s, C-2), 140.1 (s, C-6), 157.4 (s, C-9), 162.3 (s, C-10), 165.8 (s, C-7) ppm.
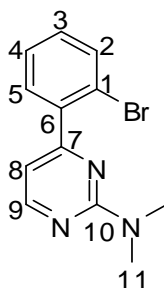
4-(2-Bromophenyl)-2-(pyrrolidin-1-yl)pyrimidine (6b). 6b was synthesized with the same procedure as described for **5** from pyrrolidinylguanidinium sulfate, yield: 11.5 g (92%). $C_{14}H_{14}BrN_3$ (304.19): calcd. C, 55.28; H, 4.64; N, 13.81; found C, 55.01; H, 4.82; N, 13.29. ^{1}H NMR (CDCl$_3$, 400.13 MHz, 20 °C): δ = 1.94 (t, $^3J_{HH}$ = 6.6 Hz, 4 H, H-12), 3.59 (t, $^3J_{HH}$ = 6.7 Hz, 4 H, H-11), 6.71 (d, $^3J_{HH}$ = 5.0 Hz, 1 H, H-8), 7.16-7.22 (m, 1 H, H-3), 7.33 (td, J_{HH} = 6.5, 1.2 Hz, 1 H, H-4), 7.50 (dd, J_{HH} = 7.7, 1.7 Hz, 1 H, H-5), 7.60 (dd, J_{HH} = 8.0, 1.1 Hz, 1 H, H-2), 8.34 (d, $^3J_{HH}$ = 5.0 Hz, 1 H, H-9) ppm. ^{13}C NMR (CDCl$_3$, 100.61 MHz, 20 °C): δ = 25.5 (s,

Experimental

C-12), 46.6 (s, C-11), 109.3 (s, C-8), 121.4 (s, C-1), 127.4 (s, C-4), 130.1 (s, C-3), 131.1 (s, C-2), 133.5 (s, C-5), 140.1 (s, C-6), 157.4 (s, C-9), 160.3 (s, C-10), 165.9 (s, C-7) ppm.
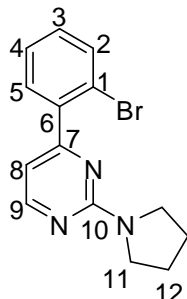
[2-(4-(2-Dimethylamino)pyrimidinyl)phenyl]diisopropylphosphine **(7a).** Under an atmosphere of nitrogen 1.00 g (3.60 mmol) of **6a** was dissolved in 25 ml dry THF and the temperature was reduced to –78 °C. Then 2.47 ml (3.96 mmol) of n-butyllithium were added dropwise during 15 min and the mixture was stirred for 1 h. 0.66 ml (3.96 mmol) of chlorodiisopropylphosphine was added dropwise during 10 min and the mixture was stirred for another 2 h at –78 °C. Then the mixture was allowed to warm up to RT and the reaction was stirred over night. Removing the solvent by vacuum, the product was purified by column chromatography (silica gel, ethyl acetate/hexane 5:1), yield: 0.76 g (67 %, white solid). $C_{18}H_{26}N_3P$ (315.39): calcd. C, 68.55; H, 8.31; N, 13.32; found C, 68.31; H, 8.43; N, 13.13. ^{1}H NMR (CDCl$_3$, 400.13 MHz, 20 °C): δ = 0.93 (dd, , $^3J_{HH}$ = 7.0 Hz, $^3J_{HP}$ = 12.3 Hz, 6 H, H-2i), 1.06 (dd, $^3J_{HH}$ = 7.0 Hz, $^3J_{HP}$ = 14.4 Hz, 6 H, H-2i), 2.06- 2.18 (m, 2 H, H-1i), 3.20 (s, 6 H, H-11), 6.59 (d, $^3J_{HH}$ = 5.0 Hz, 1 H, H-8), 7.35-7.42 (m, 3 H, H-3, H-4, H-5), 7.60 (m, 1 H, H-2), 8.31 (d, $^3J_{HH}$ = 5.0 Hz, 1 H, H-9) ppm. ^{13}C NMR (CDCl$_3$, 100.61 MHz, 20 °C): δ = 20.1 (d, $^2J_{CP}$ = 11.8 Hz, C-2i), 20.2 (d, $^2J_{CP}$ = 18.4 Hz, C-2i), 24.8 (d, $^1J_{CP}$ = 13.6 Hz, C-1i), 37.3 (s, C-11), 110.8 (d, $^4J_{CP}$ = 5.6 Hz, C-8), 127.9 (s, C-5), 128.6 (s, C-3), 129.3 (d, $^4J_{CP}$ = 5.9 Hz, C-4), 132.64 (d, $^2J_{CP}$ = 3.1 Hz, C-2), 134.9 (d, $^1J_{CP}$ = 23.0 Hz, C-1), 148.1 (d, $^2J_{CP}$ = 27.2 Hz, C-6), 156.5 (s, C-9), 161.8 (s, C-10), 168.9 (s, C-7) ppm. ^{31}P NMR(CDCl$_3$, 100.61 MHz, 20 °C): δ =

160

Experimental

–2.71 (s) ppm.
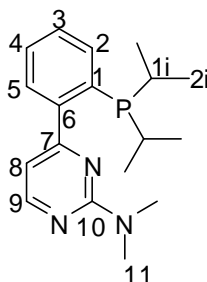
[2-(4-(2-Dimethylamino)pyrimidinyl)phenyl]dicyclohexylphosphine **(7b).** Under an atmosphere of nitrogen 1.00 g (3.60 mmol) of **6a** was dissolved in 25 ml dry THF and the temperature was reduced to –78 °C. Then 2.47 ml (3.96 mmol) of *n*-butyllithium were added dropwise during 15 min and stirred for 1 h. 0.99 ml (3.60 mmol) of chlorodicyclohexylphosphine were added dropwise during 10 min and the mixture was stirred for another 2 h at –78 ºC. Then the mixture was allowed to warm up to RT and the reaction mixture was stirred over night. After removing the solvent in vacuum, the product was purified by column chromatography (silica gel, ethyl acetate/hexane 5:1), yield: 0.77 g (55 %). $C_{24}H_{34}N_3P$ (395.52): calcd. C, 72.88; H, 8.66; N, 10.62; found C, 72.82; H, 8.46; N 10.57. ^{1}H NMR (CDCl$_3$, 400.13 MHz, 20 °C): δ = 1.03-1.30 + 1.50-1.95 (2 × m, 22 H, H-1*c*, H-2*c*,H-3*c* & H-4*c*), 3.20 (s, 6 H, H-11), 6.54 (m, 1 H, H-8), 7.33-7.42 (m, 3 H, H-3, H-4, H-5), 7.60 (m, 1 H, H-2), 8.30 (d, $^3J_{HH}$ = 5.0 Hz, 1 H, H-9) ppm. ^{13}C NMR (CDCl$_3$, 100.61 MHz, 20 °C): δ = 26.5 + 27.28 + 27.30 + 27.4 + 29.7 + 29.8 + 30.4 + 30.6 + 34.8 + 34.9 (observed complexity due to P-C splitting for C-2*c* to C-4*c*), 37.4 (s, C-11), 110.8 (d, $^4J_{CP}$ = 5.8 Hz, C-8), 127.9 (s, C-5), 128.6 (s, C-3), 129.3 (d, $^4J_{CP}$ = 6.1 Hz, C-4), 133.0 (s, C-2), 134.2 (d, $^1J_{CP}$ = 23.1 Hz, C-1), 148.1 (d, $^2J_{CP}$ = 27.8 Hz, C-6), 156.3 (s, C-9), 161.8 (s, C-10), 169.0 (s, C-7) ppm. ^{31}P NMR (CDCl$_3$, 100.61 MHz, 20 °C): δ = –11.00 (s) ppm.

Experimental
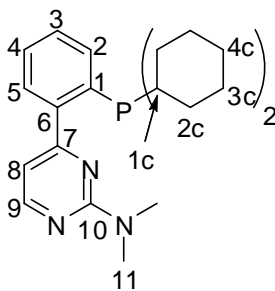
[2-(4-(2-Pyrrolidino)pyrimidinyl)phenyl]dicyclohexylphosphine (7c). 2.78 g (9.14 mmol) of **6b** were dissolved in 25 ml dry THF and the temperature was reduced to –78 ºC. Then 6.30 ml (10.05 mmol) of *n*-butyllithium were added dropwise during 15 min and the reaction mixture was stirred for 1 h. After adding 2.00 ml (9.14 mmol) of chlorodicyclohexylphosphine dropwise during 10 min, the mixture was stirred for another 2 h at –78 ºC. Then the reaction mixture was allowed to warm up to RT and it was stirred over night. Removing the solvent in vacuum, the product was purified by chromatography (silica gel, ethyl acetate/hexane 5:1), yield: 1.58 g (45 %). $C_{26}H_{36}N_3P$ (421.56): calcd. C, 74.08; H, 8.61; N, 9.97; found C, 73.36; H, 9.10; N 9.42. ^{1}H NMR (CDCl$_3$, 400.13 MHz, 20 ºC): δ = 1.05-1.30 + 1.50-1.93 (2 × m, 22 H, H-1*c to* H-4*c*), 1.97 (m, 4 H, H-11), 3.60 (m, 4 H, H-12), 6.54 (d, $^3J_{HH}$ = 5.0 Hz, 1 H, H-8), 7.34-7.41 (m, 3 H, H-3, H-4, H-5), 7.60 (m, 1 H, H-2), 8.30 (d, $^3J_{HH}$ = 5.0 Hz, 1 H, H-9) ppm. ^{13}C NMR (CDCl$_3$, 100.61 MHz, 20 ºC): δ = 25.7 (s, C-12), 26.5 + 27.28 + 27.30 + 27.4 + 29.7 + 29.8 + 30.4 + 30.6 + 34.8 + 35.0 (observed complexity due to P-C splitting for C-(2-4)*c*), 46.82 (s, C-11), 110.9 (d, $^4J_{CP}$ = 5.8 Hz, C-8), 127.8 (s, C-5), 128.6 (s, C-3), 129.3 (d, $^4J_{CP}$ = 6.0 Hz, C-4), 133.0 (d, $^2J_{CP}$ = 3.1 Hz, C-2), 134.2 (d, $^1J_{CP}$ = 22.6 Hz, C-1), 148.5 (d, $^2J_{CP}$ = 28.1 Hz, C-6), 156.6 (s, C-9), 160.2 (s, C-10), 169.0 (d, $^3J_{CP}$ = 4.6 Hz, C-7) ppm. ^{31}P NMR (CDCl$_3$, 100.61 MHz, 20 ºC): δ = –10.99 (s) ppm.

Experimental
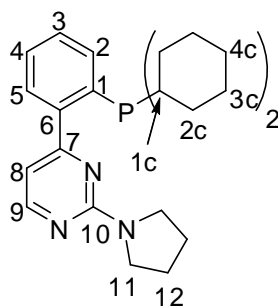
[2-(4-(2-Pyrrolidino)pyrimidinyl)phenyl]di(*p*-tolyl)phosphine (7d). Under an atmosphere of nitrogen 0.59 g (1.93 mmol) of **6b** was dissolved in 20 ml dry THF and the temperature was reduced to –78 °C. Then 1.27 ml (2.04 mmol) of *n*-butyllithium were added dropwise during 15 min and the mixture was stirred for 1 h and then 0.44 ml (1.93 mmol) of di-*p*-tolylchlorophosphine were added dropwise during 10 min and the mixture was stirred for another 2 h at –78 °C. Then the mixture was allowed to warm up to RT and the reaction mixture was stirred over night. After removing the solvent by vacuum the product was purified by column chromatography (silica gel, ethyl acetate/hexane 5:1), yield: 0.55 g (65 %, white solid). $C_{28}H_{22}N_3P$ (437.52): calcd. C, 76.87; H, 6.45; N, 9.60; found C, 75.72; H, 6.73; N, 9.63. ^{1}H NMR ([D$_6$]DMSO, 400.13 MHz, 20 °C): δ = 1.50-1.95 (br., 4 H, H-12), 2.28 (s, 6 H, H-13), 2.60-3.40 (br., 4 H, H-11), 6.68 (d, $^3J_{HH}$ = 4.9 Hz, 1 H, H-8), 6.97 (ddd, J_{HH} = 7.7, 3.9, 1.0 Hz , 1 H, H-2), 7.00-7.06 (m, 4 H, H-*m*), 7.12-7.17 (m, 4 H, H-*o*), 7.39 (td, $^3J_{HH}$ = 7.5, 1.5 Hz, 1 H, H-3), 7.47 (td, J_{HH} = 7.5, 1.3Hz, 1 H, H-4), 7.59 (ddd, J_{HH} = 7.6, 4.2, 1.2 Hz, 1 H, H-5), 8.29 (d, $^3J_{HH}$ = 5.0 Hz, 1 H, H-9) ppm. ^{13}C NMR ([D$_6$]DMSO, 100.61 MHz, 20 °C): δ = 20.8, 24.9, 45.7, 108.4, 126.7, 128.7, 128.8, 129.0, 129.1, 129.2, 133.3, 134.5, 134.9, 135.9, 137.8, 144.8, 157.7, 159.3, 166.4 ppm. ^{31}P NMR ([D$_6$]DMSO, 161.98 MHz, 20 °C): δ = –13.76 (s) ppm.

Experimental
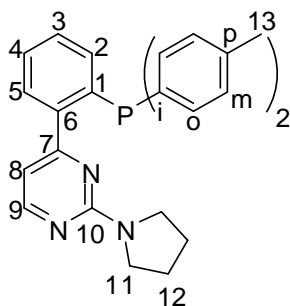
1-Dimethylamino-3-phenyl-3-oxo-1-propene (8). 36.38g (333.00 mmol) of DMF-DMA and 20.07g (167.00 mmol) of acetophenone were added in EtOH (80 ml) and refluxed for 24 h. The colour changed from yellow to dark orange. By concentrating the solvent in vacuum and adding pentane, a yellow solid precipitated. The yellow precipitate was filtrated and washed with diethyl ether and dried in vacuum, yield: 26.6g (91 %). $C_{11}H_{13}NO$ (175.23): calcd. C, 75.40; H, 7.48; N, 7.99; found C, 75.18; H, 7.33; N, 7.95. ^{1}H NMR ([D_6]DMSO, 400.13 MHz, 20 °C): δ = 2.88 + 3.11 (2 × s, 6 H, H-1), 5.83 (d, $^3J_{HH}$ = 12.3 Hz, 1 H, H-3), 7.40-7.50 (m, 3 H, H-7, H-8), 7.74 (d, $^3J_{HH}$ = 12.3 Hz, 1 H, H-2), 7.92 (d, $^3J_{HH}$ = 7.1, 2 H, H-6) ppm. ^{13}C NMR ([D_6]DMSO, 100.61 MHz, 20 °C): δ = 37.0 + 44.4 (2 × s, C-1), 90.9 (s, C-3), 127.2 (s, C-6), 128.1 (s, C-7), 130.7 (s, C-8), 140.3 (s, C-5), 154.1 (s, C-2), 185.7 (s, C-4) ppm.
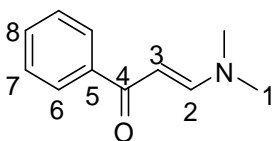
4-Phenylpyrimidin-2-amine (11a). 2.62 g (114.02 mmol) of sodium were added to dry ethanol (150 ml) and the mixture was stirred until all sodium reacted with ethanol to give sodium ethanolat. After adding 8.72 g (71.60 mmol) of guanidinium nitrate and 10.00 g (57.00 mmol) of **8**, the mixture was refluxed over night. After removing the solvent, the residue was dissolved in CH_2CH_2 (50 ml) and after concentrating, diethyl ether (5 ml) was added. Keeping

Experimental

the mixture in the refrigerator, the product precipitated which was filtrated and dried in vacuum, yield: 7.16g (73 %, colorless solid). $C_{10}H_9N_3$ (171.20): calcd. C, 70.16; H, 5.30; N, 24.54; found C, 69.95; H, 5.35; N, 24.33. ^{1}H NMR ([D$_6$]DMSO, 400.13 MHz, 20 °C): δ = 6.68 (br., 2 H, NH$_2$), 7.12 (d, $^3J_{HH}$ = 5.1 Hz, 1 H, H-3), 7.45-7.55 (m, 3 H, H-7, H-8), 8.07 (m, 2 H, H-6), 8.31 (d, 2 H, $^3J_{HH}$ = 5.1 Hz, 1 H, H-2) ppm. ^{13}C NMR ([D$_6$]DMSO, 100.61 MHz, 20 °C): δ = 105.8 (s, C-3), 126.7 (s, C-4), 128.7 (s, C-7), 130.5 (s, C-8), 137.0 (s, C-5), 159.0 (s, C-2), 163.6 (s, C-4), 163.8 (s, C-1) ppm.
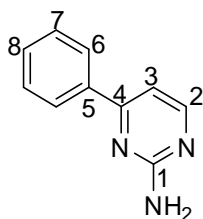
Potassium 4-(pyridin-2-yl)pyrimidine-2-thiolate (11d). **11d** was synthesized according to procedures published in the literature.[218] 17.00 g (95.38 mmol) of **9**, 10.89 g (143.06 mmol) of thiourea and 8.01 g (143.00 mmol) of KOH were added in EtOH (60 ml) and refluxed for 24 h. Then solvent was evaporated and the residue was dissolved in dichloromethane (50 ml). After washing the organic phase with water (2 × 10 ml), the organic phase was dried over magnesium sulfate. After removing the solvent in vacuum, the product was recrystallized from ethanol, yield: 21.68 (93%, yellow solid). $C_9H_6KN_3S$ (227.33): calcd. C, 47.55; H, 2.86; N, 18.48; S, 14.11; found C, 47.47; H, 2.93; N, 18.37; S, 14.27. ^{1}H NMR ([D$_6$]DMSO, 400.13 MHz, 20 °C): δ = 7.34 (d, $^3J_{HH}$ = 4.9 Hz, 1 H, H-3), 7.44 (ddd, J_{HH} = 7.4, 4.8, 1.1 Hz, 1 H, H-8), 7.91 (td, J_{HH} = 7.7, 1.8 Hz, 1 H, H-7), 8.11 (d, 1 H, $^3J_{HH}$ = 4.9 Hz, 1 H, H-2), 8.30 (d, 1 H, $^3J_{HH}$ = 7.9 Hz, H-6), 8.63 (dd, J_{HH} = 4.7, 0.8 Hz, 1 H, H-9) ppm. ^{13}C NMR ([D$_6$]DMSO, 100.61 MHz, 20 °C): δ = 106.0 (s, C-3), 120.5 (s, C-6), 124.6 (s, C-8), 136.9 (s, C-7), 149.1 (s, C-9), 155.4 (s, C-5), 155.9 (s, C-2), 159.8 (s, C-4), 189.1 (s, C-1) ppm.

Experimental
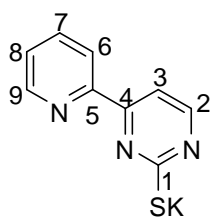
_N_-(Diphenylphosphino)-4-phenylpyrimidin-2-amine (12a). Under an atmosphere of nitrogen 2.00 g (11.68 mmol) of **11a** were added to 20 ml of dry THF. Then the solution was cooled in an ice bath to 0 °C and 1.70 ml (12.26 mmol) of freshly dried NEt$_3$ were added. After adding 2.20 ml (11.68 mmol) of chlorodiphenylphosphin dropwise with a syringe in 15 minutes, the reaction mixture was stirred at room temperature for 65 h and then was filtered, to remove NEt$_3$·HCl. After removing the solvent the desired product was recrystallized from ethanol/pentane, yield: 2.68 g (64%, colorless solid). C$_{22}$H$_{18}$N$_3$P (355.37): calcd. C, 74.35; H, 5.11; N, 11.82; found C, 74.23; H, 5.29; N, 11.80. ^{1}H NMR ([D$_6$]DMSO, 400.13 MHz, 20 °C): δ = 7.32-7.42 (m, 7 H, H-3, H-_m_, H-_p_), 7.47-7.58 (m, 7 H, H-7, H-8, H-_o_), 8.10 (m, 2 H, H-6), 8.24 (d, $^2J_{HP}$ = 8.4 Hz, 1-H, NH), 8.46 (d, $^3J_{HH}$ = 5.2 Hz, 1 H, H-2) ppm. ^{13}C NMR (DMSO-d6, 101 MHz, 20 °C): δ = 107.9 (s, C-3), 126.9 (s, C-6), 128.3 (d, $^3J_{CP}$ = 6.6 Hz, C-_m_), 128.8 (s, C-_p_), 128.9 (s, C-7), 130.8 (s, C-8), 131.2 (d, $^2J_{CP}$ = 22.1 Hz, C-_o_), 136.4 (s, C-5), 139.9 (d, $^1J_{CP}$ = 15.0 Hz, C-_i_), 159.2 (s, C-2), 163.2 (d, $^2J_{CP}$ = 17.4 Hz, C-1), 163.5 (s, C-4) ppm. ^{31}P NMR ([D$_6$]DMSO, 161.98 MHz, 20 °C): δ = 24.64 (s) ppm.
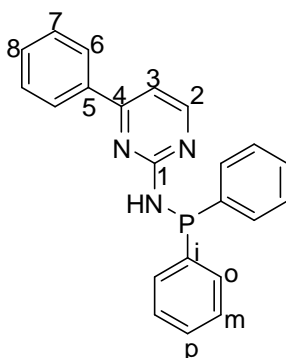
Experimental

***N*-(Diphenylphosphino)-4-(pyridin-2-yl)pyrimidin-2-amine (12b).** The synthesis of **12b** was carried out as described for **12a** from **11b**, yield: 3.75 g (90%). $C_{21}H_{17}N_4P$ (356.36): calcd. C, 70.78; H, 4.81; N, 15.72; found C, 69.65; H, 4.98; N, 15.48. ^1H NMR ([D_6]DMSO, 400.13 MHz, 20 °C): δ = 7.33-7.43 (m, 6 H, H-*m*, H-*p*), 7.49-7.56 (m, 5-H, H-8, H-*o*), 7.68 (d, $^3J_{HH}$ = 5.0 Hz, 1 H, H-3), 7.98 (td, J_{HH} = 7.8, 1.5 Hz, 1 H, H-7), 8.29-8.34 (m, 2 H, H-6, NH), 8.56 (d, $^3J_{HH}$ = 5.1 Hz, 1 H, H-2), 8.70 (d, $^3J_{HH}$ = 4.2 Hz, 1 H, H-9) ppm. ^{13}C NMR (DMSO-d6, 101 MHz, 20 °C): δ = 108.0 (s, C-3), 121.0 (s, C-6), 125.6 (s, C-8), 128.3 (d, $^3J_{CP}$ = 6.6 Hz, C-*m*), 128.9 (s, C-*p*), 131.2 (d, $^2J_{CP}$ = 22.1 Hz, C-*o*), 137.4 (s, C-7), 139.7 (d, $^1J_{CP}$ = 14.9 Hz, C-*i*), 149.5 (s, C-9), 153.5 (s, C-5), 159.6 (d, $^4J_{CP}$ = 2.2 Hz, C-2), 162.8 (s, C 4), 163.3 (d, $^2J_{CP}$ = 17.2 Hz, C 1) ppm. ^{31}P NMR ([D_6]DMSO, 161.98 MHz, 20 °C): δ = 24.95 (s) ppm.
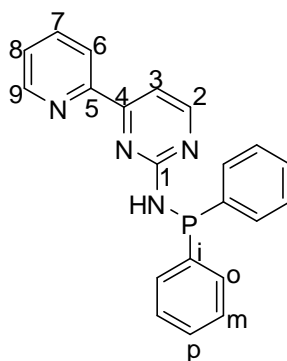
***N*-(Diphenylphosphino)-4-(pyridin-2-yl)-6-phenylpyrimidin-2-amine (12c).** The synthesis of **12c** was carried out as described for **12a** from **11c** with longer reaction time (3 days), yield: 3.94 g (78%, yellow solid). $C_{27}H_{21}N_4P$ (432.46): calcd. C, 74.99; H, 4.89; N, 12.96; found C, 74.35; H, 5.52; N, 12.83. ^1H NMR ([D_6]DMSO, 600 MHz, 20 °C): δ = 7.36-7.42 (m, 6 H, H-*m*, H-*p*), 7.51-7.60 (m, 8 H, H-8, H-12, H-13, H-*o*), 8.01 (td, J_{HH} = 7.7, 1.7 Hz, 1 H, H-7), 8.18 (dd, J_{HH} = 6.5, 3.0 Hz, 2 H, H-11), 8.22 (s, 1 H, H-3), 8.37 (d, $^3J_{HH}$ = 7.9 Hz, 1 H, H-6), 8.40 (d, $^1J_{HP}$ = 7.4 Hz, 1 H, NH), 8.76 (d, $^3J_{HH}$ = 4.0 Hz, 1 H, H-9) ppm. ^{13}C NMR (DMSO-d6, 151

MHz, 20 °C): δ = 103.4 (s, C-3), 121.2 (s, C-6), 125.8 (s, C-8), 127.0 (s, C-11), 128.4 (d, $^3J_{CP}$ = 6.6 Hz, C-m), 128.9 (s, C-p), 128.9 (s, C-12), 131.0 (s, C-13), 131.4 (d, $^2J_{CP}$ = 22.0 Hz, C-o), 136.7 (s, C-10), 137.4 (s, C-7), 139.9 (d, $^1J_{CP}$ = 14.8 Hz, C-i), 149.5 (s, C-9), 153.7 (s, C-5), 163.5 (d, $^2J_{CP}$ = 16.3 Hz, C-1), 164.0 (s, C-2), 165.1 (s, C-4) ppm. ^{31}P NMR ([D$_6$]DMSO, 243 MHz, 20 °C): δ = 25.24 (s) ppm.
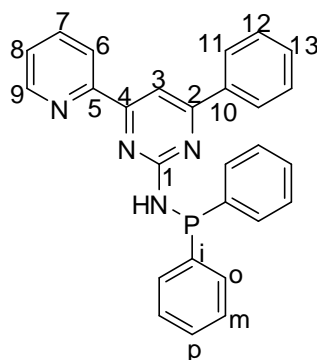
2-(Diphenylphosphinothio)-4-(pyridin-2-yl)pyrimidine (12d). The synthesis of **12d** was carried out as described for **12a** from **11d**, yield: 3.49 g (80%, yellow solid). C$_{21}$H$_{16}$N$_3$PS (373.41): calcd. C, 67.55; H, 4.32; N, 11.25; S, 8.59; found C, 65.56; H, 5.01; N, 10.87; S, 8.69. ^{1}H NMR ([D$_6$]DMSO, 400.13 MHz, 20 °C): δ = 7.40-7.47 (m, 6-H, H-m, H-p), 7.54 (m, 1H, H-8), 7.59-7.62 (m, 4 H, H-o), 7.93 (m, 1 H, H-7), 8.07-8.12 (m, 2 H, H-3, H-6), 8.72 (m, 1 H, H-9), 8.78 (d, $^3J_{HH}$ = 5.2 Hz, 1 H, H-2) ppm. ^{13}C NMR (DMSO-d6, 101 MHz, 20 °C): δ = 113.5 (s, C-3), 121.4 (s, C-6), 126.3 (s, C-8), 128.6 (d, $^3J_{CP}$ = 6.6 Hz, C-m), 129.8 (s, C-p), 132.5 (d, $^2J_{CP}$ = 22.6 Hz, C-o), 135.6 (d, $^1J_{CP}$ = 25.1 Hz, C-i), 137.6 (s, C-7), 149.9 (s, C-9), 152.3 (s, C-5), 159.5 (d, $^4J_{CP}$ = 3.0 Hz, C-2), 162.5 (d, $^4J_{CP}$ = 2.6 Hz, C-4), 169.4 (d, $^2J_{CP}$ = 12.1 Hz, C-1) ppm. ^{31}P NMR ([D$_6$]DMSO, 161.98 MHz, 20 °C): δ = 17.18 (s) ppm.

Experimental
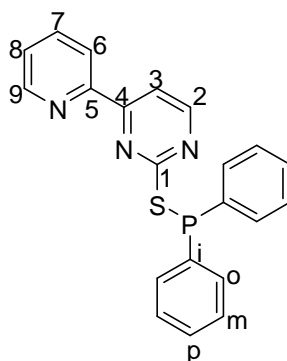
2-(Diisopropylphosphinothio)-4-(pyridin-2-yl)pyrimidine (13b). Under an atmosphere of nitrogen 1.00 g (4.39 mmol) of **11d** was weighted in a Schlenk flask and dried under vacuum. 30 ml of dry THF were added and the mixture was cooled in an ice bath to 0 °C. 0.91 ml (6.58 mmol) of NEt$_3$ was added. After adding 0.78 ml (4.85 mmol) of chlorodiisopropylphosphine dropwise with a syringe in 15 minutes the colour of the mixture changed from yellow to white by increasing the temperature to RT. The mixture was stirred for another 3 h and then it was filtered. Removing the solvent gave the product which was dried under vacuum, yield: 1.19 g (89 %, pale yellow). C$_{15}$H$_{20}$N$_3$PS (305.38): calcd. C, 59.00; H, 6.60; N, 13.76; S, 10.50; found C, 58.11; H, 6.29; N, 11.68. ^{1}H NMR ([D$_6$]DMSO, 600.1 MHz, 20 °C): δ = 1.11-1.17 (m, 12-H, H-2i), 2.05-2.15 (m, 2 H, H-1i), 7.58 (dd, J_{HH} = 6.7, 4.9 Hz, 1 H, H-8), 8.02-8.08 (m, 2 H, H-3, H-7), 8.46 (d, $^3J_{HH}$ = 7.9 Hz, 1 H, H-6), 8.71-8.76 (m, 2 H, H-2, H-9) ppm. ^{13}C NMR (DMSO-d6, 101 MHz, 20 °C): δ = 15.5 (2 × d, 19.5, 18.9), C-2i), 24.8 (d, $^2J_{CP}$ = 23.0, C-2i), 113.8 (s, C-3), 121.3 (s, C-6), 126.2 (s, C-8), 137.7 (s, C-7), 149.8 (s, C-9), 159.1 (d, C-2), 152.7 (s, C-5), 162.3 (s, C-4), 171.0 (d,$^2J_{CP}$ = 14.0, C-1). ^{31}P NMR ([D$_6$]DMSO, 161.98 MHz, 20 °C): δ = 54.58 (s) ppm.

Experimental
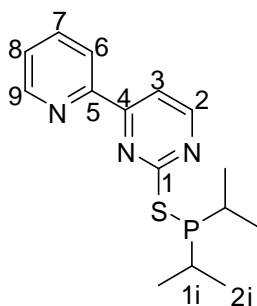
$N^2,N^{2'}$-Bis(diphenylphosphino)-4,4'-bipyrimidine-2,2'-diamine (12e). Under an atmosphere of nitrogen 0.11 g (0.58 mmol) of **11e** was added to 30 ml of THF then the solution was cooled in an ice bath to 0 °C and 0.24 ml (1.86 mmol) of NEt$_3$ was added. After adding 0.23 ml (1.22 mmol) of chlorodiphenylphosphine dropwise with a syringe in 15 minutes, the mixture was stirred at room temperature. Monitoring the reaction by NMR showed that the reaction was completed in 3 days. To remove NEt$_3$·HCl, the mixture was filtered and the solvent removed. Crystallization of the crude material from dry ethanol gave the desired solid product, yield: 0.28 g (86%, pale yellow). C$_{32}$H$_{26}$N$_6$P$_2$ (556.54): calcd. C, 69.06; H, 4.71; N, 15.10; found C, 69.56; H, 4.58; N, 15.23. ^{1}H NMR ([D$_6$]DMSO, 400.13 MHz, 20 °C): δ = 7.34-7.41 (m, 12 H, H-*m*, H-*p*), 7.48-7.54 (m, 10 H, H-8, H-*o*), 7.56 (d, $^3J_{HH}$ = 5.0 Hz, 2 H, H-3), 8.43 (d, $^3J_{HP}$ = 8.2 Hz, 2 H, NH), 8.61 (d, $^3J_{HH}$ = 5.0 Hz, 2 H, H-2) ppm. ^{13}C NMR (DMSO-d6, 101 MHz, 20 °C): δ = 108.3 (s, C-3), 128.4 (d, $^3J_{CP}$ = 6.6 Hz, C-*m*), 129.0 (s, C-*p*), 131.4 (d, $^2J_{CP}$ = 22.0 Hz, C-*o*), 139.7 (d, $^1J_{CP}$ = 14.7 Hz, C-*i*), 160.1 (s, C-2), 161.5 (s, C-4), 163.4 (d, $^2J_{CP}$ = 17.4 Hz, C-1) ppm. ^{31}P NMR ([D$_6$]DMSO, 161.98 MHz, 20 °C): δ = 25.17 (s) ppm.
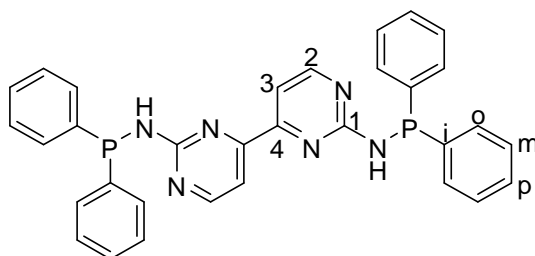
Experimental

5.5. Complex Synthesis

General Synthesis of the Palladium Complexes: 14a-c and **15a-c** were obtained by treating $(C_6H_5CN)_2PdCl_2$ with ligands **4a-f** in equivalent molar amounts according to the following general method: A solution of the appropriate ligand **4a-f** (0.30 mmol) in CH_2Cl_2 (5 ml) was added to a solution of 0.115 g (0.30 mmol) of $(C_6H_5CN)_2PdCl_2$ in CH_2Cl_2 (20 ml). The mixture was stirred for 16 h at room temperature. Addition of diethyl ether (50 ml) caused precipitation of the product, which was further washed two times with diethyl ether (20 ml) and dried in the vacuum giving yields of 80-95 %.

{[2-(4-(2-Amino)pyrimidinyl)phenyl]diphenylphosphine}dichloridopalladium(II),   14a. From **4a**, yield: 0.15 g (93 %, yellow solid). $C_{22}H_{18}Cl_2N_3PPd$ (532.68): calcd. C, 49.60; H, 3.41; N, 7.89; found C, 49.35; H, 3.62; N, 7.80. ^1H NMR ([D_6]DMSO, 400.13 MHz, 20 °C): not det. NH_2, $\delta = 6.89$ (d, $^3J_{HH} = 4.7$ Hz, 1 H, H-8), 7.18 (m, 2 H, H-2), 7.23-7.68 (m, 10 H, H-o, H-m, H-p), 7.78 (t, $^3J_{HH} = 7.8$ Hz, 1 H, H-3), 7.91 (t, $^3J_{HH} = 7.8$ Hz, 1 H, H-4), 8.09 (m, 1 H, H-5), 8.23 (d, 1 H, H-9) ppm. ^{31}P NMR ([D_6]DMSO, 161.98 MHz, 20 °C): $\delta = 31.27$ (s) ppm.
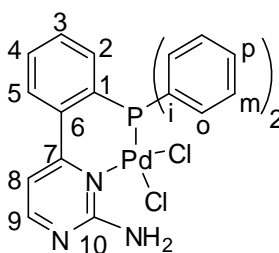
{[2-(4-(2-ethylamino)pyrimidinyl)phenyl]diphenylphosphine}dichloridopalladium(II),

14b. From **4b**, yield: 0.15 g (90 %, yellow solid). $C_{24}H_{22}Cl_2N_3PPd$ (560.74): calcd. C, 51.41; H, 3.95; N, 7.49; found C, 51.07; H, 3.93; N, 7.33. ^1H NMR ([D_6]DMSO, 400.13 MHz, 20 °C): $\delta = 1.13$ (t, $^3J_{HH} = 7.0$ Hz, 3 H, H-12), 3.51 (br., 2 H, H-11), 6.87 (d, $^3J_{HH} = 5.1$ Hz, 1 H, H-8), 7.19 (m, 1 H, H-2), 7.25-7.72 (m, 10 H, H-o, H-m, H-p-H), 7.78 (t, $^3J_{HH} = 7.8$ Hz, 1 H, H-3),

Experimental

7.91 (t, $^3J_{HH}$ = 7.8 Hz, 1 H, H-4), 8.11 (m, 1 H, H-5), 8.29 (d, 1 H, H-9), 8.50 (br., 1 H, NH) ppm. ^{31}P NMR ([D$_6$]DMSO, 161.98 MHz, 20 °C): δ = 30.71 (s) ppm.
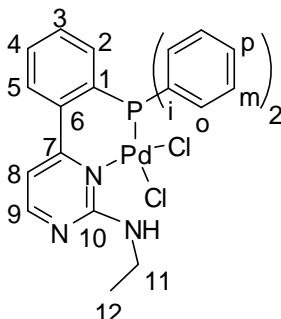
{[2-(4-(2-octhylamino)pyrimidinyl)phenyl]diphenylphosphine}dichloridopalladium(II), 14c. From **4c**, yield: 0.17 g (89 %, pale yellow solid). C$_{30}$H$_{34}$Cl$_2$N$_3$PPd (644.91): calcd. C, 55.87; H, 5.31; N, 6.52; found C, 55.17; H, 3.66; N, 7.02. ^{1}H NMR (CDCl$_3$, 400.13 MHz, 20 °C): δ = 0.89 (br., 3 H, H-18), 1.20-1.750 (br., 14 H, H-12, H-13, H-14, H-15, H-16 and H-17), 3.25-3.57 (br., 2 H, H-11), 6.44 (s, 1 H, H-8), 7.20-7.75 (m, 14 H, H-*o*, H-*m*, H-*p*, H-2, H-3, H-4, H-5) 8.03 (s, 1 H, H-9), 8.42 (br., 1H NH) ppm. ^{31}P NMR (CDCl$_3$, 100.61 MHz, 20 °C): δ = 30.88 (s) ppm.
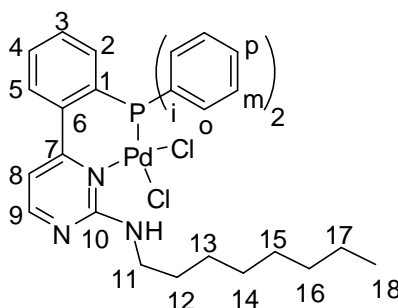
{[2-((2-dimethylamino)pyrimidin-κC^5-1-ium-4-yl)phenyl]diphenylphosphine}dichlorido-palladium(II), (15a). From **4d**, yield: 0.15 g (87 % yellow solid). C$_{24}$H$_{22}$Cl$_2$N$_3$PPd (560.74): calcd. C, 51.41; H, 3.95; N, 7.49; found C, 52.98; H, 3.98; N, 7.78. ^{1}H NMR ([D$_6$]DMSO,

172

Experimental

400.13 MHz, 20 °C): not det. NH, δ = 3.14 (s, 6 H, H-11), 6.84 (br., 1 H, H-2), 7.30-7.50 (m, 10 H, H-o, H-m, H-p), 7.59 (m, 1 H, H-3), 7.75 (t, $^3J_{HH}$ = 7.0 Hz, 1 H, H-4), 8.45 (m, 1 H, H-5), 8.52 (s, 1 H, H-9) ppm. ^{31}P NMR ([D$_6$]DMSO, 161.98 MHz, 20 °C): δ = 29.69 (s) ppm.
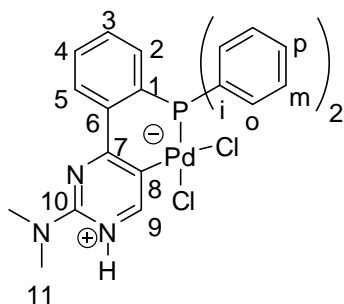
{[2-((2-pyrrolidino)pyrimidin-κC^5-1-ium-4-yl)phenyl]diphenylphosphine}dichloride-palladium(II), (15b). From **4e**, yield: 0.15 g (85 % yellow solid). C$_{26}$H$_{24}$Cl$_2$N$_3$PPd (586.78): calcd. C, 53.22; H, 4.12; N, 7.16; found C, 53.47; H, 4.11; N, 7.16. ^{1}H NMR ([D$_6$]DMSO, 400.13 MHz, 20 °C): δ = not det. NH, 1.93 (br., 4 H, H-12), 3.51 (br., 4 H, H-11), 6.84 (br., 1 H, H-2), 7.30-7.50 (m, 10 H, H-o, H-m, H-p), 7.58 (m, 1 H, H-3), 7.75 (t, $^3J_{HH}$ = 7.9 Hz, 1 H, H-4), 8.45 (m, 1 H, H-5), 8.51 (s, 1 H, H-9) ppm. ^{31}P NMR ([D$_6$]DMSO, 161.98 MHz, 20 °C): δ = 29.67 (s) ppm.
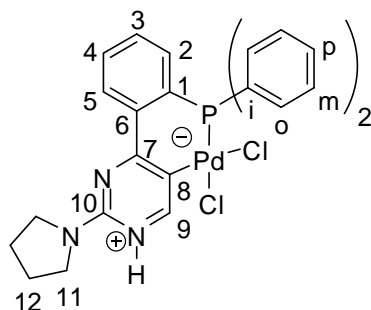
{[2-((2-piperidino)pyrimidin-κC^5-1-ium-4-yl)phenyl]diphenylphosphine}dichloride-palladium(II), (15c). From **4f**, yield: 0.15 g (83 % yellow solid).

Experimental

$C_{27}H_{26}Cl_2N_3PPd\cdot(CH_2Cl_2)_{0.67}$: calcd. C, 50.54; H, 4.19; N, 6.53; found C, 50.79; H, 4.14; N, 6.40. ^{1}H NMR ([D$_6$]DMSO, 400.13 MHz, 20 °C): δ = not det. NH, 1.59 (br., 6 H, H-12, H-13), 3.68 (br., 4 H, H-11), 6.84 (br., 1 H, H-2), 7.32-7.42 (m, 4 H, H-*o*), 7.44-7.54 (m, 6 H, H-*m*, H-*p*), 7.58 (m, H-3), 7.75 (t, $^3J_{HH}$ = 7.4 Hz, 1 H, H-4), 8.40 (m, H-5), 8.52 (s, 1 H, H-9) ppm. ^{31}P NMR ([D$_6$]DMSO, 161.98 MHz, 20 °C): δ = 29.60 (s) ppm.
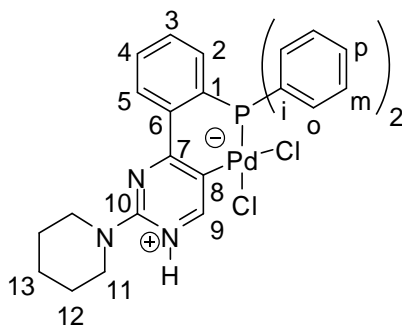
Bis[μ-(acetato-κ*O*:κ*O*')]bis[(diphenylphosphino-κ*P*)-2-(4(2-dimethylamino)pyrimidin-κ*C*^{5}-1yl)phenyl]dipalladium (II), (16). From **4d**. A solution of 0.23 g (0.60 mmol) **4d** in dry CH_2Cl_2 (20 ml) were added dropwise to a solution of 0.13 g (0.60 mmol) $Pd(O_2CCH_3)_2$ in dry CH_2Cl_2 (20 ml). The mixture was stirred at RT over night. After concentration, addition of pentane (20 ml) caused precipitation of the product, which was then washed twice with pentane (10 ml) and dried in vacuum, yield: 0.60 g (91%, orange solid). $C_{52}H_{50}N_6O_4P_2Pd_2$ (1097.78): calcd. C, 56.89; H, 4.59; N, 7.66; found C, 56.20; H, 5.03; N, 7.25. ^{1}H NMR ([D6]DMSO, 400.13 MHz, 20 °C): 1.18 (s, 3 H, H-12), 3.07 (s, 6 H, H-11), 6.60-6.75 (m, 3 H, H-2, H-*o*), 7.25-7.58 (m, 9 H, H-*o*, H-*m*, H-*p*, H-3), 7.64 (m, 1 H, H-4), 8.00 (m, 1 H, H-5), 8.74 (s, 1 H, H-9) ppm. ^{31}P NMR ([D6]DMSO, 161.98 MHz, 20 °C): δ = 32.86 (s) ppm.

Experimental
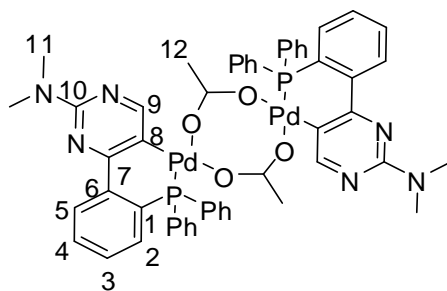
***trans*-Dichloridobis{[4-(4-(2-ethylamino)pyrimidinyl)phenyl]diphenylphosphine}-**

palladium(II), (17). A solution of 0.5 g (1.30 mmol) **2b** in dry CH_2Cl_2 (20 ml) was added

dropwise to a solution of 0.25 g (0.65 mmol) $(C_6H_5CN)_2PdCl_2$ in dry CH_2Cl_2 (20 ml). The

mixture was stirred at RT over night. After concentration, the addition of diethylether (30 ml)

caused precipitation of the product, which was then washed twice with diethylether (20 ml) and

dried in vacuum. Suitable crystals for X-ray diffraction were obtained either from diffusion of

diethyl ether to a solution of complex in $CHCl_3$, or slow evaporation of solution of the complex

in methanol, yield: 0.60 g (91%, orange solid). $C_{48}H_{44}Cl_2N_6O_8P_2Pd.2CH_3OH$ (1008.26): calcd.

C, 59.56; H, 5.20; N, 8.34; found C, 59.80; H, 5.32; N, 7.74. ^1H NMR ($CDCl_3$, 400.1 MHz, 20

°C): 1.26 (t, $^3J_{HH}$ = 7.2 Hz, 6 H, H-10), 3.52 (m, 2 H, H-9), 5.15 (br., 2 H, N-H), 6.94 (d, $^3J_{HH}$

= 5.2 Hz, 2 H, H-6), 7.37-7.48 (m, 12 H, H-*o*, H-*p*), 7.71-7.78 (m, 12 H, H-*m*, H-2), 8.03 (d,

$^3J_{HH}$ = 7.9 Hz, 4 H, H-3), 8.33 (d, $^3J_{HH}$ = 4.2 Hz, 2 H, H-7) ppm. ^{13}C NMR ($CDCl_3$, 100.61

MHz, 25 °C): δ = 15.9, 35.5, 106.7, 126.7, 128.3, 128.4, 128.4, 129.4, 130.9, 135.2, 135.3,

135.3, 138.1, 139.4, 158.6, 158.7, 164.1 ppm. ^{31}P NMR (CDCl3, 161.98 MHz, 20 °C): δ =

23.08 (s) ppm.
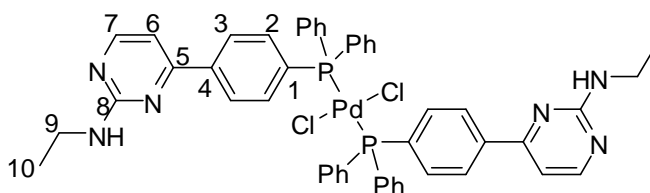
Experimental

[*N*-(Diphenylphosphino)2-amine-4-(pyridin-2-yl)pyrimidine(chlorido)palladium(II)]

hexafluorophosphate, (20). A solution of 0.1 g (0.28 mmol) of **12b** in CH_2Cl_2 (10 ml) was added dropwise to a solution of 0.106 g (0.28 mmol) $(C_6H_5CN)_2PdCl_2$ in CH_2Cl_2 (10 ml). Then 0.067 g (0.36 mmol) of potassium hexafluorophosphate were added. The mixture was stirred over night and the precipitated yellow solid was filtered and potassium chloride as well as excess of potassium hexafluorophosphate was washed with water (3 × 5 ml). Suitable crystals for X-ray crystal structure determination were obtained by slow diffusion of ether vapor into DMSO-EtOH-CHCl$_3$ solution of the complex, yield: 0.19 g (94 %, yellow solid). $C_{22}H_{17}Cl_2F_6N_3P_2Pd \cdot DMSO$ (721.33): calcd. C, 38.30; H, 3.21; N, 7.77; S, 4.45; found C, 38.32; H, 3.60; N, 7.73; S, 5.16. ^1H NMR ([D$_6$]DMSO, 400.13 MHz, 20 °C): δ = 7.58-7.75 (m, 7 H, H-*m*, H-*p*, H-3), 7.85-8.10 (m, 5 H, H-*o*, H-8), 8.40 (t, $^3J_{HH}$ = 7.6 Hz, 1 H, H-7), 8.60 (d, $^3J_{HH}$ = 7.5 Hz, 1 H, H-6), 8.75-8.83 (m, 2 H, H-2, H-9), 11.1-11.7 (br., 1 H, NH) ppm. ^{31}P NMR ([D6]DMSO, 161.98 MHz, 20 °C): δ = −144.20 (sep), 65.64 (s) ppm.
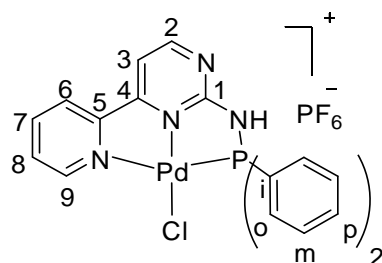
[*N*-(Diphenylphosphino)2-amine-4-(pyridin-2-yl)-6-phenylpyrimidine(chlorido)pallad-

ium(II)] chloride, (21). A solution of 0.22 g (0.51 mmol) **12c** in dry CH_2Cl_2 (20 ml) were added dropwise to a solution of 0.2 g (0.51 mmol) $(C_6H_5CN)_2PdCl_2$ in dry CH_2Cl_2 (20 ml). The mixture was stirred at RT over night. After concentration, addition of diethylether (30 ml) caused precipitation of the product, which was then washed twice with diethylether (20 ml) and dried in vacuum. yield: 0.19 g (94 %, yellow solid). $C_{27}H_{21}Cl_2N_4PPd$ (609.78): calcd. C, 53.18;

Experimental

H, 3.47; N, 9.19; found C, 52.82; H, 3.61; N, 9.73. ^{1}H NMR ([D$_6$]DMSO, 400.13 MHz, 20 °C): δ = 7.58-7.79 (m, 9 H, H-*o*, H-*m*, H-13), 8.00-8.10 (m, 5 H, H-*p*, H-12, H-7), 8.42 (d, 2 H, H-11), 8.55 (m, 1 H, H-8), 8.80 (s, 1 H, H-3), 8.86 (m, 1 H, H-6), 9.11 (m, 1 H, H-9), 11.2-11.8 (br., 1 H, NH) ppm. ^{31}P NMR ([D6]DMSO, 161.98 MHz, 20 °C): δ = 67.81 (s) ppm.
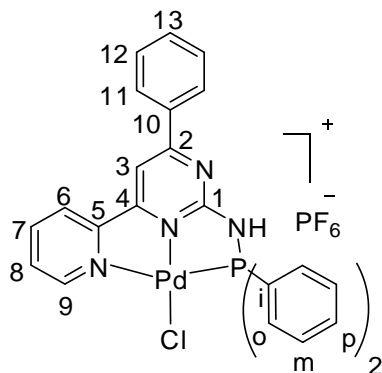
[*N*-(diphenylphosphino)2-amine-4-phenylpyrimidin]dichloridopalladium(II), (23). A solution of 0.50 g (1.41 mmol) **12a** in CH$_2$Cl$_2$ (10 ml) was added dropwise to a solution of 0.54 g (1.41 mmol) (C$_6$H$_5$CN)$_2$PdCl$_2$ in CH$_2$Cl$_2$ (20 ml). The product tended to precipitate from the reaction solution and optimized yields were obtained by adding excessive amounts of diethyl ether (10 ml) in the reaction mixture. The product was filtered, washed twice with diethyl ether and dried under vacuum. Suitable crystals for X-ray crystal structure determination were obtained by slow diffusion of ether vapor into DMSO-Ethanol solution of the complex, yield: 0.65 g (87%, orange solid). C$_{22}$Cl$_2$H$_{18}$N$_3$PPd.DMSO (532.70): calcd. C, 47.19; H, 3.96; N, 6.88; found C, 47.07; H, 3.92; N, 6.86. ^{1}H NMR ([D$_6$]DMSO, 400.13 MHz, 20 °C): δ = 7.55-7.61 (m, 2 H, H-7), 7.62-7.66 (m, 5-H, H-8, H-*m*), 7.70-7.75 (m, 2 H, H-*p*), 7.80 (d, $^3J_{HH}$ = 6.5 Hz, 1 H, H-3), (m, 4 H, H-*o*), 8.19 (d, $^3J_{HH}$ = 7.3 Hz, 2 H, H-6), 9.29 (d, $^3J_{HH}$ = 6.5 Hz, 1 H, H-2), 10.84 (s, 1 H, NH) ppm. ^{31}P NMR ([D$_6$]DMSO, 161.98 MHz, 20 °C): δ = 63.34 (s) ppm.

Experimental
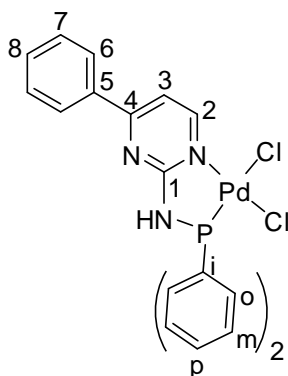
5.6.   Synthesis of Hybrid Materials

[2-{2-(Diphenylphosphanyl)phen-2-yl}pyrimidin-4-yl]-3-(triethoxysilyl)prop-1-yl   urea (25). 1.56 g (6 mmol) of [(3-triethoxysilyl)prop-1-yl]isocyanate were added to 1.50 g (4.22 mmol) of **4a** and the mixture was heated to 200 ℃ for 1 h. After cooling to RT, the residue was recrystallized from CH_2Cl_2/n-hexane (1:1), which gave desired product, yield: 1.83 g (72%; light yellow powder.). $C_{32}H_{39}N_4O_4Psi$ (602.74): calcd. C, 63.77; H, 6.52; N, 9.30; found C, 63.53; H, 6.45; N, 9.23. ^1H NMR ([D6]DMSO, 400.13 MHz, 20 °C): δ = 0.57 (m, 2 H, H-14), 1.07 (m, 9 H, H-16), 1.57 (m, 2 H, H-13), 3.20 (m, 2 H, H-12), 3.67 (m, 6 H, H-15), 6.93 (m, 1 H, H-2), 7.00 (d, $^3J_{HH}$ = 4.8 Hz, 1 H, H-8), 7.25-7.15 (m, 4 H, H-*m*), 7.38-7.30 (m, 6 H, H-*o*, H-*p*), 7.44 (t, $^3J_{HH}$ = 7.4 Hz, 1 H, H-3), 7.51 (t, $^3J_{HH}$ = 7.4 Hz, 1 H, H-4), 7.59 (m, 1 H, H-5), 8.42 (d, $^3J_{HH}$ = 4.7 Hz, 1 H, H-9), 9.09 (br., 1 H, NH-b), 9.27 (br., 1 H, NH-a) ppm. ^{13}C NMR (DMSO-d6, 101.61 MHz, 20 °C): δ = 7.4 (s, C-14), 18.1 (s, C-16), 23.2 (s, C-13), 42.0 (s, C-12), 57.7 (s, C-15), 113.9 (s, C-8), 128.7 (d, $^3J_{CP}$ = 7.4 Hz, C-*m*), 129.0 (s, C-2), 129.1 (s, C-*p*), 129.7 (s, C-3), 130.0 (d, $^3J_{CP}$ = 2.8 Hz, C-4), 133.3 (s, C-5), 135.9 (d, $^1J_{CP}$ = 20.34 Hz, C-1), 133.4 (d, $^2J_{CP}$ = 21.3 Hz, C-2), 136.3 (d, $^1J_{CP}$ = 11.9 Hz, C-*i*), 141.6 (d, $^1J_{CP}$ = 19.4 Hz, C-6), 153.5 (s, C-9), 157.3 (s, C-10), 158.5 (s, C-7), 166.2 (s, C-11) ppm. ^{31}P NMR ([D_6]DMSO, 161.98 MHz, 20 °C): δ = –9.51 ppm (s).

Experimental
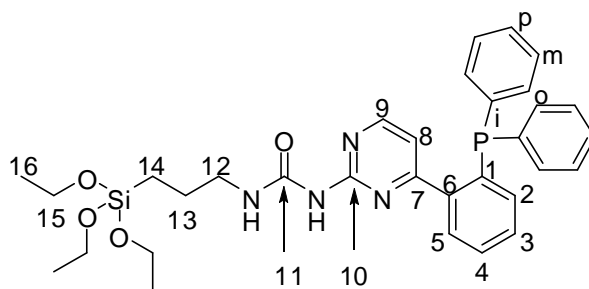
{[2-((3-(triethoxysilyl)prop-1-yl-urea)pyrimidin-κC5-1-ium-4-yl)phenyl]diphenyl phosphine}dichlorideopalladium(II), (26). A solution of 1.00 g (1.66 mmol) ligand **25** in CH$_2$Cl$_2$ (30 ml) was added dropwise to a solution of (C$_6$H$_5$CN)$_2$PdCl$_2$ (0.64 g, 1.66 mmol) in CH$_2$Cl$_2$ (30 ml). The mixture was stirred at RT for 1 h. By adding pentane (50 ml), the product was precipitated, which was then filtered and washed twice with pentane (20 ml) and dried in vacuum, yield: 1.25 g (75%, orange solid). C$_{30}$H$_{34}$Cl$_2$N$_4$O$_4$PPdSi (751.00): calcd. C, 47.98; H, 4.56; N, 7.46; found C, 47.82; H, 4.89; N, 7.21. ^{1}H NMR ([D6]DMSO, 600 MHz, 20 °C): δ = 0.40 (m, 2 H, H-14), 1.05 (m, 3 H, H-16), 1.55 (m, 2 H, H-13), 3.13 (m, 2 H, H-12), 3.43 (m, 3 H, H-15), 6.83 (s, 1 H, H-2), 7.30-7.38 (m, 4 H, H-m), 7.41-7.55 (m, 6 H, H-*o*, H-*p*), 7.57 (m, 1 H, H-3), 7.77 (m, H-4), 8.26 (s, 1 H, H-5), 8.81 (s, 1 H, H-9), 9.5-10.5 (br., 1 H, NH-a) ppm. ^{13}C NMR ([D6]DMSO, 151 MHz, 25 °C): δ = 11.2, 18.6, 23.6, 42.1, 56.1, 128.55, 130.0, 131.4, 131.8, 132.2, 133.9, 143.6, 154.0 ppm. ^{31}P NMR ([D$_6$]DMSO, 161.98 MHz, 20 °C): δ = 30.13 (s) ppm.
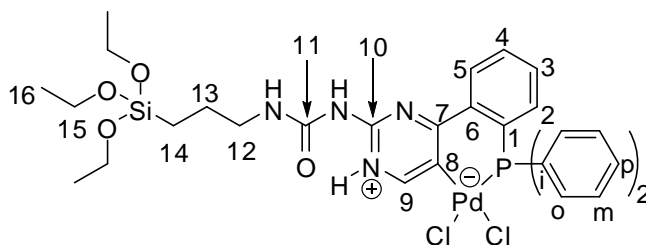
[2-{4-(Diphenylphosphanyl)phen-2-yl}pyrimidin-4-yl]-3-(triethoxysilyl)prop-1-yl urea

Experimental

(27). 2.50 g (10.11 mmol) of [(3-triethoxysilyl)prop-1-yl]isocyanate were added to 1.77 g (4.98 mmol) of **2a** and the mixture heated to 170 °C for 1 h. After cooling to RT, the residue was recrystallized from methanol and washed with diethylether-hexane (1:1), which gave desired product, yield: 2.28 g (76%, light yellow powder). $C_{32}H_{39}N_4O_4PSi$ (602.74): calcd. C, 63.77; H, 6.52; N, 9.30; found C, 63.91; H, 6.11; N, 8.92. ^{1}H NMR (CDCl$_3$, 400.1 MHz, 20 °C): δ = 0.70 (m, 2 H, H-12), 1.21 (t, $^3J_{HH}$ = 7.0 Hz, 9 H, H-14), 1.86 (m, 2 H, H-11), 3.81 (q, $^3J_{HH}$ = 7.0 Hz, 6 H, H-13), 4.05 (m, 2 H, H-10), 7.30 (d, $^3J_{HH}$ = 7.5 Hz, 1 H, H-6), 7.33-7.40 (m, 10 H, H-*o*, H-*m*, H-*p*), 7.41-7.45 (m, 2 H, H-2), 8.17 (d, $^3J_{HH}$ = 7.3 Hz, 2 H, H-3), 8.70 (d, $^3J_{HH}$ = 7.5 Hz, 1 H, H-7) ppm. ^{13}C NMR (CDCl$_3$, 100.61 MHz, 20 °C): δ = 7.9 (s, C-12), 18.4 (s, C-14), 21.0 (s, C-11), 46.0 (s, C-13), 58.6 (s, C-10), 106.7 (s, C-6), 128.7 (d, $^3J_{CP}$ = 6.1 Hz, C-3), 129.0 (d, $^3J_{CP}$ = 7.4 Hz, C-*m*), 129.6 (s, C-*p*), 133.8 (d, $^2J_{CP}$ = 7.2 Hz, C-2), 134.2 (d, $^2J_{CP}$ = 20.2 Hz, C-*o*), 135.8 (d, $^1J_{CP}$ = 10.5 Hz, C-*i*), 137.7 (s, C-4), 146.9 (d, $^1J_{CP}$ = 15.9, Hz C-1), 148.0 (s, C-7), 153.6 (s, C-8), 153.7 (s, C-5), 172.2 (s, C-9) ppm. ^{31}P NMR (CDCl$_3$, 161.98 MHz, 20 °C): δ = –4.18 (s) ppm.
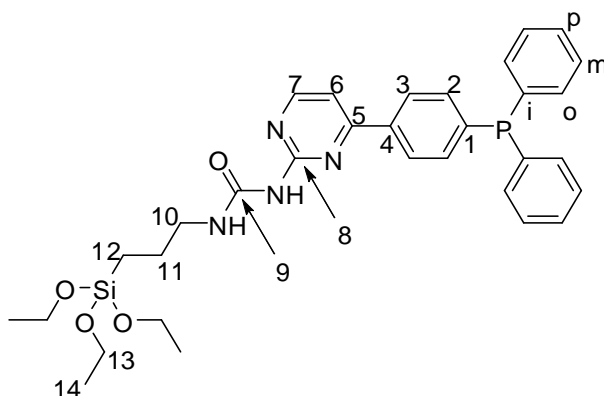
trans-**Dichloridobis{[2-{4-(diphenylphosphanyl)phen-2-yl}pyrimidin-4-yl]-3-(triethoxy-silyl)prop-1-yl urea}palladium(II), (28).** A solution of 0.63 g (1.05 mmol) ligand **27** in dry CH$_2$Cl$_2$ (20 ml) was added dropwise to a solution of (C$_6$H$_5$CN)$_2$PdCl$_2$ (0.20 g, 0.52 mmol) in

Experimental

dry CH_2Cl_2 (20 ml). The mixture was stirred at RT for 1 h. The colour changed from orange to yellow. After concentration, addition of pentane (40 ml) caused precipitation of the product, which was then washed twice with pentane (20 ml) and dried in vacuum, yield: 0. 72 g (92%, orange solid). $C_{64}H_{78}Cl_2N_8O_8P_2PdSi_2$ (1382.80): calcd. C, 55.59; H, 5.69; N, 8.10; found C, 56.07; H, 5.36; N, 7.93. ^{1}H NMR (CDCl$_3$, 400.1 MHz, 20 °C): δ = 0.70 (m, 2 H, H-12), 1.21 (t, $^3J_{HH}$ = 7.0 Hz, 9 H, H-14), 1.86 (m, 2 H, H-11), 3.81 (q, $^3J_{HH}$ = 7.0 Hz, 6 H, H-13), 4.05 (m, 2 H, H-10), 7.33 (d, $^3J_{HH}$ = 7.4 Hz, 1 H, H-6), 7.41-7.46 (m, 4 H, H-*m*), 7.48-7.52 (m, 2 H, H-*p*), 7.74-7.80 (m, 6 H, H-2, H-*o*), 8.21 (d, $^3J_{HH}$ = 8.1 Hz, 2 H, H-3), 8.76 (d, $^3J_{HH}$ = 7.4 Hz, 1 H, H-7) ppm. ^{13}C NMR (CDCl$_3$, 100.61 MHz, 25 °C): δ = 7.9 (s, C-12), 18.4 (s, C-14), 21.0 (s, C-11), 46.1 (s, C-13), 58.6 (s, C-10), 106.9 (s, C-6), 128.2 (m, C-3), 128.7 (m, C-*m*), 131.4 (s, C-*p*), 135.3 (m, C-2), 135.6 (m, C-*o*), 135.7 (d, C-*i*), 137.5 (m, C-1), 138.3 (s, C-4), 148.0 (s, C-7), 153.6 (s, C-8), 153.7 (s, C-5), 172.1 (s, C-9) ppm. ^{31}P NMR (CDCl3, 161.98 MHz, 20 °C): δ = 23.90 (s) ppm.
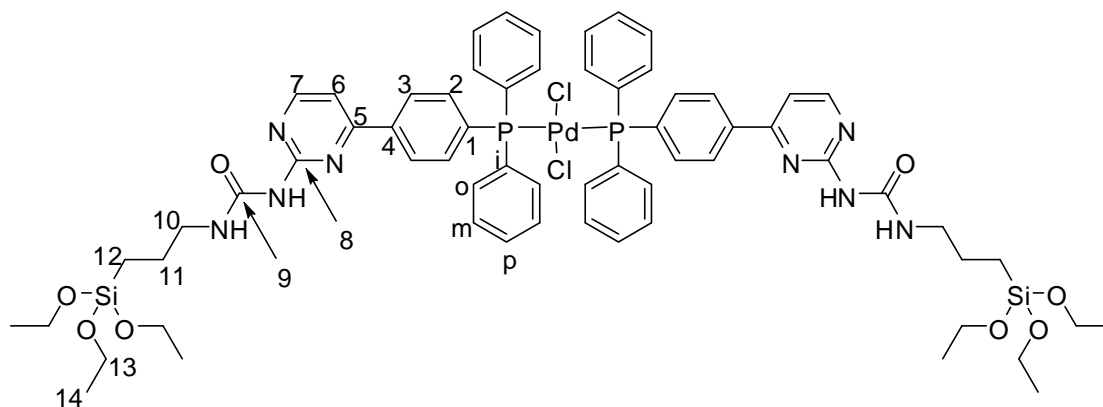
Preparation of 26@SiO$_2$ or 26@MCM-41. Compound **26** was immobilized on MCM-41 or SiO$_2$ according to a standard procedure: A solution of 0.5 g (0.66 mmol) of **25** in dry CHCl$_3$ (60 ml) was added to a suspension of MCM-41 or SiO$_2$ (1.10 g) in dry toluene (120 ml). The mixture was stirred for 18 h at 100 ºC. The solid was filtered off and washed with CH$_2$Cl$_2$ in a

Experimental

Soxhlet apparatus for 24 h. Finally, the solid was dried in vacuum at 50 ºC for 5 h to obtain **26@MCM-41** or **26@SiO₂**.

26@SiO₂. A pale yellow product was obtained. Elemental analysis for **26@SiO₂**: C, 9.61; H, 1.33; N, 1.58; which corresponds to a loading of 0.28 mmol/g. IR (KBr, cm^{-1}): 3438 (m, br.), 2979 (w), 1666 (m), 1589 (w), 1540 (w), 1543 (w), 1092 (s, br.), 963 (m), 798 (m), 472 (s, br.). ^{29}Si CP-MAS NMR (Solid-state, 79.5 MHz): δ = –111.20 (s), –100.99 (br., m), –47.64 (br., m) ppm. ^{13}C CP-MAS NMR (Solid-state, 100.6 MHz): δ = 9.4, 16.4, 23.0, 43.1, 58.2, 130.9 (br.), 141.6, 156.1, 161.8 ppm. ^{31}P CP-MAS NMR (Solid-state, 162.0 MHz): δ = 36.52 (s) ppm.

26@MSM-41. A pale yellow product was obtained. Elemental analysis for **26@MSM-41**: C, 11.84; H, 1.58; N, 1.77; which corresponds to a loading of 0.31 mmol/g. IR (KBr, cm^{-1}): 3403 (m, br.), 3062 (w), 2980 (w), 1666 (m), 1590 (w), 1543 (w), 1438 (w), 1074 (s, br.), 962 (m), 804 (m), 455 (s, br.). ^{29}Si CP-MAS NMR (Solid-state, 79.5 MHz): δ = –100.12 (br., m), –51.78 (br., m) ppm. ^{13}C CP-MAS NMR (Solid-state, 100.6 MHz): δ = 9.0, 16.3, 23.0, 43.0, 58.3, 133.0 (br.), 141.5, 156.0, 161.9 ppm. ^{31}P CP-MAS NMR (Solid-state, 162.0 MHz): δ = 36.9 (s) ppm.

Experimental

Preparation of 28@ SiO₂ and 28@MCM-41. Compound **28** was immobilized on MCM-41 and SiO₂ according to a previously reported procedure used in Thiel's group. A solution of 0.2 g (0.14 mmol) of **28** dissolved in 5 ml of dry CH₂Cl₂ and 15 ml of toluene was added to a suspension of 0.50 g of SiO₂ or MCM-41 in 50 ml of dry toluene. The mixture was stirred for 12 h at 100 °C. The solid was filtered off and washed with CH₂Cl₂ in a Soxhlet apparatus for 24 h. Finally, the solid was dried in vacuum at 50 ºC to obtain **28@ SiO₂** or **28@MCM-41**.

28@SiO₂. A pale yellow product was obtained. Elemental analysis for **28@SiO₂**: C, 10.75; H, 1.44; N, 1.63; which corresponds to a loading of 0.2 mmol/g. IR (KBr, cm⁻¹): 3418 (m, br.), 2978 (w), 1759 (w), 1682 (m), 1626 (m), 1571 (w), 1540 (w), 1496 (w), 1438 (m), 1393 (m), 1343 (m), 1045 (s, br.), 961 (m), 798 (m), 481 (s, br.). ²⁹Si CP-MAS NMR (Solid-state, 79.5 MHz): δ = –110.39 (s), –100.91 (br., m), –45.90 (br., m) ppm. ¹³C CP-MAS NMR (Solid-state, 100.6 MHz): δ = 8.55, 16.60, 23.0, 47.1, 57.98, 110.01, 128.78 (br.), 135.00, 155.12, 175.21, ppm. ³¹P CP-MAS NMR (Solid-state, 162.0 MHz): δ = 21.94 (s) ppm.

183

Experimental
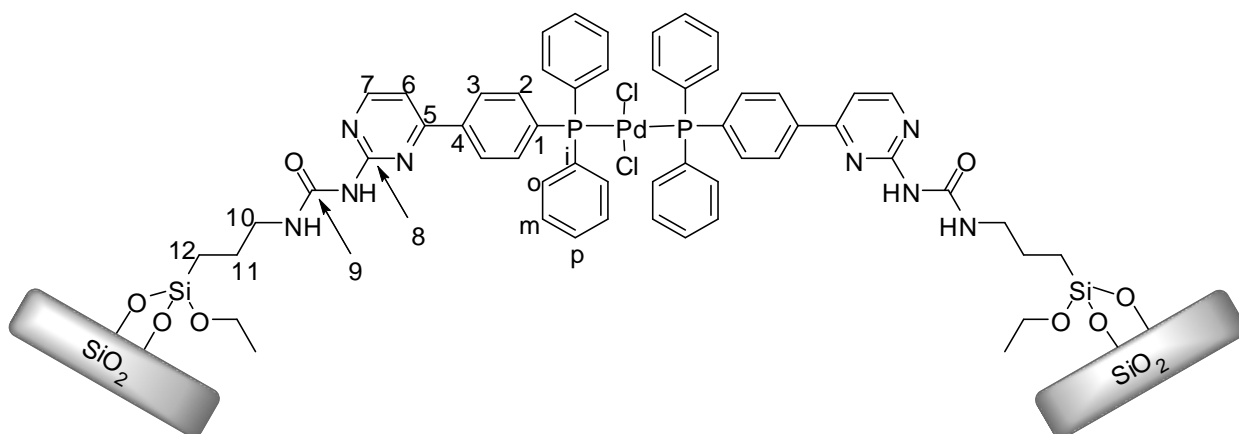
28@MCM-41. A yellow product was obtained. Elemental analysis for **28@MCM-41**: C, 7.39; H, 1.19; N, 1.04; which corresponds to a loading of 0.13 mmol/g. IR (KBr, cm^{-1}): 3420 (m, br.), 2974 (w), 1625 (m), 1569 (w), 1437 (w), 1395 (w), 1057 (s, br.), 954 (m), 792 (m), 462 (s, br.). ^{29}Si CP-MAS NMR (Solid-state, 79.5 MHz): δ = –99.92 (br., m), –44.89 (br., m) ppm. ^{13}C CP-MAS NMR (Solid-state, 100.6 MHz): δ = 8.63, 16.19, 20.44, 46.68, 58.73, 110.00, 128.74 (br.), 154.47, 174.54 ppm. ^{31}P CP-MAS NMR (Solid-state, 162.0 MHz): δ = 36.2 (s) ppm.
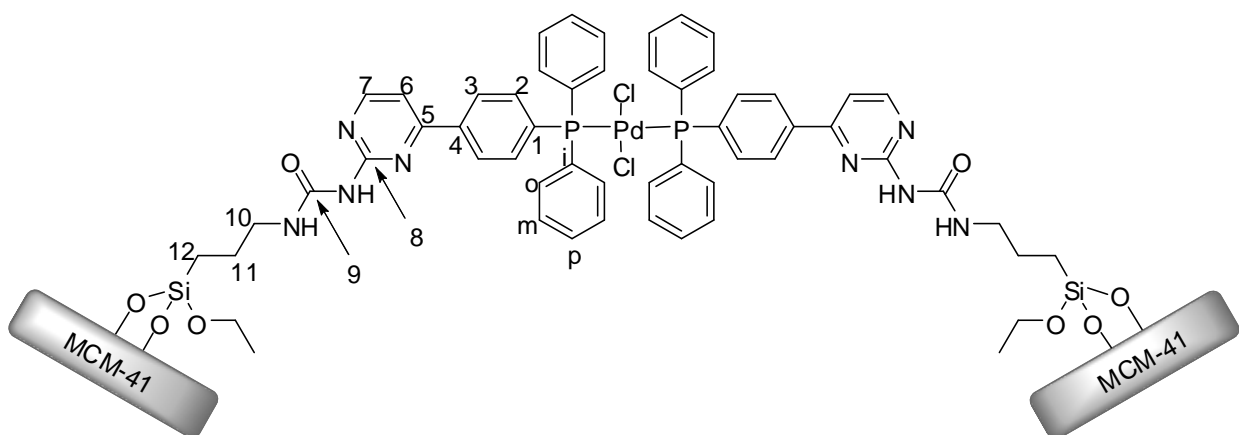
References

6.   References

1. K. J. Laidler, J. H. Meiser, *Physical Chemistry, Benjamin/Cummings* **1982**, 423.

2. A. Corma, *Chem. Rev*. **1997**, *97*, 2373.

3. A. Wight, M. Davis, *Chem. Rev*. **2002**, *102*, 3589.

4. F. Hoffmann, M. Cornelius, J. Morell, *Angew. Chem.*, **2006**, *118*, 3290; *Angew. Chem. Int. Ed.* **2006**, *45*, 3216.

5. A. Corma, H. Garcia, *Adv. Synth. Catal*. **2006**, *348*, 1391.

6. G. J. Hutchings, *Chem. Commun*. **1996**, 301.

7. J. Grunes, J. Zhu, G. A. Somorjai, *Chem. Commun*. **2003**, 2257.

8. A. Corma, *Catal. Rev. Sci. Eng*. **2004**, *46*, 369.

9. R. A. Sheldon, *Chem. Commun*. **2008**, 3352.

10. E. Lindner, T. Schneller, F. Auer, H. A. Mayer, *Angew. Chem.* **1999**, *111*, 2288; *Angew. Chem Int. Ed*. **1999**, *38*, 2155.

11. C. A. Tolman, *Chem. Rev*. **1977**, *77*, 313.

12. A. G. Orpen, N. G. Connelly, *Organometallics* **1990**, *9*, 1206.

13. D. S. Marynick, D. S. *J. Am. Chem. Soc*. **1984**, *106*, 4064.

14. A. G. Orpen, N. G. Connelly, *J. Chem. Soc., Chem. Commun*. **1985**, 1310.

15. F. Natalie, A. G. Orpen, J. N. Harvey, *Coord. Chem. Rev*. **2009**, *253*. 704.

16. J. C. Jeffrey, T. B. Rauchfuss, *Inorg. Chem*., **1979**, 18, 2658.

17. P. Braunstein, F. Naud, *Angew. Chem.* **2001**, *113*, 702; *Angew. Chem. Int. Ed.* **2001**, *40*, 680.

18. J. Holz, R. Kadyrov, S. Borns, D. Heller, A. Börner, *J. Organomet. Chem.* **2000**, *603*, 61.

19. T. E. Barder, S. D. Walker, J. R. Martinelli, S. L. Buchwald, *J. Am. Chem. Soc*. **2005**, *127*, 4685.

References

20. H. Weissman, L. J. W. Shimon, D. Milstein, *Organometallics* **2004**, *23*, 3931.

21. J. Andrieu, P. Braunstein, F. Naud, R. D. Adams, *J. Organomet. Chem.* **2000**, *601*, 43.

22. F. Y. Kwong, W. H. Lam, C. H. Yeung,K. S. Chan, A. S. C. A. Chan, *Chem. Commun*. **2004**, 1922.

23. W. M. Dai, Y. A. Zhang, *Tetrahedron Lett*. **2005**, *46*, 1377.

24. X. Bei, H. W. Turner, W. H. Weinberg, A. S. Guram, J. L. Petersen, *J. Org. Chem.* **1999**, *64*, 6797.

25. S. Pautz, R. Fawzi, M. Steimann, *Organometallics* **1998**, *17*, 3006.

26. R. W. Wegman, A. G. Abatjoglou, A. M. Harrison, *J. Chem. Soc. Chem. Commun*. **1987**,1891.

27. A. Weigt, S. Bischoff, Phosphorus Sulfur Silicon Relat. Elem. **1995**, *102*, 91.

28. L. Gall, P. Laurent, L. Toupet, J.-Y. Salaün, H. Abbayes, Organometallics **1997**, *16*, 3579.

29. S. Bischoff, A. Weigt, H. Mießner, B. Lücke, J. Mol. Catal. A **1996**, 339.

30. E. Lindner, T. Schneller, F. Auer, H. A. Mayer, *Angew. Chem.* **1999**, *111*, 2288; *Angew. Chem. Int. Ed*. **1999**, *38*, 2154.

31. F. A. Jalón, B. R. Manzano, F. G. Torre, A. M. López-Agenjo, A. M. Rodríguez, W. Weissensteiner, T. Sturm, J. Mahía, J. Maestro, *J. Chem. Soc., Dalton Trans.* **2001**, 2417.

32. Z. Weng, S. Teo,L. L. Koh, T. S. A. Hor, *Organometallics* **2004**, *23*, 4342.

33. L. C. Liang, P. S. Chien, M. H. Huang, *Organometallics* **2005**, *24*, 353.

34. G. R. Newkome, *Chem. Rev*. **1993**, *93*, 2067.

35. C. Abu-Gnim, I. Amer, *J. Mol. Catal*. **1993**, *85*, L275.

36. K. P. Langhans, O. Stelzer, *Chem. Ber.* **1987**, *120*, 1707.

37. O. Herd, K. P. Langhans, O. Stelzer, N. Weferling, W. S. Sheldrick, *Angew. Chem.* **1993**, *105*, 1097; *Angew. Chem., Int. Ed*., **1993**, *32*, 1058.

38. O. Herd, A. Heßler, K. P. Langhans, O. Stelzer, W. S. Sheldrick, N. Weferling, *J.*

Organomet. Chem. **1994**, *475*, 99.

39. A. Heßler, J. Fischer, S. Kucken, O. Stelzer, *Chem. Ber*. **1994**, *127*, 481.

40. F. Bitterer, O. Herd, A. Hessler, M. Kühnel, K. Rettig, O. Stelzer, W. S. Sheldrick, S. Nagel, N. Rösch, *Inorg. Chem*. **1996**, *35*, 4103.

41. F. Bitterer, O. Herd, M. Kühnel, O. Stelzer, N. Weferling, W. S. Sheldrick, J. Hahn, S. Nagel, N. Rösch, *Inorg. Chem*. **1998**, *37*, 6408.

42. D. J. Brauer, P. Machnitzki, T. Nickel, O. Stelzer, *Eur. J. Inorg. Chem*. **2000**, 65.

43. D. J. Brauer, S. Schenk, S. Roßenbach, M. Tepper, O. Stelzer, T. Häusler, W. S. Sheldrick, *J. Organomet. Chem*. **2000**, *598*, 116.

44. O. Herd, D. Hoff, K. W. Kottsieper, C. Liek, K. Wenz, O. Stelzer, W. S. Sheldrick, *Inorg. Chem*. **2002**, *41*, 5034.

45. A. Reis, W. R. Thiel, DE 102008039167.

46. A. Reis.; Dissertation, Technishe Universität Kaiserslautern, **2008**.

47. A. Reis, D. Dehe, S. Farsadpour, I. Munstein, Y. Sun, W. R. Thiel, *New J. Chem*. **2011**, *35*, 2488.

48. H. U. Blasé, A. Indolese, A. Schnyder, *Curr. Science* **2000**, *78*, 1336.

49. J. M. Brown, S. Woodward, *J. Org. Chem.* **1991**, *56*, 6803.

50. S. Vyskocil, M. Amrcina, V. Hanus, M. Polasekand P. Kocovsky, *J. Org. Chem.* **1998**, *63*, 7738.

51. H. Takaya, K. Mashima, K. Koyano, M. Yagi, H. Kumobayashi, T. Taketomi, S. Akutagawa, R. Noyori, *J. Org. Chem*. **1986**, *51*, 629.

52. B. Drießen-Hölscher, J. Kralik, F. Agel, C. Steffens, C. Hu, *Adv. Synth. Catal*. **2004**, *346*, 979.

53. A. E. S. Gelpke, H. Kooijman, A. L. Spek, H. Hiemstra, *Chem. Eur. J*. **1999**, *5*, 2472.

54. D. Evans, J. A. Osborn, G. Wilkinson, *J. Chem. Soc. A*, **1968**, 3133.

References

55. M. Beller, B. Cornils, C. D. Frohning, C. W. Kohlpaintner, *J. Mol. Catal. A Chem*. **1995**, *104*, 17.

56. E. P. Kündig, P. Meier, *Helv. Chim. Acta* **1999**, *82*, 1360.

57. A. Meijere, F. Diederich, *Metal-Catalyzed Cross-Coupling Reactions*, 2rd ed., Wiley-VCH: Weinheim, **2008**.

58. M. Hingst, M. Tepper, O. Stelzer, *Eur. J. Inorg. Chem.* **1998**, 73.

59. I. Sagasser, G. Helmchen, *Tetrahedron Lett.* **1998**, *39*, 261.

60. W. S. Knowles, *Angew. Chem.* **2002**, *114*, 2096; *Angew. Chem., Int. Ed.* **2002**, *41*, 1998.

61. R. Noyori, *Angew. Chem.* **2002**, *114*, 2108; *Angew. Chem., Int. Ed.* **2002**, *41*, 2008.

62. N. Miyaura, K. Yamada, A. Suzuki, *Tetrahedron Lett.* **1979**, *20* (36), 3437.

63. R. F. Heck, J. P. Nolley, *J. Org. Chem.* **1972**, *37* (14), 2320.

64. D. Milstein, J. K. Stille, *J. Am. Chem. Soc.* **1978**, *100*, 3636.

65. A. O. King, N. Okukado, E. Negishi, *J. Chem. Soc. Chem. Commun.* **1977**, *19*, 683.

66. K. Sonogashira, *J. Organomet. Chem.* **2002**, *653*, 46.

67. D. S. Surry, S. L. Buchwald, *Chem. Sci.* **2011**, *2*, 27.

68. Y. Hatanaka, T. Hiyama, *J. Org. Chem.* **1988**, *53*, 918.

69. L. J. Goossen, N. Rodríguez, C. Linder, *J. Am. Chem. Soc.* **2008**, *130*, 15248.

70. J. Flapper, H, Kooijman, M, Lutz, A. L. Spek, P. W. N. M. Van Leeuwen, C. J. Elsevier, P. C. J. Kamer, *Organometallics* **2009**, *28*, 1180.

71. J. Flapper, P. W. N. M. Van Leeuwen, C. J. Elsevier, P. C. J. Kamer, *Organometallics* **2009**, *28*, 3264.

72. J. Flapper, H, Kooijman, M, Lutz, A. L. Spek, P. W. N. M. Van Leeuwen, C. J. Elsevier, P. C. J. Kamer, *Organometallics* **2009**, *28*, 3272.

73. L. O. Tabla, I. Matas, P. Palma, E. Alvarez, J. Campora, *Organometallics* **2012**, *31*, 1006.

74. K. Takuya, N. Shusuke, Y. Kenji, N. Kyoko, *J. Am. Chem. Soc.* **2007**, *129*, 8948.

References

75. M. Kawatsura, J. F. Hartwig, *J. Am. Chem. Soc*. **2000**, *122*, 9546.

76. G. Kiss, *Chem. Rev*. **2001**, *101*, 3435.

77. Sun, Y.; Ahmed, R.; Beller, M.; Thiel, W. R. *Organometallics* **2004**, *23*, 5260.

78. Seubert, C.; Sun, Y.; Thiel, W. R. *J. Chem. Soc., Dalton Trans.* **2009**, 4971.

79. Sun, Y.; Grasser, J.; Herdtweck, E.; Thiel, W. R. *J. Organomet. Chem*. **2006**, *681*, 2891.

80. B. Lippert, Coord. Chem. Rev. **2000**, *200*, 487.

81. W. B. Parker, *Chem. Rev.* **2009,** *109,* 2880.

82. L. Taghizadeh Ghoochany, *Dissersion,* Kaiserslautern, **2012**.

83. L. Wang, *Dissersion,* Kaiserslautern, **2011**.

84. L. Wang, A. Reis, A. Seifert, T. Philippi, S. Ernst, M. Jia, W. R. Thiel, *Dalton Trans*. **2009**, 3315.

85. S. Shylesh, M. Jia, A. Seifert, S. Adappa, S. Ernst, W. R. Thiel, *New J. Chem*. **2009**, *33*, 717.

86. S. Shylesh, J. Schweitzer, S. Demeshko, V. Schnemann, S. Ernst, W. R. Thiel, *Adv. Synth. Catal*. **2009**, *351*, 1789.

87. S. Shylesh, L. Wang, W. R. Thiel, *Adv. Synth. Catal*. **2010**, *352*, 425.

88. S. Shylesh, V. Schnemann, W. R. Thiel, *Angew. Chem.* **2010**, *122*, 3504; *Angew. Chem. Int. Ed*. **2010**, *49*, 3428.

89. J. Tang, L. Wang, G. Liu, Y. Liu, Y. Hou, W. Zhang, M. Jia, W. R. Thiel, *J. Mol. Catal. A-Chem*. **2009**, *313*, 31.

90. Y. Sun, A. Hienzsch, J. Grasser, E. Herdtweck, W. R. Thiel, *J. Organomet. Chem.* **2006**, *691*, 291.

91. D. Dehe, *Dissersion,* Kaiserslautern, **2012**.

References

92. A. K. Pleier, H. Glas, M. Grosche, P. Sirsch, W. R. Thiel, *Synthesis*, **2001**, *1*, 55.

93. J. G. Cordaro, J. K. McCusker, R. G. Bergman, *Chem. Commun.*, **2002**, 1496.

94. D. Benito-Garagorri, V. Bocokic, K. Mereiter, K. Kirchner, *Organometallics*. **2006**, *25*, 3817.

95 A. Bollmann, K. Blann, J. T. Dixon, F. M. Hess, E. Killian, H. Maumela, D. S. McGuinness, D. H. Morgan, A. Neveling, S. Otto, M. Overett, A. M. Z. Slawin, P. Wasserscheid,S. Kuhlmann. *J. Am. Chem. Soc.* 2004, *126*, 14712

96. L. Taghizadeh G.; Dissertation, Technische Universität Kaiserslautern, **2012**.

97. S. Kealey, N. J. Long, P. W. Miller, A. J. P. White, P. B. Hitchcock, A. Gee*a, Dalton Trans.* **2007**, 2823.

98. T. Iwata, Y. Miyake, Y. Nishibayashi, S. Uemura, *J. Chem. Soc.*, *Perkin Tran* **2002**, *1*, 1548.

99. S. M. Nobre, A. L. Monteiro, *Journal of Molecular Catalysis A* **2009**, *13*, 65.

100. J. Flapper, P. W. N. M. van Leeuwen, C. J. Elsevier, P. C. J. Kamer, *Organometallics* **2009**, *28*, 1180.

101. P. A. Aguirre, C. A. Lagos,S. A. Moya,C. Zuniga, C. Vera-Oyarce, E. Sola, G. Peris, J. C.Bayon, *Dalton Trans* **2007**, 5419.

102. F. Speiser, P. Braunstein, *Organometallics* **204**, *23*, 2625.

103. P. Koovsky, S. Vyskocil, I. Cisarova, J. Sejbal, I. Tislerova, M. Smrina, G. C. Lloyd-Jones, S. C. Stephen, C. P. Butts, M. Murray, V. Langer, *J. Am. Chem. Soc*. **1999**, *121*, 7714.

104. J. W. Faller, N. Sarantopoulos, *Organometallics* **2004**, *23*, 2008.

105. U. Christmann, D. A. Pantazis, J. Benet-Buchholz, J. E. McGrady, F. Maseras, R. Vilar, *J. Am. Chem. Soc.* **2006**, *128*, 6376.

106. R. Pratap, D. Parrish, P. Gunda, D. Venkataraman, M. K. Lakshman, *J. Am. Chem. Soc.* **2009**, *131*, 12240.

References

107. C. J. Moulton, B. L. Shaw, *J. Chem. Soc., Dalton Trans*. **1976**, 1020.

108. J.-F. Gong, Y.-H. Zhang, M.-P. Song, C.Xu, *Organometallics* **2007**, *26*, 6487.

109. Y. Motoyama, K. Shimozono, H. Nishiyama, *Inorg. Chim. Acta* **2006**, *359*, 1725.

110. B. Ines, R. SanMartin, Fa Churruca, E. Dominguez, M. K. Urtiaga, M. I. Arriortua, *Organometallics* **2008**, *27*, 2833.

111. P. Wehman, R. E. Rülke, V. E. Kaasjager, P. C. J. Kamer, H. Kooijman, A. L. Spek, C. J. Elsevier, K. Vrieze, P. W. N. M. van Leeuwen, *J. Chem. Soc., Chem. Commun*. **1995**, 331.

112. R. E. Rülke, V. E. Kaasjager, P. Wehman, C. J. Elsevier, P. W. N. M. van Leeuwen, K. Vrieze, J. Faanje, K. Goubitz, A. L. Spek, *Organometallics* **1996**, *15*, 3022.

113. A. Del Zotto, E. Zangrando, W. Baratta, A. Felluga, P. Martinuzzi, P. Rigo, *Eur. J. Inorg. Chem*. **2005**, 4707.

114. E. Balaraman, B. Gnanaprakasam, L. J. W. Shimon, D. Milstein, *J. Am. Chem. Soc*. **2010**, *132*, 16756.

115. C. Gunanathan, Y. Ben-David, D. Milstein, *Science* **2007**, *317*, 790.

116. J. Zhang, G. Leitus, Y. Ben-David, D. Milstein, *Angew. Chem.*, **2006**, *118*, 1131; *Angew. Chem., Int. Ed.* **2006**, *45*, 1113.

117. J. Zhang, G. Leitus, Y. Ben-David, D. Milstein, *J. Am. Chem. Soc.* **2005**, *127*, 10840.

118. E. Balaraman, C. Gunanathan, J. Zhang, L. J. W Shimon, D. Milstein, *Nature, Chem*. **2011**, *3*, 609.

119. B. Zhang, C. Wang, J. F. Gong, M. P. Song, *Journal of Organometallic Chemistry* **2009**, *694*, 2555.

120. T. Kimura, Y. Uozumi, *Organometallics* **2006**, *25*, 4883.

121. D. Morales-Morales, C. Grause, K. Kasaoka, R. Redon, R. E. Cramer, C. M. Jensen, *Inorg.*

Chim. Acta **2000**, *300-302*, 958.

References

122. R. B. Bedford, S. M. Draper, P. N. Scully, S. L. Welch, *New J. Chem.* **2000**, *24*, 745.

123. R. A. Begum, D. Powell, K. Bowman-James, *Inorganic Chemistry* **2006**, *45*, 964.

124. J. A. Loch, M. Albrecht, E. Peris, J. Mata, J. W. Faller, R. H. Crabtree, *Organometallics* **2002**, *21*, 700.

125. D. A. Burrows, M. F. Mahon, M. Varrone, *J. Chem. Soc., Dalton Trans.* **2003**, 4718.

126. S. M. Aucott, A. M. Z. Slawin, J. D. Woollins, *J. Chem. Soc., Dalton Trans.* **2000**, 2559.

127. T. G. Appleton, H. C. Clark, L. E. Manzer, *Coord. Chem. Rev.* **1973**, *10*, 335.

128. X.-F. Wu, P. Anbarasan, H. Neumann, M. Beller, *Angew. Chem.*, **2010**, *122*, 9231; *Angew. Chem. Int. Ed.* **2010**, *49*, 9047.

129. R. F. Heck, *Acc. Chem. Res.* **1979**, *12*, 146.

130. I. P. Beletskaya, A. V. Cheprakov, *Chem. Rev.* **2000**, *100*, 3009.

131. E. Negishi, C. Copéret, S. Ma, S.-Y. Liou, F. Liu, *Chem. Rev.***1996**, *96*, 365.

132. E. Negishi, A. O. King, N. Okukado, *J. Org. Chem.* **1977**, *42*, 1821.

133. E. Negishi, *Acc. Chem. Res.* **1982**, *15*, 340.

134. E. Negishi, L. Anastasia, *Chem. Rev.* **2003**, *103*, 1979.

135. N. Miyaura, K. Yamada, A. Suzuki, *Tetrahedron Lett.* **1979**, *20*, 3437.

136. N. Miyaura, A. Suzuki, *J. Chem. Soc., Chem.Commun.* **1979**, 866.

137. S. Kotha, K. Lahiri, D. Kashinath, *Tetrahedron* **2002**, *58*, 9633.

138. K. C. Nicolaou, J. M. Ramanjulu, S. Natarajan, S. Bräse, H. Li, C. N. C. Boddy, F. Rübsam, *Chem. Commun.* **1997**, 1899.

139. A. Markham, K. L. Goa, *Drugs* **1997**, *54*, 299.

140. R. Capdeville, E. Buchdunger, J. Zimmermann, A. Matter, *Nat. Rev. Drug Discovery* **2002**, *1*, 493.

141. J. Boren, M. Cascante, S. Marin, B. Comin-Anduix, J. J. Centelles, S. Lim, S. Bassilian,

References

S. Ahmed, W. N. Lee, L. G. Boros, *J. Biol. Chem.* **2001**, *276*, 37747.

142. M. F. Lipton, M. A. Mauragis, M. T. Maloney, M. F. Veley, D. W. VanderBor, J. J. Newby, R. B. Appell, E. D. Daugs, *Org. Process Res. Dev.* **2003**, *7*, 385.

143. S. Kaye, J. M. Fox, F. A. Hicks, S. L. Buchwald,. *Adv. Synth. Catal.* **2001**, *343*, 789.

144. H. Tomori, J. M. Fox, S. L. Buchwald, *J. Org. Chem.* **2000**, *65*, 5334.

145. M. Kertesz, C. H. Choi, S. Yang, *Chem. Rev.***2005**, *105*, 3448.

146. S. Lightowler, M. Hird, *Chem. Mater.* **2005**, *17*, 5538.

147. A. A. C. Braga, N. H. Morgon, G. Ujaque, F. Maseras, *J. Am. Chem. Soc.* **2005**, *127*, 9298.

148. N. Miyaura, *J. Organomet. Chem.* **2002**, *653*, 54.

149. R. Martin, S. L. Buchwald, *Acc. Chem. Res.* **2008**, 41, 1461.

150. A. F. Littke, G. C. Fu, *Angew. Chem.*, **2002**, *114*, 4350; *Angew. Chem. Int. Ed.* **2002**, *41*, 4176.

151. A. Zapf, R. Jackstell, F. Rataboul, T. Riermeier, A. Monsees, C. Fuhrmann, N. Shaikh, U. Dingerdissen, M. Beller, *Chem. Commun.* **2004**, 38.

152. A. Zapf, A. Ehrentraut, M. Beller, *Angew. Chem.* **2000**, *112*, 4315; *Angew. Chem. Int. Ed.* **2000**, *39*, 4153.

153. R. B. Bedford, C. S. J. Cazin, S. L. Hazelwood, *Angew. Chem.*, **2002**, *114*, 4294; *Angew. Chem.Int. Ed.* **2002**, *41*, 4120.

154. R. B. Bedford, S. L. Hazelwood, M. E. Limmert, *Chem. Commun.* **2002**, 2610.

155. R. B. Bedford, S. L. Hazelwood, M. E. Limmert, D. A. Albisson, S. M. Draper, P. N. Scully, S. J. Coles, M. B. Hursthouse, *Chem. Eur. J.* **2003**, *9*, 3216.

156. B. Karimi, P. F. Akhavan, *Chem. Commun.* **2009**, 3750.

157. J. Yin, M. P. Rainka, X.-X. Zhang, S. L. Buchwald, *J. Am.Chem. Soc.* **2002**, *124*, 1162.

158. G. Altenhoff, R. Goddard, C. W. Lehmann, F. Glorius, *J. Am. Chem. Soc.* **2004**,

References

126,15195.

159. A. Schmidt, A. Rahimi, *Chem. Commun.* **2010**, *46*, 2995.

160. M. J. Burns, I. J. S. Fairlamb, A. R. Kapdi, P. Sehnal, R. J. K. Taylor, *Org. Lett*. **2007**, *9*, 539.

161. A. T. Lindhardt, M. L. H. Mantel, T. Skrydstrup, *Angew. Chem.*, **2008**, *120*, 2708; *Angew. Chem. Int. Ed.* **2008**, *47*, 2668.

162. A. S. Guram, X. Wang, E. E. Bunel, M. M. Faul, R. D. Larsen, M. J. Martinelli, *J. Org. Chem.* **2007**, *72*, 5104.

163. K. Billingsley, S. L. Buchwald, *J. Am. Chem. Soc*. **2007**, *129*, 3358.

164. C. A. Fleckenstein, H. Plenio, *Green Chem.* **2007**, *9*, 1287.

165. B. H. Lipshutz, B. R. Taft, *Org. Lett*. **2008**, *10*, 1329.

166. A. F. Littke, C Dai, G. C. Fu, *J. Am. Chem. Soc.* **2000**, *122*, 4020.

167. Q. Dai, W. Gao, D. Liu, L. M. Kapes, X. Zhang, *J. Org. Chem.* **2006**, *71*, 3928.

168. C. Zhang, J. Huang, M. L. Trudell, S. P. Nolan, *J. Org. Chem.* **1999**, 64, 3804.

169. A. C. Hillier, G. A. Grasa, M. S. Viciu, H. M. Lee, C. Yang, S. P. Nolan, *J. Organomet. Chem.* **2002**, 69.

170. G. A Grasa, M. S. Viciu, J. Huang, C. Zhang, M. L. Trudell, S. P. Nolan, *Organometallics* **2002**, *21*, 2866.

171. O. Navarro, R. A. Kelly, S. P. Nolan, *J. Am. Chem. Soc.* **2003**, *125*, 16194.

172. N. Marion, O. Navarro, J. Mei, E. D. Stevens, N. M. Scott, S. P. Nolan, *J. Am. Chem. Soc*. **2006**, *128*, 4101.

173. O. Diebolt, P. Braunstein, S. P. Nolan, C. S. Cazin, *J. Chem. Commun.* **2008**, 3190.

174. B. Crociani, S. Antonaroli, A. Marini, U. Matteoli, A. Scrivanti, *Dalton Trans.* **2006**, 2698.

175. S. Doherty, J. G. Knight, T. H. Scanlan, M. R. J. Elsegood, W. Clegg, *J. Organometal.*

194

Chem. **2002**, *650*, 231.

176. A. Scrivanti, V. Beghetto, U. Matteoli, S. Antonaroli, A. Marini, F. Mandoj, R. Paolesseb, B. Crocianib, *Tetrahedron Lett.* **2004**, *45*, 5861.

177. Z. Weng, S. Teo, L. Lin Koh, T. S. A. Hor, *Organometallics* **2004**, *23,* 4342.

178. A. Scrivanti, V. Beghetto, U. Matteoli, S. Antonaroli, A. Marinib, B. Crocianib, *Tetrahedron* **2005**, *61*, 975.

179. K. L. Billingsley, K. W. Anderson, S. L. Buchwald, *Angew. Chem.*, **2006**, *118*, 3564; *Angew. Chem. Int. Ed.* **2006**, *45*, 3484.

180. S. D. Walker, T. E. Barder, J. R. Martinelli, S. L. Buchwald, *Angew. Chem.*, **2006**, *116*, 1907; *Angew. Chem. Int. Ed.* **2004**, *43*, 1871.

181. H.Weissman, L. J. W. Shimon, D. Milstein, *Organometallics* **2004**, *23,* 3931.

182. C. C. Ho, S. Chatterjee, T. L. Wu, K. T. Chan, Y. W. Chang, T. H. Hsiao, H. M. Lee, *Organometallics* **2009**, *28,* 2837.

183. Z. Weng, S. Teo, T. S. A. Hor, *Acc. Chem. Res.* **2007**, *40*, 676.

184. C. Amatore, A. Jutand, *Acc. Chem. Res*. **2000**, *33*, 314.

185. C. Baleizão, A. Corma, H. Garcia, A. Leyva, *Chem. Commun.* **2003**, 606.

186. R. B. Bedford, C. S. J. Cazin, M. B. Hursthouse, M. E. Light, K. J. Pike, S. Wimperis, *J. Organomet. Chem.* **2001**, *633*, 173.

187. E. B. Mubofu, J. H. Clark, D. J. Macquarrie, *Green Chem.* **2001**, *3*, 23.

188. S. Paul, J. H. Clark, *Green Chem.* **2003**, *5*, 635.

189. J. Horniakova, T. Raja, Y. Kubota, Y. Sugi, *J. Mol. Catal. A-Chem.* **2004**, *217*, 73.

190. O. Vassylyev, J. Chen, A. P. Panarello, J. G. Khinast, *Tetrahedron Lett*. **2005**, *46*, 6865.

191. M. Trilla, R. Pleixats, M. Wong Chi Man, C. Bied, J. J. E. Moreau, *Tetrahedron Lett*. **2006**, *47*, 2399.

192. M. Trilla, R. Pleixats, M. Wong Chi Man, C. Bied, J. J. E. Moreau, *Adv. Synth. Catal*.

References

2008, *350*, 577.

193. S. Paul, J. H. Clark, *J. Mol. Catal. A-Chem.* **2004**, *215*, 107.

194. L. Dong-Hwan,C. Minkee, Y. Byung-Woo, R. Ryong, T. Abu, H. Shahin, J. Myung-Jong , *Adv. Synth. Catal.* **2009**, *351*, 2912.

195. M. Michau, M. Barboiu, R. Caraballo, C. Arnal-H_rault, P. Periat, A. van der Lee, A. Pasc, *Chem. Eur. J.* **2008**, *14*, 1776.

196. M. Michau, R. Caraballo, C. Arnal-H_rault, M. Barboiu, *J. Membr. Sci.* **2008**, *321*, 22.

197. L. Zhonghua,T. Demei, Z. Chuanfang, *Phosphorus, Sulfur, and Silicon and the Related Elements*, **2000**, *165*, 99.

198. P. Ferreira, I. S. Gonçalves, F. E. Kühn, A. D. Lopes, M. A. Martins, M. Pillinger, A. Pina, J. Rocha, C. C. Romão, A. M. Santos, T. M. Santos, A. A. Valente, *Eur. J. Inorg. Chem.* **2000**, 2263.

199. K. Albert, E. Bayer, *J. Chromatogr.* **1991**, *544*, 345.

200. S. Farsadpour, L. Taghizadeh Ghoochany, Y. Sun, W. R. Thiel, *Eur. J. Inorg. Chem.* **2011**, 4603.

201. Z. Zhou, A. W. Franz, S. Bay, B. Sarkar, A. Seifert, P. Yang, A. Wagener, S. Ernst, M. Pagels, T. J. J. Müller, W. R. Thiel, *Chem. Asian J.* **2010**, *5*, 2001.

202. A. Fidalgo, L. Ilharco, *Chem. Eur. J.* **2004**, *10*, 392.

203. E. Geidel, H. Lechert, J. Dçbler, H. Jobic, G. Calzaferri, F. Bauer, *Microporous Mesoporous Mater.* **2003**, *65*, 31.

204. D. E. De Vos, M. Dams, B. Sels, P. A. Jacobs, *Chem. Rev.* **2002**, *102*, 3615.

205. B. Marler, U. Oberhagemann, S. Vortmann, H. Gies, *Microporous Mater.* **1996**, *6*, 375.

206. S. Jana, B. Dutta, R. Bera, S. Koner, *Langmuir* **2007**, *23*, 2492.

207. H. Yang, G. Zhang, X. Honga, Y. Zhua, *J. Mol. Catal. A Chem.* **2004**, *210*, 143.

208. K. S. W. Sing, D. H. Everett, R. A. W. Haul, L. Mouscou, R. A. Pierotti, J. Rouquerol, T.

References

Siemieniewska, *Pure Appl. Chem*. **1985**, *57*, 603.

209. V. Polshettiwar, C. Len, A. Fihri, *Coord. Chem. Rev*. **2009**, *253*, 2599.

210. A. M. Trzeciak, J. J. Ziółkowski, *Coord. Chem. Rev*. **2007**, *251*, 1281.

211. L. Yin, J. Liebscher, *Chem. Rev*. **2007**, *107*, 133.

212. N. T. S. Phan, M. V. D. Sluys, C. W. Jones, *Adv. Synth. Catal*. **2006**, *348*, 609.

213. J. G. J. de Vries, *J. Chem. Soc. Dalton Trans*. **2006**, 421.

214. A. Biffis, M. Zecca, M. Basato, *J. Mol. Catal. A-Chem*. **2001**, *173*, 249.

215. K. Kçhler, R. G. Heidenreich, J. G. E. Krauter, M. Pietsch, *Chem. Eur. J*. **2002**, *8*, 622.

216. T. Noel, S. L. Buchwald, *Chem. Soc. Rev*. **2011**, *40*, 5010. And references cited therein.

217. *Arbeitsmethoden in der Organischen Chemie*; Hünig, S.; Kreitmeier, P.; Märkl, G.; Sauer, J. LOB-Lehmanns, Berlin, **2008**.

218. F. Wang, A. W. Schwabacher, *Tetrahedron Lett.* **1999**, *40*, 4779.

Index

7. Index

7.1. Crystal Structure Data

7.1.1. Crystal Data and Structure Refinement for 4a.

Empirical formula	$C_{22}H_{18}N_3P$
Formula weight	355.36
Crystal colour and habit	colorless prism
Crystal size (mm)	0.28 x 0.18 x 0.16
Temperature (K)	150(2)
Wavelength (Å)	1.54184
Crystal system	Triclinic
Space group	P-1

Unit cell dimensions
$a = 7.6009(2)$ Å $\quad \alpha = 89.235(2)^o$
$b = 7.8075(3)$ Å $\quad \beta = 89.139(2)^o$
$c = 48.9141(10)$ Å $\quad \gamma = 69.160(3)^o$

Volume (Å^3)	2712.45(14)
Z	6
Calculated density (Mg/m^3)	1.305
Absorption coefficient (mm^{-1})	1.413
F(000)	1116
θ-range for data collection (^{o})	3.62/62.61
Index ranges	$-8 \le h \le 7, -8 \le k \le 8, -55 \le l \le 56$
Reflections collected	24323
Independent reflections	8464 ($R_{int} = 0.0209$)
Completeness to $\theta = 62.61^o$	98.0 %
Absorption correction	Semi-empirical from equivalents (Multiscan)
Max. and min. transmission	1.00000 and 0.87933
Refinement method	Full-matrix least-squares on F^2
Data/restraints/parameters	8464/342/831
Goodness-of-fit on F^2	1.066
Final R indices [$I>2\sigma(I)$]	$R_1 = 0.0341, wR_2 = 0.0922$
R indices (all data)	$R_1 = 0.0386, wR_2 = 0.0943$
Largest diff. Peak and hole (e·Å^{-3})	0.258/–0.648

Definitions:

$$R_1 = \frac{\sum \left\| F_o \right| - \left| F_c \right\|}{\sum \left| F_o \right|} \qquad wR_2 = \sqrt{\frac{\sum \left[w \left(F_o^2 - F_c^2 \right)^2 \right]}{\sum \left[w \left(F_o^2 \right)^2 \right]}}$$

$$GooF = \sqrt{\frac{\sum \left[w \left(F_o^2 - F_c^2 \right) \right]}{(n - p)}} \qquad \text{n = number of reflections; p = number of parameters}$$

Index

Notes on the refinement of 4a.

The hydrogen atoms, which are bound to the nitrogen atoms N3, N6, and N9, were located in the difference Fourier synthesis, and were refined semi-freely with the help of a distance restraint, while constraining their *U*-values to 1.2 times the *U(eq)* values of corresponding nitrogen atoms. All the other hydrogen atoms were placed in calculated positions and refined by using a riding model. For this crystal structure, an asymmetric unit consists of 3 independent target molecules, one of which was disorderd in the two unsubstituted phenyl- rings.

7.1.2. Crystal Data and Structure Refinement for 4f.

Empirical formula	$C_{27}H_{26}N_3P$
Formula weight	423.48
Crystal colour and habit	colorless prism
Crystal size (mm)	0.25 x 0.21 x 0.18
Temperature (K)	150(2)
Wavelength (Å)	1.54184
Crystal system	Monoclinic
Space group	$P2_1/n$
Unit cell dimensions	$a = 10.7084(2)$ Å $\quad \alpha = 90^o$
	$b = 8.8315(1)$ Å $\quad \beta = 90.199(2)^o$
	$c = 23.3496(4)$ Å $\quad \gamma = 90^o$
Volume (Å^3)	2208.19(6)
Z	4
Calculated density (Mg/m^3)	1.274
Absorption coefficient (mm^{-1})	1.240
F(000)	896
θ-range for data collection (^{o})	3.79/62.72
Index ranges	$-8 \leq h \leq 12, -10 \leq k \leq 10, -26 \leq l \leq 24$
Reflections collected	14940
Independent reflections	3521 ($R_{int} = 0.0193$)
Completeness to $\theta = 62.72^o$	99.6 %
Absorption correction	Semi-empirical from equivalents (Multiscan)
Max. and min. transmission	1.00000 and 0.65611
Refinement method	Full-matrix least-squares on F^2
Data/restraints/parameters	3521/0/280
Goodness-of-fit on F^2	1.104
Final R indices [$I > 2\sigma(I)$]	$R_1 = 0.0336$, $wR_2 = 0.0877$
R indices (all data)	$R_1 = 0.0361$, $wR_2 = 0.0888$
Largest diff. peak and hole (e·Å^{-3})	0.320/–0.291

Index

Definitions:

$$R_1 = \frac{\sum \left\| F_o \right| - \left| F_c \right\|}{\sum |F_o|}$$

$$wR_2 = \sqrt{\frac{\sum \left[w \left(F_o^2 - F_c^2 \right)^2 \right]}{\sum \left[w \left(F_o^2 \right)^2 \right]}}$$

$$GooF = \sqrt{\frac{\sum \left[w \left(F_o^2 - F_c^2 \right) \right]}{(n - p)}}$$

n = number of reflections; p = number of parameters

Notes on the refinement of 4f.

All the hydrogen atoms were placed in calculated positions and refined by using a riding model.

7.1.3. Crystal data and structure refinement for 12a.

Identification code	11133o
Empirical formula	C22 H18 N3 P
Formula weight	355.36
Temperature	150(2) K
Wavelength	1.54184 Å
Crystal system	Monoclinic
Space group	P2$_1$/n
Unit cell dimensions	a = 11.7563(2) Å α= 90°.
	b = 7.7007(1) Å β= 100.178(2)°.
	c = 20.4757(3) Å γ= 90°.
Volume	1824.53(5) Å^3
Z	4
Density (calculated)	1.294 Mg/m^3
Absorption coefficient	1.401 mm^{-1}
F(000)	744
Crystal colour and habit	Colorless prism
Crystal size	0.17 x 0.07 x 0.07 mm^3
Theta range for data collection	4.06 to 62.57°.
Index ranges	–13<=h<=13, –8<=k<=7, –22<=l<=23
Reflections collected	11312
Independent reflections	2914 [R(int) = 0.0219]
Completeness to theta = 62.57°	99.9 %
Absorption correction	Semi-empirical from equivalents (Multiscan)
Max. and min. transmission	1.00000 and 0.31289
Refinement method	Full-matrix least-squares on F^2
Data / restraints / parameters	2914 / 1 / 238
Goodness-of-fit on F^2	1.095

Index

Definitions:

$$R_1 = \frac{\sum \left\| F_o \right| - \left| F_c \right\|}{\sum \left| F_o \right|}$$

$$wR_2 = \sqrt{\frac{\sum \left[w \left(F_o^2 - F_c^2 \right)^2 \right]}{\sum \left[w \left(F_o^2 \right)^2 \right]}}$$

$$GooF = \sqrt{\frac{\sum \left[w \left(F_o^2 - F_c^2 \right) \right]}{(n - p)}}$$

n = number of reflections; p = number of parameters

Notes on the refinement of 12a.

The hydrogen atom H3N, which is bound to the nitrogen atom N3, was located in the difference Fourier synthesis, and was refined semi-freely with the help of a distance restraint, while constraining their *U*-values to 1.2 times the *U(eq)* value of N3. All the other hydrogen atoms were placed in calculated positions and refined by using a riding model.

7.1.4. Crystal Data and Structure Refinement for 14a.

Empirical formula	$C_{22}H_{18}Cl_2N_3PPd$	
Formula weight	532.66	
Crystal colour and habit	yellow prism	
Crystal size (mm)	0.22 x 0.09 x 0.09	
Temperature (K)	150(2)	
Wavelength (Å)	1.54184	
Crystal system	Monoclinic	
Space group	P2$_1$/n	
Unit cell dimensions	a = 10.37080(10) Å	α= 90°
	b = 14.7430(2) Å	β= 90.4240(10)^o
	c = 13.7009(2) Å	γ= 90°
Volume (Å^3)	2094.77(5)	
Z	4	
Calculated density (Mg/m^3)	1.689	
Absorption coefficient (mm^{-1})	10.325	
F(000)	1064	
θ-range for data collection (^{o})	4.41/62.60	
Index ranges	$-11 \leq h \leq 11, -16 \leq k \leq 16, -15 \leq l \leq 15$	
Reflections collected	14832	

Index

Independent reflections   3342 (R_{int} = 0.0244)
Completeness to θ= 62.60°   99.9 %
Absorption correction   Semi-empirical from equivalents (Multiscan)
Max. and min. transmission   1.00000 and 0.25249
Refinement method   Full-matrix least-squares on F^2
Data/restraints/parameters   3342/2/268
Goodness-of-fit on F^2 1.076
Final R indices [$I>2\sigma(I)$] R_1 = 0.0215, wR_2 = 0.0558
R indices (all data) R_1 = 0.0232, wR_2 = 0.0565
Largest diff. peak and hole (e·Å^{-3})   0.536/–0.459

Definitions:

$$R_1 = \frac{\sum \left\| F_o \right| - \left| F_c \right\|}{\sum \left| F_o \right|}$$

$$wR_2 = \sqrt{\frac{\sum \left[w \left(F_o^2 - F_c^2 \right)^2 \right]}{\sum \left[w \left(F_o^2 \right)^2 \right]}}$$

$$GooF = \sqrt{\frac{\sum \left[w \left(F_o^2 - F_c^2 \right) \right]}{(n-p)}}$$

n = number of reflections; p = number of parameters

Notes on the refinement of 14a.

The hydrogen atoms H3A and H3B, which are bound to the nitrogen atom N3, were located in the difference Fourier synthesis, and were refined semi-freely with the help of a distance restraint, while constraining their U-values to 1.2 times the $U(eq)$ value of N3. All the hydrogen atoms were placed in calculated positions and refined by using a riding model.

7.1.5. Crystal Data and Structure Refinement for 15a.

Identification code   1136o
Empirical formula   C24 H22 Cl2 N3 P Pd
Formula weight   560.72
Temperature   150(2) K
Wavelength   1.54184 Å
Crystal system   Monoclinic
Space group   P2$_1$/n
Unit cell dimensions   a = 9.6797(1) Å α= 90°.
                                     b = 16.7909(2) Å β= 95.074(1)°.
                                     c = 16.9032(3) Å γ= 90°.
Volume   2736.53(6) Å^3

Index

Z	4
Density (calculated)	1.361 Mg/m^3
Absorption coefficient	7.930 mm^{-1}
F(000)	1128
Crystal colour and habit	yellow block
Crystal size	$0.10 \times 0.04 \times 0.03$ mm^3
Theta range for data collection	3.72 to $62.62°$.
Index ranges	$-11 <= h <= 11$, $-19 <= k <= 17$, $-19 <= l <= 17$
Reflections collected	20197
Independent reflections	4376 [R(int) = 0.0692]
Completeness to theta = $62.62°$	99.7 %
Absorption correction	Semi-empirical from equivalents (Multiscan)
Max. and min. transmission	1.00000 and 0.43126
Refinement method	Full-matrix least-squares on F^2
Data / restraints / parameters	4376 / 1 / 285
Goodness-of-fit on F^2	0.969
Final R indices [I>2sigma(I)]	R1 = 0.0330, wR2 = 0.0870
R indices (all data)	R1 = 0.0388, wR2 = 0.0887
Largest diff. peak and hole	0.446 and -0.703 e.Å^{-3}

Definitions:

$$R_1 = \frac{\sum \left\| F_o \right| - \left| F_c \right\|}{\sum \left| F_o \right|}$$

$$wR_2 = \sqrt{\frac{\sum \left[w \left(F_o^2 - F_c^2 \right)^2 \right]}{\sum \left[w \left(F_o^2 \right)^2 \right]}}$$

$$GooF = \sqrt{\frac{\sum \left[w \left(F_o^2 - F_c^2 \right) \right]}{(n - p)}}$$

n = number of reflections; p = number of parameters

Notes on the refinement of 15a.

The hydrogen atom H2N, which is bound to the nitrogen atom N2, was located in the difference Fourier synthesis, and was refined semi-freely with the help of a distance restraint, while constraining its *U*-value to 1.2 times the *U(eq)* value of N2. All the other hydrogen atoms were placed in calculated positions and refined by using a riding model. Because of the existence of severely disordered solvents (probably the mixture of pentane, CH$_2$Cl$_2$ / CHCl$_3$ and / or H$_2$O), SQUEEZE process integrated in PLATON has been used. And the detailed information has also been posted in the final CIF file.

Index

Identification code	1166o
Empirical formula	C52 H48 N6 O4 P2 Pd2
Formula weight	1095.70
Temperature	150(2) K
Wavelength	1.54184 Å
Crystal system	Triclinic
Space group	P-1

Unit cell dimensions:
- $a = 13.3207(3)$ Å $\alpha = 80.516(3)°$.
- $b = 14.5212(5)$ Å $\beta = 81.728(2)°$.
- $c = 16.4279(6)$ Å $\gamma = 63.940(3)°$.

Volume	2806.43(17) Å^3
Z	2
Density (calculated)	1.297 Mg/m^3
Absorption coefficient	6.066 mm^{-1}
F(000)	1112
Crystal colour and habit	yellow prism
Crystal size	0.11 x 0.09 x 0.07 mm^3
Theta range for data collection	3.41 to 62.56°.
Index ranges	$-14 <= h <= 15, -16 <= k <= 14, -18 <= l <= 18$
Reflections collected	20071
Independent reflections	8924 [R(int) = 0.0208]
Completeness to theta = 62.56°	99.5 %
Absorption correction	Semi-empirical from equivalents (Multiscan)
Max. and min. transmission	1.00000 and 0.29435
Refinement method	Full-matrix least-squares on F^2
Data / restraints / parameters	8924 / 0 / 601
Goodness-of-fit on F^2	1.014
Final R indices [I>2sigma(I)]	R1 = 0.0242, wR2 = 0.0613
R indices (all data)	R1 = 0.0281, wR2 = 0.0622
Largest diff. peak and hole	0.540 and –0.602 e.Å^{-3}

Definitions:

$$R_1 = \frac{\sum \left\| F_o \right| - \left| F_c \right\|}{\sum \left| F_o \right|}$$

$$wR_2 = \sqrt{\frac{\sum \left[w \left(F_o^2 - F_c^2 \right)^2 \right]}{\sum \left[w \left(F_o^2 \right)^2 \right]}}$$

$$GooF = \sqrt{\frac{\sum \left[w \left(F_o^2 - F_c^2 \right) \right]}{(n - p)}}$$

n = number of reflections; p = number of parameters

Notes on the refinement of 16.

Because of the existence of strongly disordered EtOH, H_2O and CH_2Cl_2 / $CHCl_3$, the

Index

SQUEEZE process integrated in PLATON was applied. The detailed information has been posted in the final CIF file. All hydrogen atoms were placed in calculated positions and refined by using a riding model.

7.1.7. Crystal Data and Structure Refinement for 17.

Empirical formula	$C_{50}H_{46}Cl_8N_6P_2Pd$
Formula weight	1182.87
Crystal colour and habit	yellow prism
Crystal size (mm)	0.18 x 0.11 x 0.08
Temperature (K)	150(2)
Wavelength (Å)	1.54184
Crystal system	Triclinic
Space group	P-1
Unit cell dimensions	$a = 10.2077(4)$ Å $\alpha = 111.122(4)^o$
	$b = 11.6068(5)$ Å $\beta = 103.279(3)^o$
	$c = 12.9606(5)$ Å $\gamma = 104.884(4)^o$
Volume (Å^3)	1292.87(12)
Z	1
Calculated density (Mg/m^3)	1.519
Absorption coefficient (mm^{-1})	7.614
F(000)	600
θ-range for data collection (^{o})	3.92/62.70
Index ranges	$-11 \leq h \leq 11, -13 \leq k \leq 13, -14 \leq l \leq 13$
Reflections collected	12985
Independent reflections	4049 ($R_{int} = 0.0291$)
Completeness to $\theta = 62.70^o$	98.0 %
Absorption correction	Semi-empirical from equivalents (Multiscan)
Max. and min. transmission	1.00000 and 0.57353
Refinement method	Full-matrix least-squares on F^2
Data/restraints/parameters	4049/1/308
Goodness-of-fit on F^2	1.065
Final R indices [$I > 2\sigma(I)$]	$R_1 = 0.0382$, $wR_2 = 0.1061$
R indices (all data)	$R_1 = 0.0408$, $wR_2 = 0.1073$
Largest diff. Peak and hole (e·Å^{-3})	0.663/–0.994

Definitions:

$$R_1 = \frac{\sum \left\| F_o \right| - \left| F_c \right\|}{\sum \left| F_o \right|}$$

$$wR_2 = \sqrt{\frac{\sum \left[w \left(F_o^2 - F_c^2 \right)^2 \right]}{\sum \left[w \left(F_o^2 \right)^2 \right]}}$$

Index

$$GooF = \sqrt{\frac{\sum\left[w\left(F_o^2 - F_c^2\right)\right]}{(n-p)}}$$ n = number of reflections; p = number of parameters

Notes on the refinement of 17.

The hydrogen atom H3N, which is bound to the nitrogen atom N3, was located in the difference Fourier synthesis, and was refined semi-freely with the help of a distance restraint, while constraining its *U*-value to 1.2 times the *U(eq)* value of N3. All the other hydrogen atom positions were calculated in deal positions (riding model).

7.1.8. Crystal Data and Structure Refinement for 20.

Empirical formula	C23 H23 Cl F6 N4 O P2 Pd S
Formula weight	721.30
Temperature	150(2) K
Wavelength	0.71073 Å
Crystal system	Monoclinic
Space group	I 1 2/a 1
Unit cell dimensions	a = 14.9946(4) Å α= 90°.
	b = 10.4896(3) Å β= 93.488(3)°.
	c = 35.6091(12) Å γ= 90°.
Volume	5590.5(3) Å^3
Z	8
Density (calculated)	1.714 Mg/m^3
Absorption coefficient	1.014 mm^{-1}
F(000)	2880
Crystal size	0.37 x 0.32 x 0.16 mm^3
Theta range for data collection	2.89 to 30.00°.
Index ranges	$-14<=h<=21, -14<=k<=13, -49<=l<=50$
Reflections collected	28445
Independent reflections	8145 [R(int) = 0.0235]
Completeness to theta = 30.00°	99.8 %
Absorption correction	Semi-empirical from equivalents
Max. and min. transmission	0.8545 and 0.7053
Refinement method	Full-matrix least-squares on F^2
Data / restraints / parameters	8145 / 1 / 357

Index

Goodness-of-fit on F^2	1.046
Final R indices [I>2sigma(I)]	R1 = 0.0262, wR2 = 0.0603
R indices (all data)	R1 = 0.0354, wR2 = 0.0621
Largest diff. peak and hole	0.477 and –0.672 e.Å^{-3}

7.1.9. Crystal Data and Structure Refinement for 23.

Identification code	11261o
Empirical formula	C24 H24 Cl2 N3 O P Pd S
Formula weight	610.79
Temperature	150(2) K
Wavelength	1.54184 Å
Crystal system	Monoclinic
Space group	P2$_1$/c
Unit cell dimensions	a = 10.1518(2) Å $\quad$ α= 90°.
	b = 11.8304(2) Å $\quad$ β= 92.499(1)°.
	c = 21.8807(3) Å $\quad$ γ= 90°.
Volume	2625.37(8) Å^3
Z	4
Density (calculated)	1.545 Mg/m^3
Absorption coefficient	9.069 mm^{-1}
F(000)	1232
Crystal colour and habit	Yellow prism
Crystal size	0.14 x 0.12 x 0.11 mm^3
Theta range for data collection	4.04 to 62.63°.
Index ranges	–11<=h<=11, –10<=k<=13, –24<=l<=25
Reflections collected	17934
Independent reflections	4193 [R(int) = 0.0303]
Completeness to theta = 62.63°	99.8 %
Absorption correction	Semi-empirical from equivalents (Multiscan)
Max. and min. transmission	0.28771 and 1.00000
Refinement method	Full-matrix least-squares on F^2
Data / restraints / parameters	4193 / 0 / 304
Goodness-of-fit on F^2	1.079
Final R indices [I>2sigma(I)]	R1 = 0.0262, wR2 = 0.0680
R indices (all data)	R1 = 0.0275, wR2 = 0.0686
Largest diff. peak and hole	0.567 and –0.870 e.Å^{-3}

Definitions:

$$R_1 = \frac{\sum \left\| F_o \right| - \left| F_c \right\|}{\sum \left| F_o \right|} \qquad wR_2 = \sqrt{\frac{\sum \left[w \left(F_o^2 - F_c^2 \right)^2 \right]}{\sum \left[w \left(F_o^2 \right)^2 \right]}}$$

$$GooF = \sqrt{\frac{\sum\left[w\left(F_o^2 - F_c^2\right)\right]}{(n-p)}}$$ n = number of reflections; p = number of parameters

Notes on the refinement of 23.

The hydrogen atom H1N, which is bound to N1, was observed clearly in the difference Fourier synthesis, and then was allowed to be refined freely. All the other hydrogen atoms were placed in calculated positions and refined by using a riding model.

7.2. DFT Calculations

Quantum chemical calculations on the compounds **14a,d** and **15a,d** were performed with the program Gaussian03W [1] using the B3LYP gradient corrected exchange-correlation functional[2] in combination with the 6-31G* basis set [3] for C, H, N, P, Cl and the LANL2DZ (ECP) basis set for Pd.[4] Full geometry optimizations were carried out in *C*1 symmetry using analytical gradient techniques and the resulting structures were confirmed to be true minima by diagonalization of the analytical Hessian Matrix

1. Gaussian 03, Revision E.01, M. J. Frisch, G. W. Trucks, H. B. Schlegel, G. E. Scuseria, M. A. Robb, J. R. Cheeseman, J. A. Montgomery, Jr., T. Vreven, K. N. Kudin, J. C. Burant, J. M. Millam, S. S. Iyengar, J. Tomasi, V. Barone, B. Mennucci, M. Cossi, G. Scalmani, N. Rega, G. A. Petersson, H. Nakatsuji, M. Hada, M. Ehara, K. Toyota, R. Fukuda, J. Hasegawa, M. Ishida, T. Nakajima, Y. Honda, O. Kitao, H. Nakai, M. Klene, X. Li, J. E. Knox, H. P. Hratchian, J. B. Cross, V. Bakken, C. Adamo, J. Jaramillo, R. Gomperts, R. E. Stratmann, O. Yazyev, A. J. Austin, R. Cammi, C. Pomelli, J. W. Ochterski, P. Y. Ayala, K. Morokuma, G. A. Voth, P. Salvador, J. J. Dannenberg, V. G. Zakrzewski, S. Dapprich, A. D. Daniels, M. C. Strain, O. Farkas, D. K. Malick, A. D. Rabuck, K. Raghavachari, J. B. Foresman, J. V. Ortiz, Q. Cui, A. G. Baboul, S. Clifford, J. Cioslowski, B. B. Stefanov, G. Liu, A. Liashenko, P. Piskorz, I. Komaromi, R. L. Martin, D. J. Fox, T. Keith, M. A. Al-Laham, C. Y. Peng, A. Nanayakkara, M.
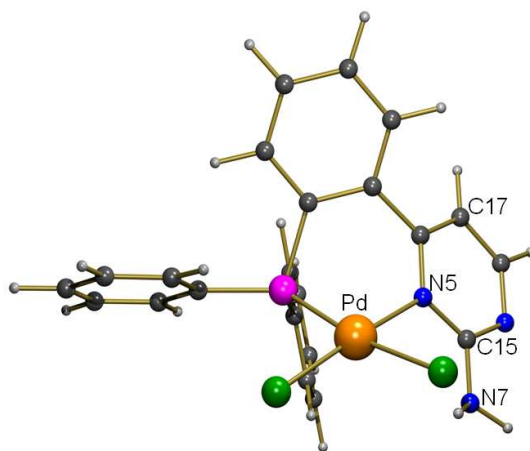
Index

Challacombe, P. M. W. Gill, B. Johnson, W. Chen, M. W. Wong, C. Gonzalez, and J. A. Pople, Gaussian, Inc., Wallingford CT, **2004**.

2. a) C. Lee, W. Yang, R. G. Parr, *Phys. Rev. B* **1988**, *37*, 785-789; b) A. D. Becke, *Phys. Rev.* **1988**, *A38*, 3098-3100; c) B. Miehlich, A. Savin, H. Stoll, H. Preuss, *Chem. Phys. Lett.* **1989**, *157*, 200-206.

3. a) P. C. Hariharan, J. A. Pople, *Theoret. Chim. Acta* **1973**, *28*, 213-222. b) M. M. Francl, W. J. Petro, W. J. Hehre, J. S. Binkley, M. S. Gordon, D. J. DeFrees, J. A. Pople, *J. Chem. Phys.* **1982**, *77*, 3654-3665.

4. P. J. Hay, W. R. Wadt, *J. Chem. Phys.* **1985**, *82*, 270-283.

Calculated structure of **14a**

SCF Done: E(RB+HF-LYP) =   -2402.03076158 A.U. after 1 cycles

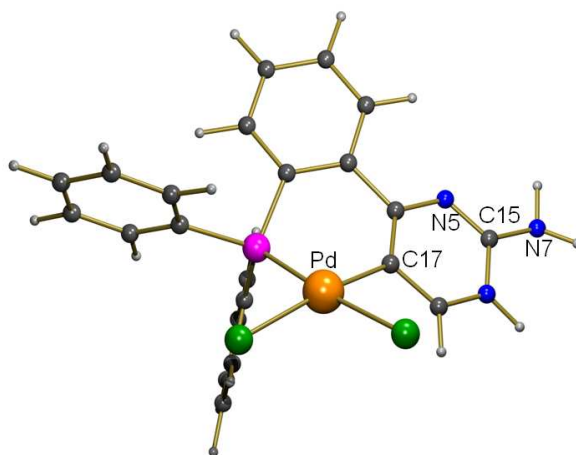Zero-point correction=   0.354271

(Hartree/Particle)

Thermal correction to Energy=   0.380744

Thermal correction to Enthalpy=   0.381689

Index

Thermal correction to Gibbs Free Energy=   0.295534

Sum of electronic and zero-point Energies=   -2401.676491

Sum of electronic and thermal Energies=   -2401.650017

Sum of electronic and thermal Enthalpies=   -2401.649073

Sum of electronic and thermal Free Energies=   -2401.735228

Dihedral angle C-N-Pd-Cl: 59.4°

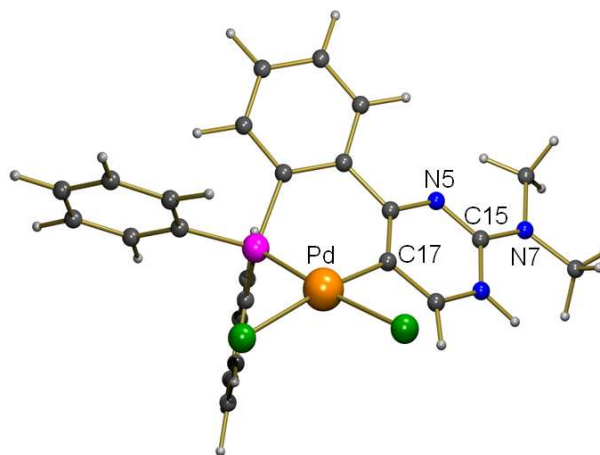Calculated structure of **14d**

SCF Done: E(RB+HF-LYP) =   -2401.98895871 A.U. after 9 cycles

Zero-point correction=   0.354011

(Hartree/Particle)

Thermal correction to Energy=   0.380951

Thermal correction to Enthalpy=   0.381895

Thermal correction to Gibbs Free Energy=   0.293409

Sum of electronic and zero-point Energies=   -2401.634948

Sum of electronic and thermal Energies=   -2401.608008

Sum of electronic and thermal Enthalpies=   -2401.607064

Index

Sum of electronic and thermal Free Energies=   -2401.695550

Dihedral angle C-C-Pd-Cl: 38.8°

Calculated structure of **15a**

SCF Done: E(RB+HF-LYP) =   -2480.62738325 A.U. after 1 cycles

Zero-point correction=   0.410779

(Hartree/Particle)

Thermal correction to Energy=   0.440480

Thermal correction to Enthalpy=   0.441425

Thermal correction to Gibbs Free Energy=   0.348030

Sum of electronic and zero-point Energies=   -2480.216604

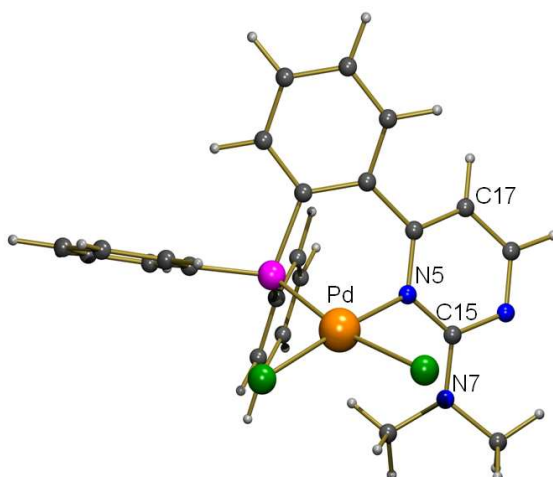Sum of electronic and thermal Energies=   -2480.186903

Sum of electronic and thermal Enthalpies=   -2480.185959

Sum of electronic and thermal Free Energies= -2480.279354

Dihedral angle C-N-Pd-Cl: 51.6°

Index

Calculated structure of **15d**

SCF Done: E(RB+HF-LYP) =   -2480.60610892 A.U. after 2 cycles

Zero-point correction=	0.410427
(Hartree/Particle)	
Thermal correction to Energy=	0.440662
Thermal correction to Enthalpy=	0.441606
Thermal correction to Gibbs Free Energy=	0.345388
Sum of electronic and zero-point Energies=	-2480.195682
Sum of electronic and thermal Energies=	-2480.165447
Sum of electronic and thermal Enthalpies=	-2480.164503
Sum of electronic and thermal Free Energies=	-2480.260721
Dihedral angle C-C-Pd-Cl:	37.0°

Calculated energies [Hartree/particle] of **14a**, **14d**, **15a** and **15d** and energy differences [Hartree/particle] resp. [kcal/mol] of (**14a-14d**) and (**15a-15d**); blue: electronic and

Index

thermal enthalpies, black: electronic and thermal free energies.
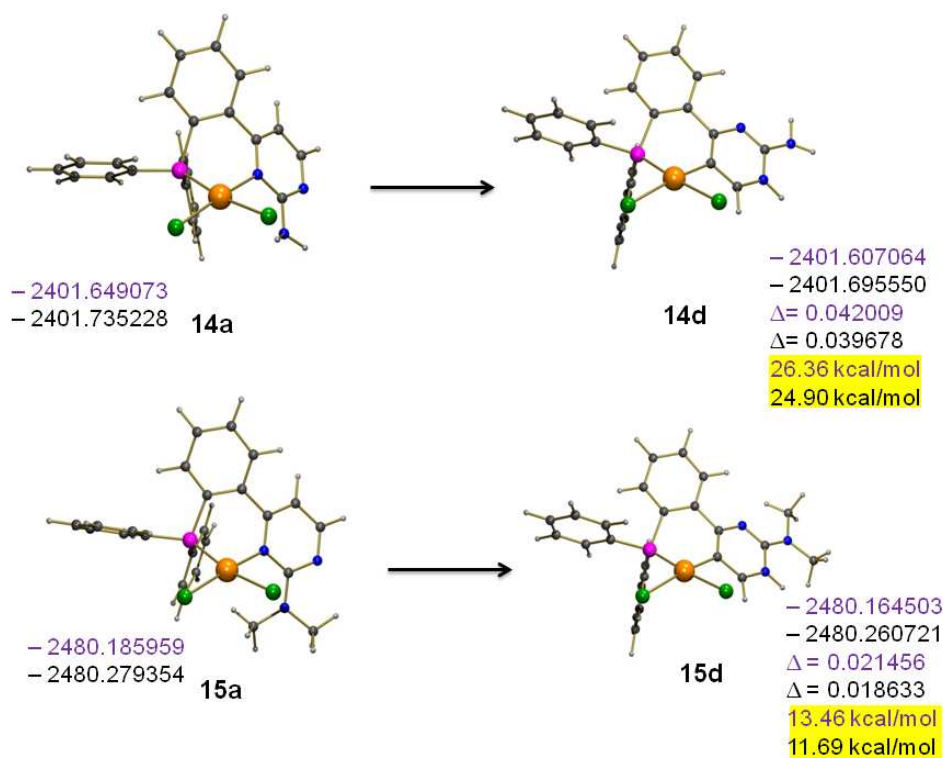
Calculated Mulliken and APT (*italics*) charges of selected atoms of compounds **14a**, **14d**, **15a** and **15d**; for the atom labeling see the figures shown above.

	14a	14d	15a	15d
Pd	–0.176	–0.201	–0.257	–0.203
	+0.437	*+0.216*	*+0.452*	*+0.228*
N5	–0.523	–0.437	–0.554	–0.471
	–0.480	*–0.795*	*–0.594*	*–0.902*
N7	–0.740	–0.750	–0.378	–0.413
	–0.695	*–0.862*	*–0.714*	*–1.000*
C15	+0.640	+0.632	+0.668	+0.695
	+0.715	*+01.041*	*+0.829*	*+1.149*
C17	–0.190	–0.047	–0.212	–0.046
	–0.470	*–0.283*	*–0.531*	*–0.275*

Index

7.3. Statutory Explanation

Hiermit bestatige ich, dass ich die vorliegende Arbeit gemäß der Promotionsordnung des Fachbereichs Chemie der Technischen Universitat Kaiserslautern selbststandig und nur unter Verwendung der angegebenen Quellen und Hilfsmittel angefertigt habe.

Kaiserslautern, August, 2012

Saeid Farsadpour

Index

Index

PERSONAL INFORMATION

Name: Saeid

Family Name: Farsadpour (Before: Nalchigar)

Nationality: Iranian

Years of Birth: July 4, 1979

Marital status: Married

EDUCATION

PhD Student at TU Kaiserslautern, August **2008** till now.

M.Sc. Inorganic Chemistry, Isfahan University of Technology **2004-2007**.

M.Sc. THESIS,

Synthesis, Characterization and Crystal Structure Determination of Novel Bispyridylamide Ligands and Binuclear Co(III), Cu(II) and Ni(II) Complexes with Deprotonated Ligands as Bulding Blocks for Supramolecular Architecture

B.S. Pure Chemistry, Azad University of Arak, Iran **2000-2004**.

PROFESSIONAL EXPERIENCE

Research Assistant, Chemistry Department, Technische Universität Kaiserslautern 2008 till now.

Synthesis of Zeolite 4A in a Pilot Plant Scale, *R&D* Department of Pars Zeolite Chemical Company, fall and winter **2007**.

Research Assistant, Chemistry Department, Isfahan University of Technology.

Assistant of Inorganic Laboratory, Fall **2005**, Spring **2006**, Fall **2006** in College of Chemistry, Isfahan University of Technology Iran.

Index

Assistant of Inorganic and Organic Laboratory, Fall **2006** and Spring **2007** in Department of Chemistry, Azad University of Arak.

Synthesis of Hydrofluoric Acid in a Larg Scale (1000 Liter per Week), Kimia Keshavarz Tehran Chemical Company, Spring and Summer **2004**.

PRESENTED PAPERS AND POSTERS

1. Intramolecular C-H Activation at an Aminopyrimidinyl Ligand: A Key to Enhanced Catalyst Activity, 8th Koordinationschemie-Treffen, Dortmund, Germany, Feb. **2012**.

2. Intramolecular C-H Activation at an Aminopyrimidinyl Ligand: A Key to Enhanced Catalyst Activity, Aachen, July, **2011**.

3. Novel Aminopyrimidinylphosphine Ligands and Their Application to the Palladium-Catalyzed Suzuki Reaction at Room Temperature, First EuCheMS Inorganic Chemistry Conference, Manchester, United Kingdom, Apr. **2011**.

4. Coordination Chemistry of Pyrimidinyl Functionalized Phosphine Ligands with Palladium(II), 7th Koordinationschemie-Treffen, Stuttgart, Germany, Feb. **2011**.

5. Coordination Chemistry of Pyrimidinyl Functionalized Phosphine Ligands towards Palladium(II) and Ruthenium(II), 9th Ferrocene Colloquium, Chemnitz, Germany, Feb. **2011**.

6. Novel Pyrimidylphosphine Palladium Complexes and their Application as Homogeneous and Heterogeneous Catalysts for Suzuki Cross Coupling Reactions
3rd EuCheMS Chemistry Congress, Nürnberg, Germany, Aug. **2010**.

7. Recovery Vanadium Pentaoxide (V_2O_5) From Residue and applications, 1st Chemistry Student Conference University of Tehran- Iran Feb. **2003**.

PUBLICATIONS

217

Index

1. Intramolecular C-H Activation at a Ruthenium(II) Complex: A Key Step for Base Free Catalytic Transfer Hydrogenation, L. Taghizadeh Ghoochany, S. Farsadpour, F. Menges, G. Niedner-Schatteburg, W.R. Thiel submitted to *Chem. Eur. J* **2012**.

2. A Covalently Supported Pyrimidinylphosphane Palladacycle as a Heterogenized Catalyst for the Suzuki-Miyaura Cross Coupling, , S. Farsadpour, L. Taghizadeh Ghoochany, S. Shylesh,G. Dörr, A. Seifert, S. Ernst, W. R. Thiel., *Chem. Cat. Chem.* **2012**, 4, 401-407.

3. Small Substituents Make Large Differences: Aminopyrimidinyl Phosphines undergoing C-H Activation, S. Farsadpour, L. Taghizadeh Ghoochany, Y. Sun, W. R. Thiel., *Eur. J. Inorg. Chem.***2011**, 4603-4609.

4. Novel *N*,*N*,*N*-Donors Giving Highly Active Ruthenium Catalysts for Transfer Hydrogenation at Room Temperature, L. Taghizadeh Ghoochany, S. Farsadpour, Y. Sun, W. R. Thiel, Accepted for *Eur. J. Inorg. Chem.* **2011**, 3431–3437. as cover paper

5. Fluoride Catalyzed P–Aryl-Coupling–a Mild Approach to Functionalized Arylphosphines, A. Reis,D. Dehe, S. Farsadpour, I. Munstein, Y. Sun, W. R. Thiel, *New. J. Chem.*, **2011**, 35, 2488-2495.

6. W. R. Thiel, A. Reis, D. Dehe, S. Farsadpour (Nalchigar) (alle TU Kaiserslautern), N. Böge, A. Kreipl (beide IP Bewertungsgesellschaft mbH), "Verfahren zur Kopplung von halogen-substituierten Aromaten mit Trialkylsilyl-substituierten Heteroatom-haltigen organischen Verbindungen", EP 09155232, eingereicht am 16.03.**2009**.

7. *N*,*N*′-Bis(8-quinolyl)pyridine-2,6-dicarboxamide, S. Meghdadi, H. R. Khavasi and S. Nalchigar *Acta Cryst.* (**2008**). E64, o431.

8. *N*,*N*'- (Methylenedi-*p*-phenylene)bis(pyridine-2-carboxamide), S. Meghdadi, H. R. Khavasi and S. Nalchigar *Acta Cryst.* (**2006**). E62, o5492.